R-08-40

KBS-3H

Description of buffer tests in 2005–2007

Results of laboratory tests

Torbjörn Sandén, Lennart Börgesson, Ann Dueck
Reza Goudarzi, Margareta Lönnqvist, Ulf Nilsson
Mattias Åkesson

Clay Technology AB

December 2008

Svensk Kärnbränslehantering AB
Swedish Nuclear Fuel
and Waste Management Co

Box 250, SE-101 24 Stockholm
Phone +46 8 459 84 00

ISSN 1402-3091
SKB R-08-40

KBS-3H

Description of buffer tests in 2005–2007

Results of laboratory tests

Torbjörn Sandén, Lennart Börgesson, Ann Dueck
Reza Goudarzi, Margareta Lönnqvist, Ulf Nilsson
Mattias Åkesson

Clay Technology AB

December 2008

Keywords: KBS-3H, Bentonite, Piping, Hydraulic pressure, Relative humidity.

Abstract

The horizontal design for the deposition of nuclear waste in granitic rock has been ongoing since 2002. Clay Technology has contributed with studies that mainly concern the behaviour and design of the bentonite buffer material. The work described in this report was a part of the design subproject and was conducted from 2005 up to mid-2007.

The results of the work and the increased general understanding of the behaviour of the buffer in KBS-3H have led to two main designs: BD (Basic Design) and DAWE (Drainage Artificial Watering and air Evacuation).

Several significant uncertainties related to the behaviour of distance blocks and buffer materials were identified in /Autio et al. 2008b/. The most important issues to be resolved were included in an extensive buffer test plan and this report presents the work carried. The critical issues (an issue is defined as critical if there is clear undertainty in fulfilling the design basis) to be resolved to produce viable designs were:

1. *Humidity-induced swelling.* This process may cause cracking and subsequent loss of bentonite as the debris falls on to the floor. There is also the possibility that the blocks could swell and come into contact with the rock wall. Both these processes will lead to a hindering of the free water flow on the tunnel floor in DAWE and may subsequently result in the erosion of bentonite material from the tunnel. This is not expected to be an issue in the BD owing to the small buffer-rock gap engineered into the design.
2. *Erosion of of filling blocks and buffer.* This process will lead either to a loss of material from the emplacement drift if it takes place before a hydraulic plug is built or to redistribution of bentonite in the emplacement drift if it takes place afterwards. Localized erosion may be harmful for both design alternatives if it results in a substantial loss or redistribution of material.
3. *Artificial wetting of distance blocks.* Both design alternatives include artificial water filling of the gap between the distance block and the rock surface as a means of improving performance of the buffer, but for different reasons. In DAWE, the entire tunnel will be filled when a functional plug has been built in order to minimize internal erosion. In BD, the slot between the distance blocks and the rock surface may be filled with water after the installation of each section in order to improve the sealing ability of the distance blocks. The hydro-mechanical interaction between the buffer, the water filled slot and the rock are important factors in the functioning of the two design alternatives.
4. *Piping through distance blocks.* In BD, the distance block section is required to hydraulically seal and isolate all container sections. Since the distance blocks cannot be installed without a gap between the blocks and the rock surface this gap must be sealed by the swelling bentonite before piping can be prevented. This requirement is very difficult to achieve at high water inflow rate, and a large number of tests have been performed in order to determine the limits of the allowable gap between the bentonite and rock and to improve the design.
5. *Hydraulic pressure on distance block end surface.* Since the distance block section in BD must hydraulically seal all container sections, there will be very high water pressure inside the supercontainer section when the air-filled volumes have been filled with water. If the water pressure propagates deeply into the joint between distance blocks or between a distance block and the supercontainer lid, unacceptably high forces will be applied on the distance blocks and on the fixing ring outside the distance block section.

In addition to the laboratory tests undertaken in order to solve the critical issues outlined previously, the following work has been carried out:

- Modelling of the mechanical performance of full-scale distance blocks and modelling of small-scale laboratory tests performed to investigate humidity-induced swelling. These modelling exercises are ongoing.
- Development of design alternatives other than BD and DAWE.
- Investigation of block properties and design of suitable composition, geometry and fabrication technique for the bentonite blocks for use in both the distance block section and within the metal sleeve portion of the supercontainer.

Piping and hydraulic pressure tests have so far shown that the distance blocks must fit tightly to both the rock surface and the lid of the supercontainer in order for them to function as required in the Basic Design layout under the harsher test conditions applied in recent tests. To ensure the proper functioning of the distance blocks, the water pressure within the emplacement drift should be artificially controlled (by use of a temporary tube placed past the distance blocks).

The Basic Design alternative has been assessed as not being robust and to contain severe uncertainties because the distance blocks were not found to function according to requirements when exposed to full hydrostatic pressure.

Sammanfattning

Utformningen av ett horisontellt slutförvar av utbränt kärnbränsle har hållit på sedan 2002. Clay Technology har bidragit med studier som huvudsakligen rör utformningen och egenskaperna hos bentonitbufferten. Arbetet som beskrivs i denna rapport ingår i ett delprojekt som rör designen av ett slutförvar och genomfördes under tiden mellan 2005 och fram till mitten av 2007.

Resultatet av arbetet och den ökade förståelsen för hur bufferten i ett KBS-3H förvar fungerar, har lett fram till två huvudutformningar: BD (Basic Design) och DAWE (Drainage Artificial Watering and air Evacuation).

Ett antal betydelsefulla osäkerheter när det gäller egenskaperna för distansblock och buffertmaterial identifierades i /Autio et al. 2008b/. De viktigaste osäkerheterna som skulle lösas ingick i en omfattande bufferttestplan och i denna rapport presenteras resultat från det arbetet. De osäkerheter som skulle lösas för att kunna producera en genomförbar och duglig design var:

1. *Svällning på grund av hög relativ fuktighet*. Denna process kan orsaka sprickbildning och därpå följande förlust av bentonitbitar som faller ner på tunnelgolvet. Det finns också en möjlighet att blocken sväller och kommer i kontakt med bergväggen. Båda dessa processer kommer att leda till att ett vattenflöde på tunnelgolvet hindras DAWE och kan leda till erosion av bentonit från tunneln. Detta förväntas inte vara en fråga som påverkar BD beroende på den smala spalt mellan berg och bentonit som är en del i denna design.
2. *Erosion av buffertblock*. Denna process kommer att leda till antingen förlust av material från deponeringstunneln om den sker innan en hydraulisk plugg är byggd eller till att material omdistribueras inom deponeringstunneln om den sker efter att pluggen är byggd.
3. *Artificiell bevätning av distansblocken*. Båda utformningsalternativen förutsätter artificiell bevätning av spalten mellan distansblock och bergyta som ett sätt att förbättra buffertens förutsättningar, men av olika anledningar. I DAWE kommer hela tunneln att fyllas, efter det att en plugg har blivit byggd, för att minska den interna erosionen. I BD kommer spalten mellan distansblock och berg att fyllas med vatten efter installationen av varje sektion, för att förbättra distansblockens tätningsmöjligheter. Den hydromekaniska påverkan mellan buffert, den vattenfyllda spalten och berget är viktiga faktorer för funktionen av de två utformningsalternativen.
4. *Kanalbildning genom distansblocken*. I BD skall distansblocken hydrauliskt täta och isolera alla supercontainersektioner. Eftersom distansblocken inte kan installeras utan en spalt mellan block och berg måste denna spalt tätas av svällande bentonit innan kanalbildning kan förhindras. Detta krav är mycket svårt att uppnå vid höga inflödeshastigheter, och ett stort antal försök har genomförts för att kunna bestämma den tillåtna gränsen för storleken på spalten mellan berg och block, för att kunna förbättra utformningen.
5. *Hydrauliskt tryck på distansblockets ändyta*. Eftersom distansblocken hydrauliskt måste täta alla containersektioner i BD, kommer höga vattentryck att byggas upp inuti supercontainersektionerna när de luftfyllda volymerna har fyllts med vatten. Om vattentrycket propagerar djupt in i spalterna mellan distansblocken eller mellan distansblocken och ändytan av supercontainern, kan oacceptabelt höga laster verka på distansblocken och den ”fixing-ring” som skall hålla allt på plats.

Förutom de laboratorieförsök som har gjorts för att lösa de osäkerheter som listats ovan, har även följande arbete utförts:

- Modellering av den mekaniska delen av ett fullskaligt distansblock samt modellering av småskaliga laboratorieförsök utförda för att undersöka svällning som sker på grund av hög relativ fuktighet. Detta modelleringsarbete pågår.
- Utveckling av andra alternativ till BD och DAWE.
- Undersökning av blockegenskaper och design av passande composition, geometri och tillverkningsteknik för både distansblock och block inuti supercontainern.

De kanalbildnings- och hydrauliska trycktester som har genomförts visar att distansblocken måste passa tätt mot både bergytan och ändytan av supercontainern för att de ska fungera som avsett i BD-utformningen med de tuffa förhållande som har rått i de senaste försöken. För att försäkra sig om att distansblocken fungerar som tänkt, måste vattentrycket i deponeringstunneln kontrolleras artificiellt (genom att ett stålrör temporärt placeras förbi distansblocken).

Det har i slutet av denna undersökning fastställts att Basic Design (BD) alternativet inte är tillräckligt robust och att det innehåller stora osäkerheter därför att distansblocken inte fungerar enligt satta krav när de utsätts för fullt hydrostatiskt tryck.

Executive summary

General

The horizontal design for the deposition of nuclear waste in granitic rock has been ongoing since 2002. Clay Technology has contributed with studies that mainly concern the behaviour and design of the bentonite buffer material. The work described in this report was a part of the design subproject and was conducted from 2005 up to mid-2007.

The results of the work and the increased general understanding of the behaviour of the buffer in KBS-3H have led to two main designs: BD (Basic Design) and DAWE (Drainage Artificial Watering and air Evacuation).

BD design alternative is based on assumption that the distance blocks will seal the supercontainer sections in wet sections stepwise in sequence independently of each other. The main idea with the BD design is to hydraulically isolate every supercontainer section from each other immediately after installation. During the installation of a deposition drift there will be no water flow from one supercontainer section to another. This is mainly achieved by the rapidly sealing distance blocks, which are designed in order to prevent all water flow between the supercontainer sections during the installation and also during the following saturation phase. Important design features specific to BD design alternative are the small, about 5 mm, gap between the distance blocks and the rock surface, requirement for a small gap between the supercontainer and the distance block and need for fixing rings to keep the distance blocks from moving when exposed to hydraulic pressure.

In the case of *DAWE design*, like in BD, fractures that could give rise to significant water flows to adjacent unsaturated drifts or transport tunnels will be avoided as supercontainer emplacement locations. The drainage of inflowing water along the floor of the drift during operations in the DAWE alternative is achieved by inclining the drift towards its entrance. There is a gap of ca. 40 mm (37.5–42.5 mm) between the distance blocks and the drift walls, which is larger than in the BD (roughly 5 mm) and should prevent any contact with the water flowing along the bottom of the drift. Furthermore, a higher initial-water-content bentonite is used to prevent humidity-induced fracturing of the distance blocks. Drainage of inflowing water along the drift floor is expected to continue until the drift or the drift compartment is plugged. Following sealing of the compartment, artificial watering takes place simultaneously with evacuation of air to avoid gas pressurisation. Steel pipes along the surface of the drift are used for watering and air evacuation. The sides of the drift are the preferred position for watering pipes to avoid possible damage during operations. Nozzles, which are directed downwards in the watering pipes, are distributed along the drift in each supercontainer section to ensure uniform inflow and minimise any axial water flow in the drift that could give rise to bentonite erosion. Water is not directly injected in the sections where the distance blocks are positioned, again to avoid possible erosion.

Critical issues studied

Several significant uncertainties related to the behaviour of distance blocks and buffer materials were identified in /Autio et al. 2008b/. The most important issues to be resolved were included in an extensive buffer test plan and this report presents the work carried out. The critical issues (an issue is defined as critical if there is clear uncertainty in fulfilling the design basis) to be resolved to produce viable designs were:

1. *Humidity-induced swelling.* This process may cause cracking and subsequent loss of bentonite as the debris falls on to the floor. There is also the possibility that the blocks could swell and come into contact with the rock wall. Both these processes will lead to a hindering of the free water flow on the tunnel floor in DAWE and may subsequently result in the erosion of bentonite material from the tunnel. This is not expected to be an issue in the BD owing to the small buffer-rock gap engineered into the design.
2. *Erosion of of filling blocks and buffer.* This process will lead either to a loss of material from the emplacement drift if it takes place before a hydraulic plug is built or to redistribution of bentonite in the emplacement drift if it takes place afterwards. Localized erosion may be harmful for both design alternatives if it results in a substantial loss or redistribution of material.

3. *Artificial wetting of distance blocks.* Both design alternatives include artificial water filling of the gap between the distance block and the rock surface as means of improving performance of the buffer, but for different reasons. In DAWE, the entire tunnel will be filled when a functional plug has been built in order to minimize internal erosion. In BD, the slot between the distance blocks and the rock surface may be filled with water after the installation of each section in order to improve the sealing ability of the distance blocks. The hydro-mechanical interaction between the buffer, the water filled slot and the rock are important factors in the functioning of the two design alternatives.
4. *Piping through distance blocks.* In BD, the distance block section is required to hydraulically seal and isolate all container sections. Since the distance blocks cannot be installed without a gap between the blocks and the rock surface this gap must be sealed by the swelling bentonite before piping can be prevented. This requirement is very difficult to achieve at high water inflow rate, and a large number of tests have been performed in order to determine the limits of the allowable gap between the bentonite and rock and to improve the design.
5. *Hydraulic pressure on distance block end surface.* Since the distance block section in BD must hydraulically seal all container sections, there will be very high water pressure inside the super-container section when the air-filled volumes have been filled with water. If the water pressure propagates deeply into the joint between distance blocks or between a distance block and the supercontainer lid, unacceptably high forces will be applied on the distance blocks and on the fixing ring outside the distance block section.

Results

The main results and conclusions are summarized below.

Humidity-induced swelling of bentonite blocks before closure

A large number of tests have been conducted using bentonite specimens exposed to a free surface of water separated by an air-filled gap. The transfer of water from the water surface via the air gap to bentonite has been studied as a function of time under different conditions. The main variables examined were gap width, initial water content of the bentonite, density of the bentonite, temperature and the size of the specimen. The water uptake and volume change of the specimen were measured. Additionally, the moisture- suction-induced cracking of the specimen was studied

The tests showed that the factor which has the greatest impact on specimen wetting is the transport of water through the air-filled gap between the water surface and the bentonite surface. The transport of water into the bentonite is always faster, which means that the wetting is much slower than when a bentonite sample is in direct contact with free water and that the relative humidity at the bentonite surface is always lower than 100%. It also means that the water content gradient in the bentonite is rather small, which is favourable for preventing cracking. The driving force for the water transport is the relative humidity gradient across the gap between the specimen and the liquid water. As a result, wetting is slower the greater the initial water contents of the bentonite and the wider the spacing. Since water transport across the gap is driven by vapour diffusion in air, the temperature also affects the wetting rate.

Modelling of the water transport with Code Bright reproduced the physically-observed conditions, lending support to the explanations put forward to describe the behaviour of water vapour transport. Physical disruption of the small specimens examined only occurred in the form of very small cracks on the exposed surface of the specimens and on specimens with low initial water content. This is attributed to the small water content gradient present, which meant that the difference in volumetric swelling was small in most specimens. Tests carried out using large specimens (blocks of 30 cm in diameter) were extremely vulnerable to cracking when the initial water ratio was lower than 20%. With an initial water content of 13%, the whole block cracked within 24 hours after it had been exposed to a free water surface at the other side of the gap. The reason why the blocks are more prone to cracking than the small specimens is probably that the stresses are smaller in the small specimens since expansion is not prevented by interlocking particle effects.

The studies of cracking and water uptake by highly compacted bentonite support a conclusion that the blocks should have high water content when installed in DAWE, preferably above 20%. The distance blocks can be produced with this water content but not the rings inside the supercontainer, since they need to have a much higher dry density.

Erosion of bentonite during and after installation

The erosion of sealing materials has so far mainly been studied in another project (Baclo), but new tests on KBS-3H buffer material are ongoing. General conclusions drawn from previous studies are that the erosion rate seems to be between 1 and 10 gram bentonite per litre of eroding water. It has also been determined that a high salt content in the water increases erosion and that the erosion rate typically decreases with time.

Consequences of artificial water filling of open slots

Tests have been carried out on bentonite blocks initially installed in a constant volume system with a gap between the blocks and the confinement. The results have shown that when the gap is initially filled, and no access is provided to additional water, the bentonite will swell, close the gap and exert a swelling-induced pressure on the confinement. With time, the water in the gap will be drawn into the interior of the specimen and the bentonite that swelled into the gap desiccates, resulting in the formation of cracks. Despite this, there still seems to be a residual swelling-induced pressure of a few hundred kPa present. This is attributed to stresses caused by the expansion of the clay that are transferred through the stiff bentonite between the cracks. Two test series are ongoing in order to further investigate these processes.

Piping past a distance block section

Three different test series have been performed in order to study the critical issue of piping past the distance blocks:

- Scale tests of a simulated distance block section on a scale of 1:10 with a test length of 1 m.
- Extending 1:10 scale tests to examine a test length of 3 m.
- Piping tests in a transparent tube to allow for direct observation of flow.

The inner diameter of the test equipment used is 175 mm and provides a 1:10 scaling, but the radial gap between the tube and the distance blocks remains at full scale.

Testing conditions are very important in determining whether the distance block section will seal and prevent piping. The test conditions used in the recent investigations were intentionally harsher than previous tests. The conditions imposed were as follows, with the conditions previously examined given in brackets for the purpose of comparison: Water inflow rate 1 l/min per section (0.1 l/min); water pressure increase rate 1 MPa/h (0.1 MPa/h); maximum water pressure 5 MPa (2 MPa). The test arrangements used varied somewhat because the emplacement design had been slightly modified since the initial tests were completed.

The tests recently completed show that the harsh hydraulic conditions applied make it difficult for the distance blocks to seal. A wide slot between the distance block and the rock surface filled with pellets does not work due to the low density of the pellets. The slot must be very narrow in order for the distance blocks to be able to generate a functional seal.

The reason why the slot between the block and the rock surface needs to be so narrow is because there is insufficient time for the distance blocks to swell and yield a high enough swelling pressure to withstand the water pressure. Consequently, sealing must be accomplished by another process. The bentonite becomes clogged in the narrow gap, which probably leads to sealing by the arching of clogged material.

Effect and extension of the hydraulic pressure on the vertical end surface of the distance blocks

The tests performed to study this issue have all been carried out on a scale of 1:10 in a testing cell with an inner diameter of 175 mm. However, as with the piping tests, the gaps have the same dimension as they would have in full scale. Since the radius of the equipment is only about 87.5 mm, radial water penetration deeper than 87.5 mm (including the initial slot) could not be studied.

The earlier tests had indicated that an axial gap of 7 mm between the lid of the supercontainer and the distance block could be acceptable and yield a radial water penetration that is limited to about 0.1 m. However, these tests were performed under the less harsh testing conditions that are mentioned above. In the new tests, both the test conditions and the gap width have been varied in order to determine the limits for the required sealing function. Earlier tests also showed that a mechanical fixing ring is required outside the distance blocks in order to support the blocks and prevent them from moving.

Tests carried out to date show that with the harsher test conditions applied in more recent tests (water inflow rate 1 l/min per section and water pressure increase rate 1 MPa/h), not even an axial slot of 2 mm could prevent an externally applied water pressure of 5 MPa from being transmitted to the centre of a block having a radius of 85 mm. When the inflow rate was lowered to 0.1 l/min the radial water penetration was 20-40 mm.

Modelling and design work

In addition to the laboratory tests undertaken in order to solve the critical issues outlined previously, the following work has been carried out:

- Modelling of the mechanical performance of full-scale distance blocks and modelling of small-scale laboratory tests performed to investigate humidity-induced swelling. These modelling exercises are ongoing.
- Development of design alternatives other than BD and DAWE.
- Investigation of block properties and design of suitable composition, geometry and fabrication technique for the bentonite blocks for use in both the distance block section and within the metal sleeve portion of the supercontainer.

General conclusions and comments

From the results of the laboratory tests the following clear statements can be made:

- The test results show that piping cannot be avoided in the Basic Design alternative unless distance block gaps are very small, the inflows are very low and the wetting /saturation times are very long.
- Recent evaluation of the very tight geometric requirements of the BD, together with study findings that the deformation of the distance blocks is unacceptably large at 5 MPa water pressure, have led to the conclusion that the Basic Design will not function reliably in its initial design.

Contents

1 Introduction

1.1 General description of sealing materials studies

This report describes the laboratory work related to the performance of the bentonite-buffer component of the KBS-3H design performed during 2005–2007 by Clay Technology. The work is a continuation of earlier studies described by /Börgesson et al. 2005/. The work on the sealing materials proposed for use in the KBS-3H design is still ongoing and so only tests that were completed before July 2007 are included in this document.

Several significant uncertainties related to the behaviour of distance blocks and buffer materials were identified in the development of KBS-3H design alternatives /Autio et al. 2008b/ to be resolved in order to produce viable designs. These issues have been studied at Clay Technology through a number of different tests and analyses over the period 2005 to 2007, and are presented in detail in Chapters 6-8. The studies on these issues are presented in this report and can be structured in the following way:

1. **Laboratory tests to assess sealing, piping and erosion**. These tests were done using two different test setups that simulated part of a deposition tunnel on a radial scale of 1:10 (inner diameter 175 mm). The length of the testing equipment was 1 and 3 m.
2. **Laboratory tests to evaluate the hydraulic pressure on the end of a distance block**. This issue was investigated in the experiment used to conduct the sealing, piping and erosion tests. In addition, special equipment was designed in order to study in greater detail the extent of the end of the distance blocks that may be exposed to high water pressure.
3. **Laboratory tests to evaluate humidity-induced swelling**. Investigations were performed on two different scales. A first testing series was conducted on a small scale and included a large number of specimens in order to acquire a database large enough to work with. The diameter of each specimen in this test series was about 50 mm and the height 40 mm. In addition, a second test series was performed on a medium scale (diameter of the specimens were about 300 mm and the height 100 mm).
4. **Scenario analyses**. Various distance block designs have been proposed and processes that may affect them have been identified.

These four studies, their results and the conclusions reached will be presented in this report. The report should be regarded as a state-of-the-art report for mid-2007.

1.2 KBS-3H design

In the KBS-3H design, 300 m-long horizontal circular deposition drifts are excavated by means of the TBM technique from a niche in the transport tunnel as shown in Figure 1-1 /Börgesson et al. 2005/. According to this design, about 40 disposal containers will be deposited in each drift.

Units consisting of one canister surrounded by buffer blocks confined by a supercontainer are manufactured elsewhere in the repository. They constitute key components and are moved into the deposition tunnels (Figure 1-2). They are separated by cylindrical “distance blocks” in order to restrict the temperature. The purpose of the distance block is also to seal off each canister position from the next, and to prevent the transport of water and bentonite along the drift.Their axial thickness will range from 3 to 6 m.

The general main objective of the KBS-3H project was to demonstrate that the KBS-3H repository design is a viable alternative to the KBS-3V design. One key objective of design was the development and design of buffer components including comprehensive laboratory testing.

The fact that the canister and the buffer material will be assembled in a prefabricated disposal container enables easier quality control of the regions closest to the canister. Since there is no deposition tunnels that will require backfilling in the KBS-3H design, the density and performance requirements of transport tunnel backfilling may be more flexible than in the KBS-3V design.

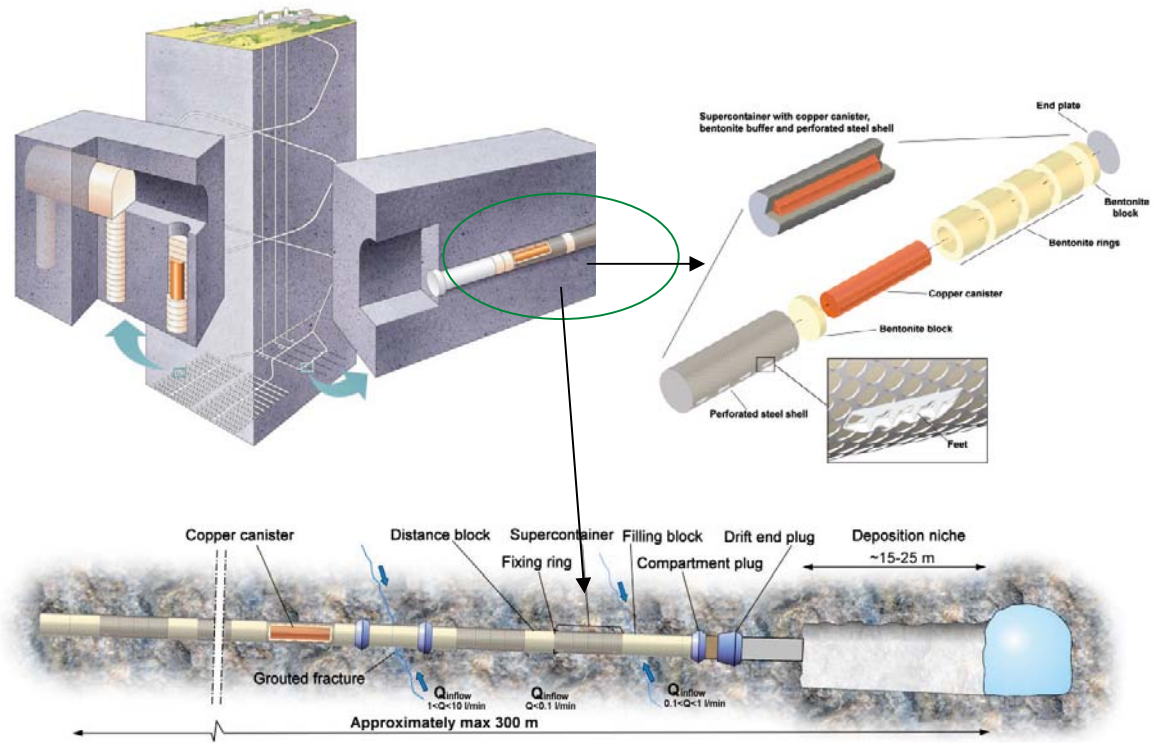

Figure 1-1. *Illustration of a transport tunnel with deposition drifts in KBS-3H.*

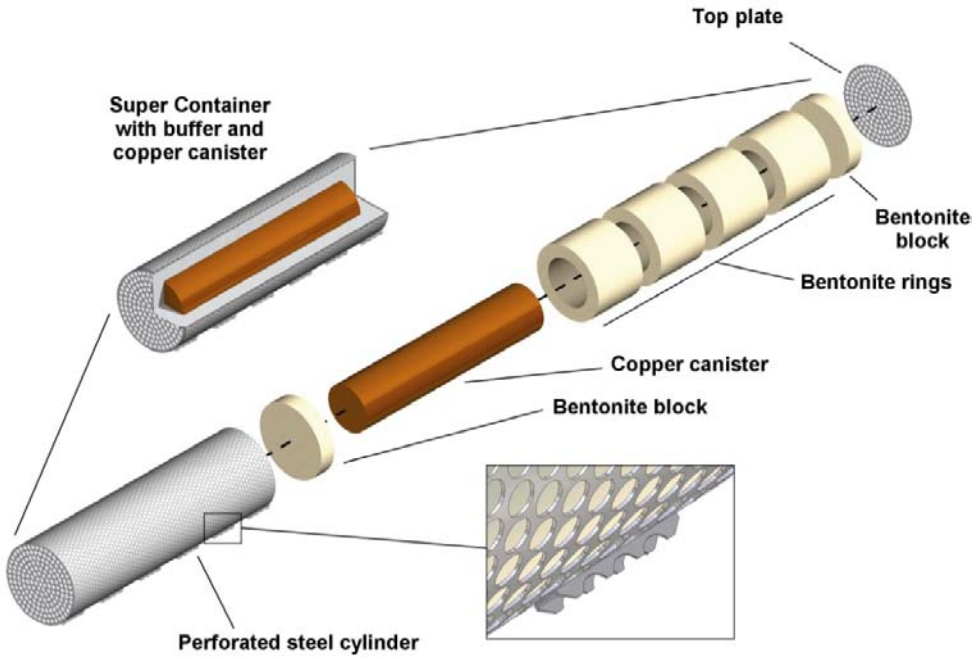

Figure 1-2. *The buffer and canister are embedded in a steel supercontainer in the KBS-3H design.*

2 Summary of work performed prior to 2005

2.1 General

The function of the buffer in the KBS-3H design has been investigated earlier by laboratory tests on small and full scale, by modeling and by scenario analyses. A summary of laboratory tests carried ouit prior to 2005 is presented in this chapter. Section 2.2 is largely reproduced from the conclusions of the report on studies of buffer behaviour in the KBS-3H design describing the work performed over the period 2002–2004 /Börgesson at al. 2005/.

During the early development of the basic design in 2004 it was concluded that there were several problems related to the presented KBS-3H design. Several of these problems related to the behaviour of KBS-3H design and scope of future research and development work were addressed in the seminar in Stockholm 9th February 2005. The most significant functional uncertainties and problems were related to uneven saturation, piping and rupturing of buffer mainly caused by heterogeneous groundwater inflow environment.

2.2 Results of earlier tests (2002–2004)

The investigations carried out over the period 2002–2004 mainly concerned the KBS-3H design alternative, in which a distance block is supposed to seal and prevent all water flow past the block during the installation phase.

2.2.1 Scaled tests

A test cell on a scale of 1:10 that allowed physical simulation of the saturation and maturation of two canister sections was constructed and tested. These tests showed that the interaction between the buffer and the perforated supercontainer in which the canisters are installed is complex, but that the system is acceptable from a safety point of view. The following observations related to the system were made:

- The bentonite swelled through the holes of the container and between the container and the simulated rock surrounding it, filling the entire slot volume.
- The swelling pressure measured outside the container and the measured average buffer density were comparable to what could be expected in a system without a container.
- The axial hydraulic conductivity of the buffer in the slot outside the container was measured and found to be about 10^{-12} m/s, higher than expected from the density and swelling pressure measurements, but still low enough to meet the requirements of a buffer.
- The perforated container was deformed/stretched by the swelling of the buffer and had ruptured at a few locations near the ends of the assembly.
- The expansion/rupturing of the perforated container is believed to be the reason for the high swelling pressure and density outside the container.
- The increased hydraulic conductivity in the slot outside the container is attributed to uneven swelling beyond the original container volume (as shown by the theoretical calculations presented in the report.

2.2.2 Sealing tests

A large number of sealing tests were performed in the laboratory. They revealed how the sealing capacity of bentonite is impaired in the presence of flowing water and how vulnerable the buffer is when the water pressure increases rapidly when the water inflow stops. These tests led to the following observations:

- Only a very low water pressure is required to disrupt the sealing process and cause permanent piping and erosion at constant water pressure (2–4 kPa) and a continuously open downstream exit for the water.
- Very small flow rates are able to hinder sealing and to induce continuous piping and ongoing erosion (less than 0.001 l/min. on the scale examined and when the exit from the system remains open). The values of 2–4 kPa and 0.001 l/min. are probably conservative since they are combined with either high water pressure or high water flow rate.
- The processes are complicated with many variables and interdependencies.
- The length of the piping channel is one parameter that influences system evolution. The longer the pipe, the better the sealing capacity of the bentonite.
- Salt in the groundwater improves the ability of the bentonite to seal, but when flow occurs it greatly increases the erosion rate.
- The hydraulic properties of the rock are very important.

After an extended period of hydration, the sealing process will be helped by overall system behaviour. Swelling at locations other than where piping or seepage is occurring is expected to tighten the plug and reduce leakage if the swelling pressure is higher than the water pressure. The distance plug is therefore expected to function adequately provided the water flow is not so high that it causes the erosion to substantially reduce the buffer density. However, it may take a long time for it to seal. The results indicate that further tests should be performed under more realistic flow and pressure conditions and that the complexity of the system requires a wide range of parameters and scenario simulations.

2.2.3 Reference scenario for testing

In the work carried out prior to 2005, the following reference scenario was selected for the subsequent tests in order to simulate natural conditions:

- A water inflow rate of 0.1 l/min. per canister section.
- A rate of water pressure increase of 100 kPa /hour when inflow is stopped.

Most distance block tests were performed on the basis of these assumptions, but other cases were tested as well.

2.2.4 Tests on a scale of 1:10 of the function of the distance block

The complex process and geometry requires the performance of scaled tests with a simulation of the basic scenario in order to gain an understanding of the processes involved. With an understanding of the processes involved, it may be possible to develop technique(s) for making the distance block function properly. The following conclusions were drawn from the results of distance block tests on a scale of 1:10 (a schematic diagram of the test ecuipment is shown in Figure 2-1):

- The filling rate and the water pressure increase rate are very important for the sealing ability. With the basic inflow scenario, the distance block would appear to seal on a scale of 1:10 when the slot between the rock and the block is 2–4 mm wide, but not for larger slots.
- If the distance block seals and prevents leakage, a water pressure will be built up outside the block and the total force from the water pressure must be taken by the block.
- A supporting ring that captures part of the water pressure outside the distance block is required.
- The sealing of the distance block works very well for the reference case, see Section 2.2.3, with the suggested solution (maximum gap of 2–4 mm between distance block/rock and a fixing ring which supports the block).
- Sealing did not occur at any water pressure higher than the reference case.
- The penetration depth of pressurized water was 15–50 mm radially into the block with the applied scale and geometry.
- The sealing function worked well for at least 90 days, although the measured force at the distance block was doubled during the first 60 days and then remained constant.
- A gap between the container and distance block should be avoided as far as possible since it increases the force on the fixing ring. If the radial gap is limited, the self-sealing behaviour assists in reducing the magnitude of the force transmitted to the fixing ring.

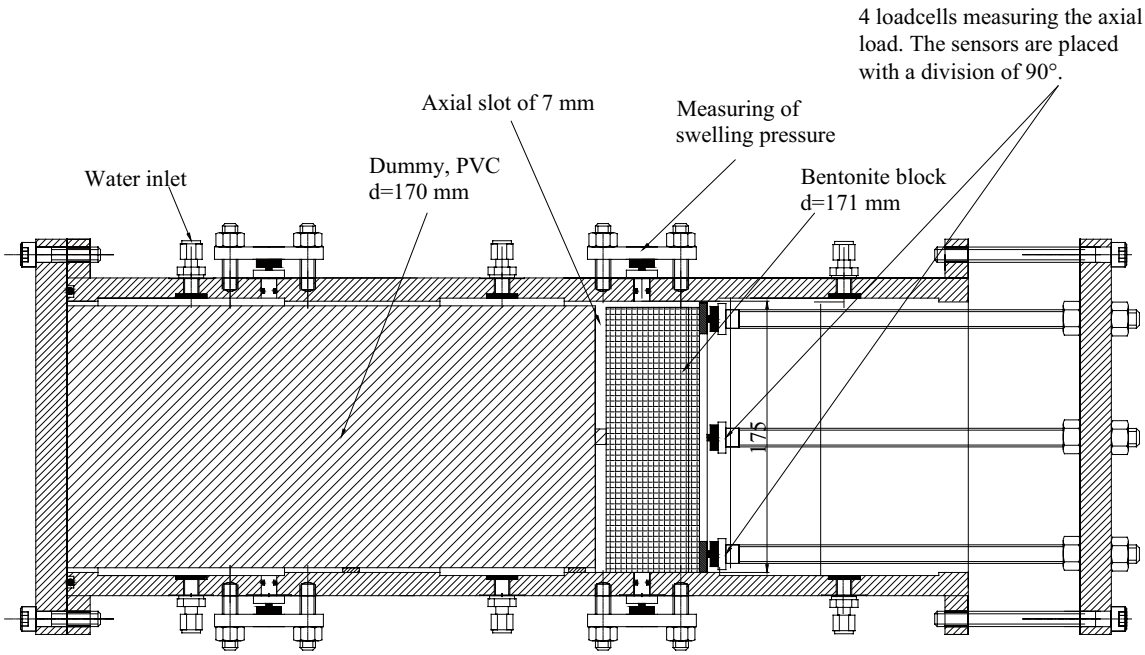

Figure 2-1. *Layout of the sealing tests on a scale of 1:10 (the axial slot was only used in some of the tests).*

2.2.5 Large-scale tests of the distance block function

Since some design parameters could not be properly tested on a scale of 1:10 and since the effect of the scale might be important, several tests were performed on almost full scale. Figure 2-2 shows an example of one of the test layouts in this test series.

The conclusions of the large-scale sealing tests were the following:

- The scale effects are strong.
- It is possible to achieve a seal using a distance block in the reference scenario provided engineering solutions such as an adequate supporting ring are used. Furthermore, either pellets should be installed in the slot or a very narrow slot (a few mm wide) is used in the assembly
- The measured total force directed down the length of the distance block caused by the transfer of a high water pressure at the upstream end of the distance block was not very high since the radial depth from the rock surface on which the water pressure acted was only 10–15 mm.
- The results also show that it is important to avoid a slot between the bentonite blocks and between a bentonite distance block and the supercontainer, although a slot of 7 mm could be handled as shown in the scale tests.

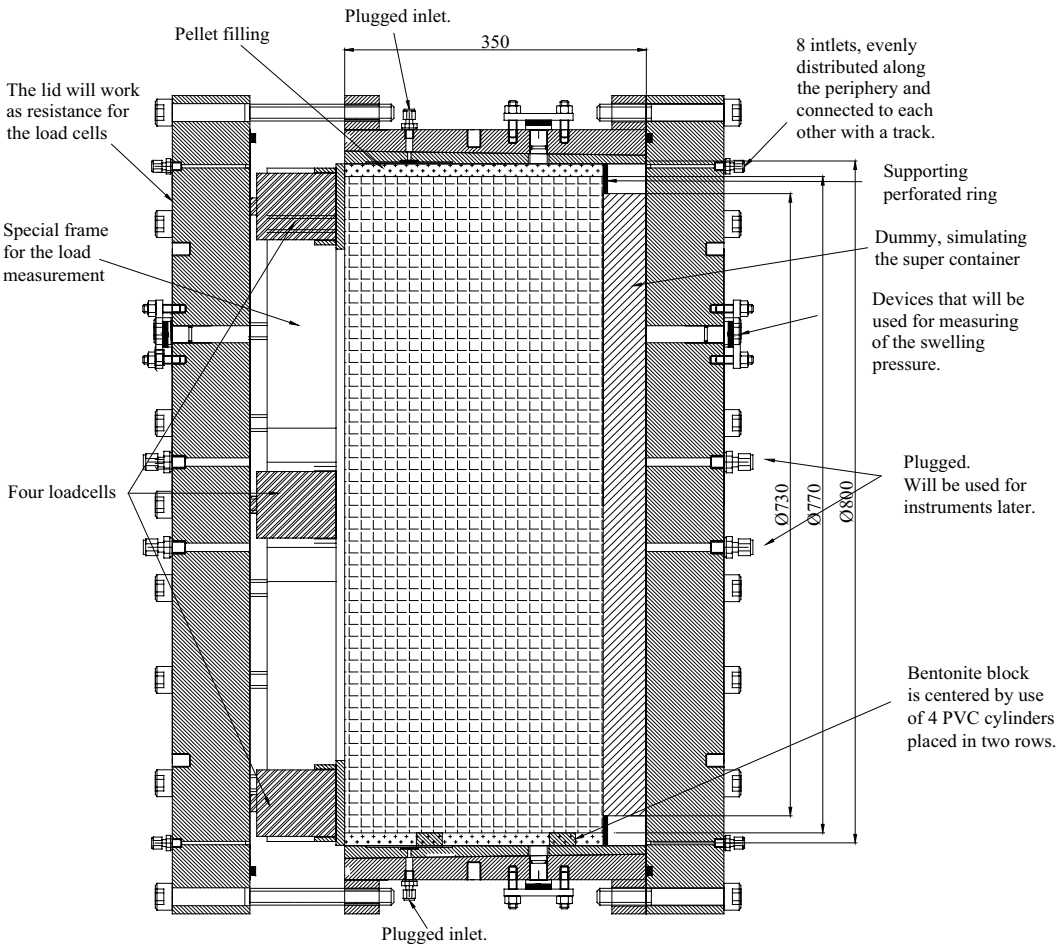

Figure 2-2. *Layout of one of the large-scale sealing tests (Test BB6). Dimensions in mm.*

2.2.6 Modelling

Analytical, numerical as well as conceptual modelling work to simulate and predict different processes were also performed. The following modelling studies were conducted:

A conceptual **KBS-3H repository has also been modelled** to assess both temperature evolution for design purposes and also the saturation rate for safety assessment. The saturation modelling showed that the time until complete water saturation is about 10 years if the rock has an average hydraulic conductivity higher than 10^{-11} m/s. The hydraulic conductivity of the rock determines the hydration rate if it is lower than 10^{-12} m/s, thereby extending the time required to achieve saturation. For example, the time to full saturation is calculated to be 100 years if K=10^{-13} m/s.

The **swelling of the bentonite** through and outside the perforated container portion of the super-container has been modelled analytically. The model describes the state after full maturation. The results showed that the optimal hole diameter is 10 cm when the present container design is used. The reduction in the swelling pressure from inside to outside the supercontainer is about 60% (resulting from reduced clay density in the outside region relative to the interior due to friction in the bentonite that prevents complete homogenisation).

The **hydro-mechanical evolution of the scale test** has been predicted by FEM-modelling of the test. The model was simplified in the sense that uniform system permeability was assumed (the effects of the perforated container were not included). Comparison with measured results showed that the general behaviour observed in the large-scale tests was fairly well predicted. The measured clay wetting was considerably slower than predicted, partly due to the influence of the container and partly due to general shortcomings in the modelling at a late stage of the water saturation phase.

2.2.7 Scenario analyses of the Basic Design

The scenario analyses carried out in the initial investigations were primarily focussed on the design alternative in which the distance block is supposed to seal the emplacement drift and prevent all water flow past the block during the installation phase (Basic Design, BD)

The conclusions from scenario analyses in combination with other investigations were that the fixing ring which is bolted to the rock can work as intended for the reference scenario and prevent piping and displacement of the distance block in one of the initially suggested design options. The ring must be fixed to the rock surface with bolts that are so strong and undeformable that the total force can be resisted without deformation. The main concern with this design is that a sudden, small displacement of the distance block could occur such that the water pressure upstream is transmitted to the entire cross-sectional area of the tunnel distance block.

The scenario description mainly refers to the base case. The consequences of higher maximum water pressure (up to 5 MPa), faster pressure build-up (up to 1,000 kPa/h) and faster water inflow rate (up to 1.0 l/min) have also been investigated. The results indicate that 5 MPa and 1,000 kPa/h. and 1.0 l/min inflows cannot be accepted. In the large-scale test a condition of 0.2 l/min (in combination with 1,000 kPa/h and 5 MPa) could barely be handled.

2.2.8 Scenario analyses of the open tunnel design

An alternative solution to the BD where the tunnel is tightly closed by the distance blocks is to keep the tunnel open by intentionally leaving a gap between the distance block and the rock surface so that the water can pass the block without interference (later developed to DAWE design). A scenario analysis was performed and although the analyses and calculations performed are of a general nature only, the conclusion was that the open tunnel design does not work unless the bentonite is protected during installation. The swelling of the buffer due to the high relative humidity in the air and the dripping of water on to the buffer may lead to degradation and erosion of the buffer.

3 Brief description of candidate designs

3.1 General

There are two different candidate designs for the KBS-3H , see Figure 3-1:

- BD (Basic Design).
- DAWE (Drainage, Artificial Watering and air Evacuation).

The BD and DAWE designs are described in the KBS-3H Design Description report /Autio et al. 2008a/. The designs include different components such as distance blocks, fixing rings and filling blocks. The distance blocks in KBS-3H are designed to separate the supercontainer sections in order to reduce temperature in the buffer and to hydraulically isolate the supercontainer sections from each other.

3.2 BD alternative

The fundamental concept behind the BD design is to hydraulically isolate all supercontainer sections from each other. This is mainly achieved by the distance block sections, which are intended to prevent all water flow between supercontainer sections during their installation and also during the saturation phase that follows.

A high hydrostatic pressure in the supercontainer section will act on parts of the cross-sectional area of the distance blocks. The displacement of the blocks is partly resisted by the friction between bentonite and rock and also by the support from the neighbouring section. In addition, a fixing ring will be used to mechanically restrain the system. The fixing ring is made of steel and is physically anchored in the rock.

Four design variations for the BD have been considered and are described in Chapter 4.3.

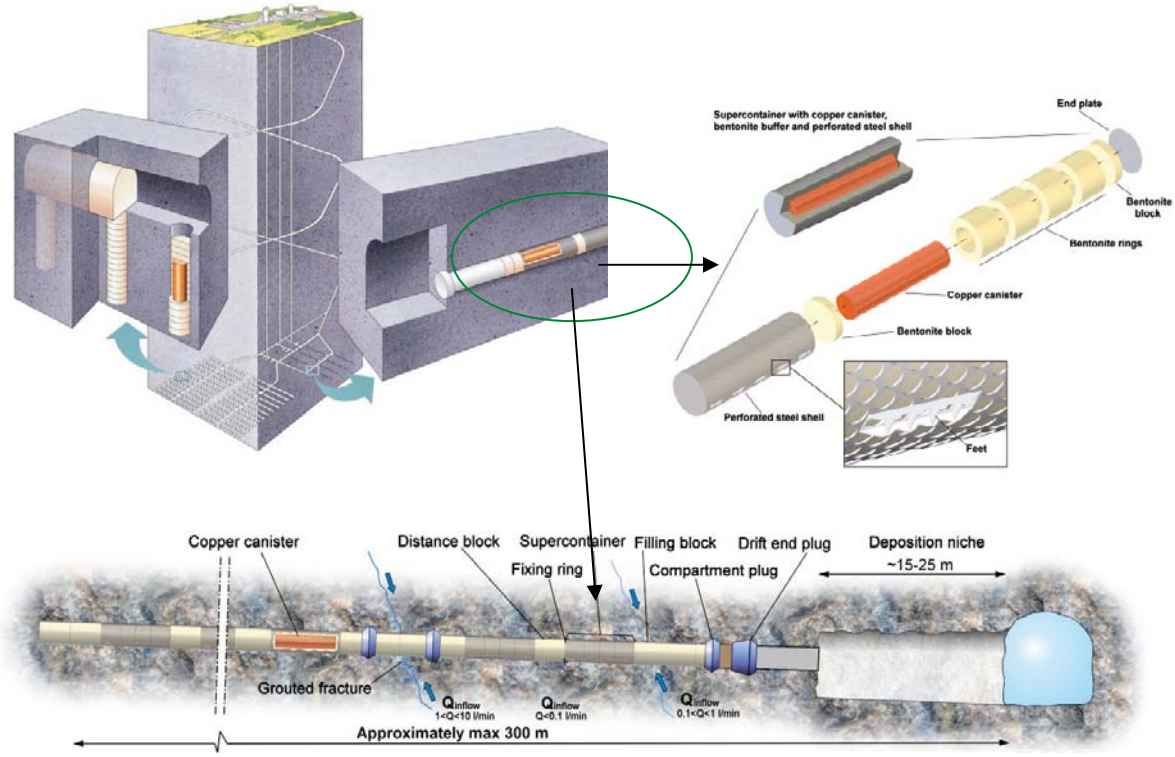

Figure 3-1. *KBS-3H repository design concept.*

3.3 DAWE alternative

The DAWE design assumes that the deposition tunnel will be kept open during the entire installation period so that water can freely flow along the floor of the tunnel. The distance blocks will be positioned centrally in the tunnel supported on feet (the same ones that support the supercontainers). The empty space between the distance blocks/supercontainer and rock will be artificial filled with water and the trapped air evacuated. The design of the distance blocks is described in Section 4.4.

4 Design of buffer components

4.1 General

The KBS-3H design incorporates a number of buffer components (bentonite originally inside the supercontainers and the bentonite distance blocks):

1. **Bentonite blocks inside the supercontainer**. Bentonite blocks of two types – ring shaped along the canister and cylindrical at the ends – will be installed in each supercontainer.
2. **Distance blocks**. Between each supercontainer section, distance blocks will be placed in order to seal each section hydraulically. Different designs are suggested. The nominal length of the distance blocks sections is 5.5 m for the Posiva reference conditions and 2.5 m for the SKB reference conditions.

This chapter describes the design of the bentonite blocks in the supercontainer and the distance blocks for the BD and DAWE designs (i.e. dimensions, initial density and initial water ratio). The water ratio is in this report defined as mass of water per mass of dry substance, where the dry mass is obtained from drying the wet samples at 105°C for 24 hours (sample weight 10–30 g). This chapter also shows results of calculations to determine the sensitivity of the final saturated density of buffer blocks to deviations from the nominal tunnel diameter (1,850 mm).

Different design alternatives related to the distance blocks in the Basic Design are also described. These different design options are based on the results of the tests described in Chapter 7.

4.2 Buffer blocks in supercontainer

4.2.1 General

A main feature of the KBS-3H design is the use of a "supercontainer". Bentonite blocks will be installed inside the perforated metal supercontainer shell that surrounds the copper canister. The final density when the blocks have become saturated after having swollen through the perforated steel container and filled the volume between the container and the rock should be between 1,950–2,050 kg/m^3 (dry density 1,481–1,637 kg/m^3). Two types of blocks will be installed: ring-shaped blocks around the canister and cylindrical blocks at each end of the container.

4.2.2 Initial conditions

The suggested supercontainer design requires blocks with a high initial density in order to provide the bentonite within the supercontainer with the ability to swell and fill the rather large slots between the container and the rock while retaining an adequately high density. The production of the blocks is described in Section 4.5.

Table 4-1 shows the dimensions and dry densities used for the calculation of the buffer conditions likely to be developed within emplacement drift occupied by the supercontainer. In Figure 4-1, the dry density of the blocks is plotted vs. the saturated density after swelling and homogenization have occurred. The tolerable variation in the dry density of the manufactured blocks is comparatively large (1,791–1,979 kg/m^3 for the ring-shaped blocks and 1,665–1,841 kg/m^3 for the cylindrical end blocks). Keeping the values within this range will allow an average density at saturation of between 1,950–2,050 kg/m^3 to be achieved in the tunnel.

4.2.3 Sensitivity to variations in the tunnel diameter

The calculations have been performed using the nominal diameter of the disposal tunnel i.e. 1,850 mm. The diameter will, however, vary and this will influence the density at saturation in the system. The plot provided as Figure 4-2 shows how the density at saturation varies with the diameter of the tunnel. The figures in the diagram assume a density at saturation of 2,000 kg/m^3 at the nominal tunnel diameter (1,850 mm). While these basic calculations have been carried out using the standard diameter of 1,850 mm, there will probably be variations in the real case.

Table 4-1. Table showing the dimensions and calculated densities of the buffer in the KBS-3H design.

Dimensions	
Rock	
Diameter tunnel, mm	1,850
Super container	
Outer diameter, mm	1,765
Inner diameter, mm	1,749
Thickness of container and end plate, mm	8
Degree of perforation	62%
Length, mm	5,546
Canister	
Outer diameter, mm	1,050
Ring-shaped block	
Outer diameter, mm	1,739
Inner diameter, mm	1,060
Cylindrical end block	
Outer diameter, mm	1,739
Calculated block data	
Ring-shaped block	
Target average density at saturation, kg/m^3	2,000
Initial block dry density, kg/m^3	1,885
Initial block void ratio	0.480
Cylindrical end block	
Target average density at saturation, kg/m^3	2,000
Initial block dry density, kg/m^3	1,753
Initial block void ratio	0.592

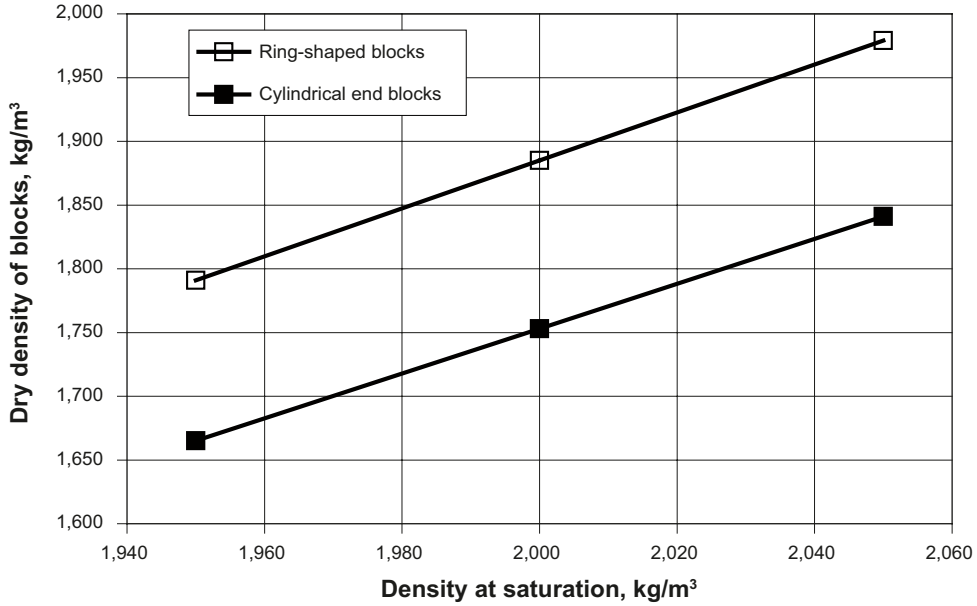

Figure 4-1. *Dry density of the blocks plotted vs. the density at saturation in the tunnel after swelling and homogenization.*

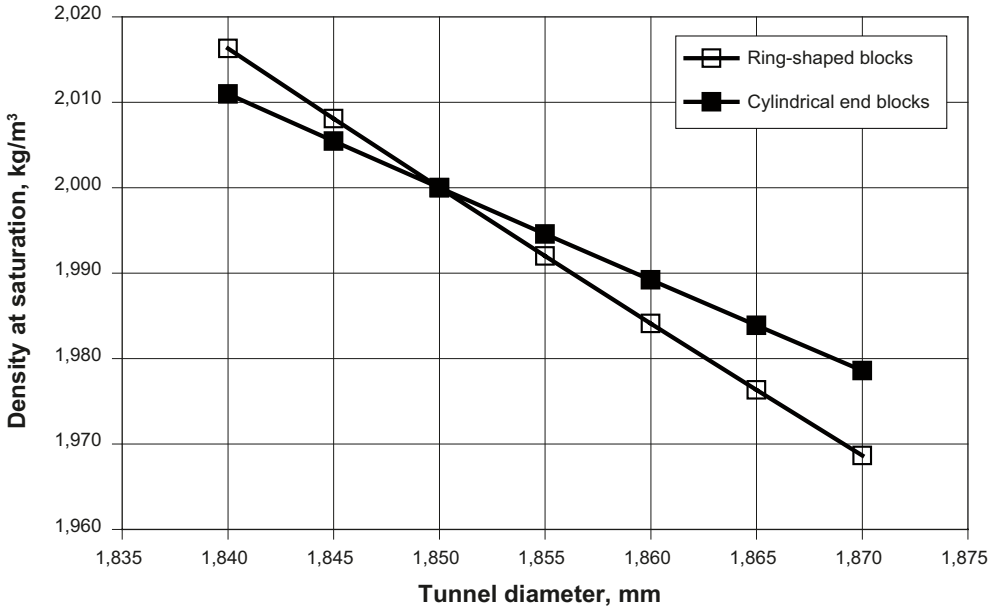

Figure 4-2. *Diagram showing the density at saturation in the tunnel after swelling and homogenization (intended density at saturation 2,000 kg/m³) plotted vs. various tunnel diameters.*

4.2.4 Sensitivity to corrosion of the supercontainer

Investigations related to the behaviour of the steel in the supercontainer during corrosion are ongoing. In order to investigate the final saturated density of the bentonite and its sensitivity to a possible volume change in the corroded steel, calculations of some extreme mechanical effects of complete corrosion have been conducted for three different cases:

1. The volume of the emplaced steel is the same after corrosion (hypothetical reference case).
2. The volume of the corroded steel is zero (hypothetical reference case).
3. The volume of the emplaced steel has been doubled after corrosion (a doubling of the volume is expected due to conversion to magnetite, which has half the density of the original metal.

The calculations made assume radial swelling only. Axial swelling/homogenization is not taken into account. Table 4-2 presents the results from the calculations for both block types. In general, it can be seen that the influence is limited for the ring-shaped blocks but larger for the end blocks as a consequence of the rather large end plate of the container.

Table 4-2. Influences of corrosion-induced change in steel volume on the final average density of the buffer in a supercontainer.

Block type	Saturated density for the different volume cases		
	Same volume kg/cm³	No volume kg/cm³	Double volume kg/cm³
Ring-shaped block	2,000	1,991	2,009
Cylindrical block	2,000	1,982	2,016

4.3 Distance block design alternatives for BD

4.3.1 General

An important component in the Basic Design, described in the KBS-3H Design description /Autio et al. 2008b/, is the distance blocks (DB) (Figure 4-3). The distance blocks are required to prevent water flow between the supercontainer (SC) sections. Ensuring the functionality of distance blocks was identified as a critical design issue in the KBS-3H test plan. The influence of the hydraulic conditions in the surrounding rock on the function of the BD is very strong, i.e. water inflow rate and water pressure increase rate.

The design and function of distance blocks in the KBS-3H design have been investigated in a number of laboratory tests /Börgesson et al. 2005 and this report/. Most of the tests have been performed on a scale of 1:10 in order to provide a timely set of results. The inner diameter of the test equipment used is 175 mm and provides a 1:10 scaling, but the radial gap between the tube and the distance blocks remains at full scale. The applied water pressure has also been "full scale" while the water flow have been scaled in order to get proper filling time.

The investigations have yielded a general conclusion that the design is apparently feasible but that additional tests are needed to confirm this. The scale effect is an example of an issue that must be studied in more detail.

The design development based on laboratory experiments resulted in four options for design of the distance blocks. Given the complexity of the system and its variability regarding inflow rates, pressure development and emplacement considerations, it is important that a number of design options be retained so as to be able to respond to the actual rock conditions encountered.

These distance block designs have so far not dealt with the issues that may arise regarding their installation.

The reference case for the first studies was:

- An inflow rate of 0.1 l/min in a supercontainer section.
- When the constant rate of inflow was discontinued, water was supplied so that a pressure increase occurred at a rate of 0.1 MPa/h up to maximum of 2 MPa.

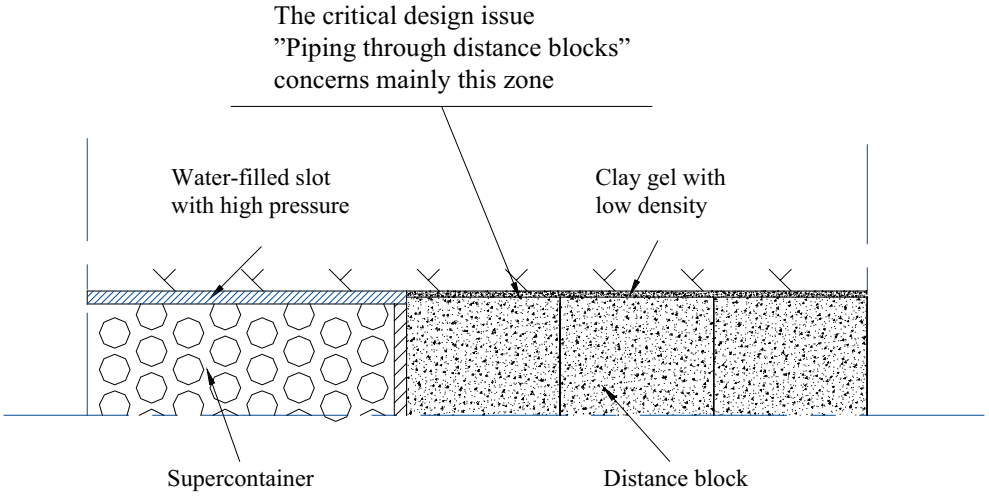

Figure 4-3. *Schematic drawing of the critical issue "piping through distance block".*

The water pressure increase rate in a section of an emplacement drift is highly uncertain and is also difficult to delineate for the purpose of analysis. Although there is currently a 0.1 l/min criterion for SC/DB emplacement sections (reference case), the water inflow rate may be higher than this value, which means that this is not a conservative delineation limit. In the interest of robustness, it is desirable to show that the system works for significantly higher inflow rates than this. Additional tests have therefore been performed, simulating these extreme cases. The conditions simulated in this test series were:

- An inflow rate of 1 l/min in a supercontainer section.
- When the inflow was stopped, a water pressure increase rate of 1 MPa/h up to maximum 5 MPa.

These conditions are very difficult for the distance blocks to handle, but a distance block design that can provide a sealing effect for these high water inflows and withstand the fast pressure increase rate is a very robust design. For the purpose of robustness, only those designs that can withstand these conditions have been proposed as being candidates for further examination.

4.3.2 Design Alternative 1 (5 mm slot)

A number of tests have been performed on a scale of 1:10 (diametrical) and with a test length of 1 m. In the test series, several parameters such as slot widths, centered and non-centered blocks, pellet-filling in the slot and also a pre-wetting of the slot have been varied. The results showed that a slot of 5 mm can be accepted under these conditions provided the slot has been pre-wetted. A design that seems to work for these extreme conditions is shown in Figure 4-4. Tests with this design and conditions were repeated three times in the laboratory.

Layout:

- Centered blocks with 5 mm slot between blocks and the rock.
- Pre-wetting of the slot.
- 3.5% salt in the water.

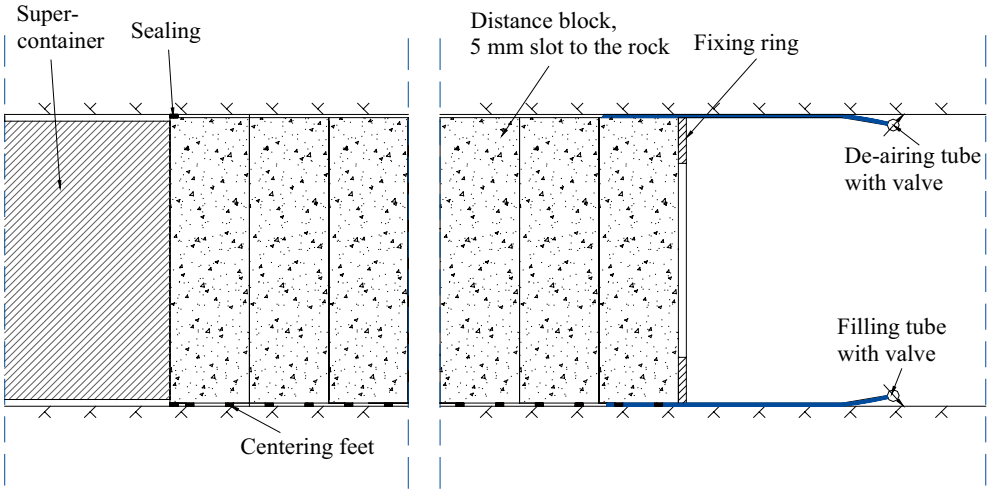

Figure 4-4. *Schematic drawing of layout distance block alternative 1.*

This layout demands that special sealing arrangements be made around the inner distance block (next to the supercontainer), and also at the outermost block (downstream face) next to the fixing-ring due to the pre-wetting of the gap bentonite/rock. These special sealing components can be rather simple, perhaps made of bentonite, since their only purpose is to withstand the pressure from the water when intentional flooding of the slot is performed (the pre-wetting).

The difference in diameter between the deposition drift and the distance blocks is only 10 mm. The small gap and the requirement to centre the block radially could be a problem for the installation. Laboratory experiments indicate that this 5 mm gap is the maximum that can be allowed for these extreme conditions without controlling the water pressure.

4.3.3 Design Alternative 2 (10 mm slot and controlled water pressure).

Tests have also been made in a test setup with a length of 3 m. In this device, an installation design with artificial control of the water pressure inside the distance blocks was tested. A drainage tube leading into the supercontainer section was installed in the slot below the distance blocks, see Figure 4-5. This drainage tube made it possible to control the water pressures in the supercontainer section and consequently give the bentonite more time for maturation (water uptake and swelling). This technique has also made it possible to increase the slot width from 5 to 10 mm, which will facilitate the installation of the distance blocks.

One of the issues discussed in connection with this layout has been the retrieval of the drainage tube. This was also successfully tested. The technique used was to pull the tube out in steps (tested with 1 m/step and 24 hours between steps), giving the bentonite time to seal the volume previously occupied by the tube. This dewatering design has been tested twice in the laboratory under the following conditions.

Layout:

- Centered blocks with 10 mm slot to the rock.
- Pre-wetting of the slot.
- 3.5% salt in the water.
- Drainage tube through the distance blocks into the supercontainer section in order to control the water pressure.

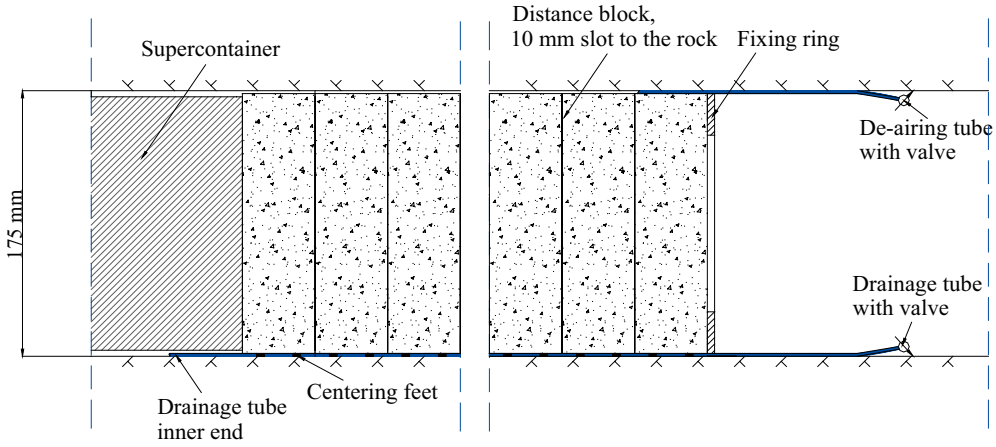

Figure 4-5. *Figure showing a schematic drawing of Alternative 2.*

Beyond the testing carried out to examine the potential viability of Alternative 2 of the BD, the simulations performed have identified three important requirements or features for the distance block design. Firstly, a temporary seal is needed around the outermost distance block where it contacts the fixing-ring. The seal can be rather simple, perhaps made of bentonite, since its only purpose is to withstand the pressure from the water when filling up the slot (the pre-wetting). The second finding of the tests is that the radial gap between the distance blocks and the surrounding rock in this layout can be increased from 5 mm (Alternative 1) to 10 mm. This will facilitate the installation of the distance blocks, but it is still rather tight. The third design requirement established is the need for a rather long time for installation maturation. The bentonite needs to be supported for about 14 days before it can withstand 5 MPa including withdrawal of the tubes. This period could perhaps be decreased if the technique is optimized.

4.3.4 Design Alternative 3 (block split into three parts)

Design Alternative 3 involves the use of a block divided into three parts in order to allow it to fit tightly to the surrounding rock, see Figure 4-6. The internal surfaces of the blocks are inclined, which means that the segments can be pushed into position and the bentonite will be forced into tight contact with the rock surface. This design could be used for the entire length of the distance block section.

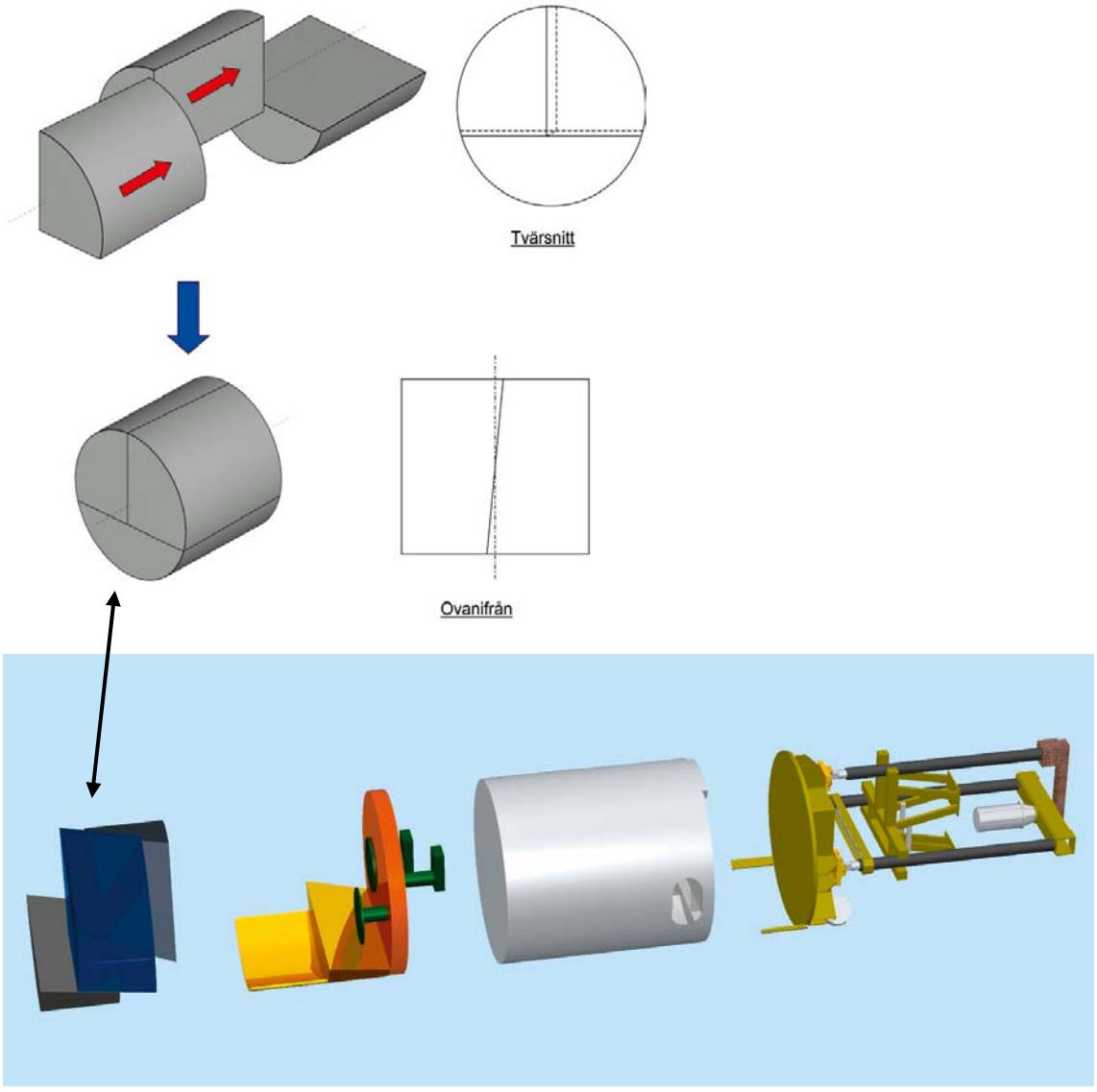

Figure 4-6. *Schematic drawing of Alternative 3 showing the divided block to the left and an example of a specially designed installation device.*

This layout has not yet been tested in any laboratory experiments. The layout is expected to cause great difficulties with regard both to the manufacture of pieces with high tolerances but also during full-scale installation in. The force needed in order to move the blocks into position could cause block breakages due to friction resistance.

Layout:

- Tight distance block; the block is divided into three parts, which means that it will be installed very tight a the rock.

4.3.5 Design Alternative 4 (block divided into one central part and an outer ring)

This design is a variation of Design Alternative 3, where a sectional block arrangement is used.

This layout has not yet been tested in any laboratory experiments. The layout is expected to cause great difficulties of the same type as for Alternative 3.

Layout:

- The same idea as proposed in Alternative 3 with tight fitting blocks, but the distance block consists of a central, somewhat conical block, with a number of outer minor fitting blocks placed in contact with the rock, see Figure 4-7. This solution means that the sealing capability of the DB is high since the block is forced into direct contact with the rock.
- It is proposed that the outer block should be 1 m thick. The distance blocks inside (upstream) of this location can result in a slot of 5 cm between the blocks and the rock, which facilitates their installation.
- The fitting blocks used to tighten the assembly will be made slightly larger than the slot and, once installed; any portion jutting out from the face of the installation will be cut off to provide a smooth face for the next stage of drift filling.

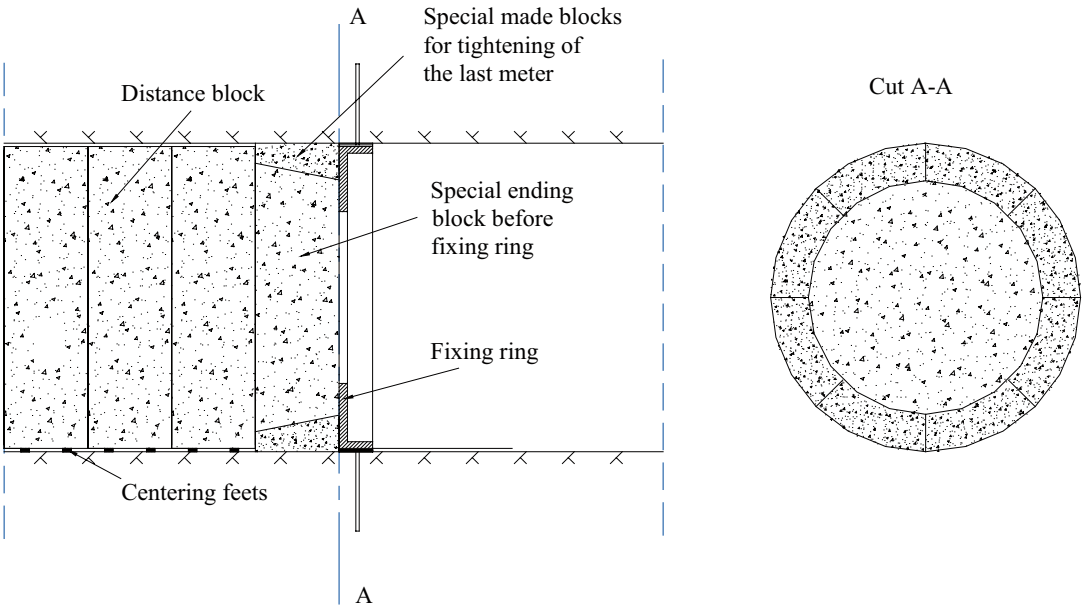

Figure 4-7. *Figure showing a schematic drawing of Layout Alternative 4.*

4.3.6 Initial conditions of distance blocks

The final density at saturation of the distance block section should be between 1,950 and 2,050 kg/m^3 (dry density 1,481–1,637 kg/m^3). The initial density of the distance blocks, before emplacement, will vary somewhat for the various designs depending on the different dimensions.

The proposed designs require blocks that result in only a small slot or no gap at all between the bentonite and the rock. The presence of a small initial gap and subsequently lower volume into which the clay must swell means that the initial density of the blocks can be somewhat lower than in BD options, where only single, massive blocks are used. In order to produce blocks of good quality, it will probably be necessary to compact them with a higher initial water ratio than would otherwise be considered (see Section 4.5).

Table 4-3 shows the dimensions and block data developed for the various design options discussed above. In Figure 4-8 the dry density of the blocks provided in Table 4-3 is plotted vs. the average density at saturation after swelling and homogenization. The range of dry density that will result in acceptable manufactured blocks is rather large. For the design option involving a single massive block where a 5 mm radial gap is present, a density range of 1,513–1,673 kg/m^3 is suitable while the split block options will require 1,481–1,637 kg/m^3 dry density in order to acquire an average density at saturation of between 1,950–2,050 kg/m^3 in the tunnel.

Table 4-3. Data used in the calculations of average block density in the distance block section of BD after swelling and saturation.

Dimensions	
Rock	
Diameter tunnel, mm	1,850
Tight distance block, 5 mm gap (Alt. 1)	
Outer diameter, mm	1,840
Tight distance block, 10 mm gap (Alt. 2)	
Outer diameter, mm	1,830
Tight distance block, split block (Alt. 3 and 4)	
Outer diameter, mm	1,850
Calculated block data	
Tight distance block, 5 mm gap (Alt. 1)	
Target average density at saturation, kg/m^3	2,000
Initial block dry density, kg/m^3	1,576
Initial block void ratio	0.771
Tight distance block, 10 mm gap (Alt. 2)	
Target average density at saturation, kg/m^3	2,000
Initial block dry density, kg/m^3	1,593
Initial block void ratio	0.752
Tight distance block, split block (Alt. 3 and 4)	
Target average density at saturation, kg/m^3	2,000
Initial block dry density, kg/m^3	1,559
Initial block void ratio	0.790

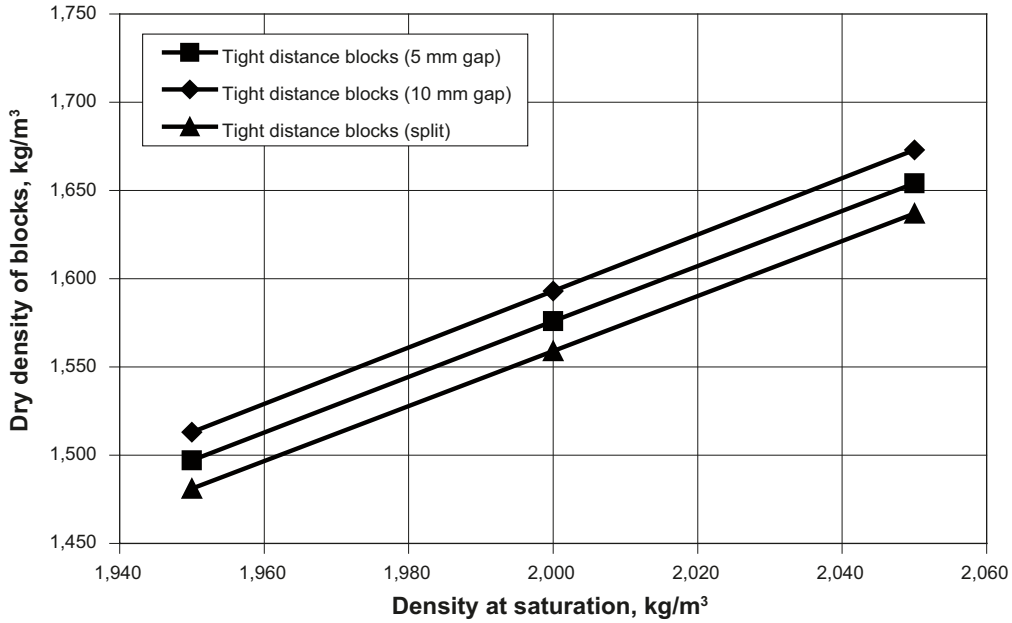

Figure 4-8. *Dry density of the blocks in the distance block section of BD plotted vs. the average density at saturation in the tunnel after swelling and homogenization.*

4.3.7 Sensitivity to variations in tunnel diameter

The required block densities are calculated using the nominal diameter of the deposition tunnel i.e. 1,850 mm. The diameter will, however, vary and this will influence the final density in the system. Figure 4-9 shows how the average bentonite density at saturation will vary with tunnel diameter. The diagram assumes an average density at saturation of 2,000 kg/m^3 at the nominal tunnel diameter (1,850 mm).

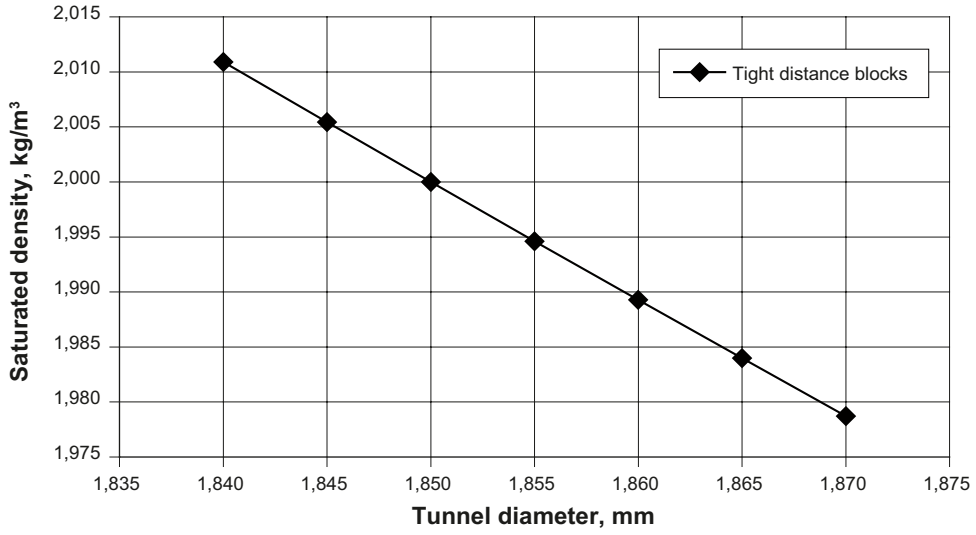

Figure 4-9. *Average density at saturation of the blocks in the distance block section of BD in the tunnel after swelling and homogenization (target density at saturation 2,000 kg/m^3 with a tunnel diameter of 1,850 mm) plotted vs. various tunnel diameters.*

4.4 Distance blocks in DAWE design

4.4.1 General

The distance blocks in the DAWE design are not intended to seal and prevent water flow between sections during the installation phase. Instead, water flow is intended to flow freely along the tunnel floor until the end plug is placed and sealed.

4.4.2 Initial conditions

The final average density at saturation of the distance blocks is between 1,950–2,050 kg/m^3 (dry density 1,481–1,637 kg/m^3). The distance blocks in the DAWE design are assumed to have the same initial diameter as the supercontainer, and would be installed directly in line with them.

Table 4-4 shows the dimensions used for the calculations and also the calculated dry density of the blocks. In Figure 4-10, the dry density of the blocks is plotted vs. the density after swelling and homogenization. The range in the dry density of the manufactured blocks that will still provide adequate saturated density is considerable. A dry density of 1,627–1,798 kg/m^3 will result in a density at saturation of between 1,950 and 2,050 kg/m^3.

Table 4-4. Dimensions used in the calculation of the dry density needed and achieved in the DAWE DB design.

Dimensions	
Rock	
Diameter tunnel, mm	1,850
Distance block	
Outer diameter, mm	1,765
Calculated block data	
Distance block DAWE	
Target average density at saturation, kg/m^3	2,000
Initial block dry density, kg/m^3	1,712
Initial block void ratio	0.629

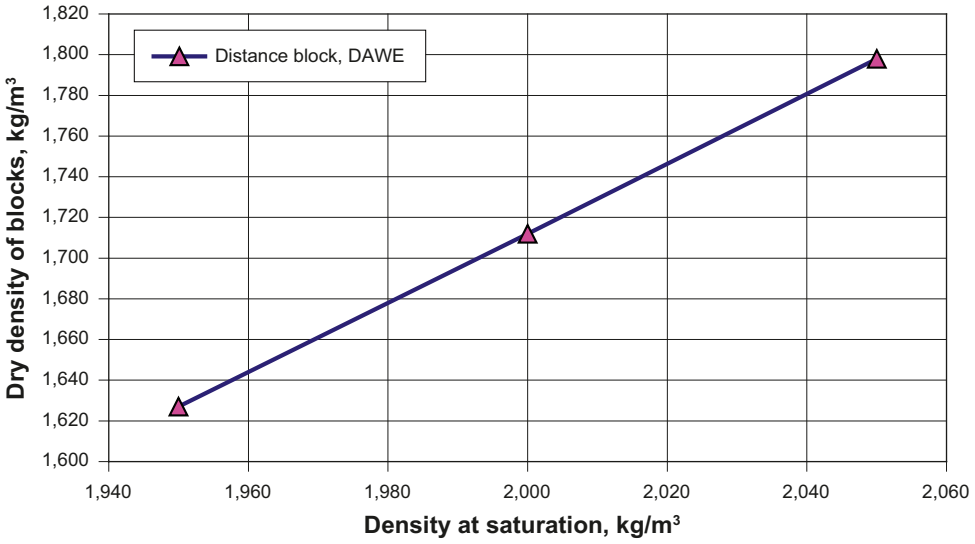

Figure 4-10. *Dry density of the DAWE distance blocks blocks plotted vs. the average density at saturation in the tunnel after swelling and homogenization.*

4.4.3 Sensitivity to variations in tunnel diameter

The required block densities are calculated using the nominal diameter of the disposal tunnel, i.e. 1,850 mm. The diameter will, however, vary and this will influence the final density in the system. Figure 4-11 shows how the average density at saturation will vary with tunnel diameter for a fixed dimension of DB. The diagram assumes an average density at saturation of 2,000 kg/m^3 at the nominal tunnel diameter (1,850 mm).

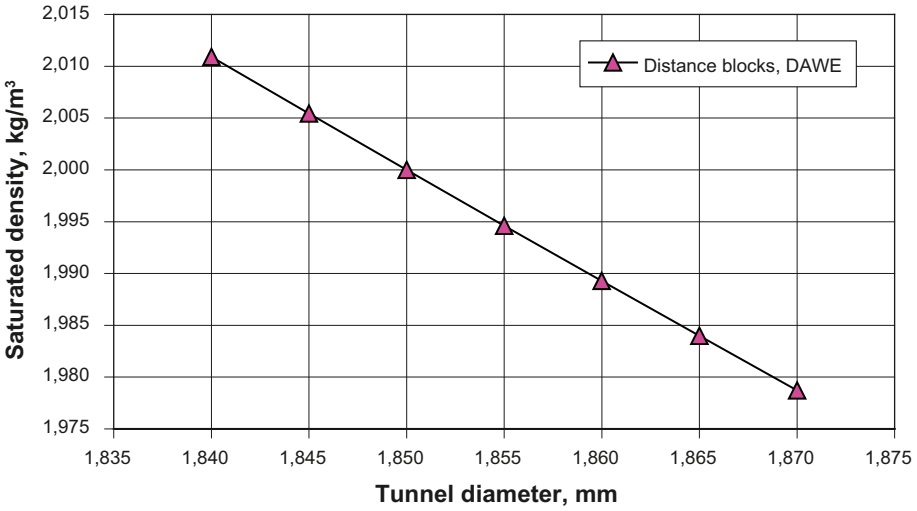

Figure 4-11. *Average density at saturation after swelling and homogenization (intended average density at saturation 2,000 kg/m^3) vs. tunnel diameter.*

4.5 Manufacture of buffer blocks

4.5.1 General

The various buffer positions and designs require bentonite blocks of different types. The blocks placed inside the supercontainer have a limited initial volume and the voids into which they are expected to swell and fill are rather large. These blocks have to be produced using bentonite with a low water ratio in order to achieve a high dry density of the blocks. In contrast, the suggested distance block designs require blocks that only result in a small slot bentonite/rock gap, which means that the initial density of the blocks can be lower while still achieving the final density of the system. In order to produce distance blocks of good quality at a lower initial dry density, it will probably be necessary to compact them with higher initial water content than that used in the supercontainer blocks. Figure 4-12 shows dry density after system equilibration vs. water ratio for different compaction pressures. The bold black line in this figure is the saturation (or zero air voids) line and hence the highest possible water ratio for a particular dry density.

Experience from the manufacture of bentonite blocks for other purposes shows that in order to obtain blocks of good quality, the compaction pressure should be at least 40 MPa and the water ratio should not exceed 26%. Lower compaction pressure could lead to problems with handling, and high water ratios create problems in connection with material handling /Johannesson et al. 1995/. Figure 4-12 shows the block density for some block types and design alternatives. The figure thus shows that the ring-shaped blocks inside the supercontainer need to be compacted at a pressure of 100 MPa and a water ratio of 10% in order to yield a sufficiently high dry density, while the large-diameter distance blocks must have a very high water ratio (~26%) in order not to have too high a density, even when compacting at a pressurte of 25 MPa. The required dry densities of the bentonite blocks for different designs and positions are shown as horizontal lines in Figure 4-12.

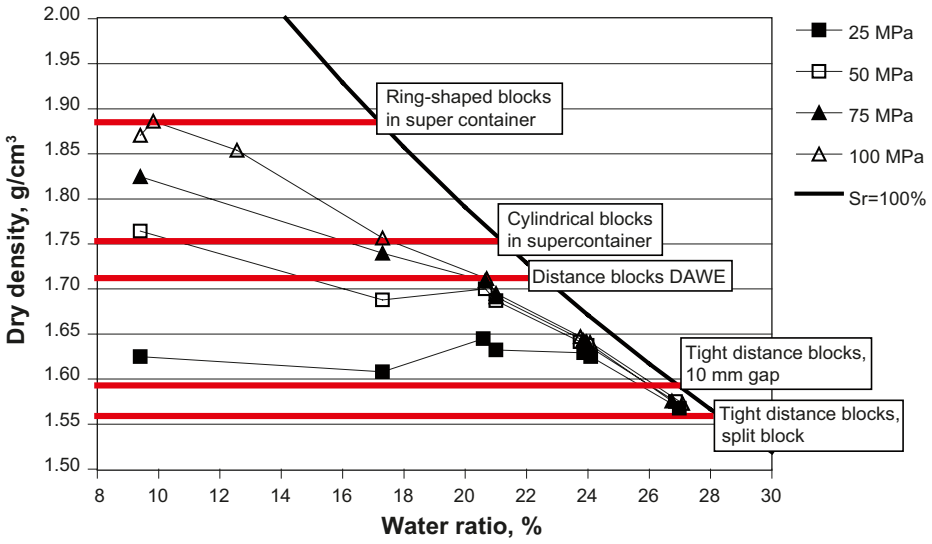

Figure 4-12. *Dry density vs. water ratio for different compaction pressures.*

5 Critical buffer issues identified

5.1 General

A number of critical design issues related to the behaviour of distance blocks have been identified in the Test Plan produced by /Autio et al. 2008a/. In this buffer test plan, issues were identified and described, and different laboratory investigations suggested. The five critical design issues associated with the buffer were identified as:

1. **Humidity-induced swelling**. The process of humidity-induced swelling and possible cracking can affect the early behaviour of distance blocks (before water saturation is achieved). This process is described in detail in Chapter 6. The magnitude of this effect depends on the design alternative selected and is evidently more significant in the case of the DAWE design. As of 2007, laboratory investigations have been undertaken and the results are presented in Chapter 6.
2. **Erosion of filling blocks and buffer**. The physical erosion of buffer, distance blocks and filling blocks will result in the transport of bentonite and, as a result, variations in the buffer density within the emplacement tunnel. Erosion may take place as a result of free–flowing water in the drift between the blocks and the rock, as channelled "piping"-type flow or as a result of flow along fractures. Since 2007, this issue has been investigated within another SKB project (Baclo), and the results of these investigations will be used in the KBS-3H project as they become available. New tests are also planned within the KBS-3H project in the years 2008 and beyond.
3. **Artificial wetting of distance blocks**. The saturation process of distance blocks has a significant impact on the sealing ability and piping resistance. The effect of wetting is different in the DAWE and BD designs. In the case of the DAWE design, artificial wetting and possible later drying and shrinkage is an important process that needs to be studied and understood. The redistribution of water within the backfill can be caused by either the thermal output of the nearby container or suction-induced water movement This aspect is also important with regard ro the issue of rock spalling (or prevention of spalling). As of 2007, laboratory investigations have been in progress, but no results are yet available.
4. **Piping through distance blocks**. In the BD design, the distance blocks are supposed to prevent water flow between supercontainer sections. The design of the distance blocks should therefore be such that no piping occurs. If piping does occur, bentonite transport may take place and if the loss of bentonite from one supercontainer section is too high, it could affect the performance of the system. Laboratory studies were completed in 2007, and the results are presented in Chapter 7
5. **Hydraulic pressure on distance block end surface**. The extent and distribution of hydraulic pressure on the inner end face of the distance blocks are important since they will affect the movement of these blocks and determine the sizing of the fixing rings in the BD design. The process associated with the development of this pressure is described in detail in Chapter 8. The main uncertainty is whether the pressure will be exerted on a narrow rim on the inner end face which is not covered by the super-container end surface or whether it is possible that the pressure will be exerted on the whole surface. Laboratory investigations have been conducted on this topic and the results are presented in Chapters 7 and 8.

5.2 Function of distance blocks

5.2.1 General

The laboratory investigations performed and described in this report mainly concern the function and behaviour of the distance blocks.

The required functions of the distance blocks are described in the KBS-3H Design description, /Autio et al. 2008a/:

1. To protect the canisters for at least 100,000 years from different Thermal, Hydrologic, Mechanical, Bacterial and Chemical (THMBC) processes and also to limit and retard the release of radionuclides from any canisters that had undetected damage.
2. To separate the canisters from each other in order to keep the temperature of the individual canisters and the overall repository at acceptable levels. The total thickness of the blocks between each supercontainer is mainly determined by the thermal conductivity of the rock and is expected to be 3–6 meters.
3. To hydraulically isolate each supercontainer section.. For the Basic Design this requirement is also valid during the installation phase.

A description of the candidate designs was provided in Chapter 3. The demands and the critical processes regarding the distance blocks are different for the two designs.

5.2.2 Critical processes investigated

The tests described in this report were performed with the following reference conditions in mind (they mostly influence the BD):

- A maximum water inflow rate of 1 l/min into the supercontainer section is required. This inflow rate will result in the empty space around the supercontainer being flooded after about 24 hours.
- After the supercontainer section has been flooded, the hydraulic pressure will start to increase at a rate of 1–5 MPa/h up to a maximum of approximately 5MPa (hydraulic head at 500 m depth). Specifics regarding rate and maximums will be site-dependant.

These conditions mean that the performance and durability demands on the blocks have increased significantly from earlier estimates where the reference conditions called for a water inflow rate that was limited to 0.1 l/min and the water pressure increased with 100 kPa/hour up to 2 MPa.

There are two critical processes related to these demands:

1. The contact between the distance block and the rock must work in combination with the fixing ring to prevent piping.
2. The force on the fixing ring caused by water pressure on the vertical surface of the distance blocks must not be too high. This is important in the sizing of the fixing ring, see also Chapter 8.

The installation period for one deposition tunnel is estimated to be 3 months, including the construction of an end plug. In the DAWE design, water will therefore be flowing along the tunnel floor for this entire period. The relative humidity in the tunnel will also be high, probably close to 100%. This will affect the bentonite blocks, which will take up water from the surrounding air.

One critical process is related to this demand:

3. The effect of high relative humidity on the distance blocks behaviour regarding swelling and cracking needs to be determined. This issue has been investigated and the results are reported in Chapter 6. In addition, a numerical modelling of the water uptake has been carried out, see Section 6.4.

Laboratory studies to evaluate the three critical processes described above were performed and the results are described in this report.

6 Humidity-induced swelling of distance blocks

6.1 Description of the issue

The buffer will absorb water from air humidity after emplacement, which may cause swelling and cracking of the buffer. Water flow in a tunnel in which the DAWE design was applied may be interfered with if pieces of bentonite fall on to the floor due to cracking or if the slot gap is reduced/closed by the swelling of bentonite. If the free flow of water is prevented or restricted, it may cause erosion of bentonite. A description of this is given by /Autio et al. 2008a/.

The water absorption of the buffer depends on the supply of water to the rock surface, the area of the supply, water transport in the air from the rock surface and the transport of moisture from the block surface into the buffer. The process of humidity-induced swelling and cracking has been studied by modelling and by experiments.

The process of humidity-induced swelling in a KBS-3H emplacement geometry (Figure 6-1) at constant temperature can be described as follows: The rock surface is wet owing to water flowing into the excavation from the rock matrix and cracks. If the relative humidity of the air in the gap between the rock surface and the bentonite block is lower than the relative humidity on the rock surface, water will evaporate to yield an increase in relative humidity. The evaporation and diffusion will take place until equilibrium in the gap is achieved. However, the water in the interior of the bentonite block is trying to reach equilibrium with the relative humidity at the surface of the bentonite. As a result, water will be absorbed from the air by the bentonite and a further increase in the evaporation and diffusion from the rock surface will result.

If the rate of the water flow in the rock to the rock surface is slower than the diffusion rate over the gap, the rock surface will dry and the relative humidity may be less than 100%. This is favourable for the buffer since the water uptake and thereby the cracking will be reduced. The condition with a slower diffusion than the water flow in the rock to the rock surface yields a relative humidity of 100% on the rock surface, which is a more critical condition for the buffer. The investigation has therefore been focused on the scenario with free water or a relative humidity of 100% being present on the rock surface. Different initial conditions of the bentonite have been studied and the experiments have been performed on different scales.

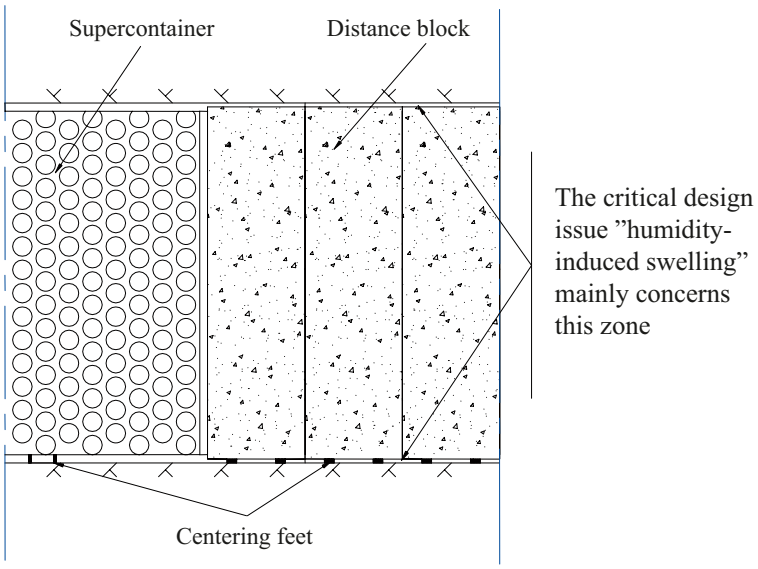

Figure 6-1. *Schematic illustration of the KBS-3H layout. The critical design issue “Humidity-induced swelling” concerns all slots in the system but especially the ones between bentonite and rock.*

Even with free water or 100% relative humidity at some distance from the buffer, the suction conditions at the surface of the buffer will not immediately come into balance with a relative humidity of 100%. The flow rate (flux) of vapour over the gap will influence the condition at the surface of the buffer, and thereby the absorption rate and swelling rate. The absorption rate and swelling rate have thus been studied by bentonite specimens placed at different gap sizes from a surface of free water.

6.1.1 Objectives

The objectives of this part of the project to evaluate critical processes were to define the water absorption rate, swelling rates and cracking of buffer surfaces with respect to time in realistic conditions, geometries and at different inflow conditions. It is important to understand this process and have a basis for modelling it. Issues for the study were to estimate:

- The influence of the initial degree of bentonite block saturation on the cracking behaviour and the water absorption rate.
- The time required for the buffer to crack sufficiently for a significant amount of buffer particles to be detached and fall to the bottom of the drift, and
- The time required for the buffer to swell sufficiently to fill the open gap between rock surfaces.

In order to investigate the block behaviour, i.e. water absorption, swelling and cracking, experiments were carried out on different scales.

6.1.2 Terminology

Water content is defined as mass of water per mass of dry substance. The dry mass is obtained from drying the wet specimen at 105°C for 24 hours.

The relative humidity is the ratio between the partial vapour pressure p and the vapour pressure at saturation p_s in %, $RH = 100 \cdot \frac{p}{p_s}$.

6.1.3 Material

The material used in the test series is MX-80 bentonite powder. MX-80 is a commercial product of sodium bentonite, produced by the Am. Coll. Co. The powder is delivered with a water ratio of about 10%. Higher water contents were achieved by adding a predetermined mass of tap water to the clay and then mixing it until a homogeneous material was produced. After powder preparation the moisture-adjusted bentonite was compacted to produce specimens at different compaction pressures.

6.2 Small-scale tests

6.2.1 General

In the small-scale tests, compacted specimens with different initial water ratios were exposed to high relative humidity. Water uptake and swelling (volume expansion) were measured continuously and the cracking of the surfaces was studied. Specimens produced using different compaction pressures (25, 50, 75 and 100 MPa), and hence having different densities, were examined. The water ratio (and by that the degree of saturation) of the specimens was varied between 10 and 25%. As a result, the initial dry density of the specimens ranged from 1.60–1.90 g/cm^3.

Three identical specimens were made for every compaction pressure and water ratio; one specimen was used for determination of the water absorption rate, one for studying the swelling/volume expansion and one was used for measurement of the initial dry density and water ratio. The test matrix required to examine all these variables is rather large, but after performing a number of initial screening tests, a limited number of tests were selected for conduct.

6.2.2 Experimental set-up

Test equipment

Determination of the water absorption rate

The compacted bentonite specimen was suspended in a tightly sealed vessel (jar) made of acrylic plastic (see Figure 6-2). The specimen was covered with a rubber membrane, leaving only one end exposed to the atmosphere within the vessel. The bottom of the vessel was filled with pure water or a salt solution of known concentration (to generate different relative humidities within the vessel). The specimen was attached to a vertical rod, which passed through the lid (Figure 6-2). This made it possible to weigh the specimen without taking it out of the jar. In order to seal off the hole when no weighing was being performed a sealing washer was mounted. The distance between the exposed bentonite surface and the water surface was kept constant during the test period. Most of the testing was performed at room temperature, but a certain number of tests were also performed in climate chambers in order to have a measure of the effects of temperature on specimen behaviour. Some of these specimens were removed from the climate chamber for the purpose of weighing.

Studying swelling/volume expansion and cracking

These tests were identical to the previous tests, but the specimens were taken out of the jar to be volumetrically measured at prescribed intervals. The specimen surfaces were also studied for cracking.

All the compacted specimens were weighed and measured with a slide caliper before and after testing. During the test period, the suspended specimens were weighed at least once a week. The specimens selected for studying volume expansion were on those occasions measured with a slide caliper. On completion of the volume change study, each specimen was divided into three slices, each of which was tested to determine water ratio and density. The density was calculated from a volume determined by weighing the specimen both above and submerged in paraffin oil. All data were recorded manually and then transferred to and stored in excel files.

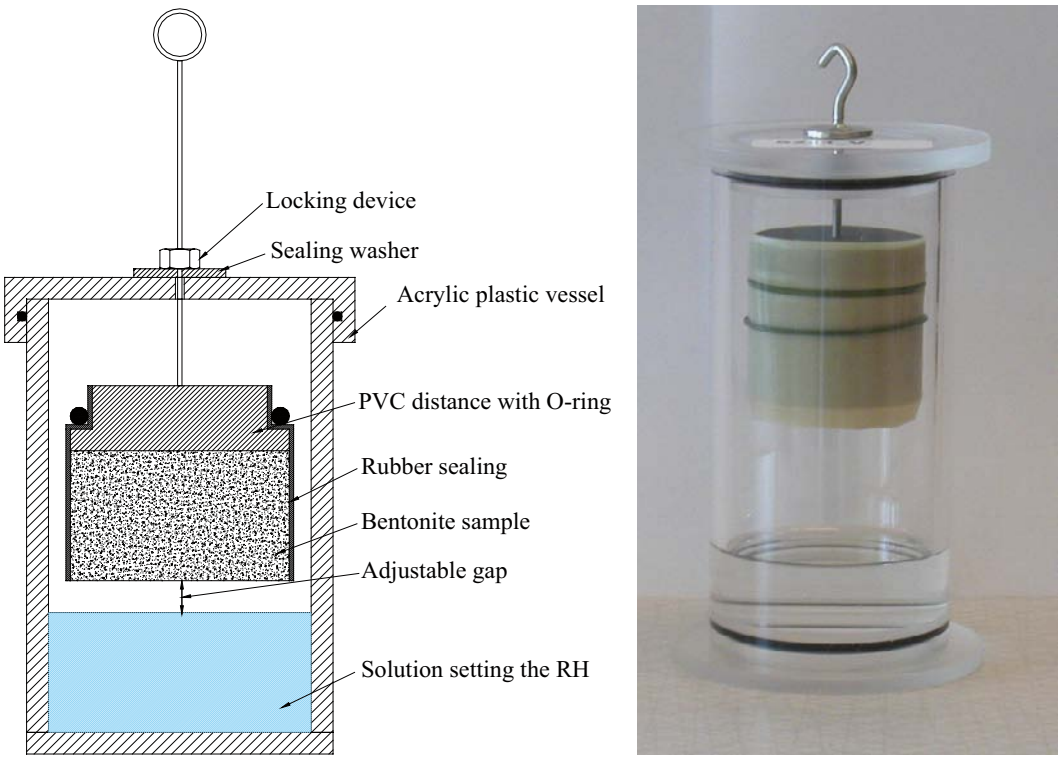

Figure 6-2. *Schematic view and a photo of the test equipment.*

Test matrix

The complete test matrix for examining compaction pressure, the initial water content of the specimens and the prescribed gap between the bentonite and water surface is shown in Table 6-1a. From this matrix a number of tests were selected with the principal focus on the most relevant parameter values, i.e. 20% water content and a gap between the bentonite and the water surface of 45 mm, which is the distance between the bentonite blocks and the rock in the DAWE design (60 mm is the anticipated gap between bentonite and rock for the blocks inside the supercontainer).

A number of additional tests were performed to check the influence of the following parameters:

1. **Influence of humidity.** All tests in the matrix were performed using pure water at the bottom of the vessel, which gives an *RH* just above the water surface of 100%. Additional tests were performed using a saturated KCl solution to produce a *RH* of about 85% just above the water surface.
2. **Influence of test temperature.** All tests shown in the matrix were performed at room temperature. In order to study the influence of the temperature, certain replicate specimens were tested at 10°C and 30°C.
3. **Influence of air movements**. It is assumed that the vapour transport rate in air is the limiting factor for the water absorption rate. In the test series, air movements inside the vessel that could serve to increase the vapour transport rate were avoided. In order to check the sensitivity to such effects, a certain number of additional tests were performed at the same conditions, but with a magnetic stirrer in the water to induce water and hence air movement.

The additional tests that examined changes in temperature or relative humidity are shown in Table 6-1b. They were performed on specimens with the same initial conditions as specimen S222. In addition to the factors mentioned above, the influence of preventing radial swelling and of a 20 mm gap size were also tested.

In the figures the specimens used to examine volume expansion have labels ending with _V, cf. S222_V.

Table 6-1a. Table showing the test matrix for the small-scale tests (tests actually performed shown as shaded boxes).

Humidity-induced swelling – test matrix for the small-scale tests												
w initial %	Compaction pressure											
	25 MPa			50 MPa			75 MPa			100 MPa		
	Gap bentonite/water			Gap bentonite/water			Gap bentonite/water			Gap bentonite/water		
	10 mm	45 mm	60 mm	10 mm	45 mm	60 mm	10 mm	45 mm	60 mm	10 mm	45 mm	60 mm
10	S110	S120	S130	S210	S220	S230	S310	S320	S330	S410	S420	S430
15	S111	S121	S131	S211	S221	S231	S311	S321	S331	S411	S421	S431
20	S112	S122	S132	S212	S222	S232	S312	S322	S332	S412	S422	S432
22	S113	S123	S133	S213	S223	S233	S313	S323	S333	S413	S423	S433
24	S114	S124	S134	S214	S224	S234	S314	S324	S334	S414	S424	S434

Table 6-1b. Table showing additional small-scale tests.

Humidity-induced swelling – test matrix for the small-scale tests						
w initial %	Additional tests starting from sample S222					
	RH = 85%	T = 10 degC	T = 30 degC	Air movement	Gap 20 mm	No radial swelling
20	S222_H	S222_T10	S222_T30	S222_A	S222_g20	S222_Dr0

Preparation

Powder with the prescribed water content was compacted at the prescribed compaction pressures in accordance with the matrix provided in Table 6-1a. The compacted specimens had diameters of 5 cm and were cut to a height of 3 cm. With few exceptions the specimens were suspended with the cut side upwards and the uncut side towards the water surface in the equipment shown in Figure 6-2.

6.2.3 Test results

All results are compared to the normal/reference specimen and base case represented by specimen S222 that is shown in all diagrams. This specimen has an initial water content of 20%, a compaction pressure of 50 MPa, a gap of 45 mm between the bentonite and water surface and the specimen was installed at room temperature (~ 20°C). In the plots of the data produced, the legends for most of the specimens contain information about the compaction pressure, the size of the gap and the initial water content, respectively. In all plots, the colours (purple, green, red, light blue, dark blue) denote the initial water contents (10%, 15%, 20%, 22%, 24%) and the shapes of the marks (x, ♦, ■ ,▲) denote the compaction pressures (25, 50, 75, 100 MPa). The tests listed in Table 6-1a–b were performed two or more times, but in the plots of the data only one of the tests is shown to make the results clearer. The results of all tests are presented in Appendix A.

Table 6-2 and Table 6-3 contain the initial and final water content and density respectively for all specimens. The tests were conducted for approximately 2,000 hours or 84 days each, and the specimens are not assumed to have reached steady state or equilibrium.

Water absorption

The absorption of water was investigated in terms of increase in mass. The initial value m_0 used in the figures is the mass determined directly after compaction and measured above the balance. After that, the mass, m_i was measured below the balance as shown in Figure 6-2. The following factors were found to have the greatest influence on the water uptake:

- The initial water content, illustrated in Figure 6-3.
- The size of the gap, illustrated in Figure 6-4.
- The temperature, illustrated in Figure 6-5.

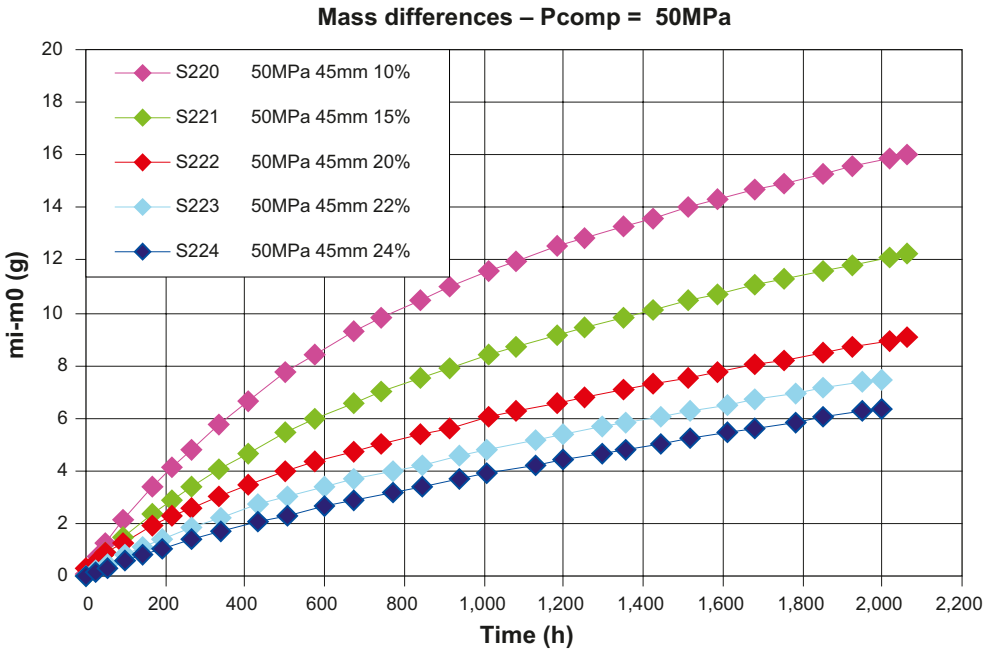

Figure 6-3. *Water absorption as a function of time examining influence of initial water content. (All specimens were compacted at 50 MPa).*

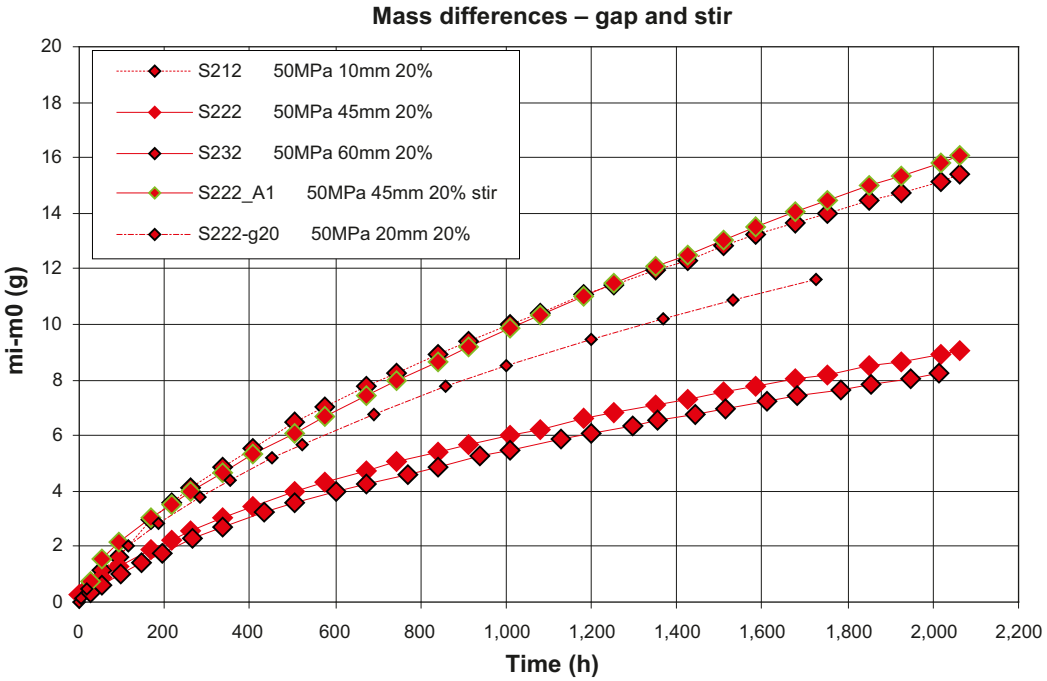

Figure 6-4. *Water absorption as a function of time examining influence of size of the gap between the water surface and the specimen. Also shown are results for specimens placed in jars with air movement (_A) induced. (All specimens were compacted at 50 MPa with an initial water content of 20%).*

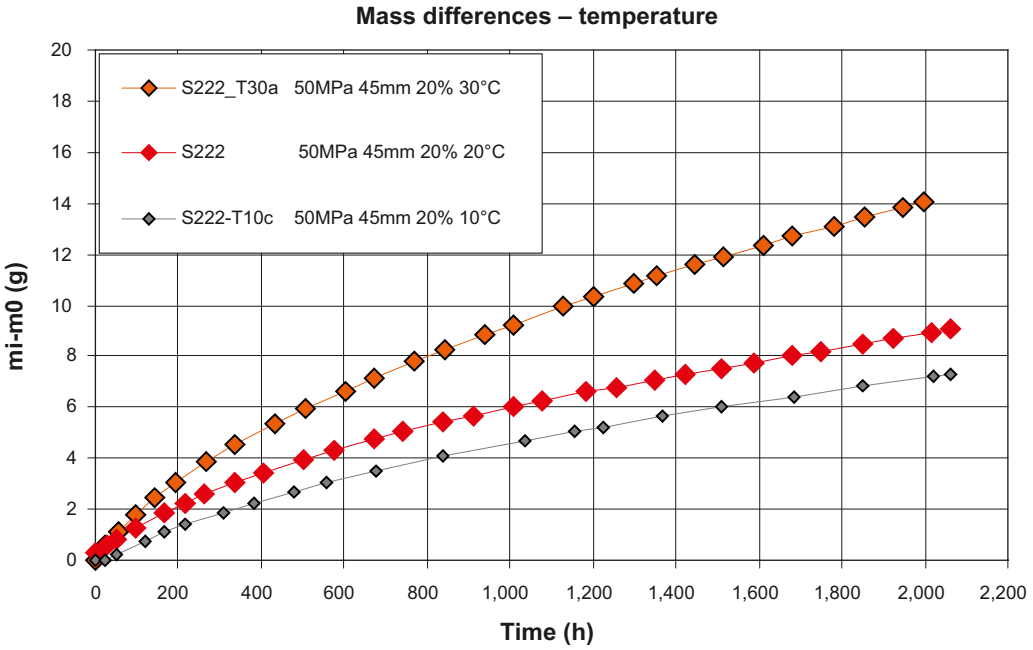

Figure 6-5. *Water absorption as a function of time showing the influence of temperature. (All specimens were compacted at 50 MPa with an initial water content of 20%).*

According to Figure 6-3, the water absorption rate is higher the lower the initial water content is. Figure 6-4 shows the influence of the size of the gap between the specimen and the water surface. The specimens placed 10 mm from the water surface and the specimens placed 45 mm from the surface with air movement show the largest and almost the same water uptake. Specimens placed 20 mm from the water surface show a water absorption rate between the specimen placed 10 mm and the base case representing a gap size of 45 mm. The absorption from specimens with a gap size of 60 mm is almost the same as the absorption from the specimen placed 45 mm from the water surface.

The influence of temperature is shown in Figure 6-5. A first attempt to investigate the influence of low temperature (10°C) was made by placing the jars in cold boxes, S222_T10a and S222_T10b. The specimens were taken out of the boxes and weighed at a temperature of 20°C, which caused visible condensation on the membranes covering the specimens and on the bottom surface of the specimens, see Appendix A6. The results of those specimens are not shown in Figure 6-5. New specimens were placed in a climate room with temperature control, S222-10c and S222-10d. In this case, the balance was placed inside the climate room and the specimens were not exposed to any temperature change during weighing. Specimens exposed to 30°C were taken out of the climate chamber and weighed at 20°C. This may have induced a small error in the absorption of these specimens, but no water droplets were visible on their surface.

Regarding the effect of compaction pressure used on the water absorption characteristics of the specimens, only a small influence was seen where water contents less than 20% were present, and at higher water contents almost no influence at all was observed, see Table 6-2. The influence of preventing radial swelling of specimen behaviour was also investigated. These specimens started with the same initial conditions as for the reference specimen, S222. The water absorption observed for a specimen prevented from swelling radially was almost the same as from specimen S222. This means that preventing radial swelling had no effect on the total amount of water absorbed.

The absorption rate is calculated from the tangent of the time curves. The absorption rates for specimens compacted at 50 MPa but with different initial water contents are shown in Figure 6-6.

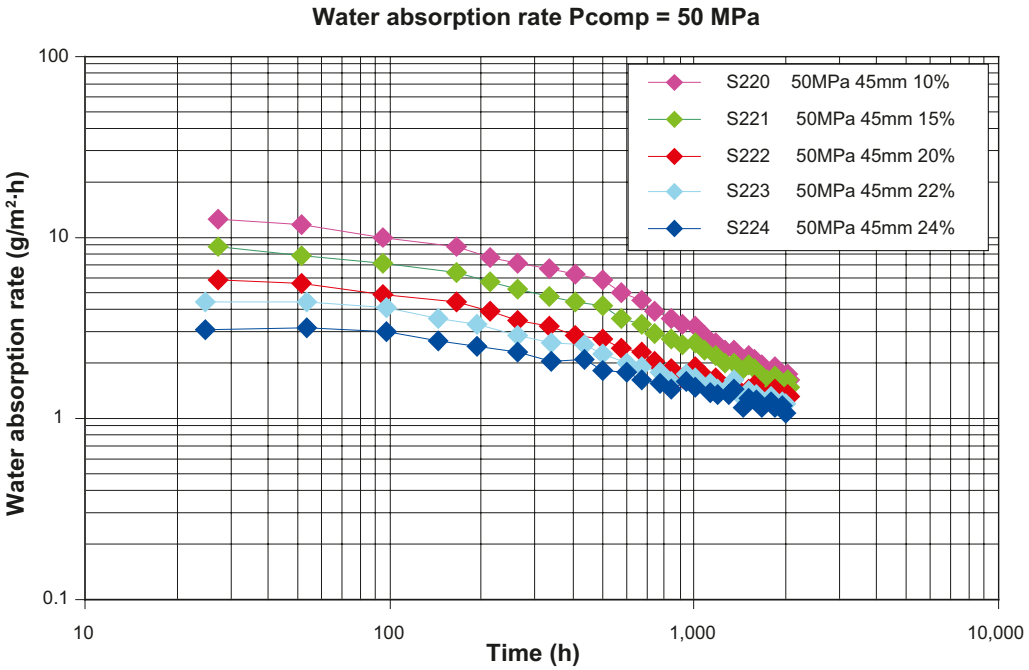

Figure 6-6. *Absorption rate evaluated from the results shown in Figure 6-3.*

In Table 6-2, the initial and final water contents for all specimens are shown and in Figure 6-7 the initial and final water contents of the main part of the specimens are shown. Since each specimen was divided into three slices, each specimen has values associated with the upper, middle and lower portions of the specimen. Both initial and final values are shown. The initial values were measured on duplicate specimens made only for the determination of initial values of water content and density.

The number of tests performed is shown in Table 6-2 and the values provided represent the average of the number of replicates performed. If the number of tests is zero, this means that the initial value is based on the reference condition (specimen S222). Two lines with S222_T10 are shown in Table 6-2; the results of the first one were not used in subsequent analyses due to problems with condensation on the specimen surface. The results of these tests were replaced by those from a second series, presented later in this table. Initial and final conditions for each specimen are shown in Appendix A1. The absorption vs. time for all tests is shown in Appendix A2.

Each specimen started with an almost homogeneous water content distribution but showed a gradient in water content at test termination. This pattern can be seen in Figure 6-7, where the three columns representing the initial water contents of each specimen have almost the same height while the columns representing the final water contents of each specimen differ slightly.

For some of the specimens placed near the water surface, S212, a dark area was seen on their lower surface, probably from water droplets. Additional trials were performed in order to check this, but droplets were not seen on these replicates.

Table 6-2. Initial and final water contents for all specimens.

Water content (%)	Initial			Number of tests	Final			Number of tests
	Upper	Middle	Lower		Upper	Middle	Lower	
S210	10.3	10.5	10.4	1	31.1	31.9	33.6	1
S122	19.5	19.5	19.5	1	27.1	27.0	27.9	2
S124	23.8	23.7	23.6	1	28.9	29.3	29.1	2
S212	19.6	19.6	19.5	1	33.7	34.4	36.1	3*
S220	10.5	10.6	10.5	1	24.8	25.2	26.1	2
S221	15.1	14.9	15.0	1	25.7	26.2	27.0	2
S222	19.4	19.5	19.5	2	27.5	28.0	28.6	3
S223	21.7	21.9	21.9	1	28.1	28.5	29.1	2
S224	23.8	23.8	23.7	1	29.0	29.3	29.9	2
S232	19.5	19.5	19.5	1	26.8	27.1	27.7	3
S322	19.6	19.6	19.4	2	27.5	27.9	28.6	3
S323	21.8	21.8	21.7	2	28.4	28.8	29.4	3
S420	10.5	10.5	10.5	1	24.8	25.4	26.3	2
S421	16.6	15.0	15.1	1	26.1	26.5	27.2	2
S422	19.6	19.6	19.5	2	27.7	28.2	28.8	3
S222_H	19.4	19.4	19.4	0	20.3	20.3	20.3	4
S222_A	19.4	19.4	19.4	0	33.7	34.4	35.6	4
S222_T10	19.4	19.4	19.4	0	34.6	36.0	38.5	4**
S222_T30	19.4	19.4	19.4	0	31.9	32.5	33.2	4
S222_T10	19.5	19.5	19.6	0	26.3	26.9	27.7	4
S222_Dr0	19.5	19.5	19.6	0	27.1	27.7	28.6	2
S222_g20	19.5	19.5	19.6	0	30.9	31.5	32.4	2

*The final water content of the lower segment is presented as an average and includes large spread.
** Erroneous tests, commented on in the text, performed in cold boxes.

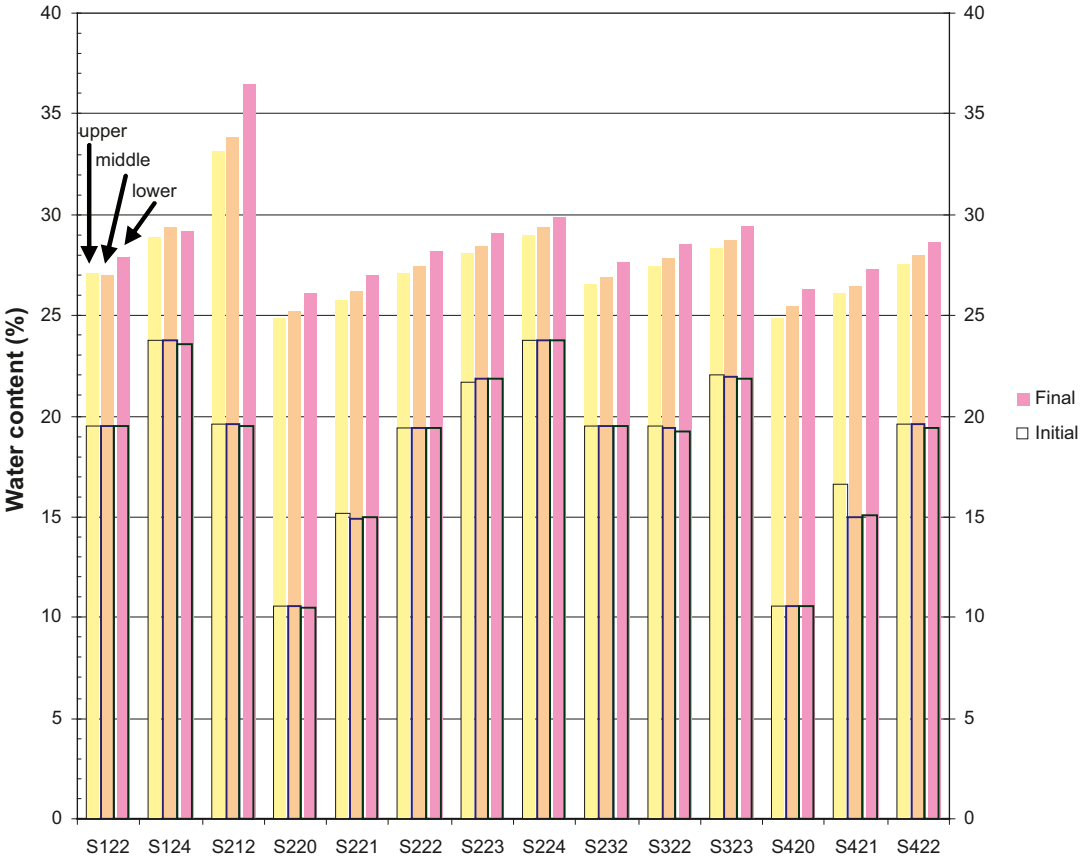

Figure 6-7. *Initial and final water content of specimens from Table 6-1a.*

The water contents shown in Table 6-2 and Figure 6-7 were measured. The water content can also be calculated w_{calc} from the initial water content w_i and the increase in mass Δm during the testing time according to Equation 6-1.

$$w_{calc} = w_i + \frac{\Delta m}{m_s} \qquad (6\text{-}1)$$

The last two columns of Appendix A1 show the water contents calculated from Equation 6-1, w(Δm), and the deviation from the average of the measured water contents, w(Δm)-w(average). For the majority of the specimens the measured water content is lower than the water content calculated from Equation 6-1. For some of the specimens the difference is as much as 1.2%. The difference can be explained by evaporation during dismantling and by water uptake in the equipment.

Swelling/volume expansion

The greatest effects on the swelling observed were associated with the initial water content, the size of the gap to the water surface and the temperature. The increase in specimen height is shown in Figure 6-8 to Figure 6-10.

The results shown in Figure 6-8 follow the same pattern as for the water absorption behaviour shown in Figure 6-3, i.e. the lower initial water content the larger absorption and the greater the increase in height. Figure 6-9 shows the influence of gap size. The results indicate that gaps of 60 mm and 45 mm between the specimen and the water surface yield approximately the same increase in height with time, which is in accordance with the absorption results shown in Figure 6-4.

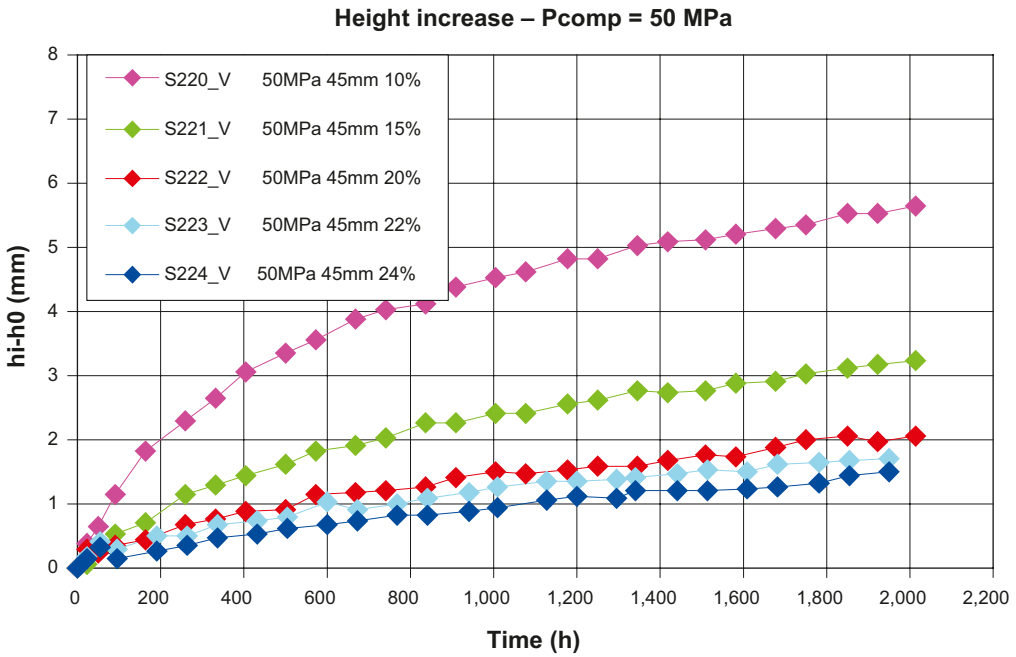

Figure 6-8. *Increase in specimen height as a function of time showing influence of initial water content. (All specimens were compacted at 50 MPa).*

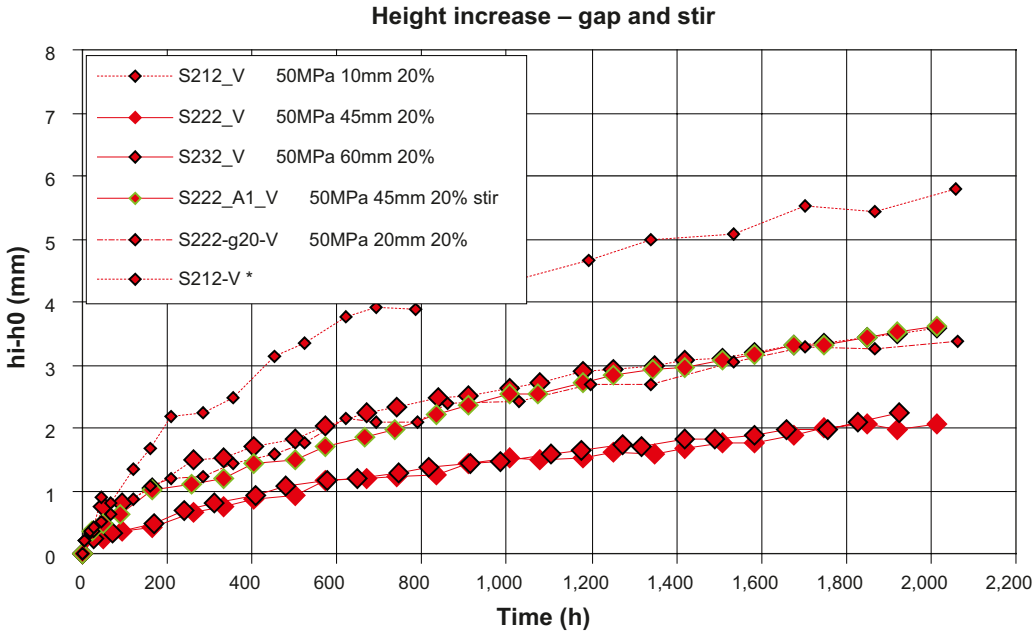

Figure 6-9. *Increase in specimen height as a function of time showing the influence of the gap between the water surface and the specimen. Also shown are specimens placed in jars with air movement (_A1_V). (All specimens were compacted at 50 MPa with an initial water content of 20%.)*

Figure 6-9 shows that the two specimens representing a gap size of 10 mm (S212) do not exhibit the same volume change. The final increase in height of the specimens was 3.5 mm and 5.8 mm respectively. A total of three specimens were placed 10 mm from the water surface. All three showed the same absorption as shown in Figure 6-4. The height and diameter of two of the specimens were measured during testing. The measured rate of increase in diameter was the same for both, but the increase in height was different (see Figure 6-9, specimen S212-V*). At the end of testing, all specimens were dismantled and their height and diameter measured. From the initial height and diameter information, a new value for the final increase in height and diameter were calculated. For all specimens the difference between the two evaluated increases in height was about ± 0.6 mm except for specimen S212-V*. For this specimen, the final increase in height was 5.8 mm (Figure 6-9), while the corresponding value from initial and final measurements was 3.5 mm which gives a difference between the two evaluations of 2.3 mm. The most probable explanation for this difference is an undetected measurement error in the height of S212-V*.

According to Figure 6-9, there is no difference between specimens placed 20 mm and those placed 45 mm from the surface when air movement occurs. If test S212-V* is not included in the data assessment, the same increase is also seen in the specimen placed 10 mm from the water surface.

Figure 6-10 shows the influence of temperature on humidity-induced swelling. Approximately the same increase in height was seen for specimens placed at 20°C and 10°C, while those placed at 30°C showed a greater increase in height. The first series of specimens placed at 10°C experienced water condensation on their surfaces, (as described previously), and so are not plotted in Figure 6-10.

Table 6-3 shows the initial and final densities for all specimens. Since each specimen was divided into three slices, each specimen has values representing the upper, the middle and their lower regions. Both initial and final values are shown. The initial values were measured on duplicate specimens made only for determining the initial water content and density values. Figure 6-11 shows the initial and final densities of some of the specimens.

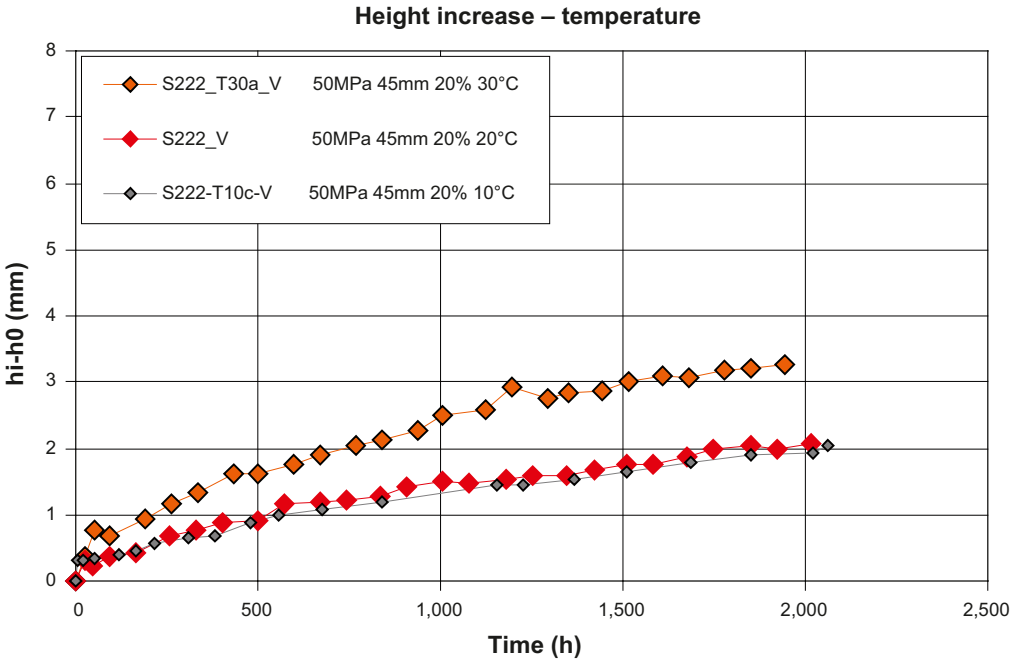

Figure 6-10. *Increase in specimen height as a function of time showing the influence of temperature. (All specimens were compacted at 50 MPa with an initial water content of 20%).*

Table 6-3. Initial and final densities for all specimens.

Density kg/m^3	Initial			Number of tests	Final			Number of tests
	Upper	Middle	Lower		Upper	Middle	Lower	
S210	1,923	1,969	1,995	1	1,585	1,542	1,569	1
S122	1,952	1,976	1,982	1	1,859	1,857	1,860	2
S124	2,019	2,026	2,025	1	1,933	1,934	1,922	2
S212	2,050	2,064	2,072	1	1,833	1,833	1,818	3
S220	1,927	1,965	1,993	1	1,665	1,660	1,661	2
S221	2,005	2,024	2,036	1	1,808	1,822	1,809	2
S222	2,065	2,069	2,074	2	1,922	1,923	1,912	3
S223	2,068	2,070	2,065	1	1,955	1,951	1,937	2
S224	2,045	2,047	2,047	1	1,960	1,956	1,943	2
S232	2,066	2,077	2,080	1	1,934	1,936	1,926	3
S322	2,014	2,096	2,097	2*	1,944	1,941	1,924	3
S323	2,073	2,073	2,074	2	1,953	1,949	1,938	3
S420	2,087	2,113	2,128	1	1,736	1,738	1,734	2
S421	2,152	2,150	2,135	1	1,887	1,875	1,851	2
S422	2,098	2,102	2,101	2	1,946	1,942	1,925	3
S222_H	2,062	2,075	2,083	0	2,023	2,034	2,038	4
S222_A	2,062	2,075	2,083	0	1,827	1,822	1,808	4
S222_T10	2,062	2,075	2,083	0	1,819	1,807	1,773	4**
S222_T30	2,062	2,075	2,083	0	1,850	1,848	1,832	4
S222_T10	2,069	2,063	2,065	0	1,946	1,947	1,936	4
S222_Dr0	2,069	2,063	2,065	0	1,949	1,943	1,913	2
S222_g20	2,069	2,063	2,065	0	1,875	1,873	1,859	2

* The initial density of the upper part is probably not correct.
** Erroneous tests, commented on in the text, performed in cold boxes.

The number of tests performed on each specimen is shown in Table 6-3 and the values represent the average of replications. If the number of tests is zero, this means that the initial value for the reference specimen S222 has been used. Two lines with S222_T10 are shown in Table 6-3, which are the same as in Table 6-2. Initial and final conditions for each specimen are shown in Appendix A1. The increase in height and diameter vs. time for all specimens are illustrated in Appendix A3 and Appendix A4.

Each specimen started with a gradient in density over the specimen and at termination the gradient was lower but in almost all specimens the region nearest the water had a markedly lower density. This can be seen in Figure 6-11 where the three columns representing the initial densities of each specimen differ within each specimen, while the columns representing the final density of each specimen differ less in height in almost all specimens.

Cracking

The cracking observed at the time of test termination is summarised in Table 6-4a and b, and Figure 6-12 shows examples of this feature. Different shadings in Table 6-4 a,b denote the type of the observed cracking (circumferential cracking and cracking on the surface closest to the water, only circumferential cracking, only circumferential cracking if any, no observed cracking). The light blue (only circumferential cracking if any) represents ambiguous results from the two or three tests conducted with the same conditions. Photos of the specimens listed in Table 6-4 (with the exception of S122, S124, S223 and S224), are provided in Appendix A5.

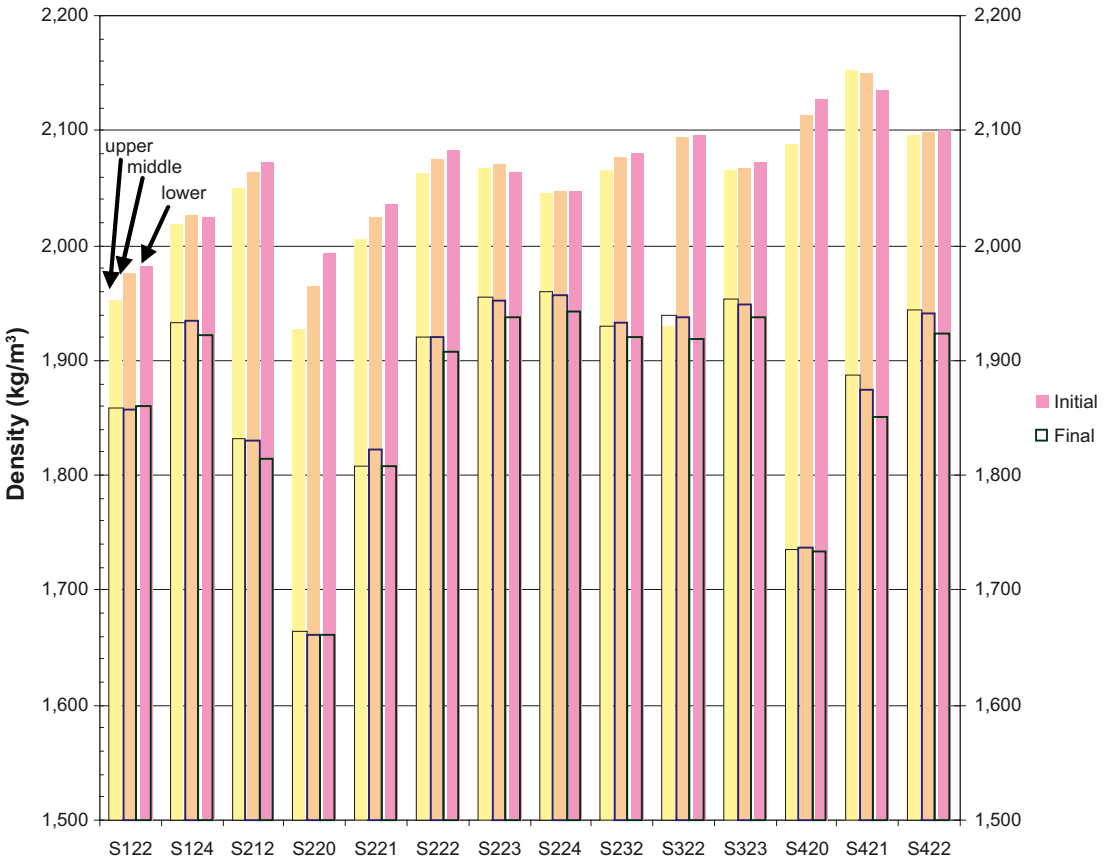

Figure 6-11. *Initial and final density of specimens listed in Table 6-1a.*

Table 6-4a Cracking observed at the end of testing. (The colours show the type of cracking from red (cracking all over the specimen) to pink, light-blue and dark-blue (no cracking observed.)

Humidity-induced swelling – test matrix for the small-scale tests														
w-initial %	Compaction pressure													
	25 MPa			50 MPa			75 MPa			100 MPa		
	Gap bentonite/water			Gap bentonite/water			Gap bentonite/water			Gap bentonite/water		
	10 mm	45 mm	60 mm	10 mm	45 mm	60 mm	10 mm	45 mm	60 mm	10 mm	45 mm	60 mm
10				S210	S220						S420	
15					S221						S421	
20		S122		S212	S222	S232		S322			S422	
22					S223			S323				
24		S124			S224							

Table 6-4b. Cracking observed at test termination on the additional specimens. (Colour coding as per Table 6-4a.)

Humidity-induced swelling – test matrix for the small-scale tests						
w initial %	Additional tests starting from sample S222					
	RH = 85%	T = 10 degC	T = 30 degC	Air movement	Gap 20 mm	No radial swelling
20	S222_H	S222_T10	S222_T30	S222_A	S222_g20	S222_Dr0

Figure 6-12. *Examples of cracking classified as red (S420), pink (S421 and light-blue (S422_V).*

Cracking was most marked on specimens starting with a low water content, and no cracking was observed on those having the highest initial water content. Of the additional tests listed in Table 6-1b, only circumferential cracking was observed, if any at all.

In addition to the observations at test termination, the following features were observed on individual specimens during the test period:

- S210: lost a small amount of material after 25 days.
- S232: a crack was observed after 13 days.
- S420: a large crack was observed after 24 days.
- On two of three types of S212 specimens, droplets were observed on the end of the specimens closest to the water (as previously described). On these specimens, cracking was observed in the dark coloured areas on the lower surface.

These individual specimen observations are provided in Appendix A6.

Uncertainties

Some of the tests for which three replicates were produced were used for an evaluation of the accuracy in the measurements. The selected specimens were S222 and S422. The accuracy was calculated as the maximum difference from the average.

Table 6-5. Average and accuracy for water contents w_f and densities ρ_f from some of the specimens for which three replicates were produced.

Specimen	Variable	Average	Accuracy
S222	Initial water content w_i (%)	19.5	±0.2
	Final water content w_f (%)	28.0	±1.1
	Initial density ρ_i (kg/m^3)	2,070	±14
	Final density ρ_f (kg/m^3)	1,919	±14
S422	Initial water content w_i (%)	19.6	±0.1
	Final water content w_f (%)	28.3	±0.8
	Initial density ρ_i (kg/m^3)	2,100	±5
	Final density ρ_f (kg/m^3)	1,938	±17

Regarding evaluation of the accuracy in the measured absorption and swelling vs. time, the calculated final values w_{calc} (according to Equation 6-1) and ρ_{calc} (according to Equation 6-2) for tests made three times were compared.

$$\rho_{calc} = \frac{m_i + \Delta m}{(h_i + \Delta d) \cdot (d_i + \Delta d)^2 \pi} \tag{6-2}$$

In Equation 6-2 m_i, h_i and d_i are the initial mass, height and diameter respectively, measured directly on the compacted specimen. Δm, Δh and Δd are the increases in mass, height and diameter respectively, measured during the test using the equipment shown in Figure 6-2. The height and diameter were measured with a slide caliper.

Table 6-6. Average and accuracy for w_{calc} and ρ_{calc}. Also shown are the deviations from the w_f and ρ_f in Table 6-5.

Specimen	Variable	Average	Accuracy	Deviation[1]
S222	w_{calc} (Equation 6-1) (%)	28.5	0.4	0.5
	ρ_{calc} (Equation 6-2) (kg/m^3)	1,877	19	–42
S422	w_{calc} (Equation 6-1) (%)	28.7	0.2	0.4
	ρ_{calc} (Equation 6-2) (kg/m^3)	1,890	19	–48

[1] Deviation from Table 6-5: ($w_{calc} – w_f$) and ($\rho_{calc} – \rho_f$).

Using the information in Table 6-5 and Table 6-6, the final water content for S222 is 28 ± 1.1% whereas the value calculated using Equation 6-1 is 28.5 ± 0.4%. The corresponding values for the final density of S222 are 1,919 ± 14 kg/m^3 determined using the paraffin oil submerging method and 1,877 ± 19 kg/m^3 from measurements taken using a slide caliper and the use of Equation 6-2.

6.2.4 Discussion of results from the small-scale tests

All of the tests identified for use in conducting the test plan have been carried out. The following observations and conclusions have been made so far:

Absorption

- The lower the initial water content, the higher the absorption rate.
- The smaller the size of the gap between the specimen and the water surface, the higher the absorption rate.
- Air movement increases the absorption rate.
- The higher the temperature, the higher the absorption rate.
- Limited influence of initial density on results.
- After 3 months, the water content difference across the specimen was less than 3% across the initially 3 cm-high specimens.

Swelling

- The lower the initial water content, the higher the swelling rate.
- The smaller size of the gap between the specimen and the water surface, the higher swelling rate.
- Air movement increases the swelling rate.
- The higher the temperature, the larger the swelling rate.
- A certain influence of the initial density was found at initial water contents of 10% and 15%. Limited influence for higher initial water contents.
- After 3 months, the density difference was less than 50 kg/m^3 along the initially 3 cm-high specimens.

Cracking

- After 3 months, cracking was most marked on specimens with low initial water content.
- After 3 months, no cracking was observed on specimens with the highest initial water content.
- Only specimens with an initial water content of 10% showed cracking on the surface next to the water surface. One of them lost a small amount of material.

Uncertainties

- The difference between the final water contents determined from oven drying and the final water contents determined from the initial water content and the increase in mass was less than 1.2%.
- The accuracy in the measured final water content is about ± 1.1% determined from selected specimens.
- The accuracy in the measured final density is about ± 17 kg/m^3 determined from selected specimens.
- A small absorption of water in the equipment took place during the testing time.
- Some of the specimens had water droplets on their surface adjacent to the water surface. The most probable explanation for this is that water had splashed on to the specimen during the movement of the jar.

6.3 Medium-scale tests

6.3.1 General

As a supplement to the small-scale tests described in Section 6.2, an additional test series was performed on a larger scale. Blocks with a diameter of 280 mm and a height of 100 mm were compacted with different water ratios (13%, 15%, 20%, 24%) and compaction pressure (50, 100 MPa). The blocks were placed in specially-made vessels in which the distance from the outer block surface to the wall was set at a prescribed value (10, 45, 60 mm). In the majority of the tests, the wall in the vessels – simulating the rock – was kept wet in order to simulate a real worst case according to Section 6.1.

6.3.2 Experimental set-up

Test equipment

A schematic view of the test equipment is shown in Figure 6-13. The bentonite block had a predefined gap between the outer block surface and the inner wall of the vessel. The ends of the blocks were covered with rubber mats and the outer periphery surface was exposed to a high relative humidity. The side wall was covered with a filter that was kept wet by circulating water through four inlets and four outlets. The filter was made of paper and so the water spread along the entire filter surface which meant that the whole “rock” surface was kept wet. The equipment operated at room temperature.

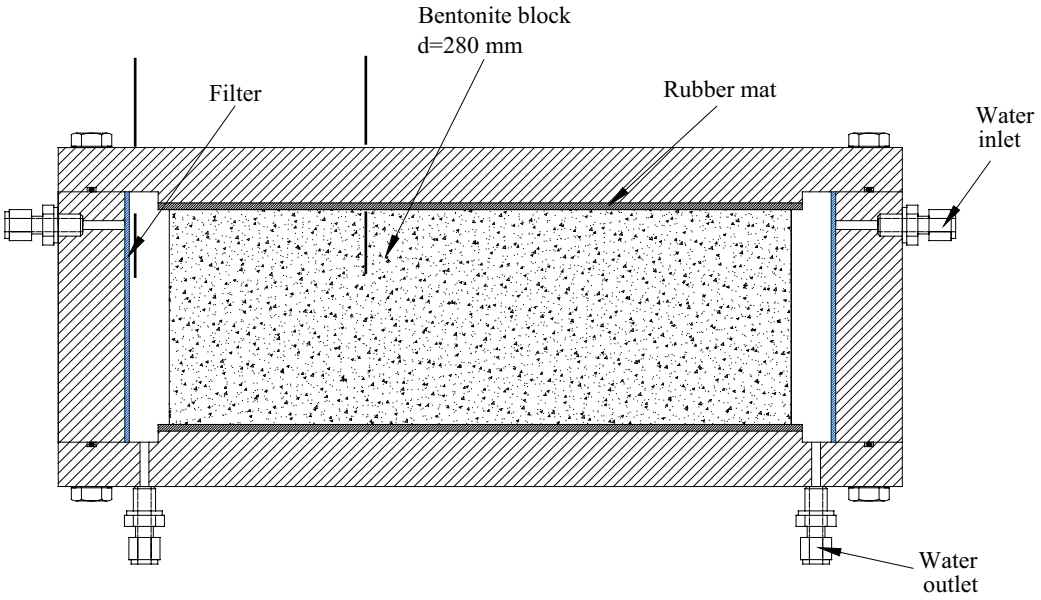

Figure 6-13. *Schematic view of the test equipment.*

The ring-shaped blocks were taken out at regular intervals in order to be weighed, measured and inspected to determine the occurrence of cracks on the surface. In order to facilitate the inspections, the vessels were placed in a special frame in which the lids could be easily locked or removed (Figure 6-14).

Test matrix

Table 6-7 shows the complete test matrix. The shaded boxes mark the tests that have been completed. All blocks/specimens were compacted at a pressure of 100 MPa except for the specimen with the highest water ratio, M153, which was compacted at 50 MPa. At high water ratios there is no advantage in having a higher compaction pressure (Figure 4-12) because the final block density will be the same and the higher pressure only makes the manufacture more difficult. Three tests, M150, M152

Figure 6-14. *Photo showing three of the test vessels after emplacement in the frame.*

Table 6-7. Test matrix for the medium-scale tests. The red-shaded boxes mark the tests performed.

Humidity-induced swelling – test matrix for the medium-scale tests						
w initial %	RH 85% Gap bentonite/water			RH 100% Gap bentonite/water		
	10 mm	45 mm	60 mm	10 mm	45 mm	60 mm
13	M110	M120	M130	M140	M150	M160
15	M111	M121	M131	M141	M151	M161
20	M112	M122	M132	M142	M152	M162
24	M113	M123	M133	M143	M153	M163

and M153, were performed with the same gap to the rock (45 mm) and with the same relative humidity (100%), but with different initial water ratios (13, 20 and 24%). Two tests, M142 and M162, were carried out in order to study the influence of the slot width (10 and 60 mm respectively) and one test, M120, was done to study the influence of relative humidity (85%) in the slot.

6.3.3 Test results

Water uptake and swelling

The water absorption from the initial state is shown in Figure 6-15 and Figure 6-16. Figure 6-15 shows the weight increase during the first 30 hours of the tests. Two of the tests, M120 (w_{ini}=13%, RH=85%) and M150 (w_{ini}=13%, RH=100%), were terminated after 8 and 24 hours respectively, due to very strong cracking which made it impossible to continue the measurements, see Figure 6-18. The graph in Figure 6-15 also shows that these two specimens had the largest water absorption rate. Two of the specimens – M162 (w_{ini}=20%, RH=100%, gap=60 mm) and M153 (w_{ini}=24%, RH=100%, gap=45 mm) – had test durations of three months, see Figure 6-16, and were still in comparatively good shape even after all this time. During the test period, the diameter of the blocks was also measured at selected intervals, Figure 6-17.

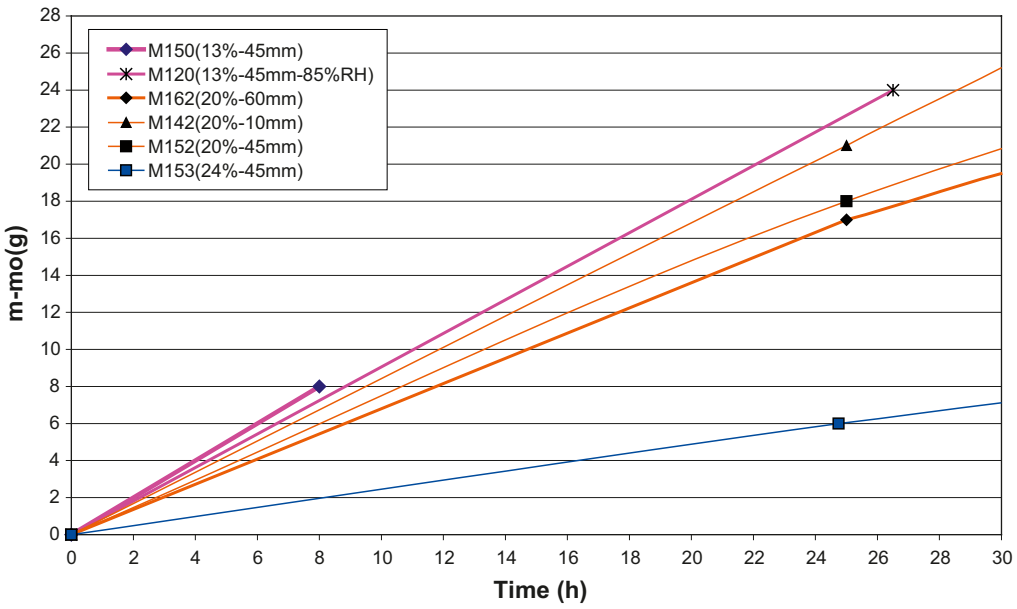

Figure 6-15. *Water absorption as a function of time for six blocks during the first 30 hours of testing.*

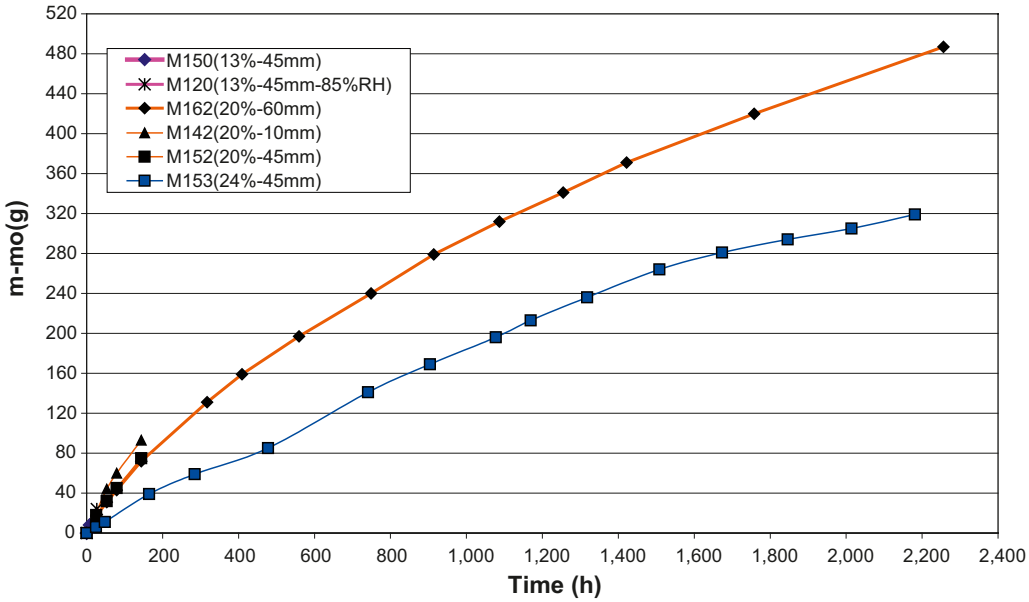

Figure 6-16. Water absorption as a function of time for six blocks.

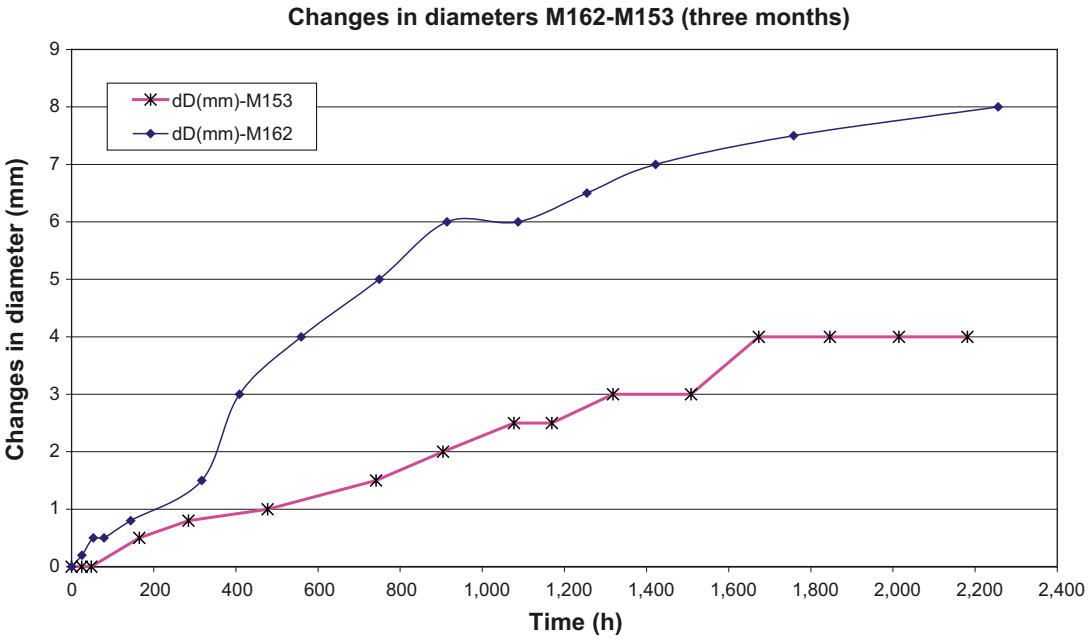

Figure 6-17. Measured change in diameter for blocks M162 (w_{ini}=20%, RH=100%, gap=60 mm) and M153 (w_{ini}=24%, RH=100%, gap=45 mm) vs. time.

Figure 6-18. *Photo showing block specimen M150 (w_{ini}=13%, RH=100%, gap=45 mm) after 8 hours.*

Cracking

These tests show that the sensitivity of the blocks to cracking is very dependent on the initial water ratio and on the distance to the wet surface. The two specimens with the lowest initial water ratio (13%) cracked into pieces during the first 24 hours. Two of the three specimens with an initial water ratio of 20% and smallest gap (10 and 45 mm) had both cracked radially within a period of only one week. The third specimen, with an initial water ratio of 20%, had a gap to the wet rock of 60 mm. After about a month of testing, a radial crack could be seen, but even after three months of testing the specimen was still in one piece, Figure 6-20. The specimen with an initial water ratio of 24% was after three months' testing still unaffected by cracking, Figure 6-21.

The following observations were noted;

Specimen M120, (w_{ini}=13%, RH=85%, gap=45 mm). The specimen had cracked completely after 24 hours.

Specimen M150, (w_{ini}=13%, RH=100%, gap=45 mm). The specimen had cracked completely after 8 hours, Figure 6-18.

Specimen M142, (w_{ini}=20%, RH=100%, gap=10 mm). Diametrical (radial) crack after 6 days.

Specimen M152, (w_{ini}=20%, RH=100%, gap=45 mm). Diametrical (radial) crack after 7 days, Figure 6-19.

Specimen M162, (w_{ini}=20%, RH=100%, gap=60 mm). Although after three months the block was still in one piece, there was a very evident diametrical (radial) crack that occurred after about one month of testing, Figure 6-20.

Specimen M153, (w_{ini}=24%, RH=100%, gap=45 mm). No cracks could be seen after three months, Figure 6-21.

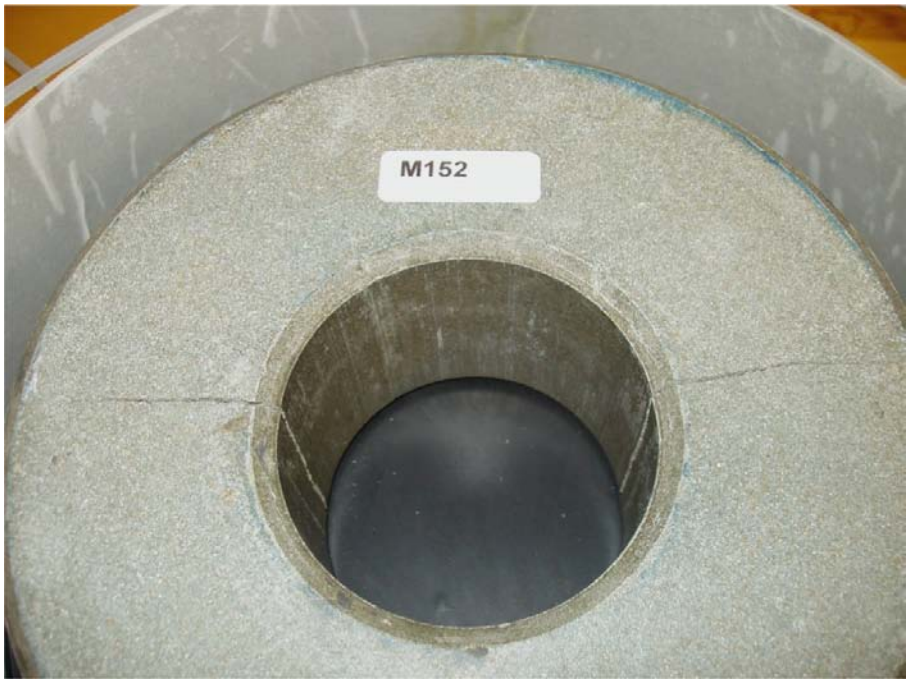

Figure 6-19. *Specimen M152 (w_{ini}=20%, RH=100%, gap=45 mm) after 7 days.*

Figure 6-20. *Specimen M162 (w_{ini}=20%, RH=100%, gap=65 mm) after 3 months. The block was still in one piece but a radial crack had developed after about one month.*

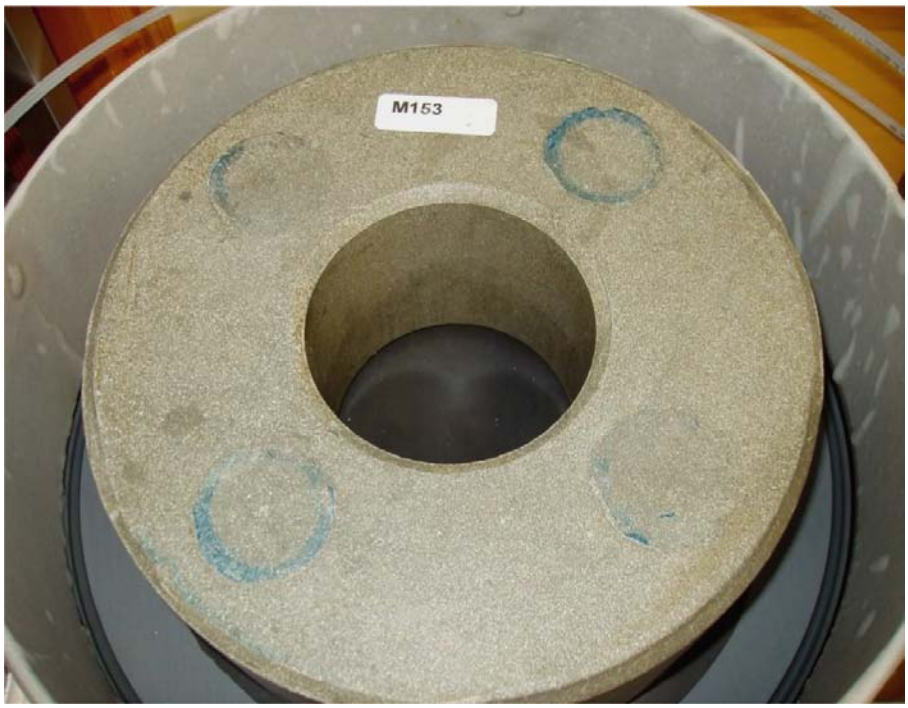

Figure 6-21. *Specimen M153 after 3 months. No cracks can be seen on the surface.*

6.3.4 Discussion of results from the medium-scale tests

The tests show that there are a number of factors that affect the susceptibility of the blocks to cracking:

- The water content – the lower the water content, the greater the amount of cracking.
- The slot width – the smaller the slot width, the greater the cracking.
- The size of the block – larger blocks seem to be more vulnerable to cracking.

The latter observation is based on the difference between the observed cracking of the small specimens and the blocks.

These observations lead to the following general understanding of the cracking process of bentonite blocks exposed to moisture:

When water is absorbed by the surface of a bentonite block, the surface starts to expand. The expansion is free to expand radially, but tangentially it will be locked in and result in the propagation of stresses in the block. These stresses become higher the greater the amount of water that is absorbed. As a result of the comparatively low strength of bentonite blocks and their brittleness, they will crack when the stresses exceed the strength. The tendency for cracking increases with the following factors:

- The main crack initiator is the magnitude of the shear stress, which in turn depends more on the stress gradient than on the stress magnitude. Thus the higher the stress gradient, the greater the cracking.
- The higher the gradient in water content distribution, the higher the gradient in stress and thus the greater the cracking.
- The faster the wetting of the higher water content gradient, the greater the cracking.
- The lower the initial water content, the higher the stress gradient and thus the stronger the cracking.
- The lower the initial water content, the faster the wetting and thus the faster the cracking.
- The smaller the gap, the faster the wetting and thus stronger the cracking.
- In small specimens, the expansion is not prevented by locked-in effects, which means that they do not crack as easily as large blocks.

Thus the very fast cracking of the blocks with low initial water content can be explained in the following way: The wetting is fast due to the high gradient in RH across the slot. The fast wetting causes a high water content gradient since the water transport from the block surface into the block cannot keep up with the wetting. The high water content gradient strongly affects the stresses in the block since the initial water content is low and the block is large enough to create interlocking effects.

The initial water content seems to be the most important factor in crack development. Since distance blocks with high water content can be fabricated, the conclusion is that they should be made with an initial water content of about 24%.

6.4 Numerical modeling of water uptake tests

6.4.1 Introduction

The water uptake tests described in Section 6.2 have been modeled using the FEM code Code_Bright v2.2 (A 3-D program for thermo-hydro-mechanical analysis in geological media. Departamento de Ingeneria del Terreno, Cartgrafica y Geofisica, UPC, Barcelona, Spain).

The tests were modeled as THM problems with constant atmospheric gas pressure. Even though the tests were performed under isothermal conditions, the thermal processes were included in the calculation to enable vapour diffusion across the gap between the water surface and the specimens. Apart from this aspect there are no relevant thermal problems to be solved.

The inclusion of mechanical processes was necessitated by the free swelling conditions. If the specimens had been modeled with a constant porosity, then the actual amount of absorbed water would have exceeded the available pore volume.

A new approach was used to mimic the retention properties of free swelling specimens. The approach consists of a parameter value adoption for the retention curve as well as for one of the mechanical parameters. This is described in detail below.

The compressibility and the thermal expansion of water were minimized in order to ensure a water density of 1,000 kg/m^3. This is the conventional value used for evaluations of void ratios. In the models, a solid density of 2,750 kg/m^3 was used for MX-80 /Karnland et al. 2,000/.

A compilation of models is given in Table 6-8. Three different bentonite materials were modeled (denoted w106, w195, and w237), each one with a specific parameter setting. Models investigating the effects of variations in conditions, i.e. gap distance and temperature, were implemented with the w195 material.

The simulation time for all models was 2,100 hours, corresponding to a duration of 3 months for each test.

Table 6-8. List of models with corresponding experiment, materials and condition variation.

Model	Experiment	Water content	Void Ratio	Gap	Temp.
w106def	S220	10.6%	0.549	45 mm	20 °C
w195def	S222	19.5%	0.584	45 mm	20 °C
w237def	S224	23.7%	0.662	45 mm	20 °C
w195g10	S212	19.5%	0.584	10 mm	20 °C
w195g60	S232	19.5%	0.584	60 mm	20 °C
w195t10	S222_T10c	19.5%	0.584	45 mm	10 °C
w195t30	S222_T30a	19.5%	0.584	45 mm	30 °C

6.4.2 Model description

Geometries and mesh

The tests were modeled as axis-symmetric 2D problems. The specimens had a diameter of 50 mm and a thickness of 30 mm. The air component was also modeled as a cylinder with a diameter of 50 mm, but with three different heights; 60, 45 and 10 mm (Figure 6-22).

The specimen was discretizied with 5 x 10 quadratic elements, slightly concentrated towards the interface between the specimen and the air. The number of elements in the air component was 60, 50 and 25 for the heights of 60, 45 and 10 mm, respectively.

Initial and boundary conditions

The initial porosities and liquid pressure of the specimens are shown in Table 6-10. The initial liquid pressure of the air material was applied as a linear distribution: from the same value as in the specimen at the specimen-air interface, to atmospheric pressure at the lower boundary.

The only boundary conditions applied were a mechanical roller boundary at the interface between the specimen and the air, and a flow boundary with atmospheric liquid pressure at the lower end of the air component (Figure 6-22). The temperature at the flow boundary was also kept constant.

Retention properties at unconfined conditions

The retention properties at unconfined conditions are fairly well-defined and can be parameterized as follows:

$$\psi = \exp(a - b \cdot w) \qquad (MPa) \qquad (6\text{-}3)$$

where ψ is suction and w is the water content. Values of the parameters a and b have been presented for three different initial water contents: 10, 17 and 27% /Dueck 2007/.

The initial water content of two of the materials used in this study (w195 and w237) fall between 17 and 27% and intermediate a-values were therefore adopted for these materials. The third material (w106) was sufficiently close to 10% for a direct adoption (see Figure 6-23 and Table 6-9).

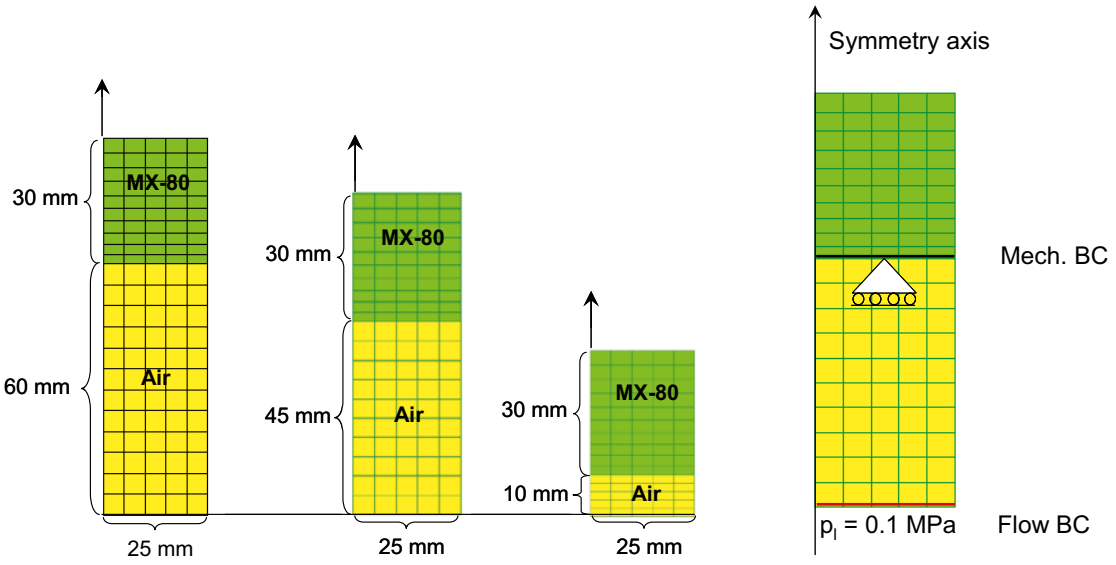

Figure 6-22. Model geometries and boundary conditions.

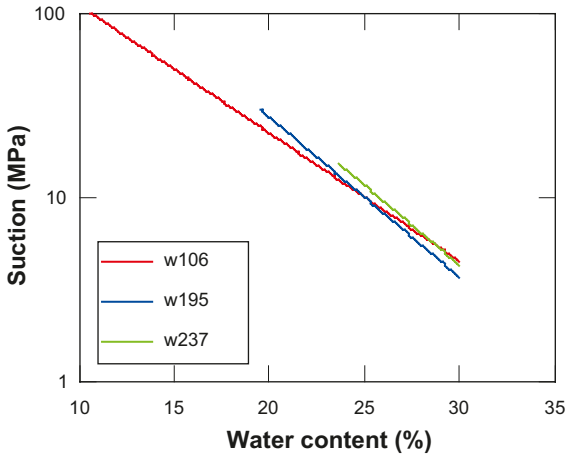

Figure 6-23. *Basic retention curves for free swelling conditions.*

The general mechanical rule for swelling is assumed to be that the air-filled void ratio ($e_M = V_g/V_s$) is constant during swelling. This type of behaviour has been found in shrinkage tests /Börgesson et al. 1995/. Applying this relationship, the degree of saturation (S) can be expressed as a function of suction:

$$S(\psi) = \frac{w(\psi)\cdot r_\rho}{e(\psi)} = \frac{e_m}{e_m + e_M} = \frac{1}{1 + \frac{e_M}{w(\psi)\cdot r_\rho}} \tag{6-4}$$

e_m is the water-filled void ratio, w is the water content and r_ρ is the solid-water density ratio.

One of the retention curves implemented in Code_Bright follows a van Genuchten expression:

$$S(\psi) = \left(1 + \left(\frac{\psi}{P_0}\right)^{\frac{1}{1-\lambda}}\right)^{-\lambda} \tag{6-5}$$

where P_0 and λ are parameters. Values of these parameters were calibrated for the different material in order to follow Equation 6-4 (see Figure 6-24 and Table 6-9).

Table 6-9. Retention and swelling parameters.

Water content	e_M	Basic relation		van Genuchten		κ_s
		a	b	P_0 (MPa)	λ	
10.6%	0.258	6.3	16	2.064	0.14	0.172
19.5%	0.048	7.3	20	0.111	0.015	0.138
23.7%	0.010	7.45	20	0.038	0.0026	0.138

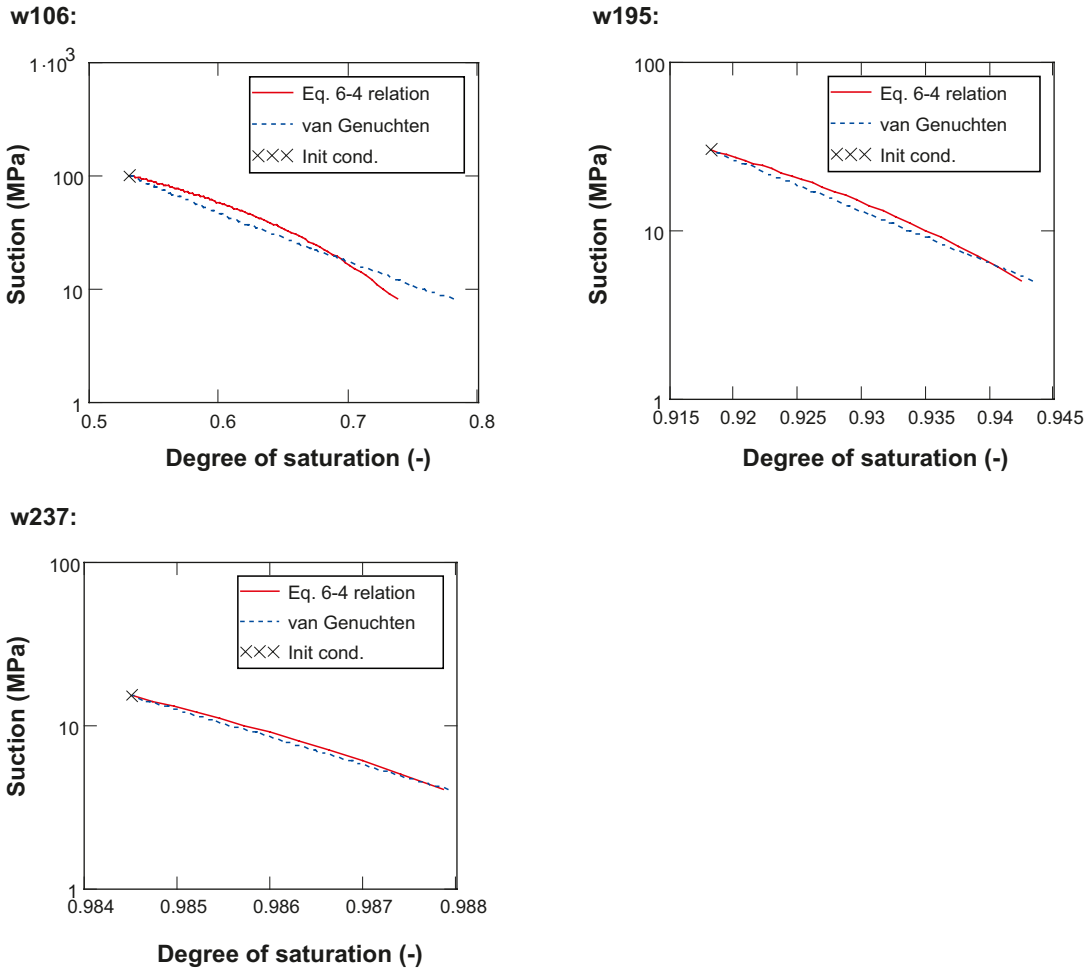

Figure 6-24. *Calibration of van Genuchten parameters (P_0 and λ) to Equation 6-4 relations.*

With the same mechanical rule as for the retention properties, i.e. that the air-filled void ratio is constant; the κ_s-module can be evaluated according to:

$$de_m = -\kappa_s \frac{d\psi}{\psi + 0.1} \tag{6-6}$$

This is the definition of the elastic swelling strain in the BBM model /Alonso et al. 1990/, but with the difference that the void ratio increment (de) is replaced by the increment in water-filled void ratio (de_m). Equation 6-6 can be rearranged and approximated as:

$$r_\rho \cdot dw \approx -\kappa_s \cdot \frac{d\psi}{\psi} \tag{6-7}$$

The inverse function of the retention curve in Equation 6-3, i.e. $w(\psi) = -(\ln(\psi) - a)/b$, has the following derivative:

$$\frac{dw}{d\psi} = -\frac{1}{\psi \cdot b} \tag{6-8}$$

The κ_s-module can be identified from Equations 6-7 and 6-8 as:

$$\kappa_s \approx \frac{r_\rho}{b} \tag{6-9}$$

Even if the rule of constant macro void ratio is not very precise, the concurrent application of the retention curve (Equation 6-4) and the swelling module (Equation 6-9) provide a means to implement a true retention curve.

Moisture transport

The liquid advective moisture transport is in the code used described by Darcy's law:

$$\vec{q} = -\frac{k \cdot k_r}{\mu} \nabla P_l \qquad (6\text{-}10)$$

k is the intrinsic permeability, k_r is the relative permeability, μ is the viscosity and P_l is the liquid pressure. The viscosity is in Code_Bright modeled with the following temperature dependence:

$$\mu(T) = A \cdot \exp\left(\frac{B}{273.15 + T}\right) \qquad (6\text{-}11)$$

where A and B is $2.1 \cdot 10^{-12}$ MPa·s and 1,808.5 K, respectively.

The intrinsic permeability of the bentonite specimens is also modeled as porosity-dependent and following Kozeny's law:

$$k(\phi) = k_0 \frac{\phi^3}{(1-\phi)^2} \frac{(1-\phi_0)^2}{\phi_0^3} \qquad (6\text{-}12)$$

The vapor diffusion follows Fick's law:

$$\vec{i} = -\phi \cdot \tau \cdot D \cdot (1 - S_r) \cdot \rho_g \cdot \nabla \omega_g^w \qquad (6\text{-}13)$$

in which the diffusion coefficient is calculated as:

$$D = 5.9 \cdot 10^{-6} \frac{(273.15 + T)^{2.3}}{P_g} \qquad (6\text{-}14)$$

Values for the intrinsic permeability of the different specimen materials were derived from /Börgesson et al. 1999/, see Table 6-10. These values are illustrated with the porosity dependence described by Equation 6-12 in Figure 6-25. The standard power law was applied for the relative permeability of the specimen materials. The vapor tortuosity factor was set to 0.3. This value has previously been used for MX-80 material /Åkesson 2006/.

The air material was modeled with a porosity value of 0.999 and a vapor tortuosity value of 1, thereby capturing the vapor diffusion across the gap (see Table 6-11). The water content of the air was suppressed by applying a very low retention curve. The liquid advective flow across the gap was eliminated by setting the relative permeability of this material to zero.

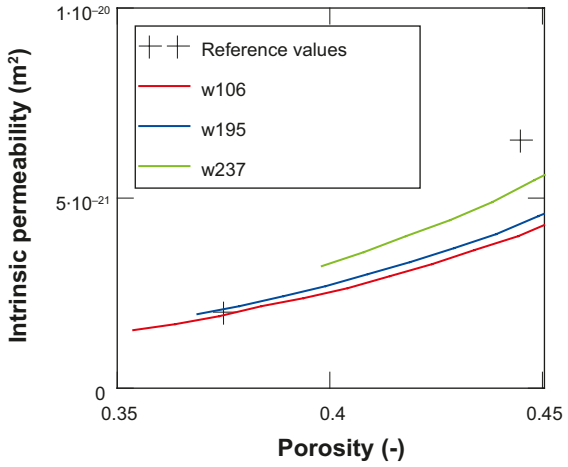

Figure 6-25. *Applied intrinsic permeability as a function of porosity. (Reference values are taken from /Börgesson et al. 1999/).*

Table 6-10. Bentonite initial porosity, liquid pressure and moisture transport parameters.

Water content	Porosity	Liquid pressure (MPa)	Intrinsic perm. (m^2)	Relative perm.	Vapor tortuosity (τ)
10.6%	0.354	–100	$1.5 \cdot 10^{-21}$		
19.5%	0.369	–29.9	$1.9 \cdot 10^{-21}$	S_r^3	0.3
23.7%	0.398	–14.9	$3.2 \cdot 10^{-21}$		

Table 6-11. Hydrodynamic parameters for air material.

Porosity	0.999
Retention parameter (P_0 and λ)	0.00001 MPa and 0.3
Intrinsic perm. (m^2)	10^{-30}
Relative perm.	0
Vapor tortuosity	1

Table 6-12. Additional mechanical parameters.

Material	Stiffness modules	Poisson's ratio
Bentonite specimen	$\kappa_i = 0.25$; $K_{min} = 10$ MPa	0.2
Air material	E = 5 MPa	0.4999

Mechanical properties

Due to the free-swelling conditions, the mechanical problem is effectively independent of the stiffness of the bentonite material. Nevertheless, properties must be assigned for the bentonite as well as for the air material (Table 6-12). The bentonite specimen was modeled as a BBM material while the air material was treated as linear elastic.

Post-processing

The evolution of average water content of the specimens was calculated in order to follow their successive mass increase. This was accomplished by analyzing model results of void ratio and degree of saturation at four nodes shown in Figure 6-26. Given the distances between these nodes, the average water content was weighted with relative initial length fractions (percentages are shown in Figure 6-26):

$$\overline{w} = \sum_i l_i \cdot w_i \tag{6-15}$$

With this weighted average, the mass increase was calculated as:

$$m_{increase} = (\overline{w} - w^{init}) \cdot V^{init} \cdot \rho_{dry}^{init} \tag{6-16}$$

The initial volume was based on a diameter of 49 mm, which is a more exact value than the 50 mm used in the model geometry.

Distributions of water content and relative humidity were evaluated as scan-lines along the symmetry axis.

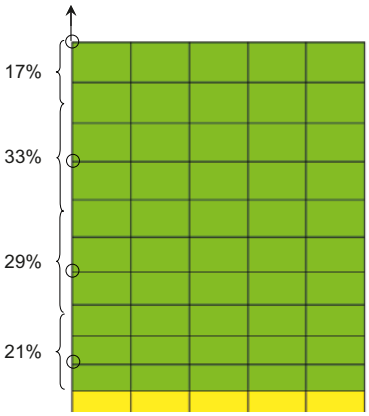

Figure 6-26. *Analyzed model nodes. Initial length fractions are marked.*

6.4.3 Results and comparisons with experimental data

Successive mass increase

The influence of the initial water content is shown in Figure 6-27. Results from three models with the same gap size and temperature, but with different initial water content, are compared with experimental results. The agreement is generally good. The main exception is the specimen with the highest water content.

The influence of the gap size between the water surface and the bentonite is shown in Figure 6-28. Results from three models are shown, representing the same initial conditions and temperature, but with different gap sizes. The results of the measurements are well represented by the models. Since the specimens are initially the same, the difference between the models has to be a result of different flow rates (rate of diffusion) in the air gap.

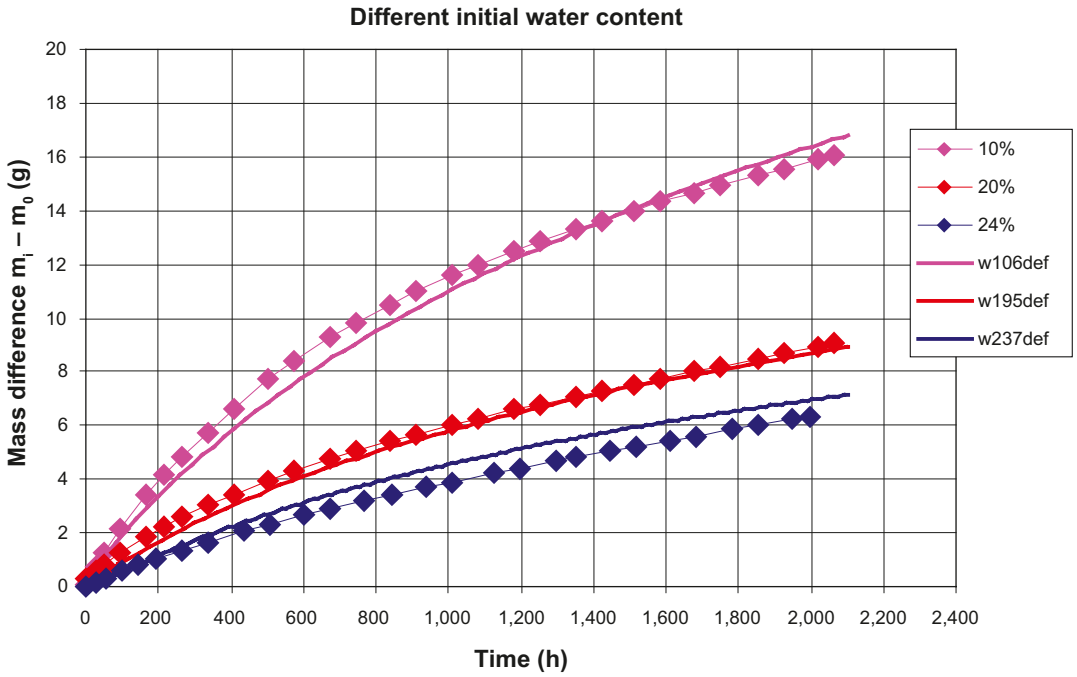

Figure 6-27. *Water absorption as a function of time showing the influence of initial water content. (Measurements from Figure 6-3 (lines with symbols) compared with model results (lines)).*

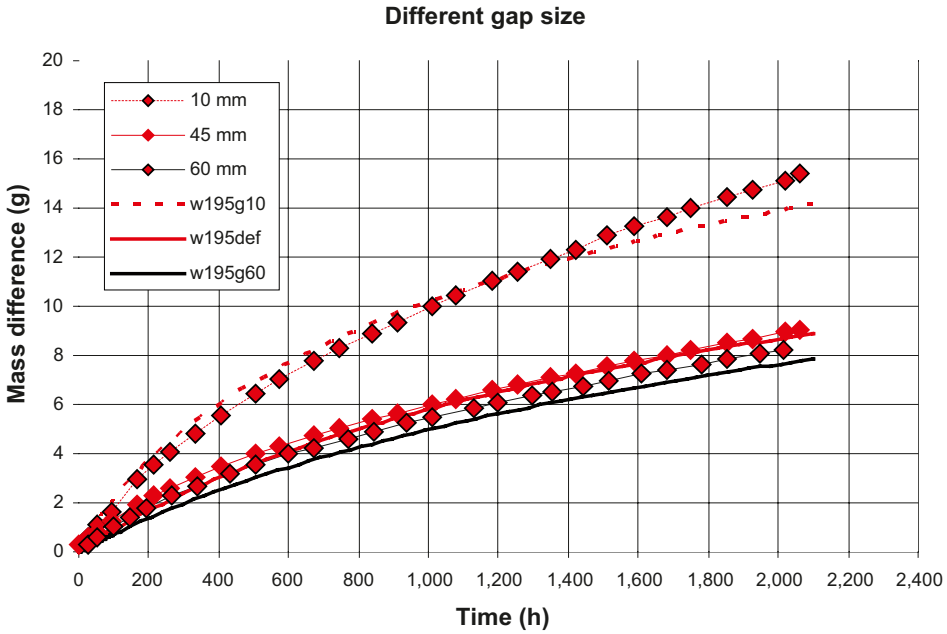

Figure 6-28. *Water absorption as a function of time showing the influence of size of the gap between the water surface and the specimen. (Measurements from Figure 6-4(lines with symbols) compared with model results (lines)).*

The influence of temperature is shown in Figure 6-29. The models concur best with the measurements at 20°C and show an increase in absorption rate with an increase in temperature, and vice versa. The deviation from the model at 20°C seems to be equal in mass difference when the temperature differs by 10°C, i.e. irrespective of whether the temperature increases or decreases. However, the measurements do not show these symmetrical results.

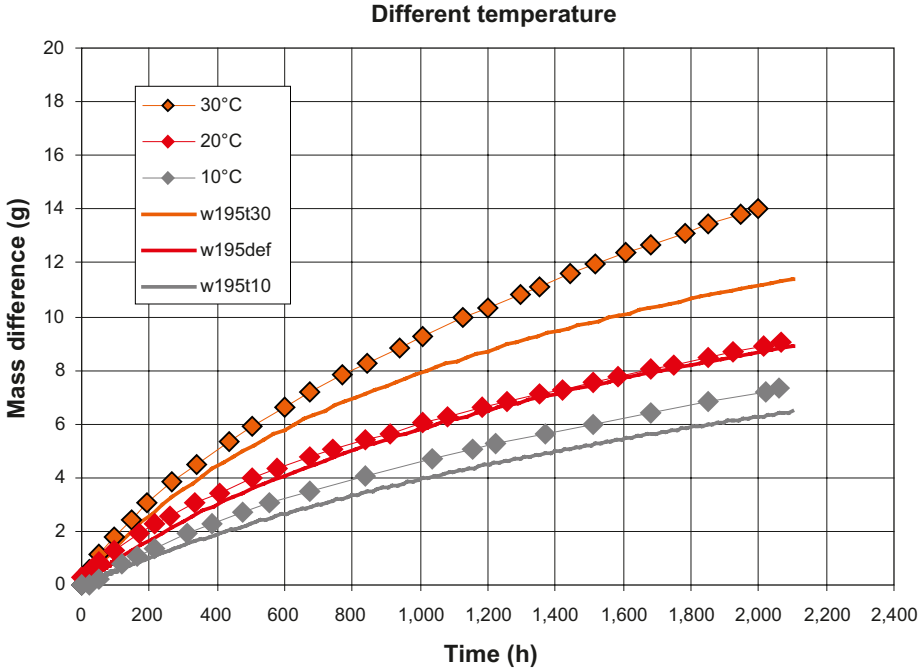

Figure 6-29. *Water absorption as a function of time showing the influence of temperature. (Measurements from Figure 6-5 (lines with symbols) compared with model results (lines)).*

Final water content distribution

To further investigate the consistency between the models and the measurements, the final distribution of water content along the specimen height was compared. The measured water contents are based on the distribution measured after termination (see Appendix A1). However, there is a difference between the average water content from the measurement w_f and the water content calculated from the increase in mass according to Equation 6-1 w_{calc}. To facilitate comparison with the models, the difference in values is taken into account by adding the difference to each of the measured water contents (upper, middle, lower).

Comparisons of modeled and experimental final distributions of water contents are shown with the same grouping as for the successive mass increase, and are presented in Figure 6-30 to Figure 6-32. It should be noted that the average water content calculated is similar to experimental results in those models that showed a close match for the mass increase (e.g. the w195def model). In general, however, the modeled gradients in water content are very low, and this characteristic is the most significant deviation from the experimental results. This result is discussed in Section 6.4.4.

Relative humidity distributions

One important reason for studying the absorption of water using numerical models was to verify whether the limiting and determining factor for the absorption rate of the bentonite is the vapour transport rate in the air as stated in /Autio et al. 2008a/. From Figure 6-28 and Figure 6-31 it can be seen that both the models and the measurements confirm that the flow rate is dependent on the size of the air gap. The flow rate is a result of different gradients in the driving potential over the air gap according to Equation 6-13. A smaller gap gives a larger gradient over the gap, which yields a more rapid transport.

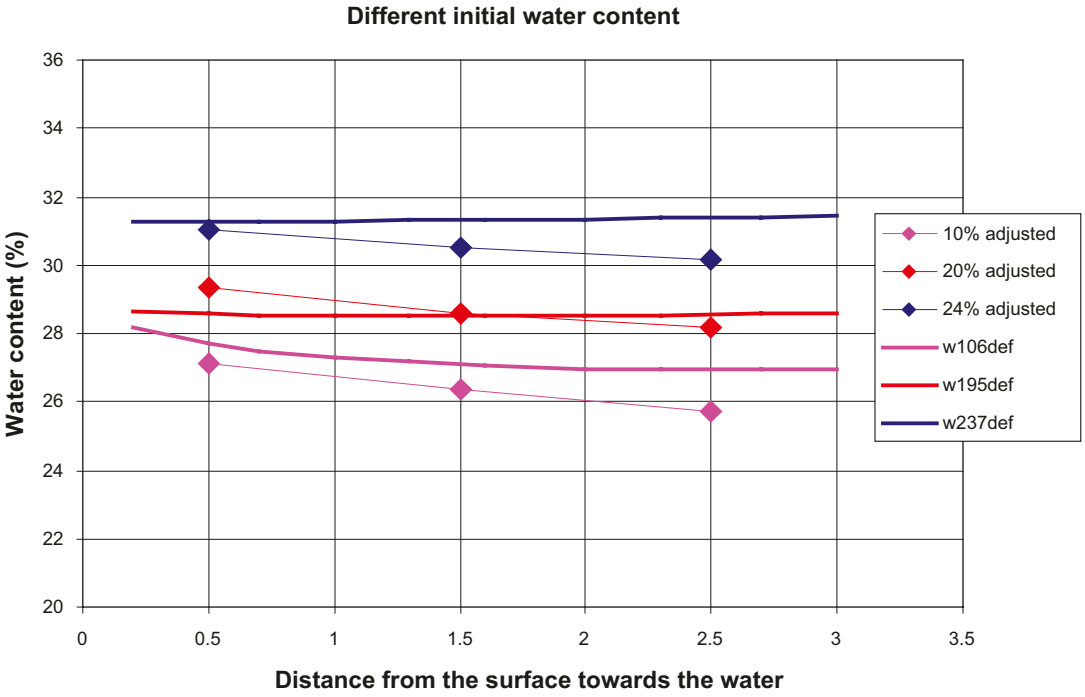

Figure 6-30. *Final distribution of modeled water content (lines) and from measurements adjusted to results from Equation 6-1 (lines with symbols) showing the influence of initial water content.*

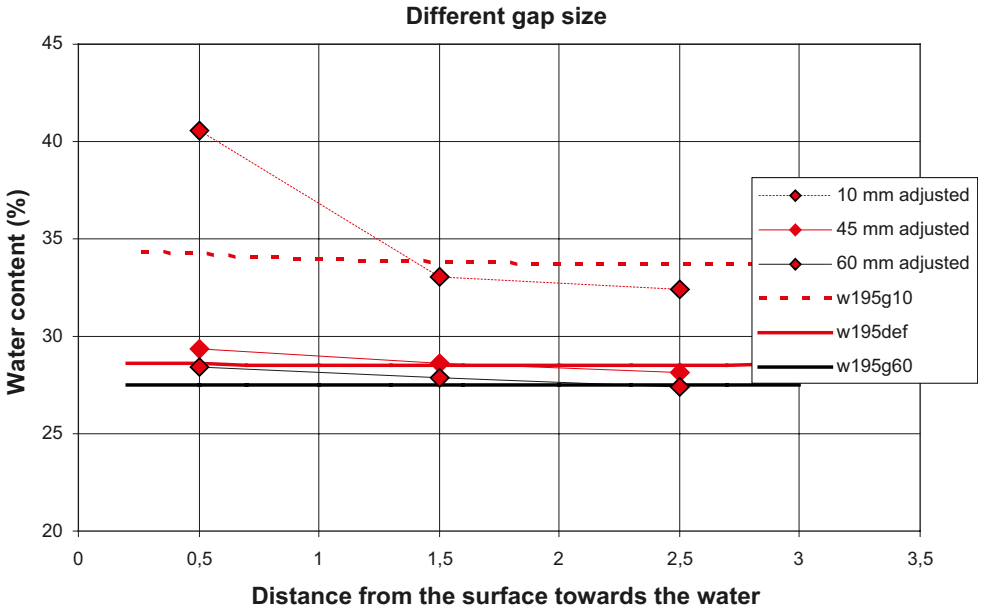

Figure 6-31. *Final distribution of modeled water content (lines) and from measurements adjusted to results from Equation 6-1(lines with symbols) showing the influence of gap sizes.*

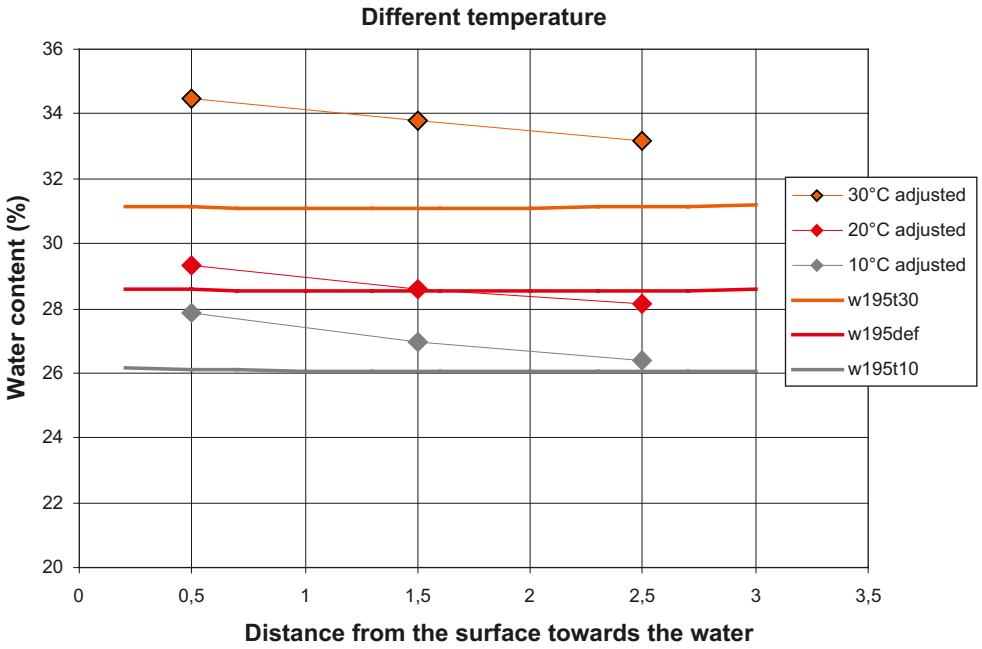

Figure 6-32. *Final distribution of modeled water content (lines) and from measurements adjusted to results from Equation 6-1 (lines with symbols) showing the influence of temperatures.*

An illustration of the influence of gap size is shown in Figure 6-33 where it can be seen that the initial gradient is larger the nearer the specimen is to the water surface. The gradient will decrease, and precisely how much the decrease is will depend on the transport rate into the bentonite. Since the final gradient in water content is low in all specimens, the moisture transport in the bentonite does not appear to be the limiting factor.

One observation can be made concerning the gradients in relative humidity at the specimen-gap interface after one week (Figure 6-33). The gradient in the specimen is apparently slightly higher than in the air gap. This reflects the fact that the flow coefficient in the specimen is lower than in the air. However, the difference is less with higher water contents. In this respect, the bentonite can be said to be a limiting factor for the absorption rate at low water contents.

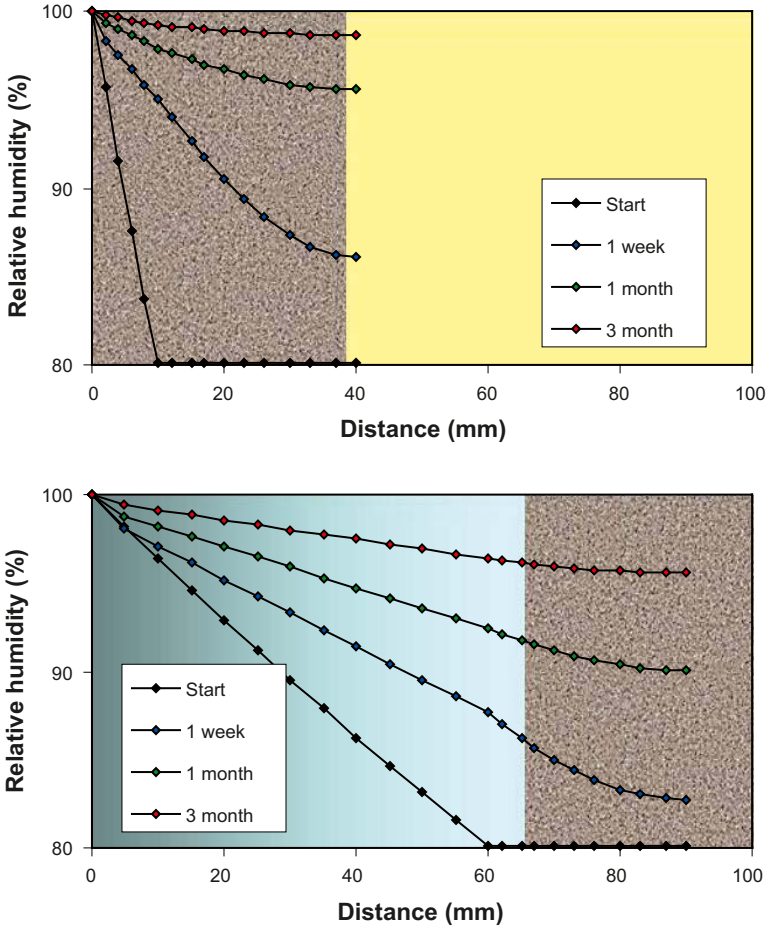

Figure 6-33. *Distributions of relative humidity in gap and specimen on four different occasions in models with w195 material. Gap sizes of 10 mm (above) and of 60 mm (below).*

6.4.4 Comments on models

Transport coefficients

The agreement with experimental mass increase supports the description of vapor diffusion across the gap and the flow coefficient value used to describe this process. The agreement also supports the flow coefficient describing the suction driven advective flow in the buffer material, although the rate appears to be overestimated at the highest water content (w237).

Mechanical swelling properties

The mechanical property describing the swelling strain is fairly well captured with the simple rule of a constant air-filled void ratio. Evaluation of the experimental volume increase data indicates that the κ_s-module used for the "base case" water content material (w195) is quite exact. For the dry material (w106) the value used underestimates the actual strain by 25%, while for the material with the highest water content (w237) the value used overestimates the strain by 4%.

Retention properties

In the course of this work, the emphasis has been placed on implementing retention properties that are as realistic as possible (following Equation 6-3). The evaluation of model results shows that this has been achieved, although further refinement can be envisaged.

It has been found that the assumed relationship between suction and void ratio, provided by the mechanical laws, is not unambiguous. Strains appear to spread from the lower part of the specimen, thereby contributing to overestimation of the void ratio in the upper part. In fact, the void ratio distributions are not really one-dimensional, which induces a small error in the calculation of the water contents. This appears to be the reason for the low water content gradients given by the models. Preliminary tests have shown that this effect can be reduced by minimizing the rigidity of the buffer material, *i.e.* by setting Poisson's ratio close to 0.5.

Moreover, the specification of the retention curve (according to Equation 6-4) can be generalized for any swelling properties (*i.e.* κ_s) by an exact integration of the strain increment. By doing this, the experimental swelling strains could be matched more closely. It also follows from this that the approximation of Equation 6-7 can be avoided. It has been found that this simplification has a certain effect on the w237 material.

Finally, there are other options than the standard van Genuchten expression (Equation 6-5) in the code used that may facilitate a more precise calibration than the one shown in Figure 6-24.

Temperature effects

The temperature influences the vapor diffusion coefficient, the water viscosity and the saturation vapor pressure in the models. These relations are apparently not sufficient to mimic the experimental results. One possible effect could be a thermal dependence of the retention properties. However, more work needs to be done in order to evaluate this possible mechanism.

6.4.5 Conclusions

The modeled mass increase is generally in good agreement with experimental results. The main exceptions are the tests performed at temperatures other than 20°C, and to some extent the test with the highest water content (w237). Moreover, the modeled distributions of water content at the end of the tests exhibit almost no gradient, in contrast to the experimental results.

Models, as well as experimental results, show that the flow rate is largely governed by the vapor diffusion across the gap, although the bentonite appears to be limiting for the absorption rate at low water contents.

The modeling results support the flow coefficients describing the vapor diffusion in air, and in general also the suction-driven advective flow in the buffer material. The models also support the retention properties, given by /Dueck 2007/, on which these models were based.

7 Piping past distance blocks

7.1 General

After the emplacement of distance blocks in the KBS-3H geometry, the bentonite is to take up water from the surrounding rock, swell and seal the drift. If high water pressures were to built up over a short period of time just after sealing, it would be possible for piping to occur, i.e. water by-pass the bentonite thereby generating a flow of water and bentonite, see Figure 7-1. It has been observed in previous tests that piping may occur at certain design and inflow conditions.

When piping starts, bentonite may erode, thereby reducing the density of the buffer locally. The erosion and transport of bentonite depends on several factors, the flow velocity being one of the most important ones.

At the time of preparting this document, experiments had been performed in three different test setups:

1. Scale 1:10, test length 1m.
2. Scale 1:10, test length 3 m.
3. Transparant tube, diameter = 0.1 m and length=1 m.

7.2 Material and water used in the tests

Bentonite

In order to facilitate the manufacture of bentonite blocks for testing purposes, it was decided to use bentonite cores that were drilled from full-scale bentonite blocks. These blocks had previously been produced for various field tests at ÄHRL (a number of spare blocks were available). The alternative would have been to manufacture a special mold and, with the aid of a large hydraulic press, produce blocks manually. Since the planned tests required blocks of different sizes, it would have been a very expensive and time-consuming task.

The full-scale blocks were manufactured to a well-defined quality and their as-manufactured density, dimension and water ratio values were well documented, see Table 7-1. The cores were machined to achieve the desired diameter. These bentonite blocks had a water ratio of either 12 or 17%, and these initial conditions were used in most of the tests. In addition, there was one spare bentonite block

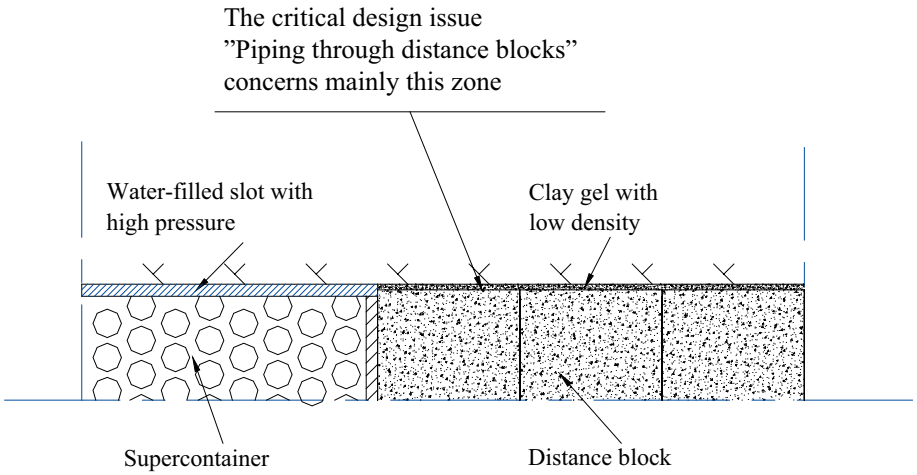

Figure 7-1. *Schematic showing a partial vertical view of the KBS-3H layout. The critical design issue “Piping through distance blocks” concerns mainly the slot between distance blocks and rock.*

Table 7-1. Table showing the basic properties of the blocks used in the piping tests.

Sample	w %	Bulk density g/cm³	Dry density g/cm³	Sr %	e
Type 1	12.5	1.93	1.71	55.71	0.623
Type 2	17.0	2.09	1.79	85.18	0.553
Type 3	21.7	2.06	1.69	94.15	0.642

available from the materials prepared for the Lasgit experiment at Äspö. The water ratio in this block was approximately 22%. A number of supplementary tests were performed with this block quality in order to provide information on the effects of saturation and density of the blocks on piping and load transfer.

All blocks used in the tests were manufactured of MX-80 bentonite, produced by the Am. Coll. Co.

Water

In this test series (two similar test series had been performed earlier, see Chapter 2), two different types ofwater were used: tap water and water with a salinity of 3.5% (50/50 NaCl/$CaCl_2$). Most tests were performed with 3.5% salt in the water.

7.3 Scale tests in 1 m-long test equipment

7.3.1 General

The function of distance blocks has been tested in three different test series on a scale of 1:10 (radial scale) in a 1 m-long test setup. The results from the first two test series were presented in the report by /Börgesson et al. 2005/. In this third test series, 14 additional tests have been completed. The basic test layout used in this series is shown in Figure 7-2. These tests were performed using what were deemed at the time to be extreme hydraulic conditions in order to test the robustness of the design. It has, however, been subsequently determined that both the tested water pressure increase rate and the maximum applied water pressure are values which can routinely occur. The test conditions examined thus far are listed below (test conditions in earlier test series are shown in brackets):

- Inflow rate: 1 l/min, corresponding to filling time of 1 day (0.1 l/min).
- Water pressure increase rate: 1–5 MPa/h (100 kPa/h).
- Maximum water pressure: 5 MPa (2 MPa).

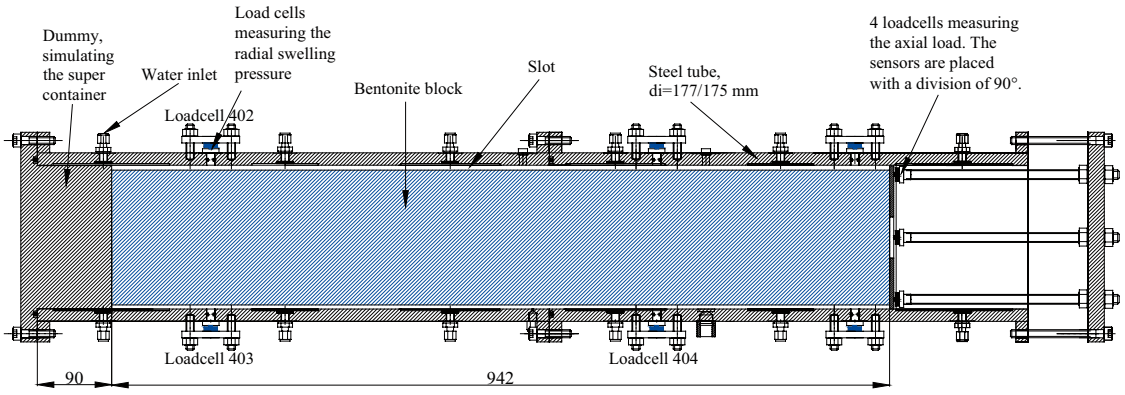

Figure 7-2. *Schematic drawing showing the test equipment used (dimensions in mm). The equipment has a radial scale of 1:10.*

7.3.2 Experimental set-up

The test variables examined are:

- Slot width.
- Slot filled with pellets or not.
- Salt content in the water.
- Pre-wetting of the slot or not.
- Initial conditions of the bentonite (degree of saturation).

The following variables were measured during the tests:

- Water pressure of the injected water.
- Water volume injected.
- Axial load on the end of the distance plug (fixing ring).
- Radial swelling pressure of the bentonite (three points).

7.3.3 Results

General

Table 7-2 shows a compilation of all tests performed in the 1 m-equipment. In total 14 tests were performed in this test series. Some comments:

- The first six tests were performed using tap water, but after finishing these tests it was decided to use water with a salinity of 3.5% which was considered to be a more realistic water type in a real repository.
- Two tests were performed with a pellet-filled slot (15 and 35 mm width) and it was concluded that a slot as wide as this would not provide the very fast sealing required. Only one type of pellet was tested. However, the behaviour observed is assumed to be the same regardless of the type of pellet used, provided their granularity and as-placed density are similar.
- Test numbers 4 to 14 included pre-wetting of the outer slot. This step was judged to increase the ability of the bentonite to seal the tunnel in a short time. See detailed description in Section 7.3.4.
- Test number 12 was a pre-test in order to study the feasibility of using a drainage tube to control the water pressure in the supercontainer section. The wetting tube was led under the distance blocks and through the fixing ring. The test also included removal/retrieval of the tube. The technique of using a drainage tube was also used in test 14 and in three tests performed in the 3 m test setup. See detailed description in Sections 7.3.5 and 7.3.6.
- Test number 13 was a special test that ran for almost four months. After filling the outer slot with water, the access to additional water was stopped. The main purpose of the test was to study the development of radial swelling pressure during the redistribution of the water. The issue of radial pressure is of particular importance with respect to support provided to the surrounding rock and to the prevention of rock spalling.
- Since the tests performed showed that the initial slot between bentonite and rock has to be very small in order to obtain rapid sealing, it will be necessary to produce blocks with a somewhat lower dry density and higher degree of saturation (in order to achieve a feasible saturated density), see Section 4.3. Test number 14 was the first test to be performed using blocks of this type.

Table 7-2. Table showing the tests performed in the 1 m-long test equipment.

Test	Arrangement	Slot top/bottom mm	Test length m	Filling time Days	Filling rate scale 1:1 l/min	Water pressure increase rate kPa/h	Maximal pressure kPa	Water type	Comments
3-1	35 mm slot filled with pellets.	35/35	0.94	1.6	0.63		350	Tap water	After filling, a constant flow of 5 l/24 h was applied. **The system did not seal.**
3-2	D bentonite 173 mm.	2/0	0.94	1.9	0.53	1,000	5,000	Tap water	Some “internal piping” during the pressure ramp. **The system seals.** Water penetration 71 cm in bottom.
3-3	D bentonite 170 mm.	5/0	0.94	1.9	0.53	1,000	820	Tap water	“Internal piping” continued with piping. **The system seals.** The outer surface completely wet.
3-4	D bentonite 170 mm. Pre wetted bentonite.	5/0	0.94	1	1	1,000	5,000	Tap water	Some “internal piping” during the pressure ramp. **The system seals.**
3-5	D bentonite 165 mm. Pre wetted bentonite.	10/0	0.94	1	1	1,000/100	4,200	Tap water	The system can not stand the fast pressure build up. The bentonite can withstand 4.2 MPa after 2 weeks.
3-6	15 mm slot filled with pellets. Pre wetted bentonite.	15/15	0.94	1	1	1,000/100	1,800	Tap water	The system can not stand the pressure build up. The bentonite can withstand 1.8 MPa after 2 weeks.
3-7	D bentonite 170 mm.	5/0	0.94	1	1	1,000	5,000	3.5% salt	The salty water increases the swelling rate and by that also the sealing effect. **The system seals.**
3-8	D bentonite 165 mm. Pre wetted bentonite.	10/0	0.94	1	1	1,000	1,600/3,600	3.5% salt	Piping at 1,600 kPa. After 12 h resttime new pressure ramp. Clay pressed out at 3,600 kPa.
3-9	D bentonite 165 mm. Pre wetted bentonite.	5/5	0.94	1	1	1,000	5,000	3.5% salt	Some “internal piping” during the pressure ramp. **The system seals.**
3-10	D bentonite 165 mm. Pre wetted bentonite.	5/5	0.94	1	1	1,000	4,600	3.5% salt	Repeating test 3-9 “Internal piping” during the pressure ramp. **The system could not take 5 MPa.**
3-11	D bentonite 165 mm. Pre wetted bentonite.	5/5	0.94	1	1	1,000	5,000	3.5% salt	Repeating test 3-9 “Internal piping” during the pressure ramp. **The system seals.**
3-12	Drainage tube under block. Pre wetted bentonite.	10/10	0.94	Controlled (7days)	Controlled	1,000	1,700/800	3.5% salt	Pre test with drainage tube. The system can not stand the fast pressure build up. Max 800 kPa after 20 days.
3-13	Pre wetted bentonite.	10/10	0.94	–	–	1,000	5,000	3.5% salt	After pre wetting of the slot, sample had no access to additional water. Water pressure was increased after 3 months.
3-14	Drainage tube, 5 mm axial slot. Pre wetted bentonite.	4/0	0.94	Controlled	Controlled	Controlled	5,000	3.5% salt	Sr block=94% The bentonite can withstand 5 MPa after 20 d

Test results

Detailed results are shown in Appendix B and a brief summary is provided below.

Test 3-1 and 3-6. These tests were performed with centred blocks and a pellet-filled slot with a width of 35 and 15 mm respectively. Tap water was used in these tests. Test number 6 also included pre-wetting of the slot.

Results: In none of the tests could the bentonite seal and withstand the water pressure applied. The specimens could, after 2 weeks of passive maturation, withstand a water pressure of 150 kPa (3-1) and 450 (3-6). After about 2 weeks of testing, the water pressure applied was increased to 350 kPa and 1,900 kPa, respectively. (Appendices B1 and B6).

Test 3-2. The blocks were placed directly on the tunnel floor with a 2 mm gap remaining at the top. Tap water was used in this test. After a maturation period of two days, a pressure ramp of 1 MPa/h was applied up to maximum 5 MPa.

Results: After some internal piping, the bentonite could withstand the applied water pressure. The arrangement for measuring the axial load was too weak in this test and the distance blocks moved several mm when the full water pressure was reached. At the beginning of the test, the water pressure could only act on a limited area in the periphery of the distance block, "the active surface", but after the movement this area increased dramatically and the water pressure could act on the whole cross-section, which resulted in an increase in the measured axial load, see more detailed information in Section 7.7. (Appendix B2.)

Test 3-3. The test layout in 3-2 with its 2 mm slot was able to handle the extreme test conditions. However, the installation of distance blocks with such a narrow slot is probably very difficult. In order to improve the layout and test the limits, the block diameter was reduced, giving a radial slot of 5 mm at the top. Tap water was also used in this test. After a filling time of two days, a pressure ramp of 5 MPa/h was applied.

Results: Internal piping occurred during the pressure ramp. The bentonite could withstand a maximum water pressure of 820 kPa before flow occurred. (Appendix B3).

Test 3-4. This test had the same test layout and test conditions as in test 3-3. In order to improve the sealing potential of the bentonite, it was decided to pre-wet the slot at the start of testing (see Section 7.3.4) and by doing so give the whole bentonite surface around the distance block access to water for 24 hours, before ramping up the water pressure (in the earlier test, water was filled from the supercontainer section bottom and reached the upper parts after about 48 h).

Results: Internal piping took place a number of times during the pressure ramp. The bentonite could withstand a maximum water pressure of 5 MPa after about 30 hours. (Appendix B4).

Test 3-5. The same test layout and test conditions as in test 3-4 but the initial slot at the top was increased to 10 mm.

Results: The bentonite could not withstand the water pressure. New pressure ramps were applied a number of times during the two-week testing period. After two weeks the specimen could withstand 4.2 MPa. (Appendix B5).

Test 3-7. The same test layout and test conditions as in test 3-4 (5 mm slot at the top) was used except that instead of tap water, water with 3.5% salinity was used.

Results: The bentonite could withstand the water pressure applied. The salt water increased the swelling rate and hence the sealing ability of the clay. It would seem that at the rather high densities applied, the use of salt water to pre-wet the system is preferable. The test also included an intentional movement of the fixing ring. Eight days after the test was started, a planned movement of the fixing ring by about 4.5 mm was made. The distance blocks were unable to withstand the 5MPa water pressure and they moved slowly towards the new location of the ring. Despite the movement of the blocks there was no water leakage. The behaviour is also described in Section 7.7. (Appendix B7).

Test 3-8. The upper slot was again increased to 10 mm (same test layout as in 3-5) but in this test the water used had a salinity of 3.5%.

Results: The bentonite could initially only withstand about 1,600 kPa water pressure. After 12 hours of rest to allow the development of radial swelling pressure, a new pressure ramp was applied. This time, the bentonite was able to withstand a pressure of 3,600 kPa. At this pressure, a movement of clay gel occurred and material was squeezed out around the fixing ring. (Appendix B8).

Test 3-9. The same test conditions were applied as in 3-8 but the blocks were centred in the tunnel (5 mm slot).

Results: The bentonite could withstand 5 MPa water pressure. There was some internal piping during the pressure increase but no throughflow occurred. (Appendix B9).

Test 3-10 and 3-11. Test number 3-9 was repeated twice.

*Result*s: Similar results were achieved in all three tests but Test 3-10 could only withstand 4.6 MPa before leakage occurred around the fixing ring. There was internal piping in all three tests during application of the pressure ramps. This test layout is probably the limit for the ability of the bentonite to seal under these extreme conditions. (Appendices B10 and B11).

Test 3-12. This was a pretest carried out in order to test the technique of using a drainage tube (see Section 7.3.5). The advantages were that both the water inflow and the water pressure increase rate could be controlled. The bentonite blocks were centred giving a 10 mm slot between the block and the rock. The filling time was set at 7 days, at the end of which a pressure ramp of 1 MPa/h was applied.

Results. The specimen could initially only withstand a maximum hydraulic pressure of 1.7 MPa. A new attempt was made 12 days later and the specimen could now only withstand 0.8 MPa. The applied pressure ramp was probably too fast. The retrieval of the drainage tube was also tested and in order to extract the steel tube (D=6mm) a force of 1.1 kN was needed. This test layout was later repeated in the 3 m-long system, see Section 7-2, but in this test the water pressure was increased in stages over a period of 2 weeks. (Appendix B12).

Test 3-13. This test included centered blocks with a radial slot of 10 mm. The slot was pre-wetted using water with a salt content of 3.5%. After initially flooding the slot, the specimen did not have access to additional water.

The test simulated the case when bentonite is installed in a dry tunnel. After the pre-wetting, it is possible that there will be no access to additional water and a re-distribution of the available water will take place. One aspect of particular importance in this test was monitoring the time-dependent development of the radial swelling. The test is valuable for understanding the possibility of preventing spalling.

Results: The test was run for almost four months. The radial swelling pressure was fairly constant at the three points throughout testing (250–500 kPa). Before test termination, the bentonite tightness against the rock was tested by applying an air pressure (up to 5 bars) in the supercontainer section. This also allowed for a check to be made of whether there was any leakage along the bentonite/rock interface. It was not possible to detect any leakage using this method. The same pressure test was repeated with water and a pressure ramp of 1 MPa/h was applied. After a number of internal piping events, it was determined that the swollen bentonite could withstand 5 MPa. (Appendix B13).

Test 3-14. This was the first test in which bentonite blocks with a high degree of saturation were tested. The bentonite blocks had an initial water ratio of 22% (Sr=94%). The blocks were placed directly on the floor of the test cell resulting in a slot width of 4 mm at the top. A drainage tube was installed in order to control the water pressure in the supercontainer section. The test simulated the design alternative using tight distance blocks that are cut into three segments before installation. In this design alternative the surfaces between the blocks are inclined, which means that the segments could be pushed into position with the bentonite in contact with the rock. The narrow slot between the bentonite and the rock in the test simulates the roughness of the rock. In addition, this test also included an initial axial slot of 5 mm between the supercontainer and the first distance block.

Results: The water pressure was increased in steps, and after about 20 days the bentonite could withstand a water pressure of 5 MPa. (Appendix B14).

7.3.4 Pre-wetting of slot

After a number of tests, it was obvious that the bentonite had difficulty in swelling and sealing the bentonite/rock slot during the short period available in these test conditions. In order to improve the potential for the bentonite to seal the slot within the prescribed time, it was decided to introduce a technique for pre-wetting of the slot.

The technique used involved two tubes passing through the fixing ring, one at the bottom and one at the top, see Figure 7-3. The lower tube is used for filling and the upper for de-airing. In the laboratory tests performed, a simple sealing was done around the innermost distance block, i.e. against the supercontainer and around the fixing ring, by applying a silicone bead. Under real conditions, this could probably be done by using bentonite gel with suitable water content. This sealing technique will, however, need to be demonstrated as being appropriate in a full-scale situation.

The main advantage of this technique is that the whole bentonite surface will gain access to water immediately after the test starts, which means that the time available for swelling and sealing increases. Thus, by the time the naturally inflowing water fills the empty space around the supercontainer, the bentonite will have already swelled and the potential for the distance plug to withstand the subsequent water pressure rise is increased.

The technique has been tested in a number of laboratory tests and has been found feasible.

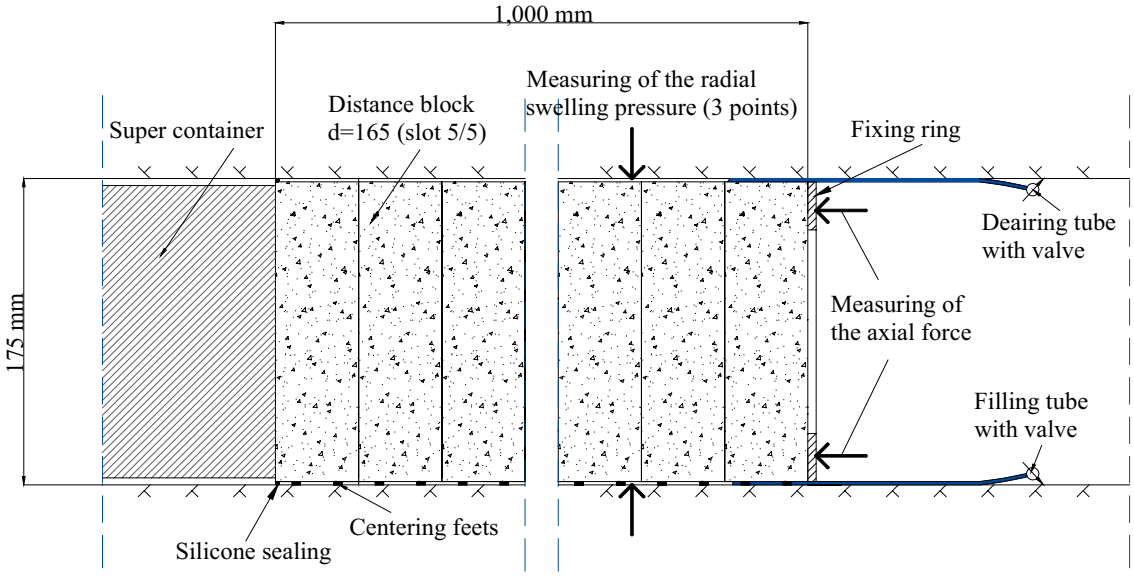

Figure 7-3. *Schematic diagram showing the technique for pre-wetting of the outer slot.*

7.3.5 Use of drainage tube

One conclusion after performing 10–11 tests in the 1-meter test equipment is that the maximum gap between bentonite and rock which the bentonite could seal within the prescribed time, including pre-wetting of the slot, is about 5 mm. The installation of distance blocks on a full-scale basis, with a diameter only 10 mm smaller than the tunnel diameter, was judged to be very difficult.

In order to improve the installation process, it was decided to use a drainage tube to control the water pressure conditions in the supercontainer section, see Figure 7-4. The tube should be led through the fixing ring, under the distance blocks and into the supercontainer section. With this tube it will be possible to control the water pressure and increase it in steps to the selected level. The bentonite will also have time to swell and seal the slot before the water pressure is applied.

The technique of using a drainage tube has been demonstrated in a number of laboratory tests and found to be potentially feasible. With this technique it was possible to double the bentonite/rock gap from 5 mm to 10 mm (see test results in Section 7.4).

7.3.6 Retrieval of drainage tube

A prerequisite for using the technique involving the use of drainage tubes is that the tubes be retrievable. The technique tested to accomplish this has been to extract the tube in steps, with a healing time of several days between each step, in order to give the bentonite time to swell and seal the remaining hole.

In two of the tests performed in the 3 m-long test equipment, see Section 7.4, the retrieval of the wetting tube was carefully tested. In each of the tests retrieval was tested by pulling the tube out in three steps and at the same time measuring the force required to do so. The test arrangement is shown in Figure 7-5. During the extraction of the tube, water pressure continues to be applied inside the tube in order to fill the volume left after withdrawal with water.

The tubes in the pull-out tests were made of stainless steel (EN 1.4436) and had an outer diameter of 6 mm and a wall thickness of 1 mm. With an ultimate tensile strength of 490 MPa for the tubes, the maximum load that could be applied was calculated to about 8 kN. The results of the force measurements during tube retrieval are shown in Figures 7-6 and 7-7. The results of the two tests are very similar. The maximum force needed was about 7 kN in both tests, which is very close to the ultimate strength limit of the tubes.

In the full scale situation, it is very important that the strength of the tubes be high enough to avoid any risk of tube rupture.

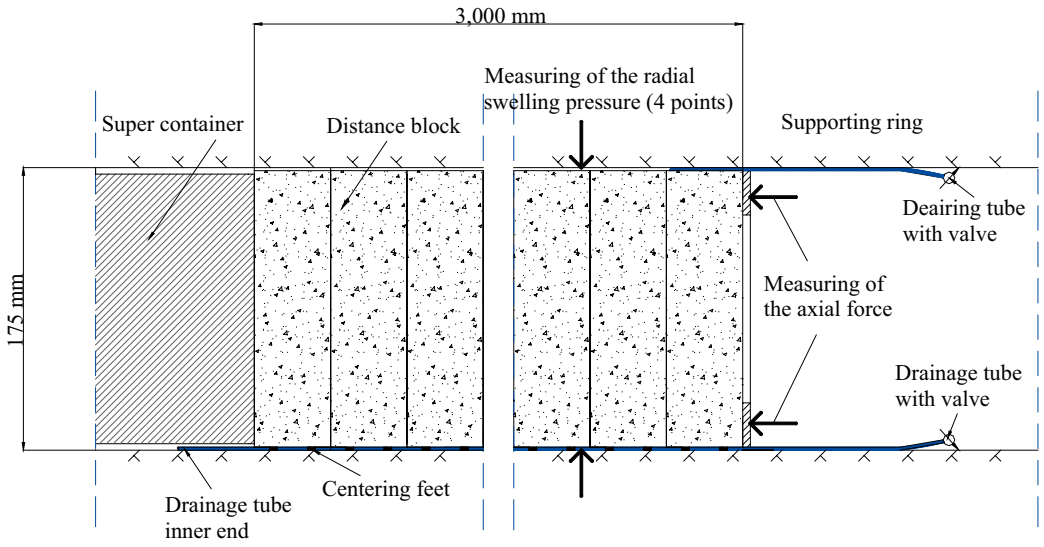

Figure 7-4. Schematic diagram showing the technique of using a drainage tube in order to control the water pressure in the supercontainer section.

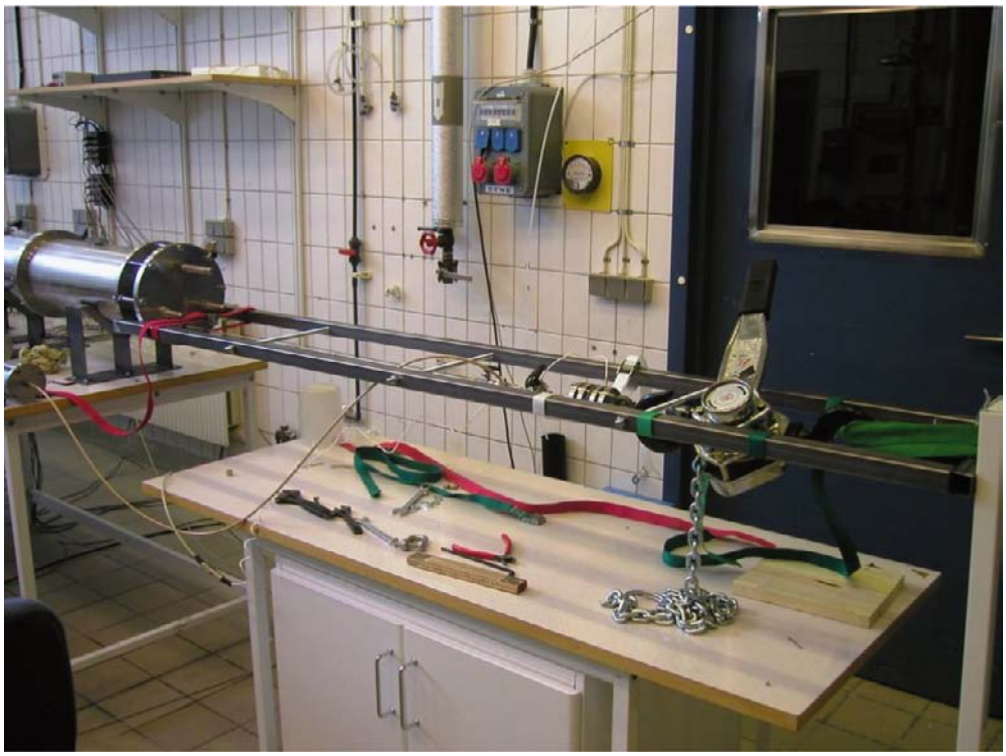

Figure 7-5. *Test arrangement used to extract the drainage tube from the bentonite.*

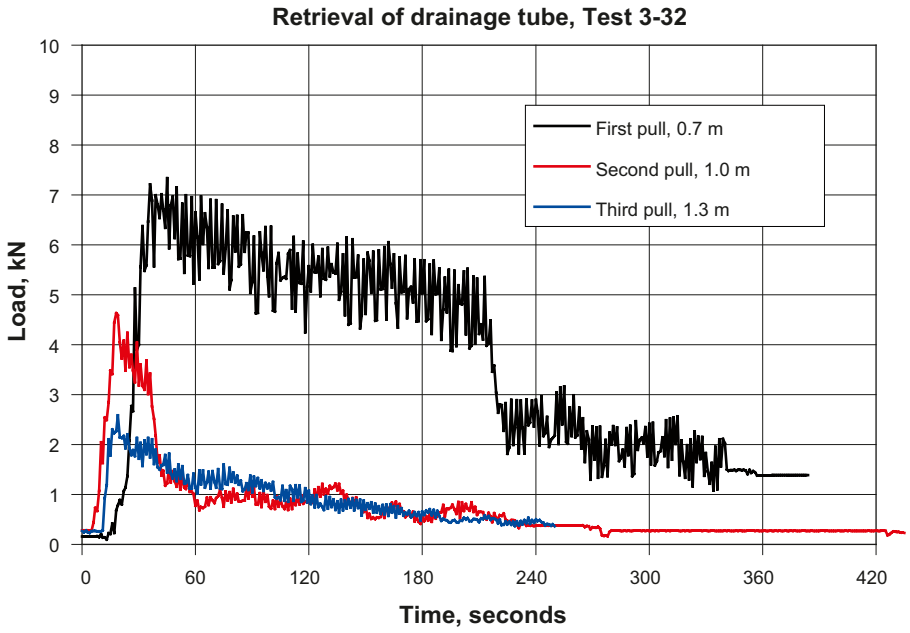

Figure 7-6. *Diagram showing the measured load during retrieval of the drainage tube in Test 3-32. After the first pull, the bentonite had a healing time of about 5 days (to swell and seal the remaining hole) and an additional 1 day after the second pull.*

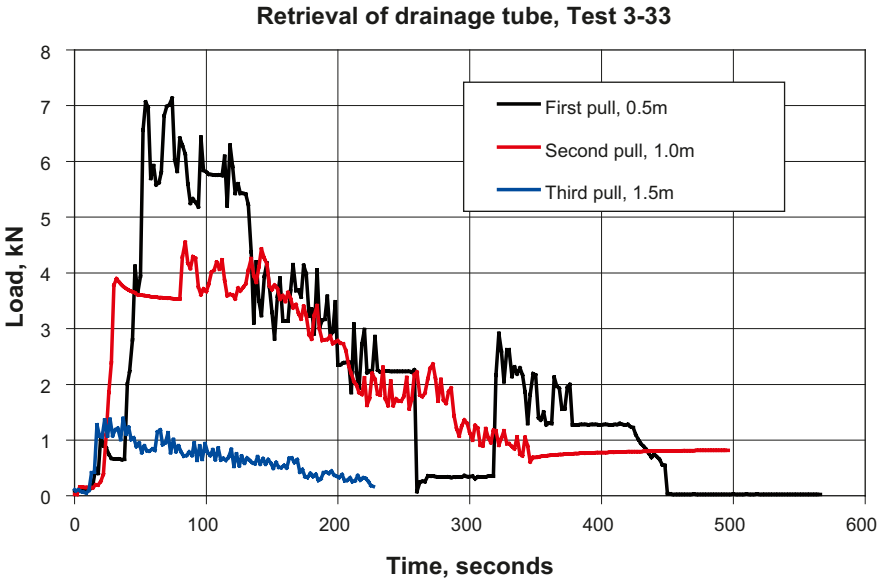

Figure 7-7. *Diagram showing the force needed in order to retrieve the drainage tube in Test 3-33. The tube was pulled out in steps. After the first pull, the bentonite had a healing time of about 3 days (to swell and seal the remaining hole) and an additional 1 day after the second pull.*

7.3.7 Example of more detailed test results, Test 3-9

Test description

The bentonite blocks in this test were centred by steel "feet" and the radial slot width between the blocks and the rock was 5 mm, see Figure 7-3. The water used in the test had a salt content of 3.5%. The space around the "distance blocks" was filled with water by the use of two tubes passing through the fixing ring, one in the bottom and one in the top. The lower tube was used for filling and the upper for de-airing. In the laboratory tests performed, simple sealing has been carried out around the innermost distance block, i.e. against the supercontainer and around the fixing ring, by applying silicone.Under real conditions; this can probably be done by using bentonite. A total amount of 3.3 litres was injected over a period of 15 minutes. The empty space in the supercontainer section was filled in 24 hours and then a pressure ramp of 1 MPa/hour was applied.

Result

Figure 7-8 shows the measured water pressure and the injected water volume. Some internal piping occurred during the pressure ramp, but after about 6 hours the applied water pressure had reached 5 MPa. Unfortunately, there was a drop in water pressure during testing caused by the pressure equipment running out of water. The axial load on the fixing ring was measured during the test and also the radial swelling pressure, Figure 7-9. These results were strongly influenced by the applied water pressure.

Photos were taken during the dismantling of the tests; see Figures 7-10 and 7-11. The pictures clearly illustrate that the slot has been filled with swelling bentonite.

This test layout was repeated in Tests 3-10 and 3-11 with almost similar results.

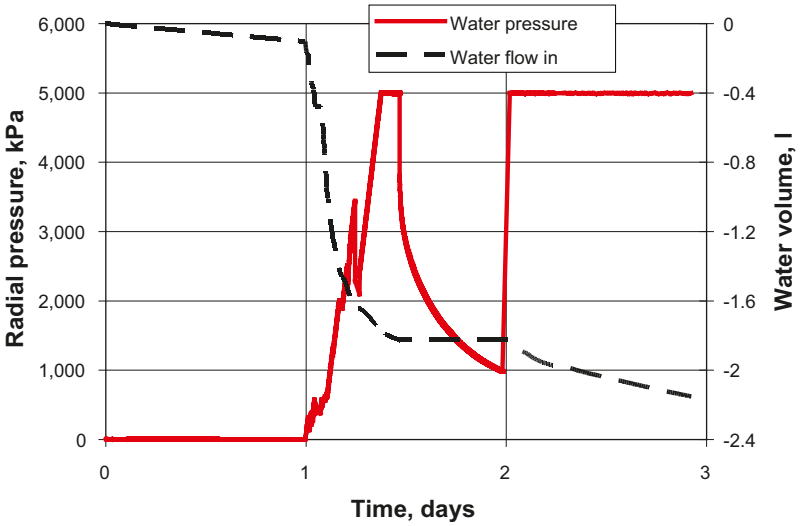

Figure 7-8. *Graph showing the water pressure build-up and the water inflow. After 24 hours, a pressure ramp was applied. The dip in pressure after about 36 hours is a result of the pressurising device being emptied of water.*

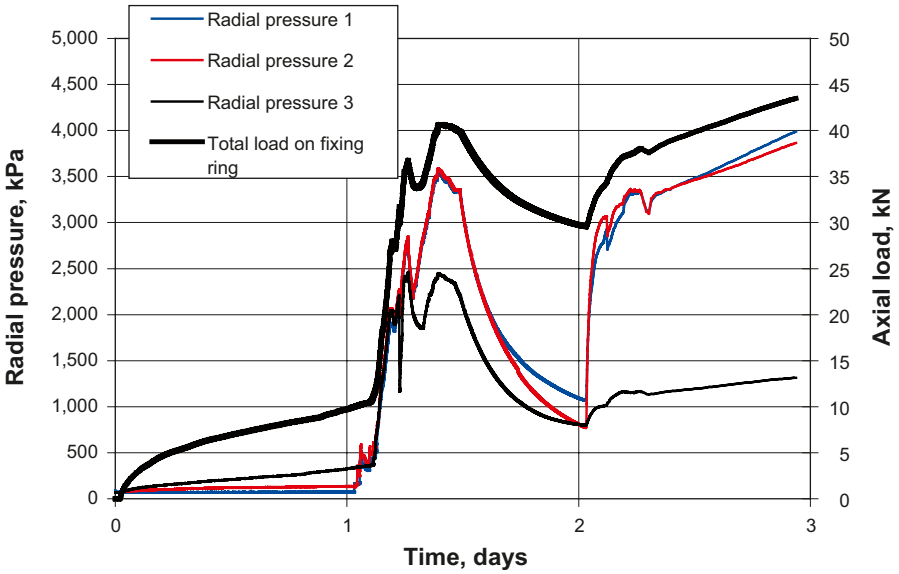

Figure 7-9. *Graph showing the axial load and the radial swelling pressure that were measured at three points.*

Figure 7-10. *Photo showing the outermost distance block just inside the fixing ring. The pre-wetted slot has been filled with swelling bentonite. Since there was no access to additional water from the "rock" after the filling, and the inner parts of the distance block were dry and had a high suction capacity, i.e. affinity for water, there was a redistribution of the available water in the slot. This redistribution resulted in minor cracks occurring in the periphery.*

Figure 7-11. *Photo of the middle of the specimen about 0.5 m from the supercontainer. The water ratio was determined in several positions with the following results: Outermost 5 mm = 30%, next 5 mm = 29%, next 5 mm = 28%, next 5 mm = 25%, and in the centre = 17%.*

7.3.8 Example of more detailed test results, Test 3-13

Test description

The bentonite blocks were centred by mean s of steel "feet" and the radial slot width between the blocks and the rock was set at 10 mm. The water used had a salt content of 3.5%. The space around the "distance blocks" was pre-wetted in the same way as in Test 3-9. A total volume of 5.5 litres was injected over a period of 30 minutes. Once the slot between the bentonite blocks and the rock had been filled, the inlet valve was closed and the specimen had no further access to additional water. This test layout was designed in order to study the mechanical interaction between the distance block and the simulated rock surface when no additional water is available. This interaction is important for the critical issue of thermally-induced spalling (brittle failure induced by thermally-induced tangential stresses occurring in the tunnel walls). The issue is of interest for both DAWE and BD.

Results

The specimen was left for 112 days with no further access to additional water. The assumption was that the water in the slot would be drawn deeper into the buffer blocks resulting in desiccation and cracking of the bentonite in the outer parts. This phenomenon has been previously induced in similar tests performed in another project (Lasgit). The results of these earlier tests showed that there were clear indications of desiccation and cracking of the surface, but also that a small swelling pressure was still acting on the walls. The radial pressure measurements in this test, Figure 7-12, showed a similar behaviour. The slot was pre-wetted and the bentonite had no access to additional water. After 112 days a water pressure ramp of 1 MPa/h was applied in the supercontainer section. A mechanical pressure from the clay was still acting on the rock surface after 112 days.

Before termination of the test, it was decided to test how well the section had been sealed. Two different methods were used:

1. Air pressure was applied in the supercontainer section (increased in steps up to 5 bar). Any possible leakage was detected by using a flow meter on the air inlet. The results of this test showed that the section seemed to have been sealed.
2. Then a water pressure ramp of 1 MPa/h was applied, Figure 7-13. After a certain amount of internal piping, the bentonite could withstand a water pressure of 5 MPa. The graph shows the applied water pressure and the water inflow. During the applied pressure ramp, internal piping occurred several times. The amount of water injected was fairly large, which showed that a lot of empty voids had been formed. Twenty-four hours after starting the pressure ramp, the maximum pressure, 5 MPa, was reached. The dip in pressure after about 8 hours is a result of the fact that the pressurising device ran out of water in the middle of the night.

Photos were taken during the dismantling of the tests, see Figures 7-14 and 7-15. In Figure 7-15, no cracks could be seen on the bentonite surface since the space from the cracks had been water filled during the final sealing test. The final testing of the sealing by applying a water pressure of course influenced the bentonite (0.8 l water was injected), and earlier cracks may have healed.

The test showed that in spite of there being no additional water available for 3.5 months of system curing and the presence of voiding (~0.8 l), a significant swelling pressure was (250–500 kPa) acting on the "rock" surface throughout the entire test. The reason for this is probably the cracks that can be seen in Figure 7-14 which were formed during the water redistribution. The cracks were formed in rather dense unsaturated bentonite, which transported inner radial stress to the "rock" surface.

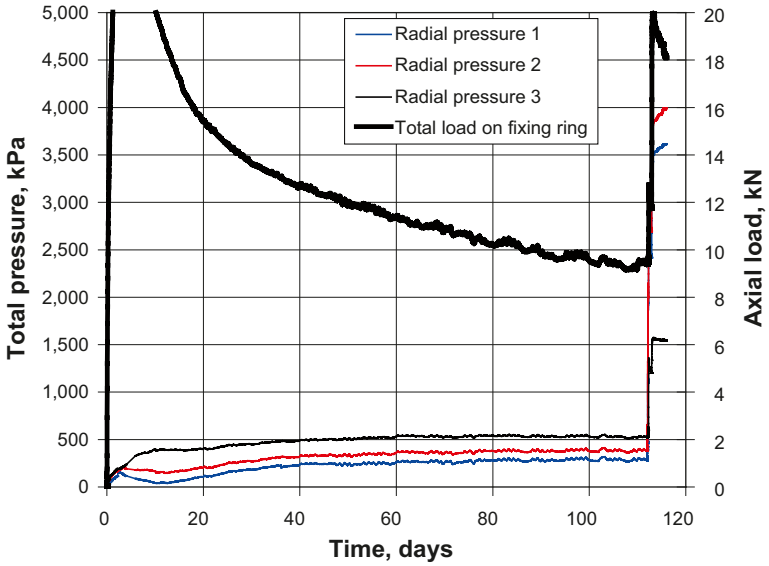

Figure 7-12. *Graph showing the axial load on the fixing ring and the radial swelling pressure measured at three points as a function of time.*

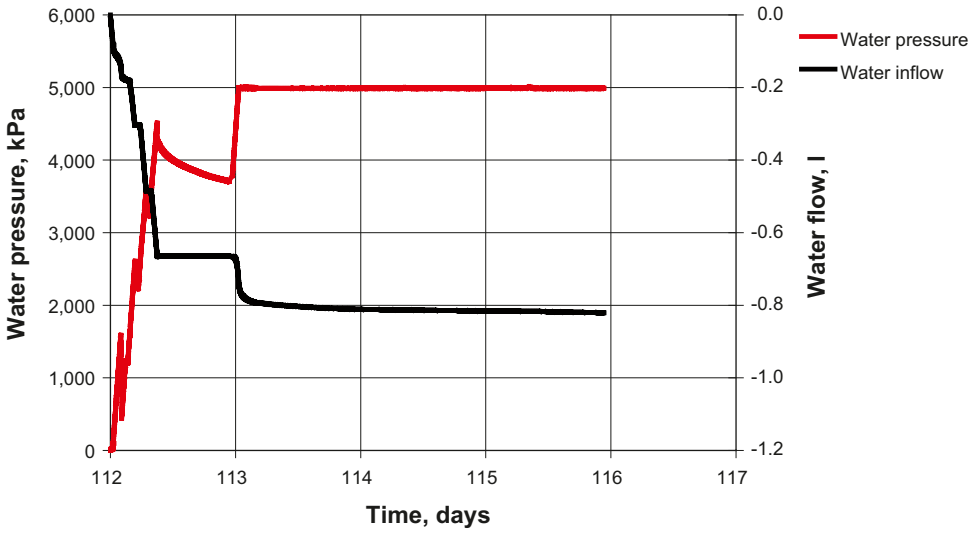

Figure 7-13. *After 112 days without access to additional water, a water pressure ramp was applied*

Figure 7-14. *Photo showing the outermost distance block after removal of the fixing ring.*

Figure 7-15. *Photo of the middle of the specimen showing part of the outer surface.*

7.4 Scale tests in 3 m-long test equipment

7.4.1 General

The tests described in Section 6.3 had a length limited to about 1 m in the 1:10 scale equipment. In order to study the influence of the test length on the piping phenomena, a new test setup with a length of 3 m was constructed and as of 2007 five tests have been conducted using this system, see Figure 7-16.

7.4.2 Experimental set-up

The equipment used is very similar to that used in the 1 m tests, the only difference being the test length, which is 3 m.

The test variables are the same as those described in Section 7.2.2.

7.4.3 Summary of results

A compilation of the tests performed in the 3 m-equipment is provided in Table 7-3. All five tests were performed using water with a 3.5% salt content. Test 3-31 was performed using bentonite blocks with a water ratio of 13.5%, while Test 3-32 and Test 3-33 were performed using blocks with a water ratio of 17%. Tests 3-34 and 3-35 were performed using bentonite blocks with a high initial water ratio (21.7%, Sr=94%).

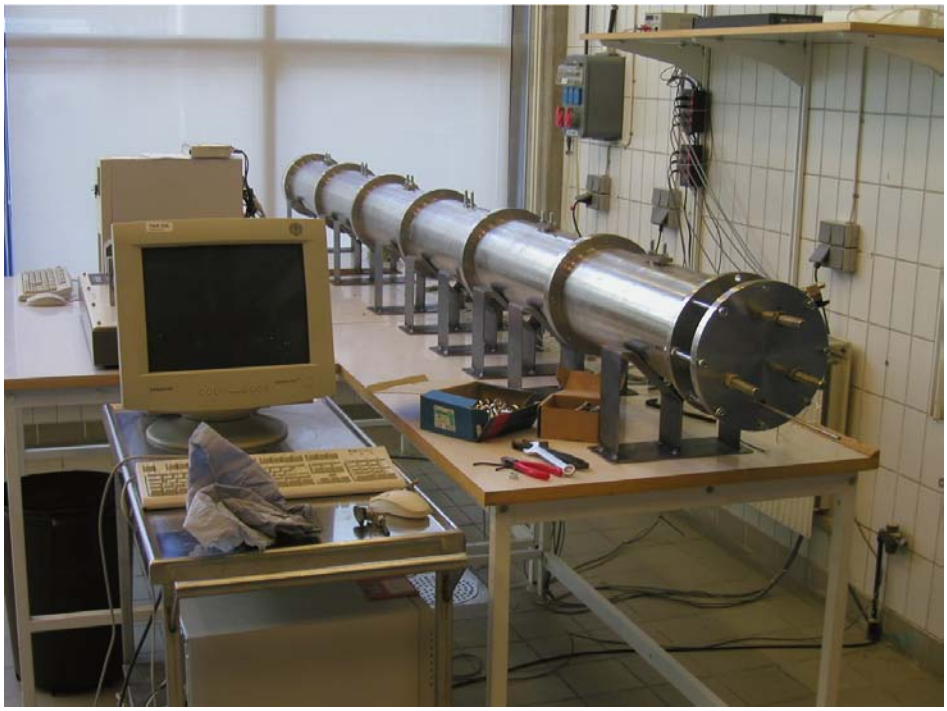

Figure 7-16. *Photo from the laboratory showing the 3 m test equipment.*

Table 7-3. Summary of tests performed in the 3 m-setup.

Test	Arrangement	Slot top/ bottom mm	Test length m	Filling time Days	Filling rate scale 1:1 l/ min	Water pressure increase rate kPa/h	Maximal pressure kPa	Water type	Comments
3-31	D bentonite 155 mm centred blocks	10/10	3.08	1	1	1,000	1,100	3.5% salt	The bentonite could not withstand the pressure. A new ramp was applied after 11 days, with the same result.
3-32	D bentonite 155 mm Drainage tube	10/10	3.10	Controlled	Controlled	Controlled	5,000	3.5% salt	The buffer could after 2 weeks withstand 5 MPa.
3-33	D bentonite 155 mm Drainage tube	10/10	3.08	Controlled	Controlled	Controlled	5,000	3.5% salt	The buffer could after 2 weeks withstand 5 MPa. Repetition of test 3-32.
3-34	D bentonite 171 mm	4/0	1.46	10	0.1	1,000	1,600	3.5% salt	The buffer could not withstand the water pressure. Only a small part of the initial slot was wetted during filling time.
3-35	D bentonite 173 mm Drainage tube, 5 mm axial slot	2/0	1.44	Controlled	Controlled	Controlled	5,000	3.5% salt	The buffer could after 3 weeks withstand 5 MPa. Small leakage along drainage tube.

Test 3-31. This was the first test performed in the 3 m equipment. In order to study the influence of the test length, it was decided to perform a test with a large bentonite-rock gap similar to the tests carried out in the 1 m equipment, where sealing was not accomplished. The blocks were centred in the "tunnel" having a radial slot of 10 mm to the walls. The slot around the distance block was pre-wetted. A total volume of about 16 litres of water was injected for a period of 30 minutes. 24 hours after the test started, a pressure ramp of 1 MPa/h was applied. This test corresponded to Test 3-5, although the latter only had a slot at the top of the distance block.

Results: The bentonite could not withstand the applied water pressure and piping occurred at a pressure of about 1,100 kPa. There was a leakage of bentonite gel around the fixing ring. A new attempt was made 11 days later with almost the same result. (Appendix B15.)

Test 3-32. The same test layout as in the previous test, i.e. centred blocks with a 10 mm radial gap to the walls. In order to control the water inflow and the water pressure increase rate in the supercontainer, a drainage tube was installed. The tube was led through the fixing ring, under the blocks and into the supercontainer section. The slot around the blocks and the empty space in the supercontainer section were filled up with water, about 16 liters over a period of 30 minutes. The water pressure was then increased in steps over a period of 2 weeks up to a maximum pressure of 5 MPa. The test also included retrieval of the drainage tube. This test corresponded almost to Test 3-12, although the water pressure rate was not controlled in that test.

Results: Two weeks after starting the test, the bentonite could withstand a water pressure of 5 MPa. After one additional week the retrieval of the drainage tube started. The tube was extracted in steps in order to give the bentonite time to heal. There was no leakage of water or gel during the retrieval. (Appendix B16).

Test 3-33. In order to study the repeatability of the experiments, test number 3-32 was repeated with exactly the same test layout.

Results: Almost the same results as in the previous test. Two weeks after the test started, the bentonite could withstand a water pressure of 5 MPa. After one additional week, retrieval of the drainage tube started. The tube was extracted in steps in order to give the bentonite time to heal the remaining hole. There was no leakage of water or gel during the retrieval. (Appendix B17.)

Test 3-34. In order to produce blocks with a dry density that yields a saturated density of 2,000 kg/m^3 and at the same time produce the comparatively narrow gaps between bentonite and rock that are needed, it will be necessary to have distance blocks with a low initial density and a rather high initial water ratio, 20–24%, see Section 4.5. This test was the first to be performed with blocks of this quality. The blocks were placed on the floor of the tunnel, i.e. not centred. The gap at the top between bentonite and the walls was 4 mm. The test simulated the design alternative using tight distance blocks, which need to be installed using a special technique. The small bentonite/rock slot in the test simulated the roughness of the rock. The water used in the test had a salt content of 3.5%. A constant flow was applied in the supercontainer section in order to simulate a void filling rate of 10 days. After 10 days, a pressure ramp (1 MPa/h) was applied.

Results: The bentonite could withstand a water pressure of about 1,700 kPa before piping occurred. A new test was carried out 2 days later with almost the same result.

When dismantling the test, it was discovered that during filling, the bentonite closest to the simulated supercontainer had swollen and sealed, and prevented water from pouring into the slot between the distance blocks and the rock. The bentonite blocks were unaffected at the top of almost the entire tube; see Figure B18-3 in Appendix B18.

Test 3-35. The test was performed with almost the same test layout as in the previous test. In order to avoid the problem of only wetting parts of the void, a drainage tube was installed. The blocks were placed on the floor of the tunnel, i.e. not centred. The gap at the top between the bentonite and the walls was 2 mm. The small bentonite/rock slot in the test simulates the roughness of the rock. In addition, this test also included an initial axial slot of 5 mm between the supercontainer and the first distance block.

The water pressure was increased stepwise to a maximum of 5 MPa.

Results: Due to the rather tight installation, it was assumed that the water pressure could be increased faster than in previous tests. Piping did, however, occur after 7 day at a water pressure of 4,000 kPa and after 11 days at 3,200 kPa. Twenty-one days after starting the test the maximum pressure, 5,000 kPa, was reached but was not maintained for a substantial time due to the fact that the pressurizing equipment was needed for other tests. Since the water pressure was being controlled externally, this kind of pressurization could be similarly regulated in a real installation. (Appendix B19.)

7.4.4 Detailed Results of Test 3-31

A schematic drawing of the test layout is shown in Figure 7-3. Table 7-4 provides input data on the installed bentonite blocks.

Test description

The bentonite blocks used in the test were centred by steel "feet" and the slot width between the blocks and the rock was 10 mm. The water used in the test had a salt content of 3.5%. The space between the super container and distance blocks was filled with water by use of the lower filling tube, see Figure 7-3. The upper tube was used to de-air the volume. A total volume of 16 litres was injected over a period of 30 minutes.

Table 7-4. Properties of the bentonite blocks installed in test number 3-31.

Installed distance blocks	
Raw material	MX-80, cores from full scale blocks
Water ratio, %	13.5
Bulk density, kg/m^3	1,950
Dry density, kg/m^3	1,720
Degree of saturation, %	60.6
Void ratio	0.617
Diameter of the blocks, mm	155
Test length, mm	3,080
Total mass of blocks installed, kg	112.05
Calculated data	
Final dry density, kg/m^3	1,343
Void ratio	1.078
Saturated density, kg/m^3	1,861

Results

Twenty-four hours after starting the test, a pressure ramp of 1 MPa/h was applied in the supercontainer section, Figure 7-17. The distance blocks could not withstand this, which resulted in piping at a pressure of 1,000–1,100 kPa. A new attempt was made after an additional 11 days, which resulted in piping at a lower pressure of about 800 kPa.

It was obvious that the bentonite had not managed to seal the slot. The measured radial swelling pressure was rather low, 50–150 kPa, Figure 7-18. As shown in Figures 7-19 and 7-20, the bentonite swelled and filled the slot, but the density at the perimeter was rather low.

At the end of testing, the water ratio was determined at several locations (Table 7-5), and in the outermost 5 mm of the cylinder it was found to be about 50%. Assuming that the specimen was saturated, this corresponds to a saturated density of 1,750 kg/m^3. The low radial swelling pressure (100–150 kPa) this density can yield is obviously too low to seal the slot for the high hydraulic pressures (5 MPa) expected.

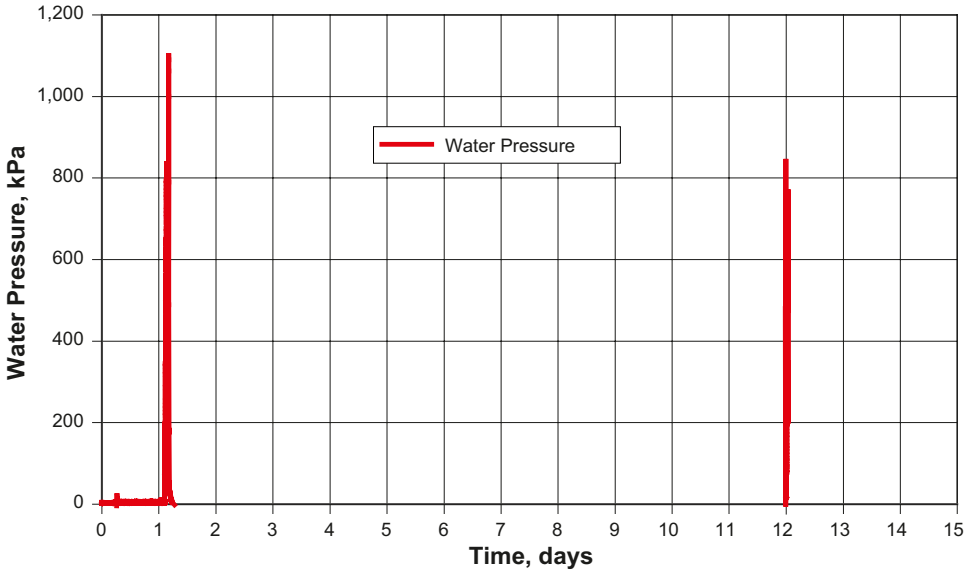

Figure 7-17. *Graph showing the water pressure applied during the test plotted vs. time. After 1 day, a pressure ramp of 1 MPa/h was applied. The specimen could withstand maximum 1,100 kPa before piping occurred. A new pressure ramp was applied after 11 more days with a similar result.*

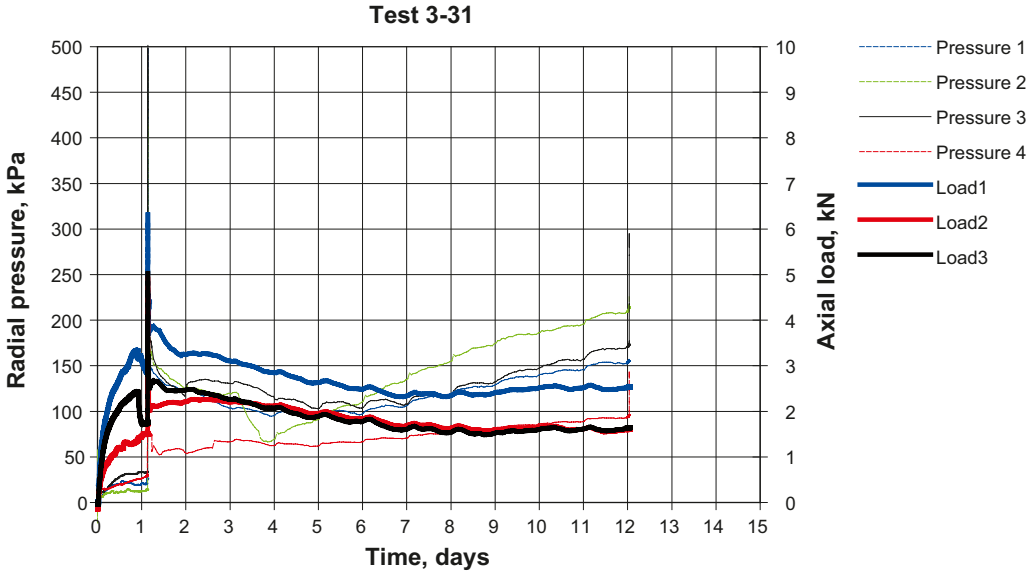

Figure 7-18. *Graph showing the measured swelling pressure at four different points and the axial load as a function of time.*

Figure 7-19. *The surface just inside the supercontainer dummy. The outer ring-shaped "active surface" can be clearly identified.*

Figure 7-20. *Photo taken during dismantling of the test, about 1.5 m from the supercontainer section. The dark ring has a width of 35–40 mm. The water ratio was determined at several locations, see Table 7-5.*

Table 7-5. Water ratio of samples taken in the wet area in a section 1.5 m from the pressurized side of Test 3-31, see Figure 7-20.

Upper part	Outermost 0–5 mm	54.5%
	5–10 mm	49.2%
	10–15 mm	44.9%
	15–30 mm	37.6%
Bottom part	Outermost 0–5 mm	46.5%
	5–10 mm	43.6%
	10–15 mm	38.4%
	15–30 mm	29.5%

7.4.5 Detailed results of Test 3-32

A schematic diagram of the test layout is shown in Figure 7-21. The input data for the installed bentonite blocks is shown in Table 7-6.

Test description

The water used in the test had a salt content of 3.5%. The empty space around supercontainer and distance blocks was filled with water by use of the lower drainage tube. The upper tube was used to de-air the slot. A total of 16 litres was injected over a 30 minute period. The slot had access to additional water from the supercontainer section via the drainage tube.

The bentonite blocks in the test were centred by steel "feet" and the slot width between the blocks and the rock was 10 mm. A photo from the installation is shown in Figure 7-22. The difference from Test 3-31 was the drainage tube that was led through the fixing ring, under the distance blocks and into the supercontainer section. This tube could be used to control the water pressure in the container section and also to "feed" the bentonite with additional water during the maturation phase. This was done by a stepwise increase of the water pressure over a period of about two weeks. This method is intensive and can probably only be used in sections with high water inflow.

Table 7-6. Summary of properties of the bentonite blocks used in Test 3-32.

Distance blocks	
Installed distance blocks	
Raw material	MX-80, cores from full-scale blocks
Water ratio, %	17.0
Bulk density, kg/m^3	2,090
Dry density, kg/m^3	1,790
Degree of saturation, %	85.2
Void ratio	0.553
Diameter of the blocks, mm	155
Test length, mm	3,099
Total mass of blocks installed, kg	123.6
Calculated data	
Final dry density, kg/m^3	1,414
Void ratio	0.973
Saturated density, kg/m^3	1,907

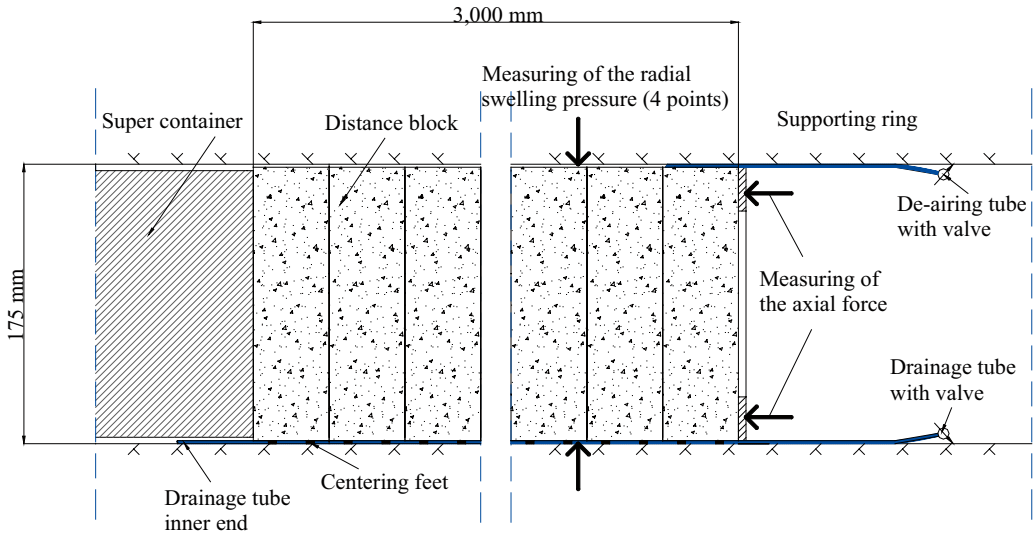

Figure 7-21. *Schematic view of the test layout.*

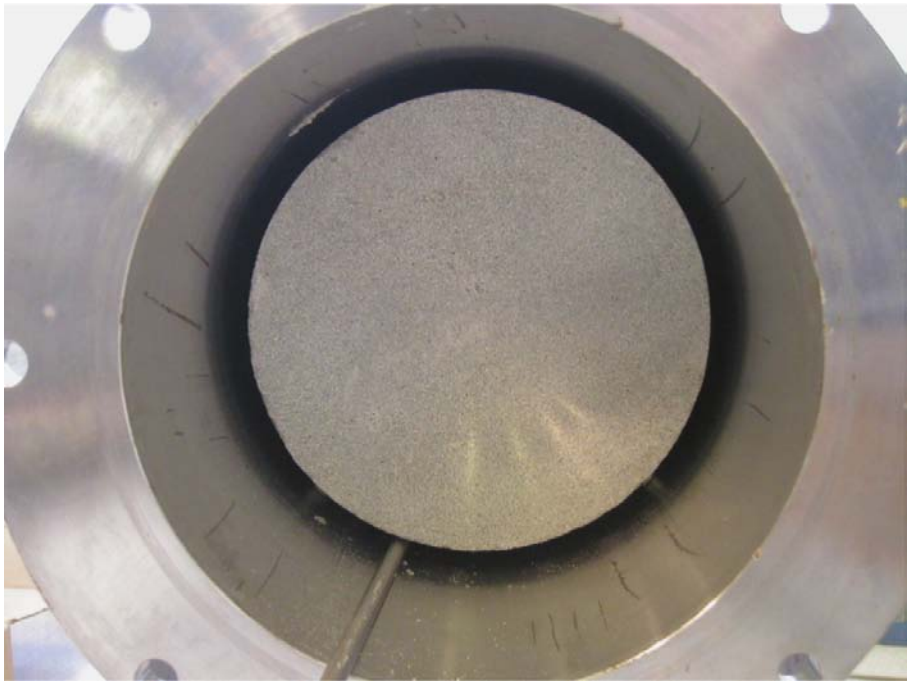

Figure 7-22. *Photo from the installation showing the centred bentonite block and the drainage tube at the bottom.*

Results

This test provided very good results. After 14 days, the water pressure applied had reached 5 MPa and the system was still tight (Figure 7-23). The axial load on the fixing ring and the radial swelling pressure were also measured, and are presented in Figure 7-24.

The retrieval of the steel tube used for wetting was also tested and a detailed description is provided in Section 7.3.6.

During the test, it was observed that the outermost bentonite block, i.e. the one closest to the fixing ring, had been forced through the fixing ring, Figure 7-25. There was a very obvious deformation of the bentonite, but there were no visible cracks in the block.

During test dismantling, samples were taken from the clay at different points and the water ratio and density were determined, see Table 7-7. The water ratio distribution at the outermost parts is shown in Figure 7-26.

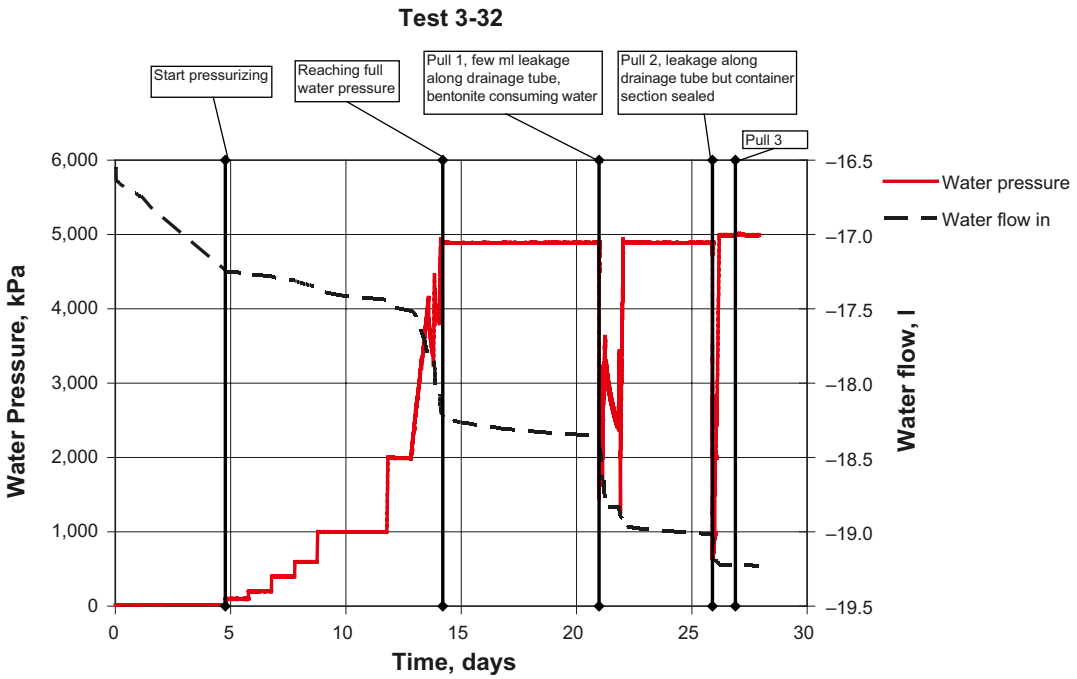

Figure 7-23. *Applied water pressure and injected water volume plotted vs. time.*

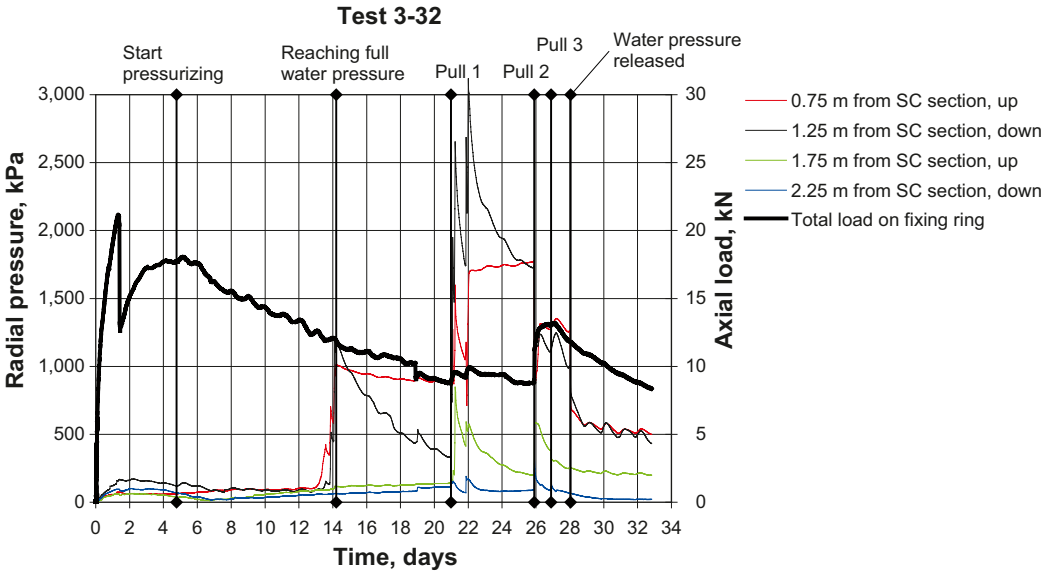

Figure 7-24. *Axial loads on the fixing ring and radial swelling pressure plotted vs. time.*

Figure 7-25. *Photo showing the fixing ring after termination of the test. The block closest to the ring has been squeezed through the central hole in the steel ring. The total displacement was estimated to be 12 mm.*

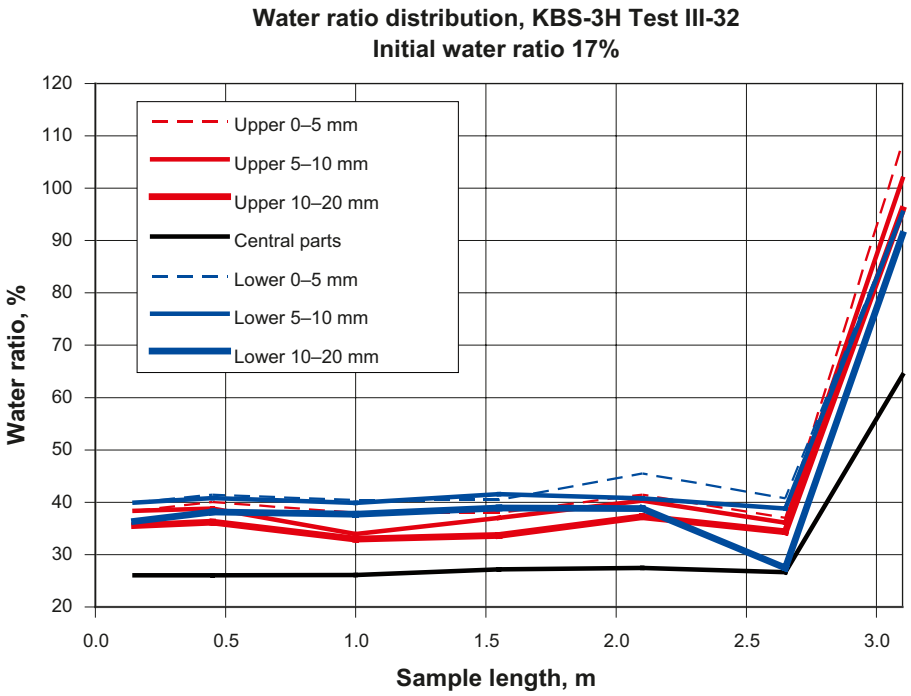

Figure 7-26. Plot showing water ratio as a function of the distance from the fixing ring.

Table 7-7. Water ratio and density of samples taken in a section 15 cm from the fixing ring.

Cut taken about 15 cm from fixing ring Examination starts at top	w %	Bulk density g/cm³	Sr %	e	Dry density g/cm³
0–10 mm	38.38	1.84	97.5	1.094	1.33
10–20 mm	35.59	1.83	93.2	1.061	1.35
20–30 mm	31.43	1.86	90.8	0.963	1.42
30–40 mm	29.20	1.92	93.3	0.870	1.49
40–50 mm	27.90	1.94	93.3	0.832	1.52
50–60 mm	27.11	1.94	91.3	0.825	1.52
60–70 mm	26.45	1.94	90.6	0.811	1.53
70–87.5 mm	26.07	1.95	90.7	0.799	1.54
87.5–105 mm	26.18	1.95	90.6	0.803	1.54
105–115 mm	27.00	1.95	92.2	0.814	1.53
115–125 mm	27.77	1.94	92.7	0.833	1.52
125–135 mm	30.03	1.90	92.4	0.904	1.46
135–145 mm	31.05	1.89	92.6	0.932	1.44
145–155 mm	33.49	1.81	88.6	1.051	1.36
155–165 mm	36.38	1.82	93.3	1.084	1.33
165–175 mm	39.96	1.80	95.5	1.163	1.29
Starting values on bentonite core	17.00	2.09	85.2	0.553	1.79

7.5 Tests performed in a transparent tube

7.5.1 General

In order to visualize the piping phenomena, a few tests have been performed in a transparent tube. These tests are intended to increase the understanding of the piping phenomena by allowing flow paths to be directly observed.

The test equipment was similar to that used in the 1:10 scale test. A key difference was that there was no measurement of radial pressure or axial load on the fixing ring. A schematic diagram is provided in Figure 7-27 and a photo in Figure 7-28. The equipment consists of a tube with an inner diameter of 100 mm made of PC (poly carbon). The wall thickness of the tube is 25 mm and the length is 1 m. The maximum allowable inner pressure is 2 MPa. This means that the tests must be designed so that piping, if it occurs, starts at a pressure of less than 2 MPa.

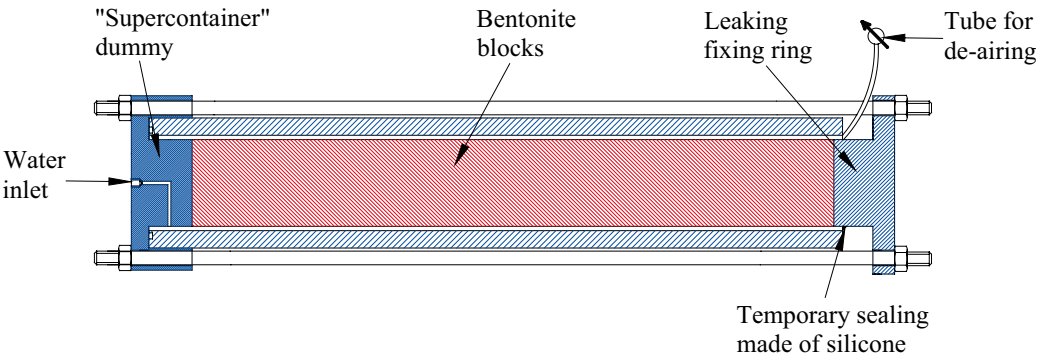

Figure 7-27. *Schematic diagram of the test equipment.*

Figure 7-28. *Photo showing the transparent tube test equipment.*

7.5.2 Experimental set-up

The original plan was to perform a number of tests where piping was achieved at different pressure levels. This could be done with different initial slot widths and different maturation times before applying the water pressure. Since only two tests have been performed, the data on the effects of varying environmental parameters are limited.

A compilation of the two tests is provided in Table 7-8.

Table 7-8. Compilation of test data.

Test	Bentonite	Water	Radial slot width (mm)	Time for maturation after filling the slot with water (Days)	Pressure ramp (kPa/h)	Maximum pressure (kPa)	Remark
1	Bulk density: 2,090 kg/m^3 Initial water content: 17%	3.5% salt	10	2	5,000	240	48 hours after the first pressure ramp, a new one was applied with almost the same results
2	Bulk density: 2,090 kg/m^3 Initial water content: 17%	3,5% salt	10	4	5,000	300	Nine days after the first pressure ramp, a new one was applied with almost the same results

7.5.3 Results

Test 1

During water filling of the slot, observations were made of how bentonite particles on the block surface would loosen from the block surface and then settle to the bottom, see Figures 7-29 and 7-30. At the end of the water filling process, a number of air pockets could be seen on the upper part of the slot. These air pockets could be seen throughout the entire test period, as can be seen in Figures 7-31, 7-32 and 7-33. During the water re-distribution (water from the outer slot is sucked into the inner parts), the shape of the air pockets changed.

Fourty-eight hours after pre-wetting of the slot started, a pressure ramp of 5 MPa/h was applied from the supercontainer section, Figure 7-34. When the water pressure reached about 240 kPa, piping occurred (the clay in the slot could not withstand the pressure and a channel was opened through which water could flow) as shown in Figure 7-35. The channel developed along the side of the tube where the material seemed to be very homogeneous and not as expected in the upper part where the air pockets were situated. After an additional 48 hours, a new pressure ramp was applied with almost the same result, Figure 7-36.

Figure 7-29. *Photo taken during the pre-wetting of the outer slot. Water has filled half way up and bentonite has discharged from the blocks and settled to the bottom.*

Figure 7-30. *Photo taken just after pre-wetting of the outer slot had finished . Bentonite has been discharged from the blocks and settled. Half the slot is still filled with clear water.*

Figure 7-31. *Photo taken from above about 0.5 hours after pre-wetting of the outer slot had finished. There are a number of air pockets present on the upper side.*

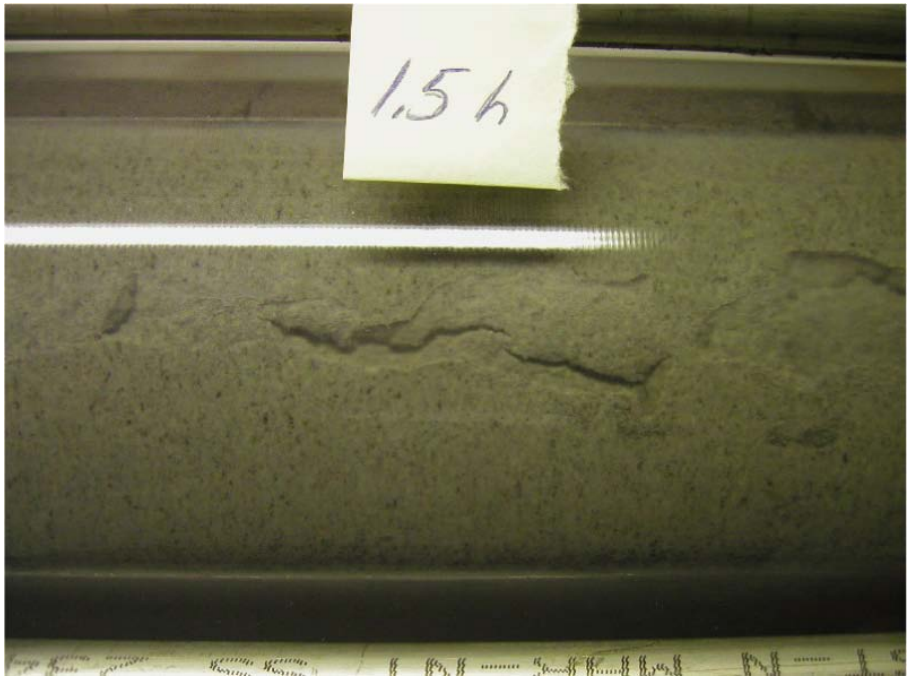

Figure 7-32. *Photo taken from above about 1.5 hours after pre-wetting of the outer slot had finished. The air pockets are still very clear.*

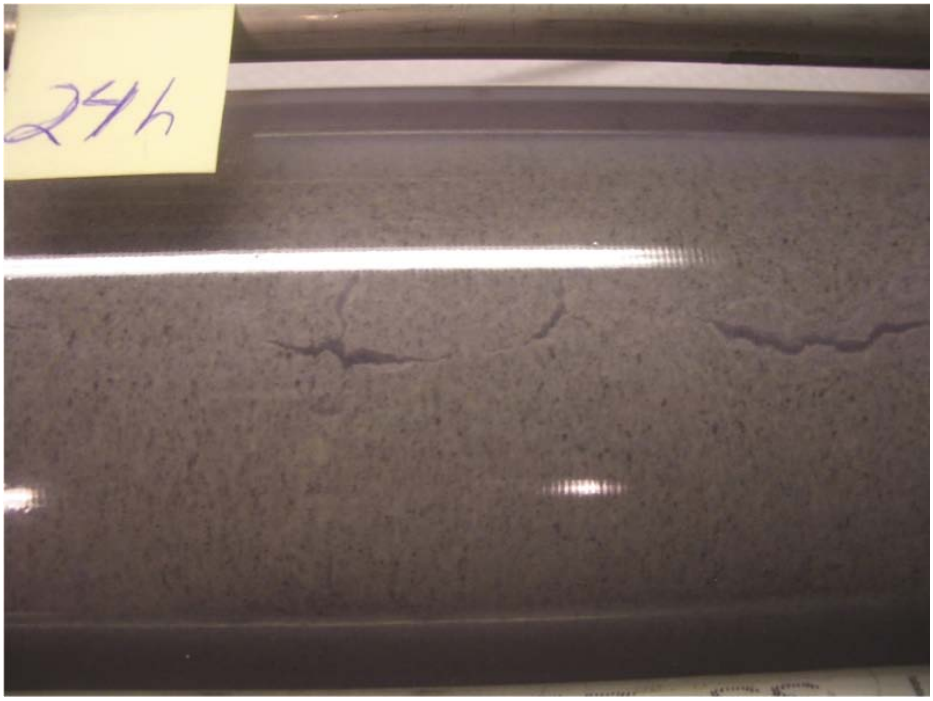

Figure 7-33. *Photo taken from above 24 hours after pre-wetting of the outer slot had finished. The air pockets are still very clear.*

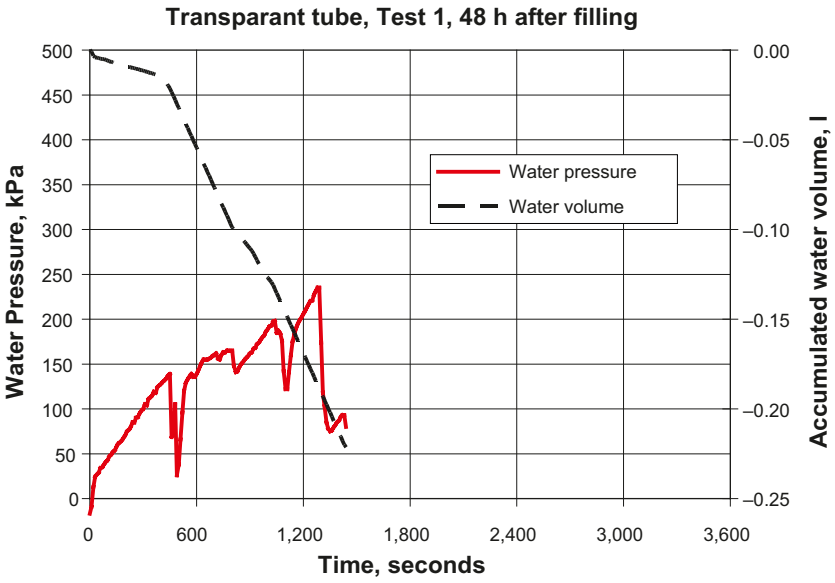

Figure 7-34. *Diagram showing the results of Test 1. Forty-eight hours after pre-wetting of the slot started, a pressure ramp was applied.*

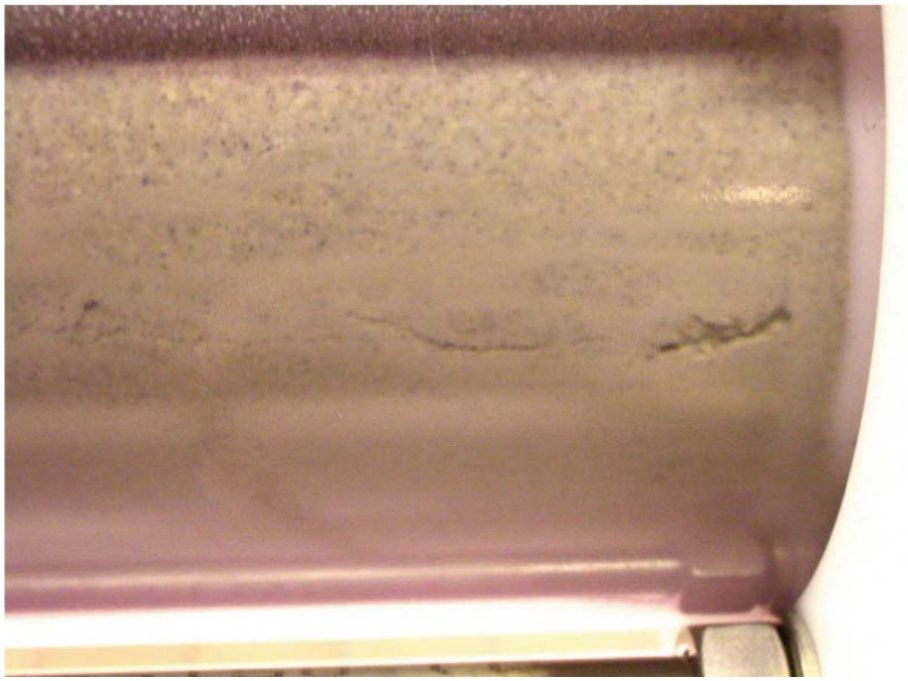

Figure 7-35. *Photo taken from side of tube showing the piping channel. For both applied pressure ramps, piping occurred in the same position.*

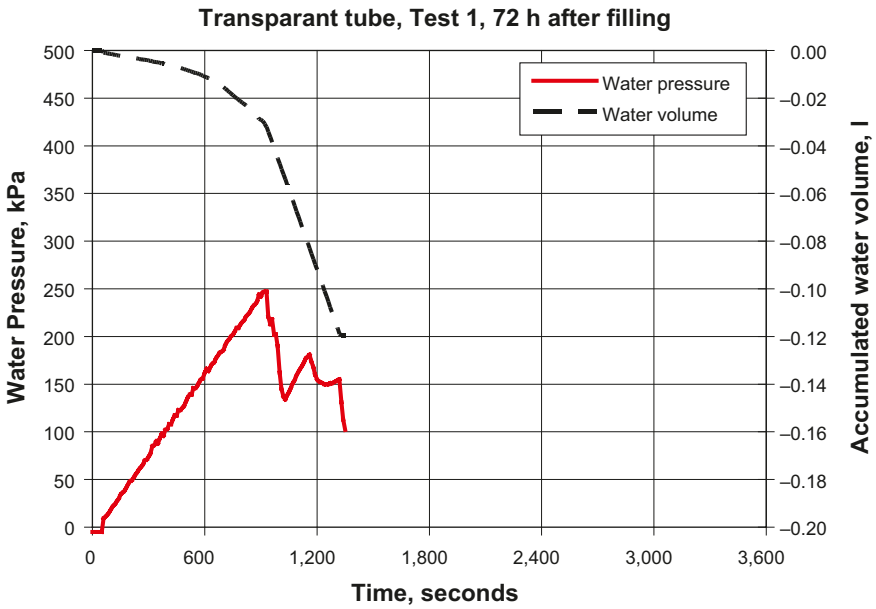

Figure 7-36. *Results of Test 1 when second pressure ramp was applied 72 hours after pre-wetting of the slot started*

Test 2

The layout of Test 2 was the same as for Test 1. In order to achieve piping at a higher water pressure, the time for homogenization was increased from 2 days to 4 days. The results of the tests were, in spite of this change, very similar. Piping was achieved at about 300 kPa (250 kPa in Test 1), Figure 7-37.

The increase in time in order to achieve piping at a higher water pressure from two to four days was obviously too small. The small difference depends probably on the fact that there is no access to additional water during the maturation time.

A new pressure ramp was applied 9 days after the test started with the same result, Figure 7-38. In this test too, the piping channel occurred in the same region.

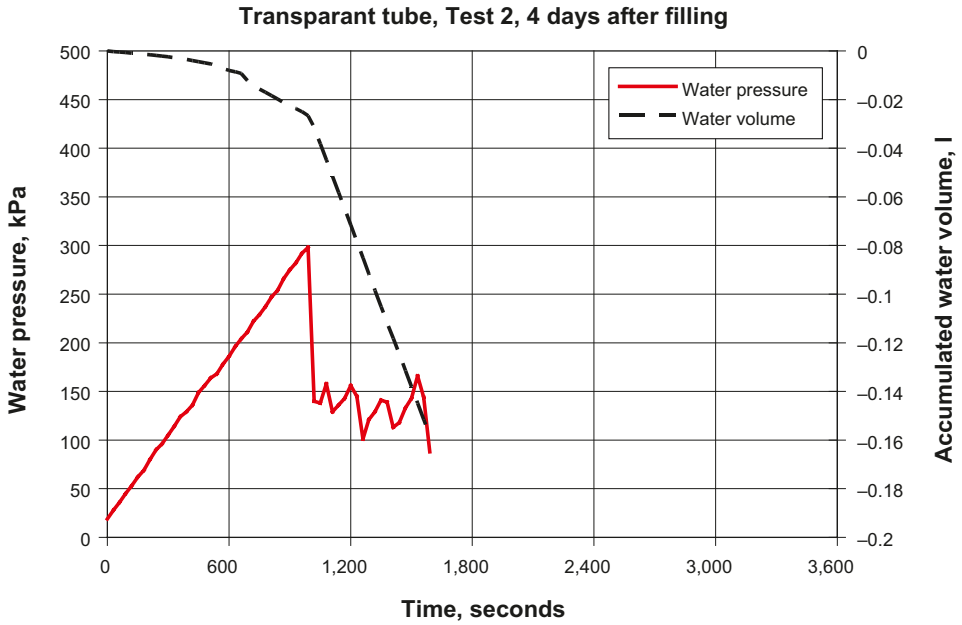

Figure 7-37. *Results of Test 2: 4 days after pre-wetting of the slot started, a pressure ramp was applied.*

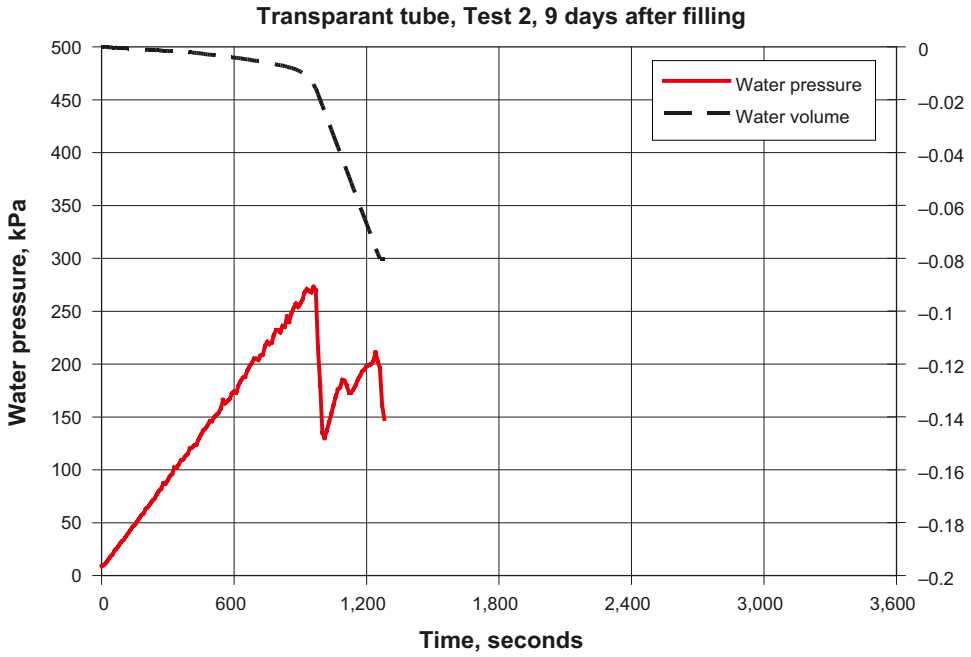

Figure 7-38. *Results from Test 2 in which a new pressure ramp was applied 9 days after pre-wetting of the slot started.*

7.6 Summary of all scale tests regarding sealing ability

7.6.1 General

A compilation of the test results is presented in Figures 7-39 and 7-40. These plots show the maximum water pressure the distance blocks could withstand before piping occurred within 2–3 days after the test started (the time is longer for the tests performed with drainage tube, i.e. under controlled water pressure conditions).

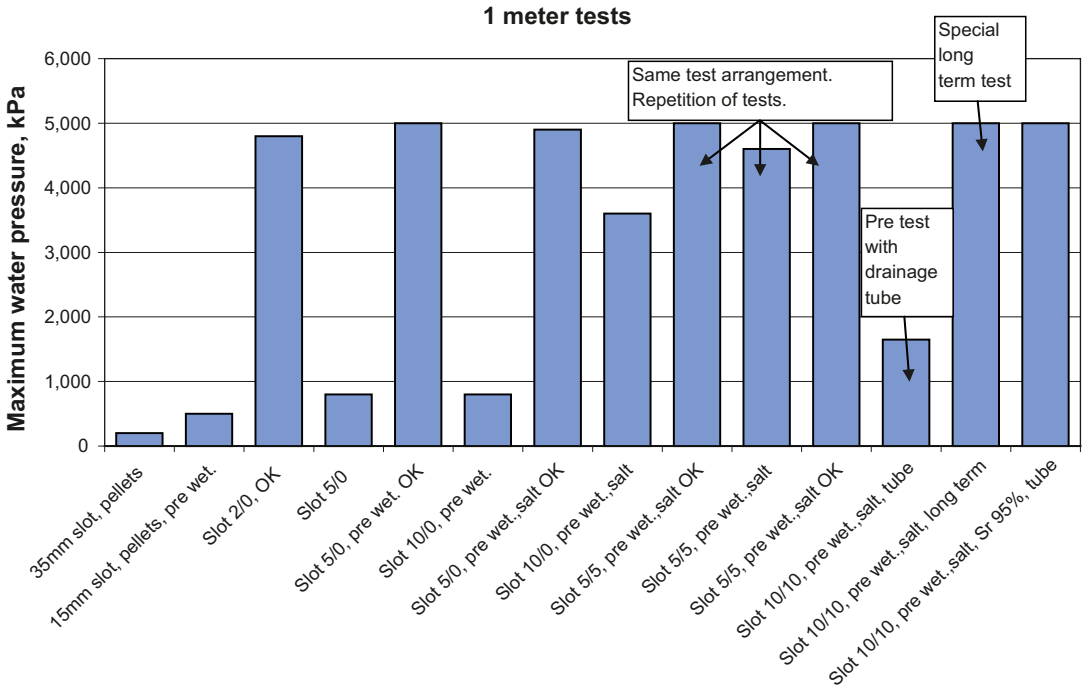

Figure 7-39. *Maximum water pressure that the installed distance blocks could resist in different test layouts before piping occurred. (The diagram shows the results of tests performed in the 1 m equipment).*

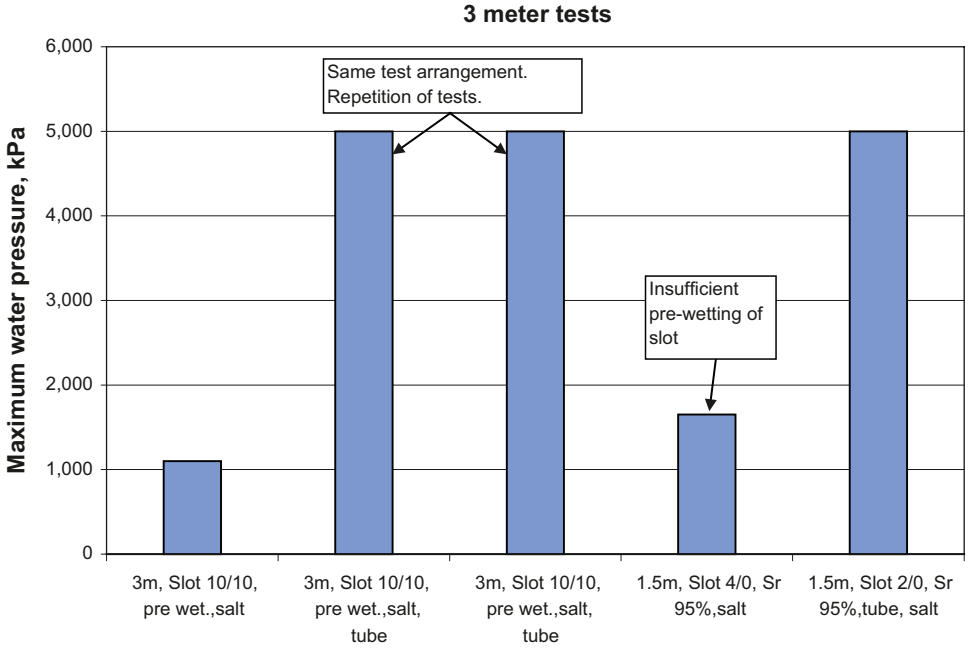

Figure 7-40. *The maximum water pressure that the installed distance blocks could resist at the different test layouts before piping occurred. (The chart shows the results from tests performed in the 3-m equipment.)*

7.6.2 Effect and extent of hydraulic pressure on distance block end surface

The extent of the hydraulic pressure exerted on the end of the distance blocks has also been investigated in these tests. The total force on the distance blocks and the sizing of the fixing rings in BD are proportional. The main uncertainty is whether the pressure is exerted on a narrow rim on the end surface, which is not covered by the supercontainer end surface, or whether it is possible that the pressure is exerted on the entire cross-sectional area.

The extent of the pressure depends on the behaviour of joints in bentonite and the initial gap between distance block and supercontainer. There are indications, from earlier investigations, that the pressure will be exerted on a rim that is less than 10 cm wide if the gap between distance block and supercontainer is 7 mm wide.

The phenomenon is investigated separately in special equipment, see Chapter 8, but data regarding the issue has also been evaluated from the piping tests in the 1 m and the 3 meter test equipment.

A summary of the measurements of the axial load on the fixing ring are provided in Figures 7-41 and 7-42. The following have been plotted:

- Measured load on the fixing ring before applying any water pressure, i.e. the load is the swelling pressure of the bentonite (blue columns).
- Measured load on the fixing ring at the maximum applied water pressure in the supercontainer section (purple columns).
- Calculated force, based on the applied water pressure and the "active surface" (the surface on which the hydraulic pressure can act) which for each sample was measured after test interruption, see example in Figure 7-19 (yellow columns).

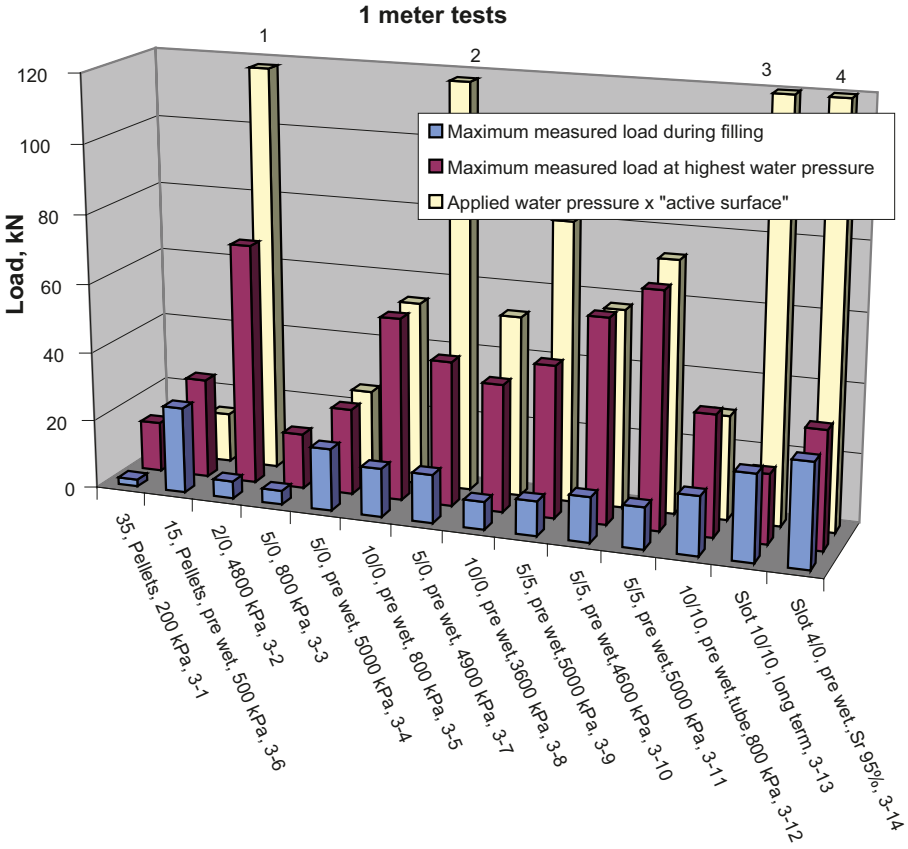

Figure 7-41. *Maximum axial load measured on the fixing ring during filling, at the highest water pressure and calculated load acting on an "active surface".*

The difference between the calculated load and that measured is the result of the friction between the bentonite and the rock. This means that the bentonite specimen length will strongly influence the load that can be taken by the friction, which can also be seen when comparing the measured load (purple columns in the middle) for the two test series, see Figures 7-41 and 7-42.

In four of the experiments performed in the 1 meter equipment (Figure 7-41) the water pressure had had access to the whole cross-sectional area that resulted in a maximum load of 120 kN (5 MPa water pressure acting on the whole cross-section area). The reason for the full access of water to the face was different in the four tests:

1. The installation of the load cells measuring the axial force was not robust enough in this test (3-2), which resulted in a small movement of the distance blocks and subsequent water filling of the resulting slot.
2. Test (3-7) included allowing a deliberate movement of the fixing ring during the test. This movement also caused a displacement of the distance blocks, which gave the water pressure access to the entire cross-section area.
3. Test 3-13 was a long-term test, running for about 4 months. In this test the whole cross-section area was also wetted.
4. Test 3-14 included an initial axial slot of 5 mm between the supercontainer and the first distance block. The slot simulates an unevenness of the supercontainer end plate.

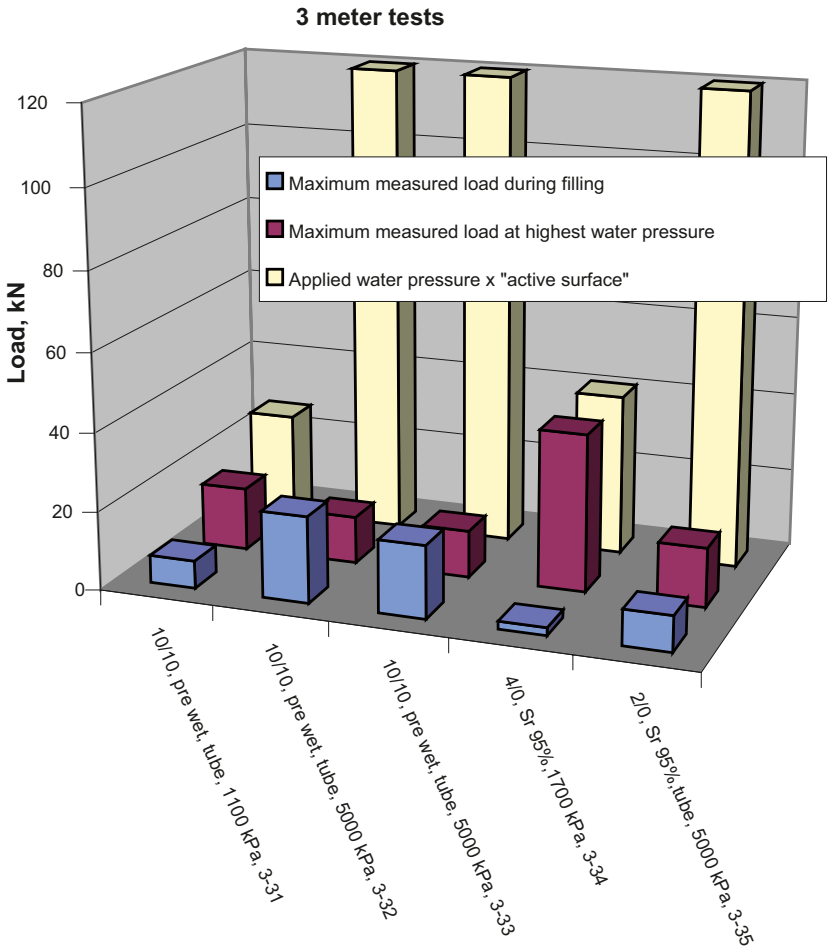

Figure 7-42. *The maximum axial load measured on the fixing ring .*

The measurements made of the axial load in the 3 m test equipment are shown in Figure 7-42. In the three tests where the bentonite sealed and could withstand 5 MPa water pressure, the active surface was similar to the whole cross-sectional area. The last test (3-35) included an initial axial slot between the supercontainer and the first distance block (same as in test 3-14), which gave the water pressure access to the whole cross-sectional area. Tests 3-32 and 3-33 both ran for a considerably longer time, 5 to 6 weeks, which could be one explanation for the complete watering (see also Figures B16-5 and B17-5 in Appendices B16 and B17 respectively, showing the water ratio distribution in the specimens). The measured total load on the fixing ring is, however, rather low. This is attributed to the fact that part of the load is taken up by the friction of the bentonite against the "rock".

7.6.3 Conclusions from the piping tests

The sealing ability of the distance blocks is limited under the severe conditions applied to them (water inflow of 1 l/min and water pressure increase rate of 1MPa/hour). The 14 tests carried out in the 1 m-long equipment and 5 tests in the 3 m-long equipment yielded the following conclusions:

- A pellet-filled slot wider than 1 cm does not function adequately under the conditions applied. The pellet density is too low and the pellets probably need more time to homogenize and increase the density by consolidation from the swelling of the bentonite blocks. Only one type of pellet was tested, but the behaviour will probably be similar regardless of the type of pellets used, provided the granularity and the final density are similar.
- When the blocks are placed directly on the floor of the deposition tunnel, leaving only a gap of 2 mm at the top, they will seal very efficiency (test only performed with tap water).
- A 5 mm slot, on one side or both sides (centred block), requires a pre-wetting of the bentonite, i.e. the slot needs to be filled with water in advance. During the subsequent water filling of the supercontainer section, the bentonite will have time to swell and seal the slot. However, after repeating this test layout three times (test 3-9, 3-10 and 3-11), it was obvious that this layout is very close to the limit of the sealing capacity.
- Installing blocks with a 10 mm slot with centred blocks is possible with special arrangements. Two tests have been performed in the 3 m equipment (Tests 3-32 and 3-33) using a drainage tube, which was led under the distance block into the supercontainer section. With this tube it was possible to control the water inflow and the water pressure in the container section. If the water pressure is increased in steps, it is possible to seal against a pressure of 5 MPa within 2 weeks. The test layout also includes a retrieval of the drainage tube. This has also been tested and seems to be feasible.
- The extent of the area on which the hydraulic pressure can act is still uncertain. The results of the scale tests, summarized in Figures 7-41 and 7-42, shows that when the water pressure had access to the whole cross-sectional area, the measured load on the fixing ring was considerably lower. There is a scale effect on this type of measurement and this may indicate a problem in full scale. If the diameter is doubled, it is uncertain whether the outer surface against the rock will also be doubled, but the cross-sectional area will be four times larger)

The results of these tests have led to the development of four different design alternatives for the distance blocks presented in Section 4.3.

8 Hydraulic pressure on distance block end surface adjacent to supercontainer

8.1 General

The phenomenon of load transfer from pressurized water through the distance blocks to the fixing ring was investigated earlier within the KBS-3H project. The phenomenon has also been investigated in connection with the study entitled "Piping through distance block tests" (see Chapter 7). In addition to these tests, a number of other studies have been completed on the problem and are reported in this chapter.

The uncertainties related to the transfer of the hydraulic pressure exerted on the end surface of the distance blocks and determining the total force on the distance blocks are important in the sizing of the fixing rings in the BD design. The principal uncertainty is whether the pressure is exerted on the narrow rim at the end of the distance block (area not covered by the supercontainer end surface), or whether it is possible that the hydraulic pressure acts on the whole end surface, see Figure 8-1.

The extent of the pressure transfer to the ends of the distance block also depends on the behaviour of joints in bentonite and the initial gap between distance block and supercontainer. There are indications from an earlier investigation that the pressure will be exerted on about a 10 cm wide rim if the gap between distance block and super-container is 7 mm wide /Börgesson et al. 2005/. This earlier investigation was conducted under different applied conditions (maximum inflow rate of 0.1 l/min and a maximum water pressure increase rate of 100 kPa/h to a maximum of 2 MPa).

The main aim of the new investigation was to measure the axial pressure between the lid of the supercontainer and the first distance block at different distances from the simulated rock surface and in so doing, determine the size of the "active surface" on which the hydraulic pressure acts.

The initial gap between the supercontainer end plate and the first distance block is calculated to be 5–6 mm, depending on unevenness of the steel plate and the bentonite and also on the difficulties in achieving a completely parallel installation. The influence of the initial gap width and how the "active area" changes with time are two important parameters that have been investigated.

Figure 8-2 shows the total force that must be taken by the fixing ring (at full scale) as a function of the width of the ring-shaped area on which the pressure acts, corresponding to "r" in Figure 8-1. The figures in the graph give no consideration to the fact that parts of the load will be taken by friction between the swollen bentonite and the rock surface.

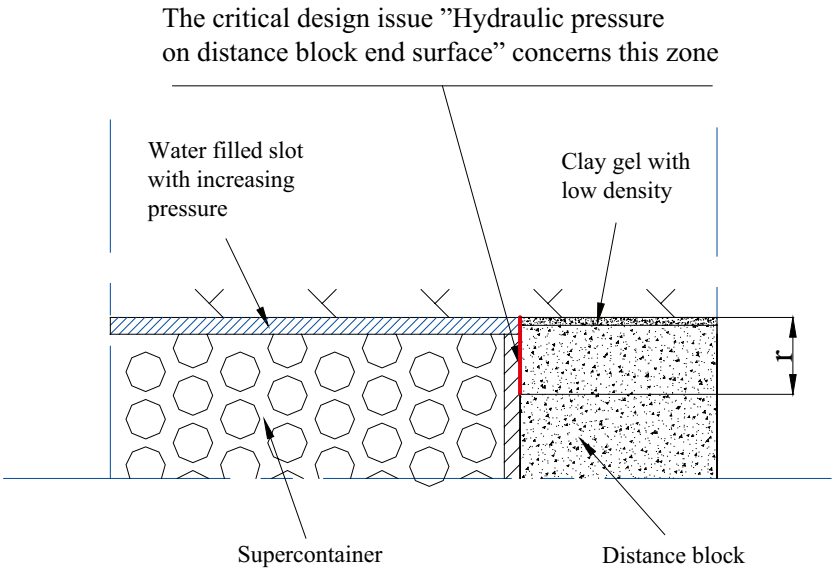

Figure 8-1. *Schematic diagram showing part of a section of the KBS-3H layout. The figure shows the zone where the critical design issue "Hydraulic pressure on distance block end surface" is relevant.*

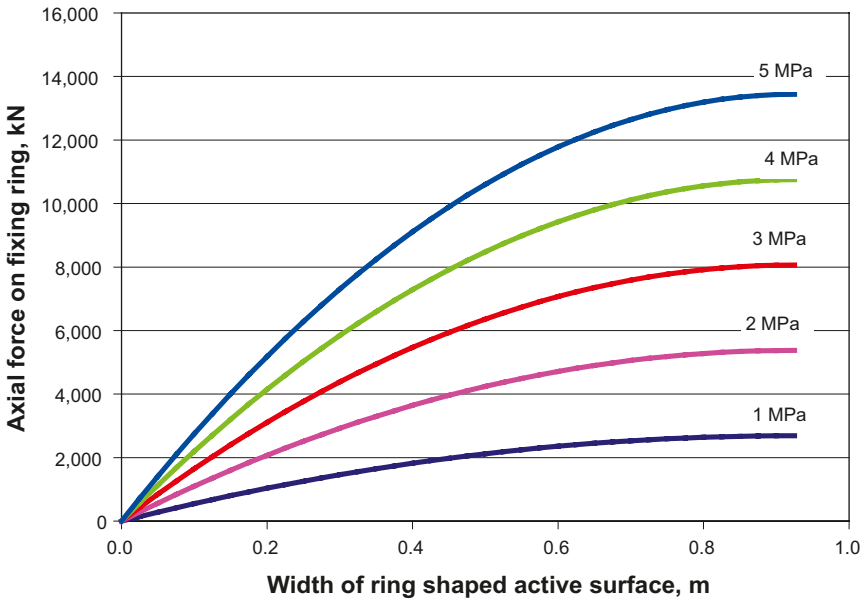

Figure 8-2. *Total force developed for different water pressures that must be taken by the fixing ring as a function of the width of the ring-shaped area on which the pressure acts ("r" in Figure 8-1).*

8.2 Experimental setup

The tests were performed using equipment specifically designed for the purpose in question and schematically described in Figure 8-3. The axial force on the fixing ring was measured in the same way as in the 1:10 scale tests. In addition, the equipment included a supercontainer dummy, on which a number of pressure sensors were mounted.

Bentonite blocks with an initial water ratio of 17% and a bulk density of 2,090 kg/m^3 have been used; see Table 6-1 in Chapter 6. Water with a salinity of 3.5% was used in all tests, see Section 6.2.

The bentonite blocks were installed with a small radial gap width at the top of about 2 mm. The parameters varied in the tests were:

- initial axial gap between distance block and supercontainer,
- water filling rate,
- water pressure increase rate.

The following variables were measured during the tests:

- axial load on the fixing ring,
- radial swelling pressure (at two points),
- axial pressure between the supercontainer end surface and the first distance block was measured using six pressure cells positioned at different radii on the supercontainer end surface, see Figures 8-3 and 8-4.

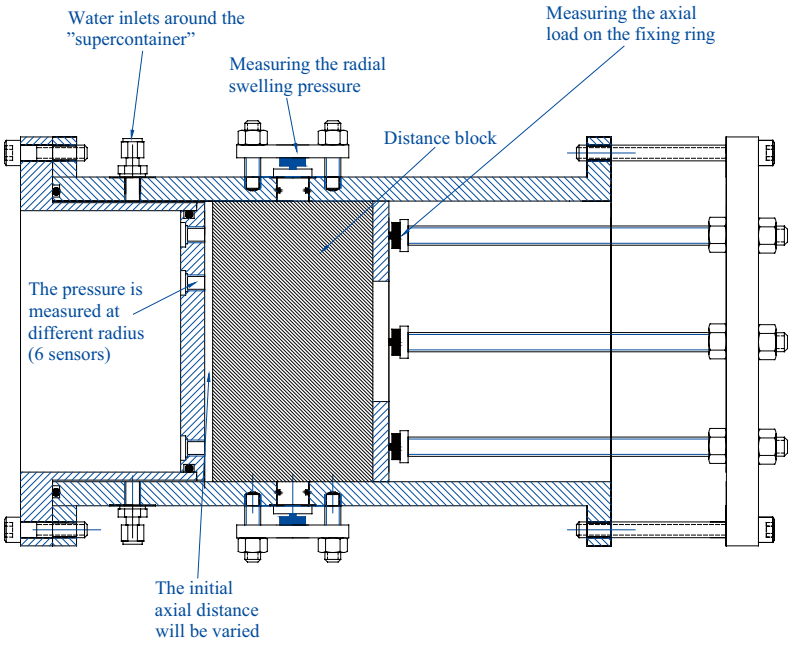

Figure 8-3. *Schematic view of the test equipment.*

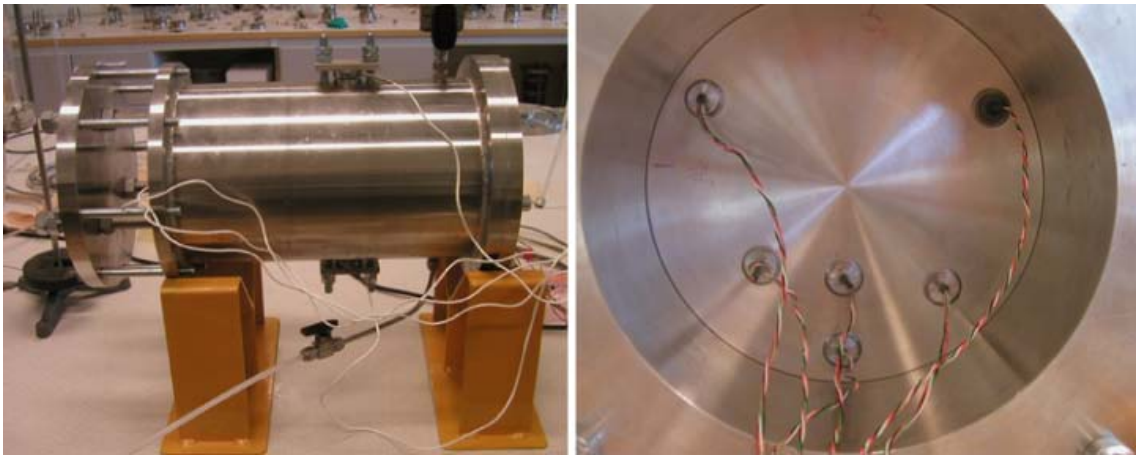

Figure 8-4. *Left: Photo of the test equipment. (Right: Photo showing the inside of the supercontainer and the six pressure cells installed at different distances from the "rock" surface.)*

8.3 Test results

Table 8-1 shows the test matrix possible for this study and the tests carried out are marked with shaded boxes. Based on previous tests and experience related to piping, the other tests were deemed to be outside the practical range of conditions in which hydraulic pressure conditions are important. In addition to the tests in Table 8-1, an alternative to Test HP104 was performed (HP404) in which all the test parameters were completely controlled. This extra test simulated the case whereby a drainage tube was used to control the water pressure within the supercontainer volume, see Section 6.3.5. A compilation of the tests and the results is shown in Table 8-2. All results from the tests are also presented in Appendices B20 to B25.

Table 8-1. Test matrix for examining the issue of hydraulic pressure on the distance block.

Hydraulic pressure on distance block			
Initial slot width, mm	**Water inflow and pressure increase rate 0.1 l/min and 0.1 MPa/h**	**0.1 l/min and 1 MPa/h**	**1 l/min and 1 MPa/h**
0	HP101	HP201	HP301
1	HP102	HP202	HP302
2	HP103	HP203	HP303
5	HP104	HP204	HP304
7.5	HP105	HP205	HP305
10	HP106	HP206	HP306

Table 8-2. Compilation of the tests and results.

Test	Initial axial slot mm	Filling rate l/min[1)]	Water pressure increase rate MPa/h	Active surface Comments
HP103	2	0.1	0.1	Width of the ring shaped active surface estimated to 20–30 mm. Obvious delay of pressure development also at the outermost parts.
HO203	2	0.1	1	Width of the ring shaped active surface estimated to 20–40 mm. Obvious delay of pressure development also at the outermost parts.
HP303	2	1	1	Active surface is 100% of the cross section area. Very small delay in pressure development at the innermost parts.
HP104	5	0.1	0.1	Active surface is 100% of the cross section area. Very small delay in pressure development at the innermost parts.
HP204	5	0.1	1	Active surface is 100% of the cross section area. The pressure response is immediate at all sensor positions.
HP404	5	Controlled	Controlled	The pressure was increased in steps with 1–2 days between every step There was an obvious delay in the pressure development up to 1,600 kPa water pressure. Active surface was then 100% of the area.

[1)] Recalculated to full scale.

8.3.1 Results of test HP103

In Test HP103, the initial slot between the supercontainer end plate and the first distance block was set at 2 mm. A water inflow rate of 0.1 l/min into a full-scale installation was simulated, i.e. the filling of the empty space in the supercontainer section took about 10 days. After finishing the filling, a water pressure ramping with an increase rate of 0.1 MPa/h was applied, which meant that after 50 hours the maximum allowed water pressure 5MPa would be reached.

In Figure 8-5, the label of each pressure sensor shows the position of the sensor on the supercontainer end plate (angle clockwise from noon and distance from rock surface). The three outermost sensors, placed at a distance of 20 mm from the rock surface, started to react slowly and with an evident delay after reaching full water pressure in the supercontainer section. After 12 days with full water pressure there was still no reaction from the sensors placed 30, 40 or 50 mm away from the “rock”.

The measurements showed that the bentonite had swelled and sealed the slot, and hence prevented the applied water pressure from acting on the full area of the distance block. These measurements were supported by the determination of the water ratio distribution on the distance block surface after finishing the tests, Figure 8-6, showing a strong radial water ratio gradient. The distribution shown in Figure 8-6 indicates the size of the “active area” and supports the pressure measurements shown in Figure 8-5.

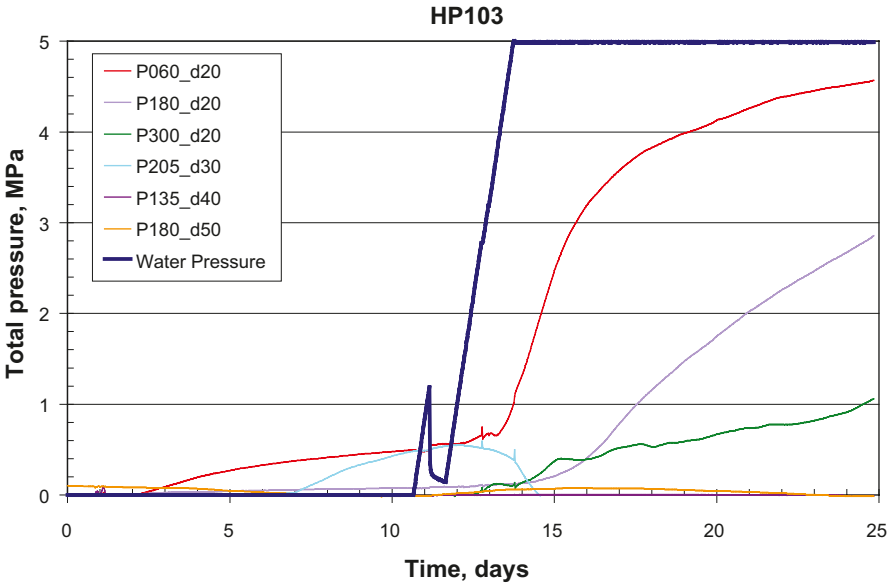

Figure 8-5. *The applied water pressure and the measured axial pressure on the supercontainer plotted vs. time for Test HP103.*

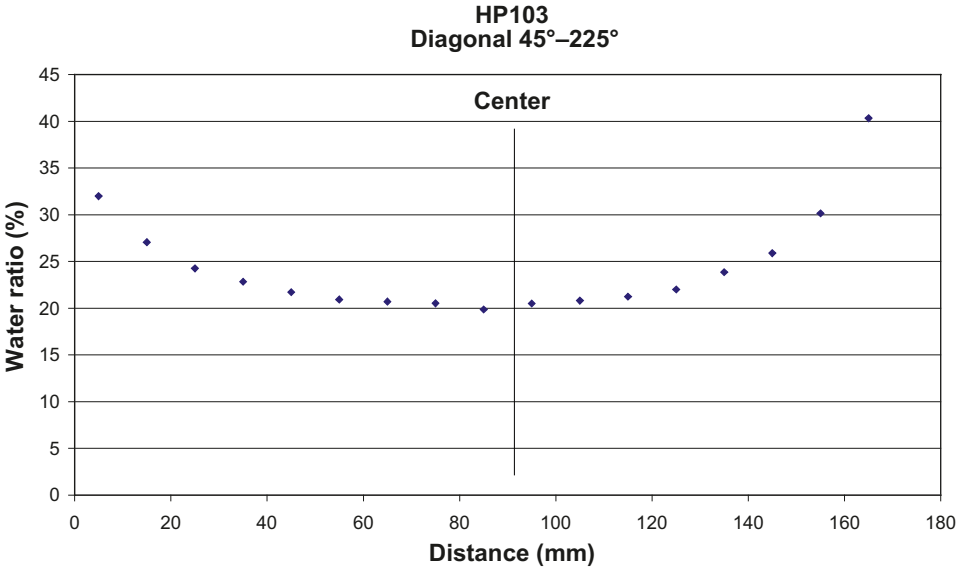

Figure 8-6. *The water ratio distribution of a 5 mm-thick bentonite slice on the distance block surface closest to the supercontainer end plate for Test HP103.*

The influence of the applied water pressure on the axial load taken by the fixing ring can be seen in Figure 8-7. The results mainly depend on two things:

- The radial swelling pressure is rather low, see Figure 8-7. This is probably related to the limited access of the system to water.
- The bentonite specimen length is rather short, about 0.15 m.

These two factors combined determine that the force which can be taken by the bentonites friction against the “rock walls” is rather small.

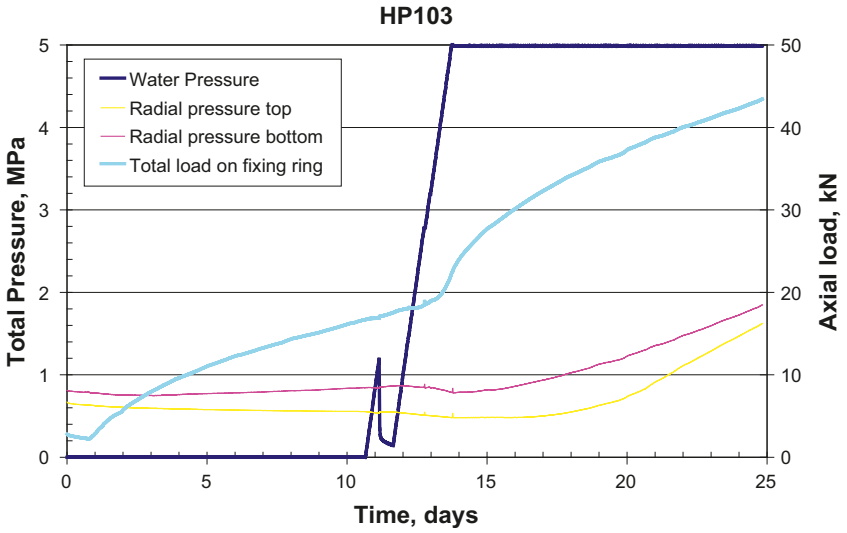

Figure 8-7. *Applied water pressure, the measured radial swelling pressure and the axial load as a function of time for Test HP103.*

8.3.2 Example of test results, Test HP303

The test conditions in Test HP303 were considerably more severe than for Test HP103. The initial axial slot between supercontainer end plate and the first distance block was 2 mm as in the previous test, but the inflow rate was increased from 0.1 l/min to 1 l/min. This simulates filling of the empty space in the supercontainer section in 1 day. The water pressurization rate was increased from 0.1 MPa/h to 1 MPa/h, which means that after 5 hours the maximum allowable water pressure of 5MPa should be reached.

The results of the pressure measurements on the supercontainer end plate are shown in Figure 8-8. In Figure 8-8 sensors from different distances from the cell wall are plotted as to their angle and distance from rock surface. All pressure sensors reacted immediately when the water pressure was increased. The measurements show that the bentonite did not have enough time to swell and seal the slot. When the water pressure started to increase, all sensors on the supercontainer end plate responded immediately and fully to the applied water pressure, establishing that the water pressure was acting on the full cross-sectional area of the distance block. These measurements were supported by the measured water ratio distribution on the distance block surface after finishing the tests, see Figure 8-9. The distribution of water ratio indicates the size of the “active area” and collaborates with the pressure measurements shown in Figure 8-8. The water ratio distribution shows that the whole surface was wetted although there was still a small radial water ratio gradient.

The influence of the applied water pressure on the measured axial load on the fixing ring was very strong, see Figure 8-10. It is obvious from this test that full water pressure will penetrate at least 9 cm from the rock surface under these conditions.

8.3.3 Bentonite shearing

In this test series a special phenomenon was noticed. In three tests (HP303, HP204 and HP404) the water pressure applied was active across the whole cross-sectional area of the distance block and the pressure reached the maximum allowed, i.e. 5 MPa. This resulted in a shear failure and the central part of the bentonite block was forced out through the hole in the fixing ring since the maximum shear strength of the bentonite blocks was exceeded, see Figure 8-11.

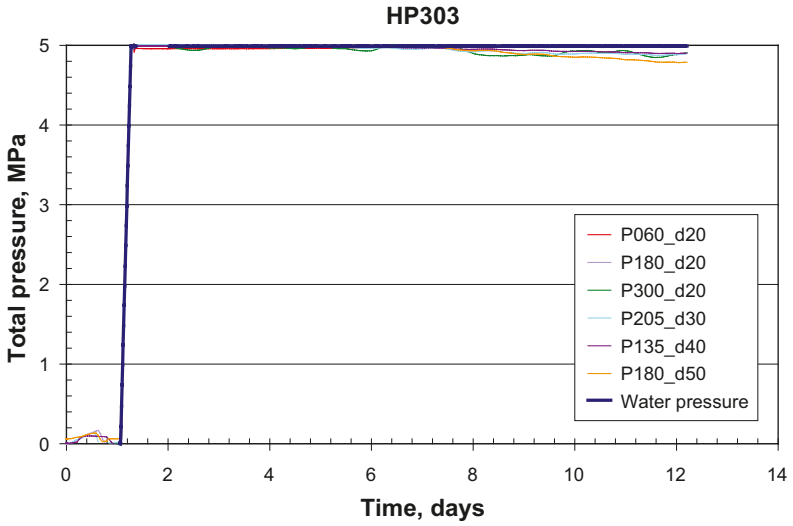

Figure 8-8. *Change in applied water pressure and the measured axial pressure on the supercontainer at different radial distance from the rock in Test HP303.*

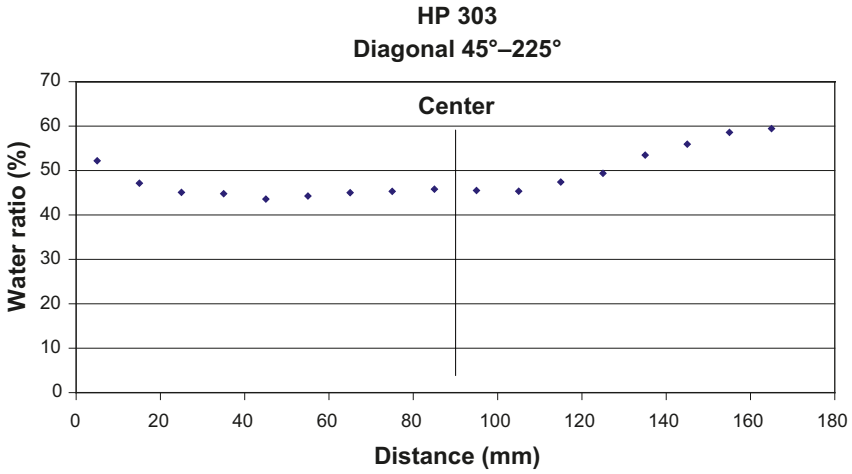

Figure 8-9. *Water ratio distribution of a 5 mm-thick bentonite slice on the distance block surface closest to the supercontainer end plate for Test HP303.*

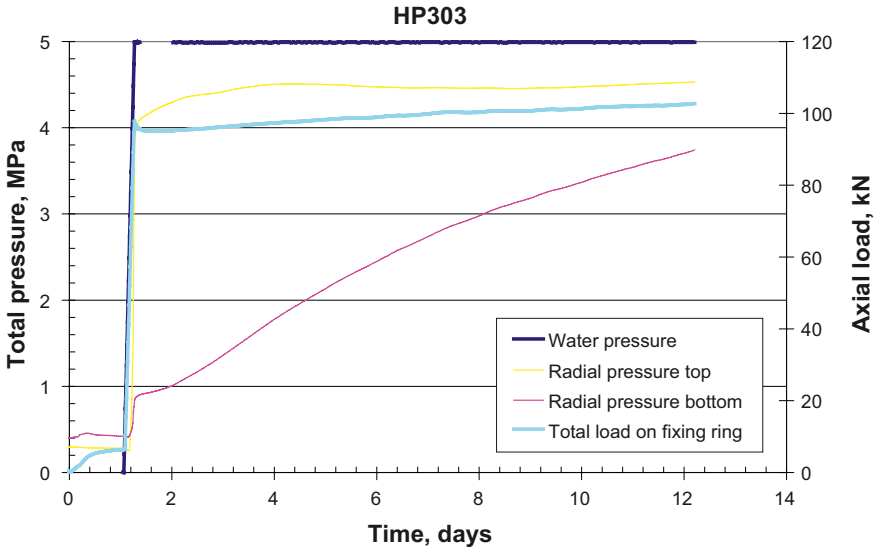

Figure 8-10. *Applied water pressure, the measured radial swelling pressure and the axial load as a function of time for Test HP303.*

Figure 8-11. *Photo showing the bentonite specimen in Test HP404 after dismantling. The central part of the block has been pushed out through the hole in the fixing ring.*

8.4 Summary and conclusions of the tests made to study the effect and extent of the hydraulic pressure on the distance block end surface

8.4.1 General

The results of the measurement of the axial load on the fixing ring have been summarized in Figure 8-12. This figure shows the following:

- The measured load on the fixing ring before applying any water pressure, i.e. the load, depends on the swelling pressure from the bentonite (blue columns).
- The measured load on the fixing ring at the maximum applied water pressure in the supercontainer section (purple columns).
- The calculated force based on the applied water pressure and the "active surface" which for each specimen is measured after test interruption, see example in Figure 6-19. (Yellow columns.)

The difference between the calculated load and the measured load is attributed to the friction between the bentonite and the rock. Since the length of the bentonite specimens in this test series is only 0.15 m, the load taken by friction between bentonite and rock is rather low.

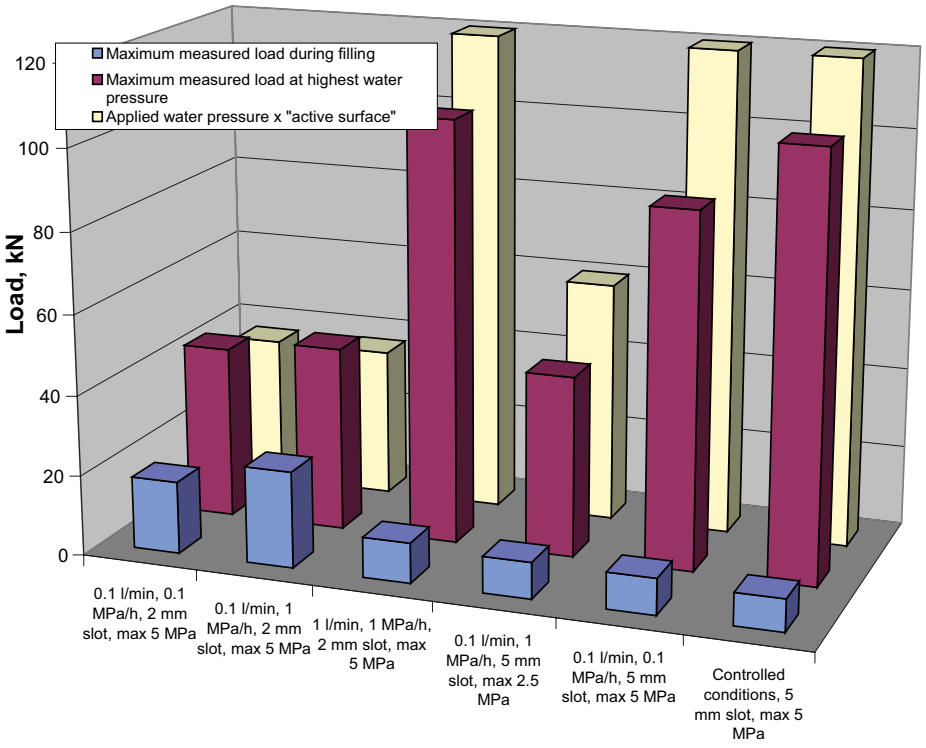

Figure 8-12. *Graph showing the maximum axial load measured on the fixing ring during filling (before applying a water pressure), at the highest water pressure and calculated load based on applied water pressure acting on an "active surface" of the distance block.*

8.4.2 Conclusions

The results of the six tests performed in this study and the results of the scale tests (1 m and 3 m tests) yielded the following conclusions regarding the penetration of water pressure into a slot between the lid of the supercontainer and the distance block end surface:

- A 2 mm axial slot will need about 10 days (corresponding to an inflow rate of 0.1 l/min) to swell and seal. A pressure increase rate of 1 MPa/h up to the maximum pressure of 5 MPa can be handled after this time. The radial penetration is 30–40 mm.
- The radial penetration in an axial slot of 5 mm is greater than 85 mm under natural conditions. With controlled conditions, i.e. the use of a drainage tube, the water penetration is limited up to a maximum pressure of 1.5–2 MPa.
- The assumption from earlier investigations that a 7 mm axial slot will result in a 100 mm radial penetration is still valid under these conditions (the reference test conditions, i.e. an inflow rate of 0.1 l/min, a water pressure increase rate of 0.1 MPa/h up to a maximum of 2 MPa).
- The scale has a major impact in this type of experiment. The maximum possible radial penetration was 87.5 mm with the equipment used.

9 Ongoing laboratory tests

9.1 General

In addition to the tests described in this report, there are some that are still running. These tests will not be finished before the middle of 2008 and the final results cannot be described in this report. Two types of tests are still running:

- **Artificial wetting of distance blocks.** This was identified as a critical design issue, see Chapter 5. The issue mainly concerns the DAWE design that includes artificial filling of water. The issue also has an influence on the rock spalling problem since spalling may be prevented if the slots are filled with water.
- **Large-scale tests.** Tests have been performed earlier within this project in order to study the processes that influence the bentonite blocks during the installation phase. Some of the results of the laboratory tests are being verified in a larger scale test.

9.2 Artificial wetting of distance blocks

9.2.1 General

Artificial water filling of the gap between the rock and the distance block is one option in the DAWE design. It has also been proposed for use in the Basic Design. In the DAWE design, the entire tunnel section will be filled with water after plugging in order to accelerate system swelling and sealing. In the BD design, it is proposed that the slot between the distance blocks and the rock wall will be flooded once the block has been installed. The initial water filling of the gaps means that water is immediately supplied to the bentonite, thereby resulting in water uptake, clay swelling and filling of the slot. However, with time, the water will be drawn deeper into the bentonite and there may be a reduction in the water content of the low-density bentonite in the slot, resulting in desiccation and cracking unless additional water is available. This phenomenon was observed in tests carried out for the LASGIT project and was investigated a scale of 1:10 in Test 3-13 (see Chapter 7).

The positive effect on the buffer if all the slots are filled with expanding bentonite may therefore be lost with time if the natural water supply is too low to satisfy the water uptake demands of the buffer. This subsequent desiccation of the perimeter region is not necessarily a long-term or system performance problem, but it is important to understand how much of the effect is left and how fast the process is. The main objectives of the tests are to find out for how long a slot will remain filled with bentonite and remain sealed under different conditions, and to find out how much the slot may be re-opened after equilibrium under conditions of dry rock.

Two types of tests were run in the laboratory (Test Type 1 and Test Type 2) representing different scales. All specimens were made of MX-80 bentonite, see for example Sections 6.1.2–6.1.3. The dry density ρ_d is defined as the ratio between the dry mass and the total volume.

9.2.2 Tests Type 1

In Test Type 1, the specimens were enclosed in stiff swelling pressure oedometers. Above each specimen a gap was left which was initially filled with water. Axial stress, radial stress and *RH* were all measured during the test.

Different conditions of initial water content, slot width and water salinity were investigated. The results are represented by stresses (measured as forces on a piston) on the clay-piston boundary with time and cracking observed at the end of the test. The gradients in water content and density over the specimen length and radius were determined after the test. Some tests are still ongoing.

Test equipment and preparation

Two specimens with prescribed water content were compacted using a compaction pressure of 50 MPa to a height of 25 mm. To obtain a total height of 50 mm including a slot of 5-8 mm, one of these specimens was sawn to a height of less than 25 mm. The two specimens were then placed on top of each other in the equipment shown in Figure 9-1. This type of equipment had previously been used in the LASGIT project. The device was sealed and *RH* measurement was performed for a period of 1–2 days to determine the initial *RH* value.

Then the lid was removed and the slot above the bentonite specimen filled with water with a pre-selected salt content. The lid was put back on, the device was sealed and no additional water was added. Radial and axial stresses were measured by load cells installed in the top lid and in the wall of the oedometer. The moisture redistribution was monitored by the *RH* sensor. After approximately 2 months, the test was terminated, the upper lid lifted and photos taken of the upper surface. The bottom plate was then removed and the specimen was pushed out of the ring.

The total mass, height and diameter were measured and the specimen was then cut into 4–6 slices and for each slice the water content and density were determined.

Test matrix

All specimens were compacted by applying a uniaxial compaction pressure of 50 MPa. Different initial water contents, slot widths and salt contents of the added water were investigated. Of the full test matrix shown in Table 9-1, only the marked tests were performed. The selected tests focus on a 20% water content and a gap of 5 mm filled with water with a salt content of 3.5%.

In addition to the tests shown in Table 9-1, four additional tests were included in this test series. The additional tests start with the same conditions as some of the specimens in Table 9-1. Two of the additional tests will be interrupted early and two will be used for illustration purpose with a transparent lid made of acrylic plastic.

Preliminary test results

The measured relative humidity, axial stress and radial stress vs. time are presented for two tests in Figures 9-2 and 9-3. The two selected specimens had initial water content of 10% and 24%. In Appendix C1, a full set of the test results are shown for all of the specimens examined.

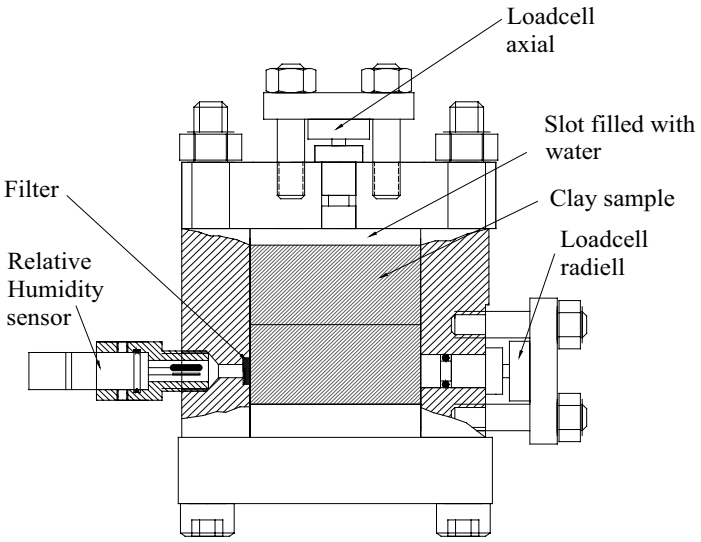

Figure 9-1. *Schematic diagram of the test equipment used for Test Type 1.*

Table 9-1. Test matrix for investigating the effect of artificial wetting of distance blocks (test type 1).

w initial %	Salt content = 1% Slot width		Salt content = 3.5% Slot width	
	5 mm	8–10 mm	5 mm	8–10 mm
10	W110	W120	W210	W220
15	W111	W121	W211	W221
20	W112	W122	W212	W222
22	W113	W123	W213	W223
24	W114	W124	W214	W224

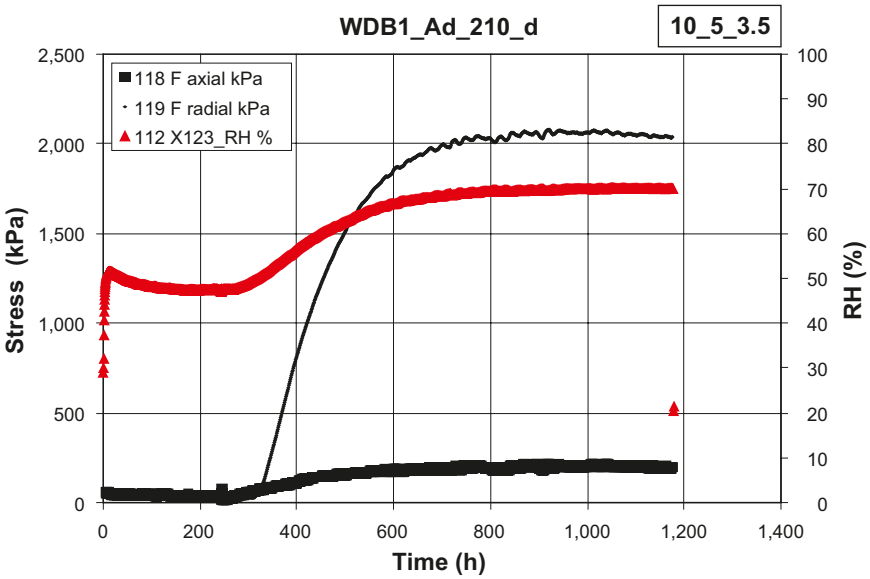

Figure 9-2. Relative humidity, axial and radial stresses vs. time from test W210. (Initial water content 10%, the slot width 5 mm and a salt content of 3.5%.)

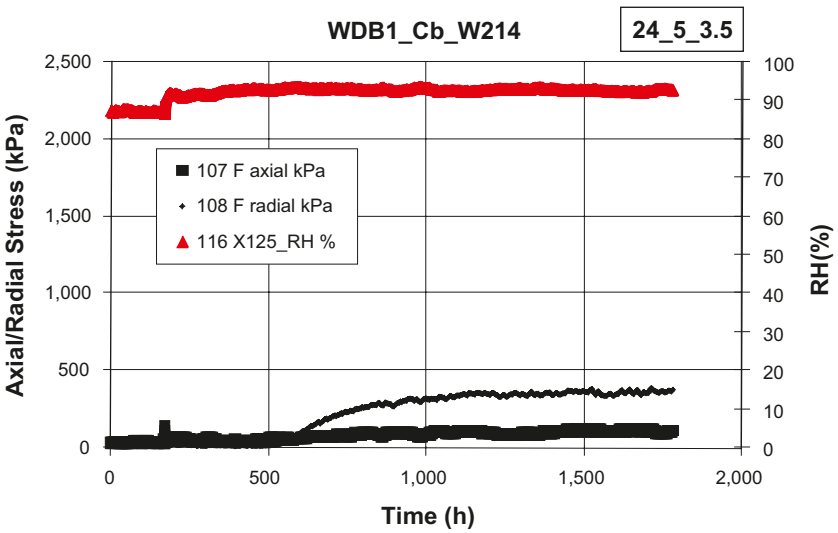

Figure 9-3. Relative humidity, axial and radial stresses vs. time from test W214. (Initial water content 24%, slot width 5 mm and a salt content of 3.5%.)

In the following graphs, the colours (blue, green, orange and red) denote the initial water content (10%, 20%, 22%, 24%) for which a maximum axial stress is associated. The end of the sample names (_t, _p) denotes that a shorter period of time was used and a lid of acrylic plastic was used. In each diagram below, the legend states: *initial water content_initial width of the slot_ salt content of the added water*.

The radial and axial stresses for all tests are plotted vs. final dry density in Figures 9-4 and 9-5, respectively.

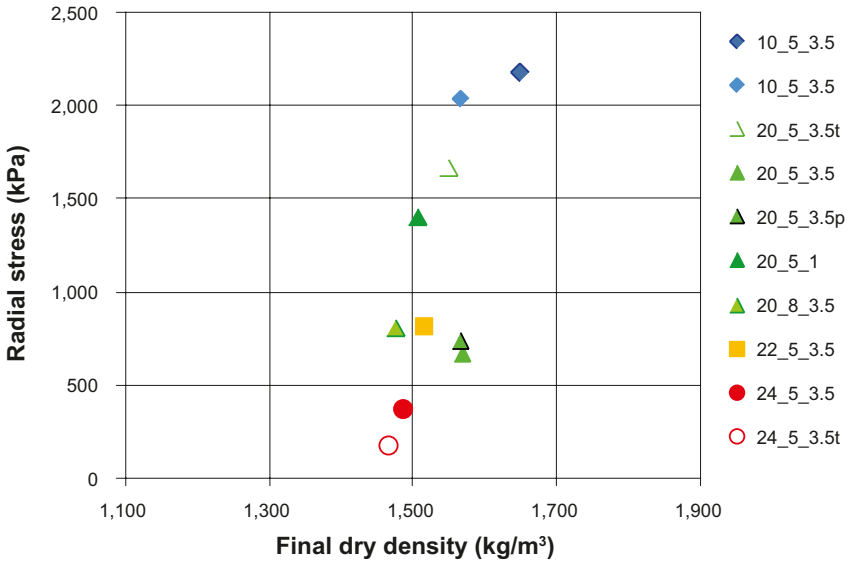

Figure 9-4. *Radial stress vs. final dry density in artificial wetting tests.*

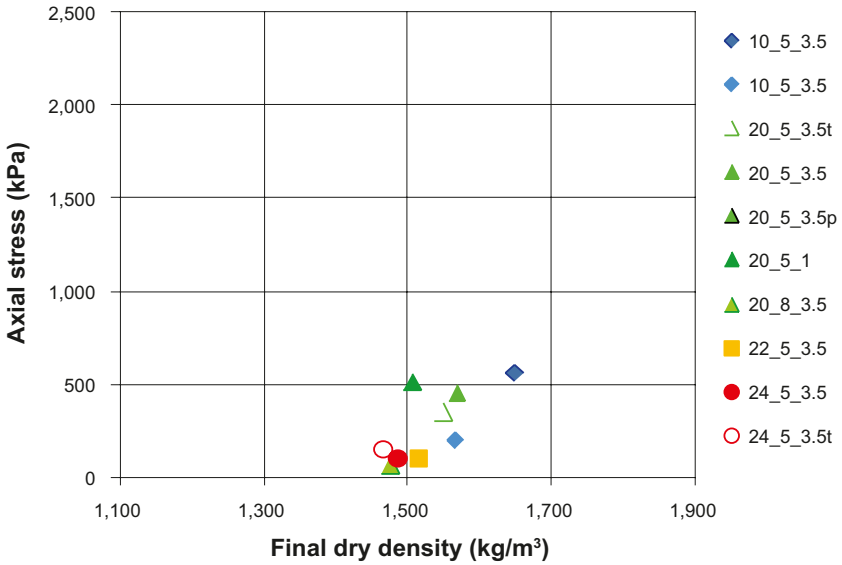

Figure 9-5. *Axial stress vs. final dry density in artificial wetting tests.*

Regarding the axial stress, there is an uncertainty in the final stress present for the tests started with a pre-stress on the piston of the same size as the final stress. This was the case for the four tests with the highest final values in Figure 9-5. However, the axial stress in all tests was lower than the radial stress, and for all tests the axial stress was lower than 600 kPa.

Gradients in water content and dry density are shown for selected samples in Figures 9-6 and 9-7, respectively. See also Appendix C2.

The water content increased in all parts of the specimen in all tests. The dry density decreased in all parts in all specimens.

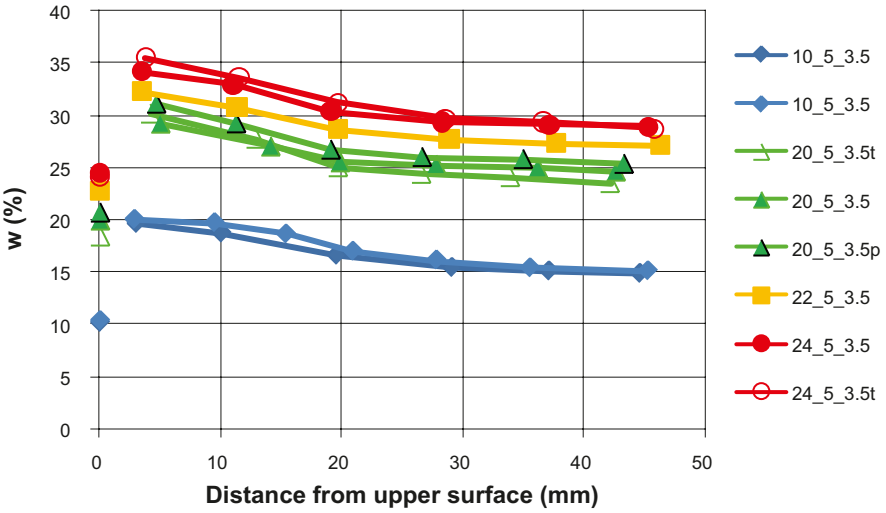

Figure 9-6. *Profiles of water content after the artificial water uptake tests. (The initial water content for each sample is marked on the y-axis as distance equal to 0 mm.)*

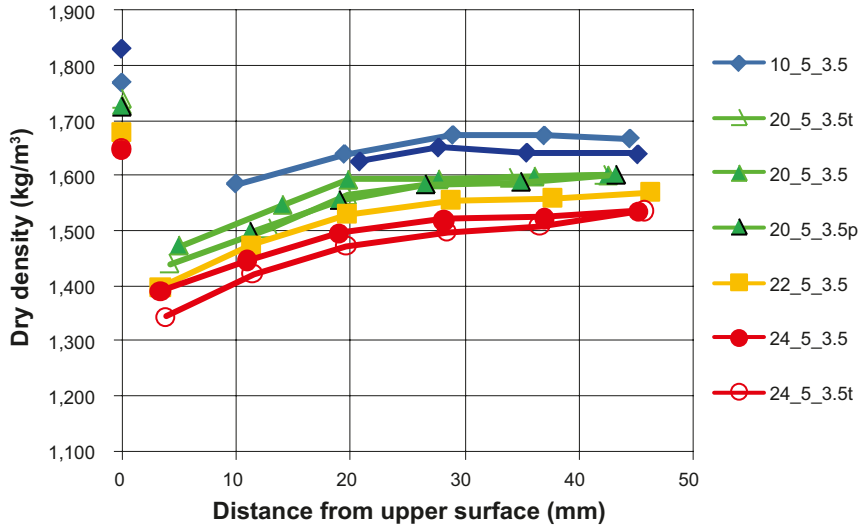

Figure 9-7. *Profiles of dry density after the artificial water uptake tests. (The initial dry density for each sample is marked on the y-axis as distance equal to 0 mm.)*

Discussion

The measured stresses increased with time in almost all tests. The only test in which a small decrease was seen in the axial stress with time was Test W210. This test started with a water content of 10%.

In all tests completed to date, all specimens showed cracking in their upper surfaces at the time of test termination, despite there being contact between the lid and the bentonite. A photo of specimen W212 taken after lifting the lid is provided as Figure 9-8 for information. Photos of all specimens taken immediately after lifting the lid are shown in Appendix C3. Photos taken through a lid made of acrylic plastic during the re-distribution of moisture are shown in Appendix C4.

A further analysis of the test results will be made when all tests have been completed.

9.2.3 Test Type 2

In Test Type 2, a 30 cm-high specimen was placed in a test cell that is similar to the apparatus used in Test Type 1. In Test Type 2, a 3 cm slot was left open on top of the specimen and in order not to induce too large an effect of water uptake at the bottom boundary a long specimen was used.

Only the axial stress at the top of the specimen was measured. The 3 cm slot was filled with water before the apparatus was closed and no additional water was then added. Two different salt contents were used in this test series. The gradient of water content and density over each specimen were determined at the end of the test.

Test equipment and preparation

A 270 mm-long cylindrical specimen with a diameter of 100 mm was sawn and trimmed out of a larger bentonite block with initial water content of 22% and dry density of 1,690 kg/m^3. The specimen was mechanically pushed into the steel cylinder in the device shown in Figure 9-9. The 3 cm gap on top of the specimen was initially filled with water of the prescribed salt content. The device was then sealed and no additional water was added. During testing, the axial stress was measured on top of the specimen. A pre-stress of approximately 50 kPa was applied on the piston where the upper part of the piston was pressed against the steel ring.The testing time was approximately 6 months for each specimen. After the test, the lid was removed and the upper surface observed to detect bentonite cracking. The gradient in water content and density were then determined over the specimen height.

Figure 9-8. *Photo taken after lifting the lid but with the specimen still inside the oedometer ring. (Specimen W212).*

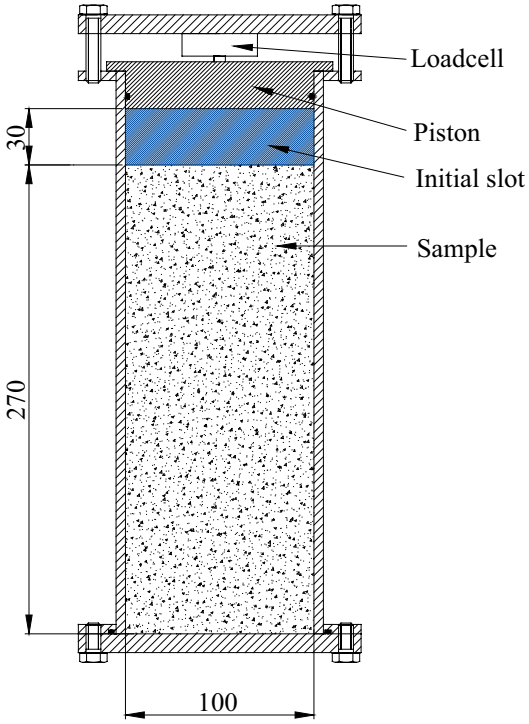

Figure 9-9. *Schematic diagram of the test equipment used for Test Type 2.*

Test matrix

Since the testing time was 6 months, only two specimens from the suggested test matrix, Table 9-2, were performed.

Preliminary test results

The measured axial stresses are shown in Figure 9-10. Before termination of the test the stresses were released by loosening the upper hexagonal nut. However, a full recovery of the originally measured axial stress was not observed. The time allowed for the system reaction was short and no additional water was added. In each graph the legend shows: *initial water content_initial width of the slot_ salt content of the added water*.

Profiles of water content and dry density are shown in Figures 9-11 and 9-12, respectively.

Table 9-2. Test matrix for investigation of the effect of artificial wetting of distance blocks, Test Type 2.

w initial %	Slot width = 3 cm Salt content	
	1%	3.5%
10	W310	W320
15	W311	W321
20	W312	W322
22	W313	W323
24	W314	W324

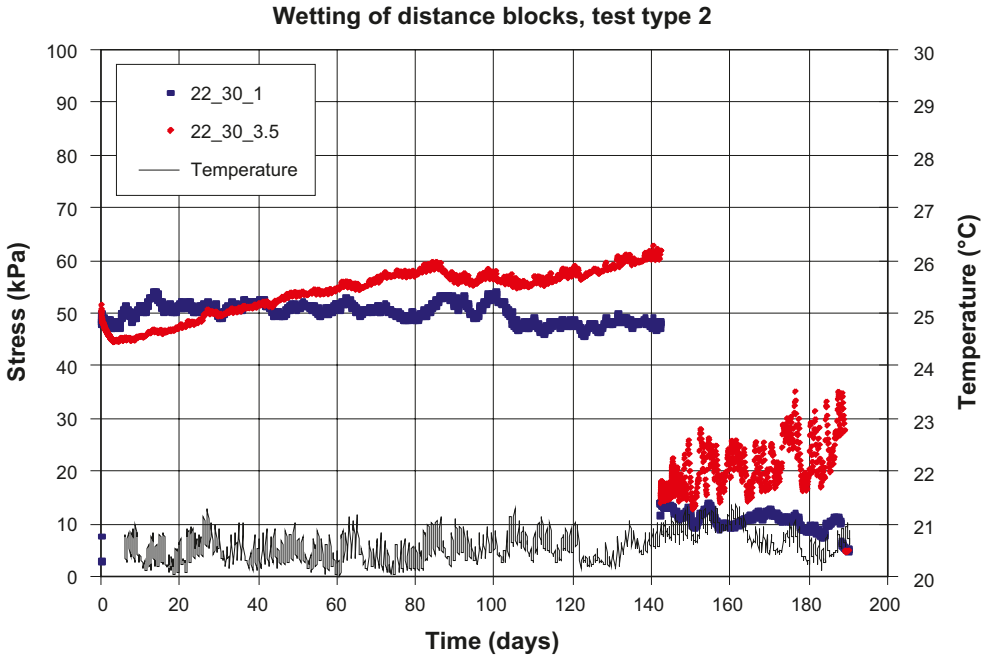

Figure 9-10. *Axial stress from Tests W313 and W323.*

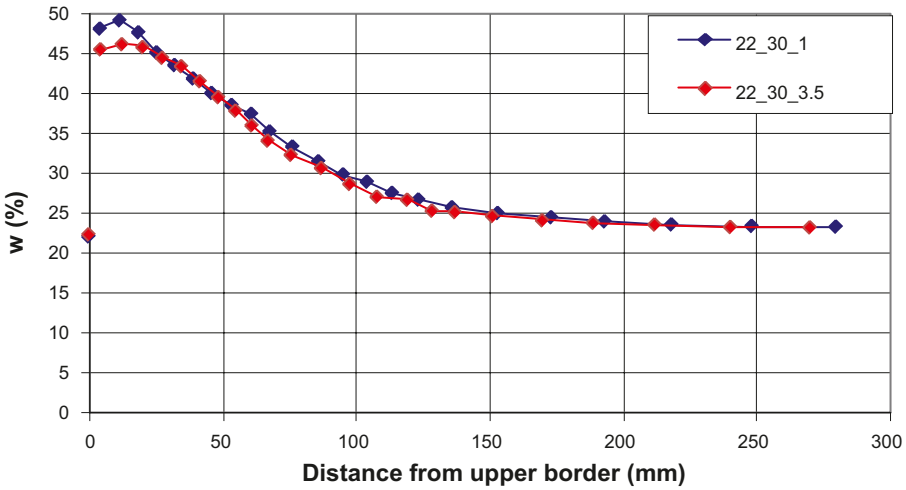

Figure 9-11. *Profiles of water content for specimens W313(blue) and W323(red). (The initial water content for each specimen is marked on the y-axis as a distance equal to 0 mm.)*

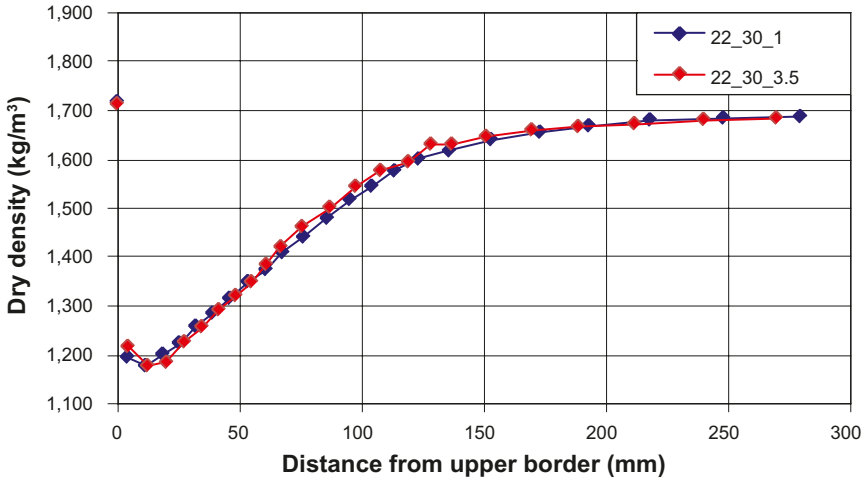

Figure 9-12. *Profiles of dry density for specimens W313(blue) and W323(red). (The initial dry density for each specimen is marked on the y-axis as a distance equal to 0 mm.)*

In all parts of both specimens, higher water content was measured at the end of the test than was present at the start of testing. In the upper part, 4 mm from the lid, the water content was lower than was observed 12 mm from the lid in both specimens. Photos of the specimens, W313 and W323, still inside the equipment and immediately after lifting the lid are shown in Figure 9-13. In Figure 9-14 these specimens are shown after dismantling.

The main region that experienced cracking in specimen W313 was seen in the cross section of the specimen and in specimen W323 the greatest degree of cracking was seen at the boundary close to the steel ring.

Discussion

No decrease in stress with time was measured, but since the stress did not fully recover after the release of the vertical confinement at the end of testing, the stress must be regarded as uncertain and in both cases was lower than 50 kPa.

Cracking was seen in both specimens at the end of testing, but the appearance of these two cracked regions was different.

Further analysis of the test results will be made when all tests carried out to evaluate the artificial wetting of distance blocks have been finished.

Figure 9-13. *Photos of specimens W313 and W323 after lifting the lid.*

Figure 9-14. *Photos of one half of the upper parts of W313 and W323.*

9.3 Large-scale tests

9.3.1 General

Tests were carried out earlier within this project that studied the processes influencing the bentonite blocks during their installation. Some of the results from the laboratory tests have been reproduced on a larger scale.

The large-scale test equipment used in the studies (Big Bertha) has an inner diameter of 800 mm. It is possible to perform tests with a length of 350 mm and 1,050 mm by using seperate sections of this two-segment equipment, or else the full length 1,400 mm can be used. The original purpose of the equipment was to simulate a section of a supercontainer, as shown in Figure 9-15, and to study the long-term homogenization process.

The two segments of the equipment are used to study two different phases of the installation. The tests mainly associated with assessing the DAWE design are:

- **Test Type 1.** In this test the behaviour of bentonite blocks installed in the supercontainer was studied by exposing them to a high relative humidity as might be caused by a wet rock surface over a long period of time. This test has been completed.
- **Test Type 2.** In the second test, a technique for artificial wetting of the space around one distance block and the following development of a radial pressure was tested. This test is still running.

Blocks made of MX-80 Wyoming bentonite at a water ratio of 10% were produced for previous tests carried out using this equipment. This water ratio is probably very close to the the ratio the blocks inside the super container will have to have in connection with installation while the distance blocks between the supercontainers will probably have an initial water ratio of 20–22% (DAWE and STC designs). This means that the blocks which were used in Test 1 were of the same quality as that planned for the full-scale solution, while the blocks used in Test 2 were actually much drier than would be used in a repository application. Another difficulty in using the previously produced blocks is their dimensions. Table 9-3 provides a listing of the blocks that were available for use in this study. The tests performed were partly adapted to the bentonite blocks available (Test 2) rather than trying to manufacture new materials with a different water ratio or density. The following blocks were used:

- Test 1. Three blocks with an outer diameter of 705 mm were used for Test 1. The blocks were originally manufactured for use inside the supercontainer.
- Test 2. One of the blocks that had an initial outer diameter of 800 mm was machined down so that the outer diameter was decreased to 715 mm. This gave a radial slot between distance block and rock of 42.5 mm, which is the same as in the full scale.

Table 9-3. Table showing blocks available for the Big Bertha test equipment.

Number of blocks	Water ratio %	D mm	h mm	Remark
8	9.5	800	350	Planned to be used in piping tests, BD
4	9.5	780	350	Planned to be used in piping tests, BD
3	9.5	705	350	From the originally planned BB tests
2	9.5	770	350	From the originally planned BB tests

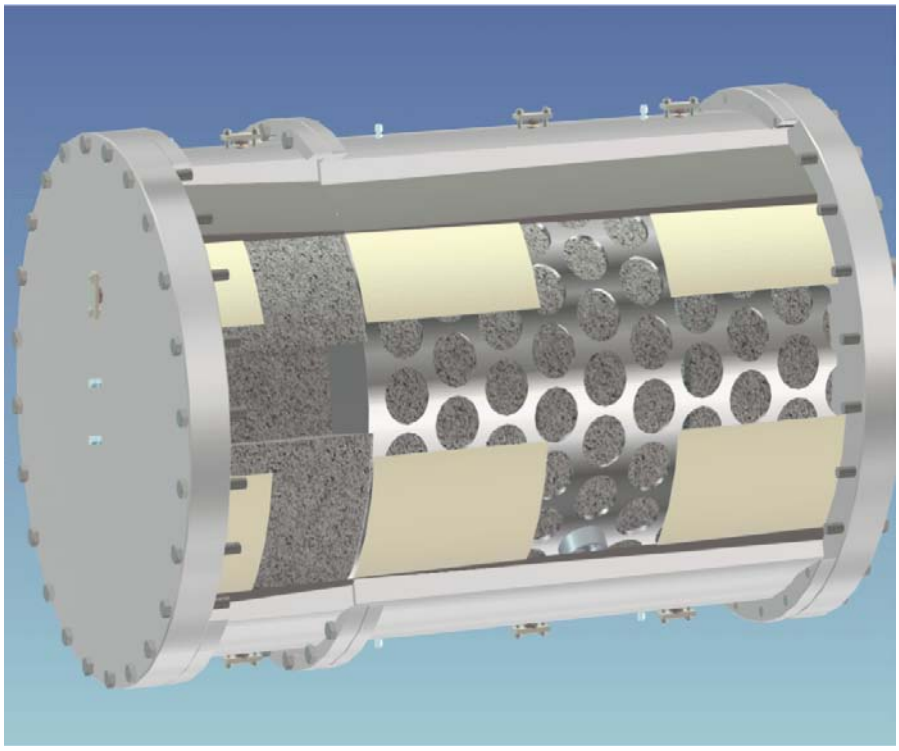

Figure 9-15. *Picture showing the Big Bertha test equipment. The original purpose of this equipment was to simulate a section of a supercontainer and to study the long-term homogenization process. The white partial covering that can be seen is filter sheets supplying the buffer with water.*

9.3.2 Test Type 1 – Study of the behaviour of bentonite blocks installed in a supercontainer when exposed to high relative humidity

Objectives

The main objectives of the test were the following:

- Study the influence of a high relative humidity on the bentonite blocks inside a supercontainer, especially related to block cracking and subsequent loss of material into the gap between the blocks and the rock.
- Measure the erosion rate of the material lost into the block-rock gap by applying an axial flow in the "tunnel".

Test description

In this test the longer segment of the outer tube was used, see Figure 9-16, together with the simulated supercontainer. Three buffer blocks with an outer diameter of 705 mm (see Table 9-3) were used in the test.

The perforated holes in the supercontainer have a diameter of 100 mm, just as planned at full scale. Laboratory tests performed previously have shown that bentonite blocks of the quality used (water ratio of about 10%) will crack and fall apart when they are exposed to high relative humidity. If this happens during the installation phase, bentonite pieces or fragments may fall to the tunnel floor and erode away from the section. In order to prevent bentonite fragments from falling to the floor it may be possible to wrap the blocks in a thin steel net with a mesh size of about 1 cm, but this remediation approach was not investigated in this study.

Figure 9-17 shows the process used in installing the simulated supercontainer. After installing the bentonite in the supercontainer and placing the whole parcel in the outer tube, which simulates the deposition tunnel, lids of Plexiglas were placed at the ends for visual supervision of the processes. The tunnel walls were partly covered with filter mats, see Figure 9-18. In these filter mats, water was circulated continuously in order to keep the relative humidity on the walls close to 100%. One of the Plexiglas lids had an outlet present in its base in order to allow for seepage water to escape.

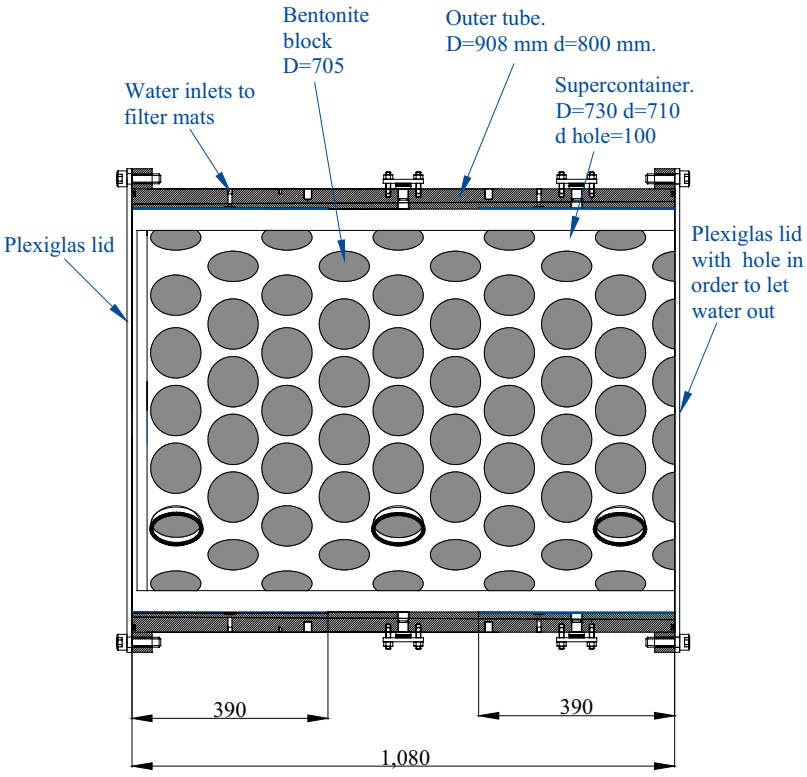

Figure 9-16. *Schematic diagram of the supercontainer test setup.*

Figure 9-17. *Installation of supercontainer simulator.* ***(Left****: The open end of the supercontainer was covered with plastic to minimize atmospheric interactions.* ***Right****: Plexiglas lids mounted in the ends to allow visual monitoring of bentonite block behaviour.*

Results of the test

Relative Humidity measurements

The total length of the test apparatus was 1,080 mm. Four filter mats, each with a width of 390 mm, were placed inside this steel "tunnel" with the filter mats only covering about half of the periphery in order not to have water dripping down onto the bentonite from the roof. (Figure 9-18). In a repository situation water would be prevented from contacting the bentonite through the use of special drip shields. The bottom (floor) part of the test cell was also left without a filter in order to perform erosion measurements along the length of the cell. A tube was connected to each of the filter mats in order to apply a constant water flow. At the point of inflow, located behind the filter mat, the water was distributed by a steel filter with a diameter of 20 mm. The water was then spread through the whole filter mat surface by capillary forces.

Three days after buffer emplacement the circulation of water was started. The flow was set at 0.2 l/min divided between four inlet points. Water was circulated in the filters throughout the entire test, excepting when an axial flow was applied in order to measure the erosion rate.

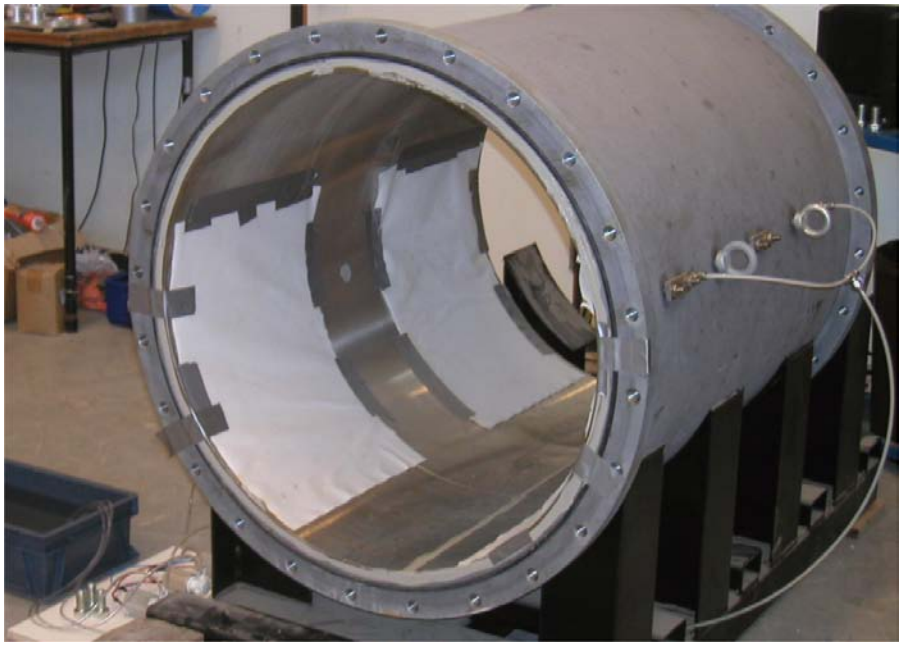

Figure 9-18. *Four filter mats were positioned on the simulated tunnel surface. Each of the filter mats was connected to a tube into which a constant flow was applied.*

Figure 9-19 shows the measured relative humidity, RH, present in the system during testing. The relative humidity and the temperature were measured at two points during the test. One sensor was positioned on the top of the supercontainer and one was positioned in the lower part. Each sensor was fixed in one of the perforated holes in the supercontainer as close as possible to the bentonite block surface. The relative humidity measured was between 70–85% with the higher values at the upper position. The reason for not measuring higher values is because the bentonite absorbed water faster than the diffusion across the air gap.

Bentonite block behaviour

Three days after emplacement in the "tunnel" the water circulation in the filter mats started. By measuring the amount of water consumed it was possible to make a rough calculation of the amount of water taken up by the bentonite during the first days of water circulation (days 2.8 – 5.2) shown in Figure 9-20.

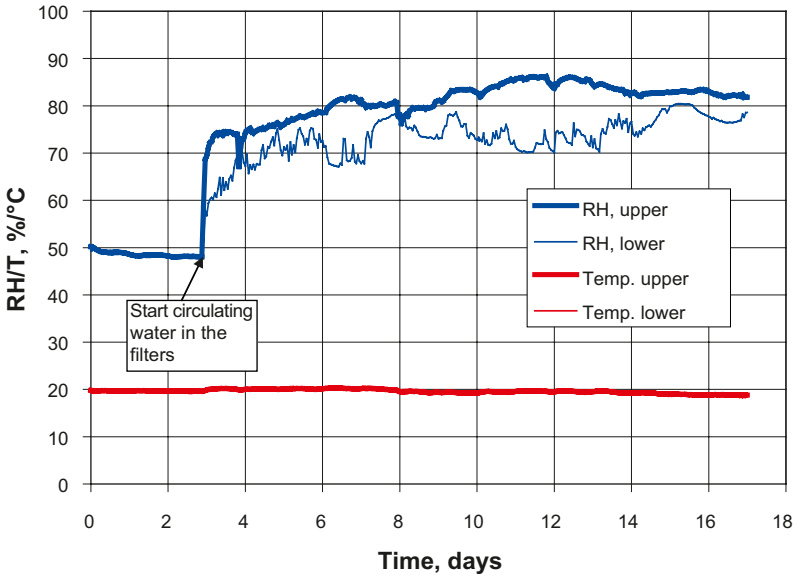

Figure 9-19. *Temperature and relative humidity measured during supercontainer simulation.*

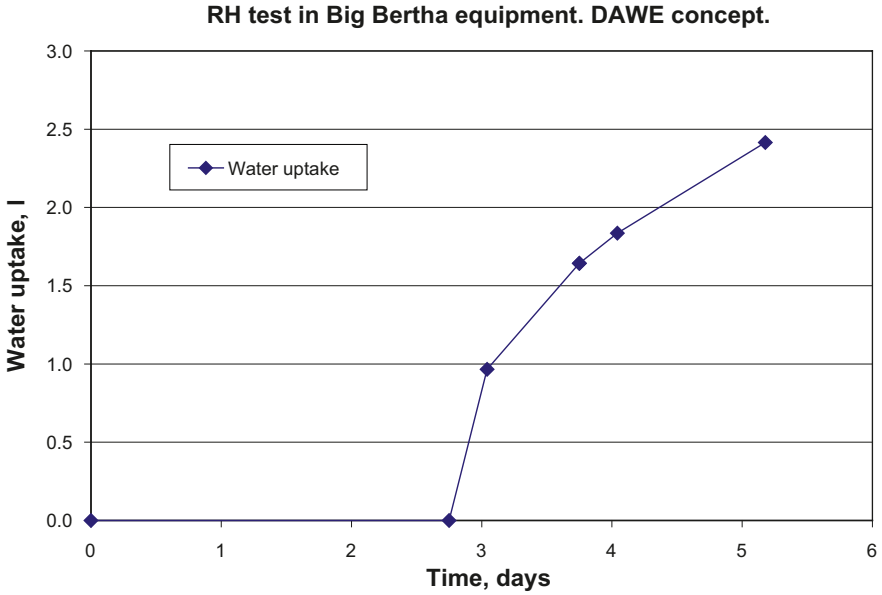

Figure 9-20. *Estimate of the water uptake during the first 2.5 days of water circulation through filter mat.*

The high relative humidity surrounding the bentonite and its uptake of water strongly affected the blocks, see Figure 9-21. The bentonite block surface cracked and flakes of bentonite fell down on to the tunnel floor, but it was noted that no large pieces fell, only flakes.

Erosion measurements

During the test, water flow into the filters was intentionally interrupted on a number of occasions, and during these periods an axial flow was applied along the tunnel floor to measure erosion of the material that had fallen from the supercontainer. The results of these tests are shown in Figure 9-22. The amount of eroded material was very low. An evident increase in the erosion rate was noticed when the water was changed from tap-water to a water with a 3.5% salt content, but after a few hours, the erosion rate also decreased to very low values for this water.

After about two weeks, so much material had fallen down to the floor and swollen in size, that the swollen clay and water moving along its upper surface had reached the base of the supercontainer, as can be seen in Figures 9-23 and 9-24.

Flaking of bentonite through perforations. *Collection of flakes on floor of "tunnel".*

Figure 9-21. *Flaking and sloughing of bentonite from the supercontainer.*

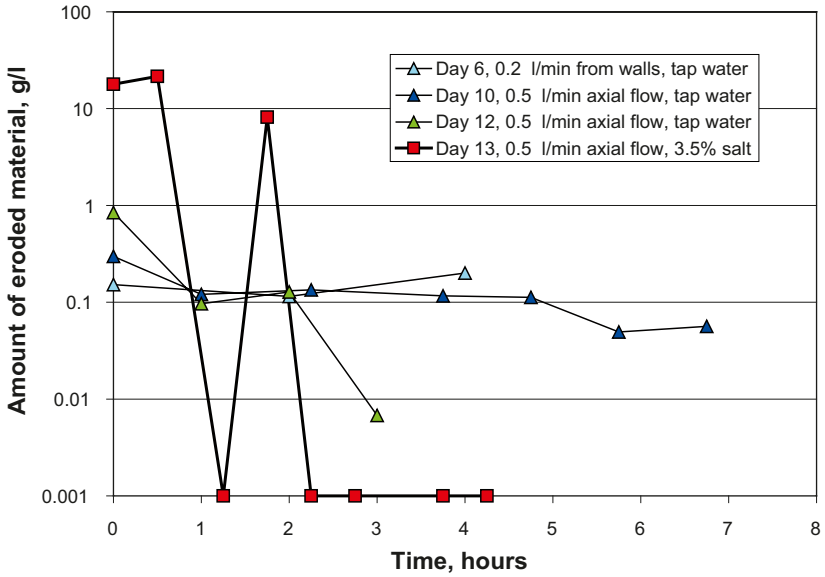

Figure 9-22. *Erosion along the floor measured on four occasions during supercontainer test.*

Figure 9-23. *View of supercontainer – "tunnel" gap after nine days of testing (note large amount of material that had fallen into the gap).*

Figure 9-24. *View on conclusion of the erosion measurement. (The amount of bentonite on the tunnel floor had increased so much that the drainage was prevented and the water level rose above the supercontainer base).*

Test Termination

The test was terminated after about two weeks. The outermost bentonite block, facing the open end of the supercontainer was strongly influenced by the high relative humidity and large cracks could be seen on its surface, even though the end had been covered with a plastic sheet to protect it (Figure 9-25).

The exposed bentonite surfaces at the locations of the perforations were also strongly influenced. The bentonite surface had cracked, producing fine flakes of material; see Figures 9-26 and 9-27. This phenomenon was very obvious on all surfaces except at the joints between the blocks. The difference is probably due to the fact that the joints allow a greater degree of localized volumetric strain preventing or delaying cracking. The water ratio of the flakes was determined to between 16 and 18% as compared with the 10% originally present.

Figure 9-25. *Cracks present on the end of the supercontainer after two weeks' exposure to high relative humidity.*

Figure 9-26. *Picture taken during the dismantling of the test. The lower part of the bentonite inside the supercontainer had been in direct contact with water.*

Figure 9-27. *Close-up view of the bentonite surface. The cracking of the bentonite surface into flakes was very obvious on all surfaces except in the joints seen in the centre of the photograph.*

Conclusions and comments

The bentonite blocks in this test were of a quality that is very close to the reference design, i.e. a dry density of 1,990 kg/m^3 and a water ratio of 10%. It will not be possible to increase the initial water ratio (which would make the block more insensitive to high relative humidity and the following cracking) due to the high dry density requirement that these internal supercontainer blocks must have.

Some conclusions that can be drawn from these tests are:

- The blocks are strongly affected by high relative humidity. On all exposed bentonite surfaces (except in the joints between the blocks), flakes of bentonite were formed. The difference in the region adjacent to the joints is probably due to the greater ability of these less constrained regions to strain without having to fail locally (2 planes of shrinkage rather than one).
- The flakes from the lower part of the supercontainer will fall to the "tunnel floor". This process started 2–3 days after installation and after a further two weeks in an environment with a high relative humidity, about 9.9 kg had fallen from the supercontainer simulation. By making a simple linear extension from the scale applied in this test to the full-scale field application, about 134 kg of bentonite will fall from a full-scale supercontainer in the first two weeks after its installation. This corresponds to about 0.8% of the total bentonite mass in a supercontainer.
- In the full-scale field application, it is expected that two supercontainers will be installed every day. The process involving the formation of bentonite flakes seems to be rather slow (2–3 days before the first flakes fell down on to the tunnel floor) which means that it will probably not be a problem during the transportation of the supercontainers into the tunnel.
- The measured erosion rate during the test was very low. To start with, tap water was used for the circulation in the filter mats. At the end of the tests, on Day 13, the tap water was replaced by salt water, 3.5% salt, and a new measurement was taken. The bentonite content was less than 0.1% in the outflowing water except for the two first hours after replacing the water. During these two hours, the sediment load in the outflow water was found to be over 2% in one measurement but then stabilized at the same low values as the earlier measurements. The bentonite that fell to the tunnel floor was quickly saturated by the water flowing along the floor, and this water did not seem to affect these wet "bentonite clumps".

- At the end of the test, so much material had fallen to the floor and swollen that the water level rose higher than the supercontainer base, which meant in turn that the lower part of the bentonite blocks had free access to water. This could also be seen during the dismantling of the test.

9.3.3 Test Type 2 – Artificial wetting of the space around distance blocks and measurement of the radial pressure

Objectives

This test is intended to simulate the situation in which distance blocks are installed in a dry tunnel according to the DAWE design. After the intentional water filling of the empty space between the SC and the tunnel walls, there will be no further access to water. The magnitude and development of the radial swelling pressure during the redistribution of the water in the bentonite has been studied on a large scale as a supplement to the small-scale tests described in Section 9.2. The mechanical interaction between the distance block and the simulated rock surface when no additional water is available is important in addressing the critical issue of thermally-induced rock spalling (brittle failure induced by thermally-induced tangential stresses occurring in the tunnel walls).

Test description

This type of test is mainly of interest for the DAWE design. Only the shorter part of the "Big Bertha" test equipment is used, giving a test length of 350 mm (Figure 9-28). One of the 800 mm diameter blocks was machined down to a diameter of 715 mm, which gave a radial slot of the same width as in a full-scale installation (42.5 mm for the distance blocks). The bentonite block was centred in the "tunnel" by the use of bolts fastened into threaded holes in the block. This design also facilitated the adjustment of the block within the slot (Figure 9-29). After installation of the block, the steel cylinder was raised and the load cells mounted. After emplacement of the block, the radial gapwas filled with water by the use of two tubes, one placed at the bottom and one at the top: The upper tube was used for de-airing while the lower one was used for filling. The water used in this test had a salt content of 1.2% (Na/Ca 50/50). This salinity was chosen since it is the concentration expected during operations in Olkiluoto.

After finishing the initial water filling of the cell, there was no access to additional water. The development of the radial swelling pressure was measured continuously at two points within the system, one at the bottom and one at the top as can be seen in Figure 9-30.

Test results and comments

The test was started on 25th October 2007 and is still running with a likely completion date in the summer of 2008.

Figure 9-31 shows the development of the radial pressure for the first 110 days of the test performance. The pressure started to increase immediately after water filling was completed. Since the water-filled slot had a width of 42.5 mm, it was obviously not the swelling pressure from the bentonite that was being measured. When a bentonite block comes into contact with water it will start to swell, and if the system is closed, i.e. no water can leak out, the water pressure will start to increase and act on the pistons intended to measure the swelling pressure. In time, water will be sucked into the bentonite and the slot will be filled with clay. This means that the water pressure will decrease and go down to zero after a certain period of time. In order to verify whether it was water pressure that had been measured in the first early phase of the test, a pressure sensor was connected to the tube that was initially used for de-airing during the water filling stage. The sensor was installed after nine days of testing. A water pressure (100–150 kPa) was measured over a period of 50 days after commencement of the test, but was then found to decrease rapidly to zero, i.e. the earlier available water had been sucked into the bentonite block.

Since the start of testing, a continuously increasing radial swelling pressure has been measured. After more than 100 days, a radial swelling pressure of between 300 and 700 kPa was noted, and it is still increasing.

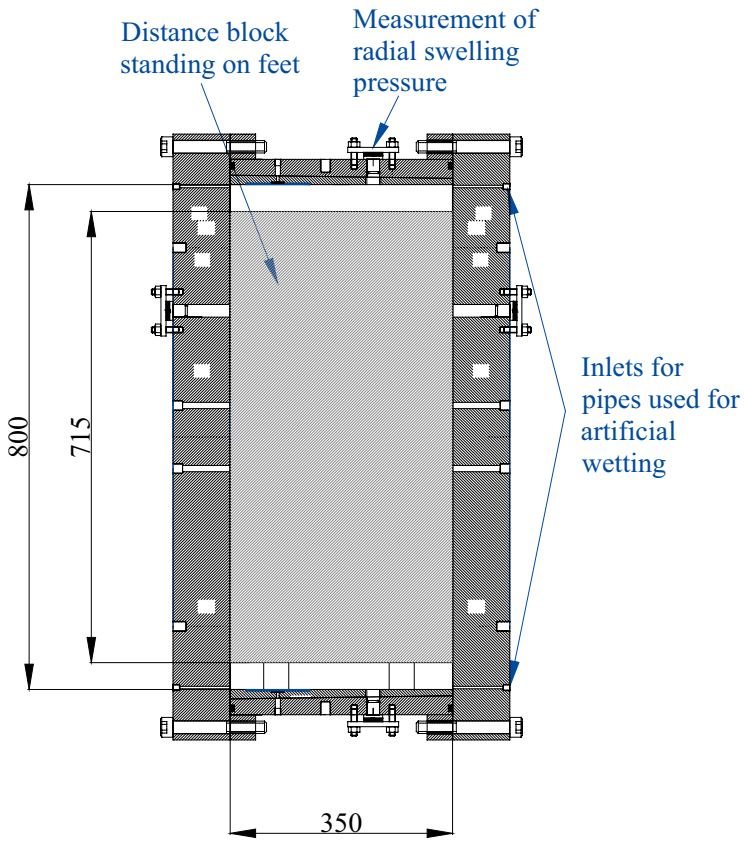

Figure 9-28. *Schematic diagram of the radial wetting test.*

Figure 9-29. *Bentonite block centred in the steel "tunnel" through the use of strong bolts.*

Figure 9-30. Completed installation of radial water uptake test.

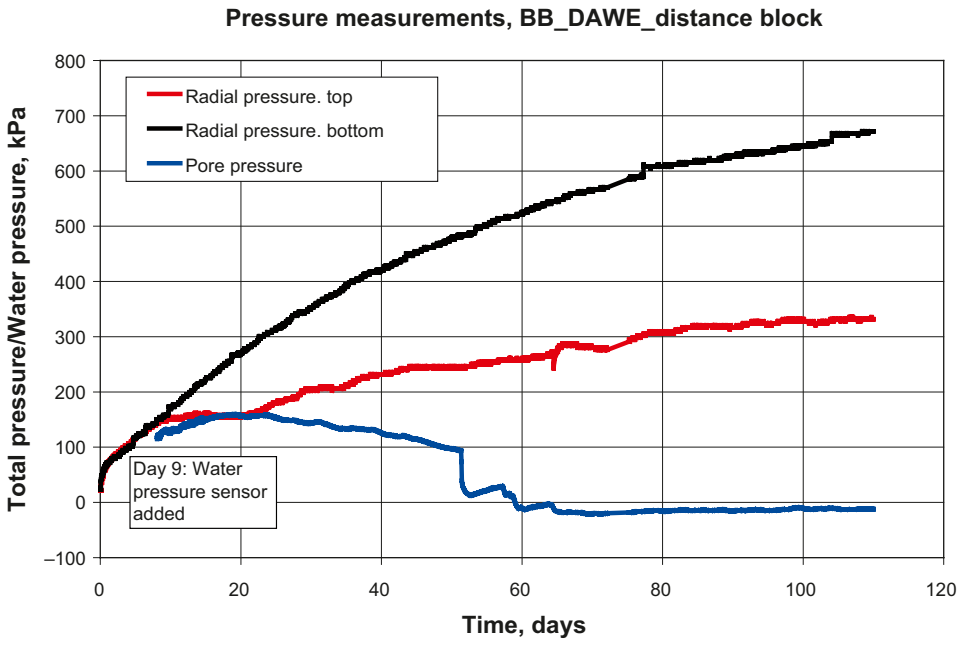

Figure 9-31. Development of radial swelling pressure and porewater suction as a function of time.

10 Conclusions

Studies related to the horizontal emplacement alternative of the KBS-3 design for the deposition of nuclear waste in granitic rock (KBS-3H) have been ongoing since 2002. Studies that mainly concern the behaviour and design of the bentonite buffer material have been described in two reports. The first, covering work conducted over the period 2002–2004, was reported by /Börgesson et al. 2005/. The work conducted from 2005 to mid-2007 is described in this report.

The results of this work have helped in creating a greater understanding of the behaviour of the buffer in the KBS-3H emplacement geometry, and have led to two main design alternatives. One of them requires that the distance blocks should hydraulically separate each container section at all times, even during the installation phase. This design is called the Basic Design (BD), and requires each distance block section to be capable of preventing piping and withstanding full hydraulic pressure immediately after installation. In the second design alternative, the tunnel is kept open for water flow until either an end plug or a temporary plug is built that is able to seal off the high hydraulic water pressure that will develop once the isolated section floods. This design alternative is called DAWE. In the latter design alternative, water may not come into contact with the buffer during installation but must flow freely on the walls and along the floor during the installation period.

The two design alternatives developed for KBS-3H offer both advantages and weaknesses. It was recognized early in the development of the alternatives that the processes related to water inflow are complicated, and that proving their functionality would not be an easy task. In early 2005, five critical issues related to the function of these designs were identified. These issues and the results from the investigations reported here are described below.

1. Humidity-induced swelling.

This process may cause cracking and subsequent loss of bentonite as debris that falls to the floor is removed by water flowing along the floor, as well as by the potential for swelling of this material so that the blocks come into contact with the rock wall. Both these consequences will lead to a hindering of the free water flow along the floor in DAWE, the subsequent fast erosion of bentonite material and its transport out of the tunnel.

A large number of tests have been performed with a bentonite specimen exposed to a free surface of water separated by an air-filled gap. The water transport from the water surface past the air-filled slot into the bentonite has been studied as a function of time under different conditions. The main variables were the gap width, the initial water content of the bentonite, the density of the bentonite, the temperature and the specimen size. The water uptake of the bentonite and the volumetric expansion of the specimens were measured, and the cracking of the specimens was studied

The tests showed that the controlling factor in the wetting process is the transport of water through the air-filled gap between the water surface and the bentonite surface. The transport of water into the bentonite is always faster than the transport through the air-filled gap, which means that the wetting is much slower than when a bentonite specimen is in direct contact with free water and that the relative humidity at the bentonite surface is always lower than 100%. It also means that the water content gradient in the bentonite is rather small, which is favourable for preventing cracking. Since the driving force behind the water transport is the gradient in relative humidity over the gap, the wetting is slower the higher the initial water content of the bentonite is and the wider the slot is. Since the water transport across the gap is driven by vapour diffusion in air, the temperature also affects the wetting rate.

Modelling of the water transport with Code Bright confirmed these processes. The transport of water across the gap and into the bentonite specimens could be very well predicted.

Cracking of the small specimens only occurred as very small cracks on the exposed surface of the specimens and on specimens with a low initial water content, since the water content gradient and thus the difference in volumetric swelling was small in most specimens. The tests with large specimens (blocks with a 30 cm diameter) showed that these were extremely vulnerable to cracking when the initial water ratio was lower than 20%. With an initial water content of 13%, the whole block cracked within no more than 24 hours after it had been exposed to a free water surface at the other side of the gap. The reason why the blocks are more vulnerable to cracking than the small specimens is probably because the stresses are smaller in the small specimens since expansion is not prevented by interlocking effects.

The conclusion that can be drawn based on this study is that the blocks should have a high initial water content when installed in DAWE, preferably above 20%. The distance blocks can be produced with this water content but not the rings inside the supercontainer, since the current design for these materials requires that they have a much higher dry density.

2. Erosion of filling blocks and buffer.

This process will lead to either a loss in the total amount of bentonite if it takes place before a tight plug is built or redistribution of bentonite in the tunnel if it takes place afterwards. Local heavy erosion may be harmful in the case of both design alternatives.

The effect of erosion has so far mainly been studied in another project (Baclo), but new tests on KBS-3H buffer material are ongoing. General conclusions drawn earlier are that the erosion rate seems to be between 1 and 10 gram bentonite per litre eroding water, that a high salt content in the water increases erosion and that the erosion rate is reduced with time.

3. Artificial wetting of distance blocks.

Both design alternatives include artificial water filling of the slot between the distance block and the rock surface as improving options, but for different reasons. In DAWE, the entire tunnel will be filled with water once a functioning plug has been built in order to minimize internal erosion. In BD, the slot between the distance blocks and the rock surface may be filled with water after the installation of each section in order to improve the sealing capacity of the distance blocks. The hydro-mechanical interaction between the buffer, the water-filled slot and the rock are important features in determining the functionality of the two design alternatives.

Tests have shown that bentonite blocks enclosed in a constant volume with an initially- water-filled gap with no access to additional water will swell, close the gap and exert a swelling pressure on the surroundings. In time, the water will be drawn into the interior of the block and the bentonite in the gap will desiccate, resulting in the formation of cracks. However, it would appear that there is still a confining pressure remaining of a few hundred kPa due to stresses arising from expansion of the inner parts that are propagating through the stiff bentonite still in contact with the rock surface. As of 2007 two test series are ongoing to further investigate these processes.

4. Piping through distance blocks.

In BD, the key requirement of the distance block section is to hydraulically seal and isolate all container sections during the installation phase as well as afterwards. Since the distance blocks cannot be installed without a gap between the blocks and the rock surface, this gap must be sealed by the swelling bentonite before piping can occur. This requirement is very difficult to achieve, especially at a high water inflow rate, and a large amount of testing has been undertaken in order to find the limits of the allowable gap between the distance block and the rock.

As of 2007, three different test series studying the critical issue of piping past the distance blocks have been completed:

- Scale tests of a simulated distance block section on a scale of 1:10 with a test length of 1 m.
- Scale tests of a simulated distance block section on a scale of 1:10 and a test length of 3 m.
- Piping tests in a transparent tube.

The conditions naturally present or defined are very important in determining whether a distance block section is able to seal and prevent piping. The test conditions used in the tests carried out over the period 2005–2007 have been harsher than those applied in previous tests. Specifically, use has been made of a water inflow rate of 1 l/min per section versus 0.1 l/min previously; a water pressure increase rate of 1 MPa/h versus 0.1 MPa/h previously; and a maximum water pressure of 5 MPa as opposed to 2 MPa previously. The test arrangements used in the tests described in this report have also been varied somewhat since the KBS-3H design was refined in 2005.

The tests show that the very severe hydraulic conditions applied in the studies performed since 2005 make it difficult for the distance blocks to seal. A wide slot between the distance block and the rock surface filled with pellets does not work due to the low density of the pellets and their low resistance to erosion. The slot must be very narrow in order to be able to seal, and as a result the following design criteria were developed:

- If no special measures are taken to help the process of emplacement drift sealing (e.g. the block is placed directly on the floor of the tunnel and left to seal on its own), the slot between the block and the rock surface at the top of the tunnel must not exceed 2 mm.
- If the slot between the block and the rock surface is artificially filled with water and the block is centred in the tunnel, the slot must not exceed 5 mm.
- If the hydraulic conditions inside the distance block section (pressure and flow) are controlled by the use of a tube past the distance blocks, the slot between the block and the rock surface can be increased, but by no more than about 10 mm. The water filling of the empty space in the super-container section and the water pressure increase are controlled in order to give the distance block about two weeks to seal before full pressure is reached. The tube can then be withdrawn in steps.

The reason why the slot between the block and the rock surface must be so narrow is that there is not time for the distance block to swell and yield a high enough swelling pressure. Consequently, the sealing must be done by another process. The narrow gap instead yields clogging of bentonite in the gap and sealing is probably achieved by the arching of clogged material.

5. Hydraulic pressure on distance block end surface.

Since the distance block section in BD must seal hydraulically, a high water pressure is likely to develop inside the supercontainer section once the open slots have been filled with water. If the water pressure propagates deeply into the joint between distance blocks or between a distance block and the supercontainer lid, there will be unacceptably high axial forces developed on the distance blocks and on thefixing ring outside the distance block section.

Tests to examine distance block movement were completed on a scale 1:10 in a device with an inner diameter of 175 mm. However, as with the piping tests, the gaps left were of the full dimension anticipated in a repository environment. Since the radius of the equipment is only about 85 mm, radial water penetration deeper than 85 mm could not be studied.

Previously, tests indicated that an axial gap of 7 mm between the lid of the supercontainer and the distance block could be accepted and yield a radial water penetration that is limited to about 0.1 m. However, these tests were carried out under the less harsh test conditions mentioned above. In the new tests, both the test conditions and the gap width were varied in order to try to find the limits of DB functionality. Earlier tests also showed that a fixing ring is required outside the distance blocks in order to support the blocks and prevent them from moving.

Tests performed to date show that with the new harsher test conditions not even an axial slot of 2 mm could prevent a water pressure of 5 MPa from propagating into the centre of a DB with a radius of 85 mm. When the inflow rate was lowered to 0.1 l/min, the radial water penetration was 20–40 mm.

The piping tests and the hydraulic pressure tests have so far shown that the distance blocks must fit very closely against both the rock surface and the lid of the supercontainer in order to function as specified in the Basic Design under harsh hydraulic conditions. To ensure proper DB function, the water pressure within the SC section should be controlled by a temporary tube placed past the DB and into the SC section. The need for an unrealistically tight fit of the DB within the emplacement drift, in combination with findings that the deformation of the distance blocks is unacceptably large at 5 MPa water pressure, have led to the preliminary conclusion that the KBS-3H Basic Design variant is unlikely to function as desired in its present form.

Additional comments

From the results of the laboratory tests the following clear statements can be done:

- The test results show that piping cannot be avoided in the Basic Design alternative unless distance block gaps are very small, the inflows are very low and the wetting /saturation times are very long.
- Recent evaluation of the very tight geometric requirements of the BD, together with study findings that the deformation of the distance blocks is unacceptably large at 5 MPa water pressure, have led to the conclusion that the Basic Design will not function reliably in its initial design.

References

SKB's (Svensk Kärnbränslehantering AB) publications can be found at www.skb.se/publications. References to SKB's unpublished documents are listed separately at the end of the reference list. Unpublished documents will be submitted upon request to document@skb.se.

Alonso E E, Gens A, Josa A, 1990. A constitutive model for partially saturated soils. Géotechnique, 40, pp 405–430.

Autio J, Johansson E, Hagros A, Börgesson L, Sandén T, Rönnqvist P-E, Eriksson M, Berghäll J, Kotola R, Parkkinen I, 2008a. KBS-3H design description 2006. SKB R-08-32, Svensk Kärnbränslehantering AB.

Autio J, Johansson E, Hagros A, Anttila P, Rönnqvist P-E, Börgesson L, Sandén T, Eriksson M, Halvarsson B, Berghäll J, Kotola R, Parkkinen I, 2008b. KBS-3H design description 2007. SKB R-08-44, Svensk Kärnbränslehantering AB.

Börgesson L, Hernelind J, 1999. Coupled thermo-hydro-mechanical calculations of the water saturation phase of a KBS-3 deposition hole. Influence of hydraulic rock properties on the water saturation phase. SKB TR-99-41, Svensk Kärnbränslehantering AB.

Börgesson L, Sandén T, Fälth B, Åkesson M, Lindgren E, 2005. Studies of buffers behaviour in KBS-3H design. Work during 2002–2004. SKB R-05-50, Svensk Kärnbränslehantering AB.

Dueck A, 2007. Results from suction controlled laboratory tests on unsaturated bentonite – verification of a model. Springer Proceedings in Physics, 112, pp 329–335.

Johannesson L-E, Börgesson L, Sandén T, 1995. Compaction of bentonite blocks. Development of technique for industrial production of blocks which are manageable by man. SKB TR 95-19, Svensk Kärnbränslehantering AB.

Karnland O, Sandén T, Johannesson L-E, Eriksen T E, Jansson M, Wold S, Pedersen K, Motamedi M, Rosborg B, 2000. Long term test of buffer material. Final report on the pilot parcels. SKB TR-00-22, Svensk Kärnbränslehantering AB.

Åkesson M, 2006. Äspö Hard Rock Laboratory. Temperature Buffer Test. Evaluation modeling – Mock-up test. SKB IPR-06-11, Svensk Kärnbränslehantering AB.

Appendix A

Appendix A1: Initial and final values of water content and density

Name	Initial conditions		Final conditions							Calculated from Δm	
	w(%)	ρ	w(top)	w(midle)	w(water)	w(average)	ρ(top)	ρ(midle)	ρ(water)	w(Δm)	w(Δm)-w(average)
	%	kg/m^3	%	%	%	%	kg/m^3	kg/m^3	kg/m^3	%	%
S122	19,5	1970,0	27,3	26,7	27,9	27,3	1857,5	1844,3	1854,6	28,5	1,2
S124	23,7	2023,3	28,8	29,3	29,9	29,3	1930,5	1933,1	1917,7	30,2	0,8
S212	19,6	2062,0	33,3	34,0	41,4	36,2	1828,3	1826,6	1804,8	35,3	-0,9
S220	10,5	1961,9	24,9	25,6	26,3	25,6	1651,8	1666,6	1665,0	26,4	0,8
S221	15,0	2021,7	25,8	26,1	27,1	26,4	1808,5	1818,9	1810,3	27,2	0,8
S222	19,4	2073,5	27,1	27,6	28,3	27,7	1918,7	1916,1	1905,0	28,7	1,0
S222_H1	19,4	2073,5	20,3	20,4	20,3	20,4	2023,1	2031,3	2035,2	20,8	0,5
S222_H2	19,4	2073,5	20,2	20,3	20,5	20,3	2018,8	2027,4	2036,7	20,7	0,4
S222_T10a	19,4	2073,5	35,8	37,6	40,7	38,0	1802,4	1788,0	1752,3	38,6	0,6
S222_T10b	19,4	2073,5	35,4	36,8	39,2	37,1	1813,7	1798,9	1761,0	37,6	0,5
S222_T30a	19,4	2073,5	32,1	32,7	33,3	32,7	1846,2	1847,3	1830,7	33,8	1,1
S222_T30b	19,4	2073,5	31,2	31,9	32,6	31,9	1862,7	1855,1	1835,7	33,2	1,2
S222_A1	19,4	2073,5	34,0	34,7	35,8	34,8	1822,4	1822,1	1802,3	35,9	1,0
S222_A2	19,4	2073,5	33,5	34,4	35,5	34,5	1833,5	1825,4	1803,8	35,5	1,0
S223	21,8	2067,4	28,1	28,6	29,2	28,7	1953,6	1948,1	1934,4	29,6	0,9
S224	23,7	2046,3	29,1	29,4	29,9	29,5	1958,0	1954,2	1940,6	30,6	1,1
S232	19,5	2074,2	26,5	27,0	27,6	27,0	1929,5	1932,6	1920,2	27,9	0,9
S322	19,4	2039,8	27,4	27,9	28,6	28,0	1937,1	1936,5	1916,7	28,7	0,7
S323	22,0	2068,3	28,5	28,8	29,5	28,9	1949,8	1946,8	1933,4	29,9	1,0
S420	10,5	2109,5	24,8	25,5	26,3	25,5	1727,0	1734,3	1725,8	26,2	0,7
S421	15,6	2145,7	26,1	26,5	27,3	26,6	1869,6	1876,5	1847,9	28,0	1,3
S422	19,5	2098,0	27,6	28,1	28,8	28,2	1942,1	1939,9	1920,7	28,9	0,8
S122_V	19,5	1970,0	26,9	27,3	28,0	27,4	1860,2	1870,3	1865,7	28,1	0,7
S124_V	23,7	2023,3	29,0	29,4	28,3	28,9	1936,3	1934,9	1926,2	30,3	1,5
S212_V	19,6	2062,0	33,0	33,8	35,1	34,0	1836,4	1834,4	1809,0	34,8	0,8
S220_V	10,5	1961,9	24,7	24,9	25,9	25,2	1677,9	1654,3	1656,6	26,2	1,0
S221_V	15,0	2021,7	25,6	26,3	27,0	26,3	1807,9	1824,9	1806,8	27,1	0,8
S222_V	19,4	2073,5	27,0	27,4	28,0	27,5	1922,0	1924,7	1910,7	28,1	0,6
S222_H1_V	19,4	2073,5	20,4	20,2	20,3	20,3	2022,0	2036,2	2041,2	20,6	0,3
S222_H2_V	19,4	2073,5	20,3	20,4	20,3	20,3	2029,4	2040,5	2040,5	20,6	0,3
S222_T10a_V	19,4	2073,5	34,1	35,1	37,2	35,5	1823,6	1814,0	1785,3	36,2	0,8
S222_T10b_V	19,4	2073,5	33,3	34,5	36,9	34,9	1837,1	1826,4	1793,2	35,7	0,8
S222_T30a_V	19,4	2073,5	31,8	32,3	32,9	32,3	1854,3	1851,1	1837,5	33,3	1,0
S222_T30b_V	19,4	2073,5	32,7	33,3	33,9	33,3	1835,7	1838,2	1825,1	34,3	1,0
S222_A1_V	19,4	2073,5	34,0	34,5	35,7	34,7	1826,9	1823,7	1823,2	35,8	1,0
S222_A2_V	19,4	2073,5	33,4	34,2	35,3	34,3	1826,7	1816,9	1803,9	35,0	0,6
S223_V	21,8	2067,4	28,0	28,3	29,0	28,4	1956,0	1954,8	1940,4	29,2	0,7
S224_V	23,7	2046,3	28,9	29,3	29,8	29,3	1961,8	1958,0	1944,6	30,3	1,0
S232_V	19,5	2074,2	26,6	26,9	27,7	27,1	1928,8	1933,0	1920,3	27,5	0,4
S322_V	19,4	2039,8	27,4	27,7	28,5	27,9	1940,1	1938,7	1920,2	28,4	0,5
S323_V	22,0	2068,3	28,3	28,7	29,4	28,8	1958,5	1950,9	1941,0	29,6	0,8
S420_V	10,5	2109,5	24,8	25,4	26,2	25,5	1744,6	1740,7	1741,7	25,9	0,4
S421_V	15,6	2145,7	26,0	26,4	27,2	26,5	1904,8	1873,5	1854,7	27,7	1,2
S422_V	19,5	2098,0	27,4	27,8	28,6	27,9	1945,6	1943,1	1925,5	28,5	0,6
S210_ph	10,4	1962,5								33,1	
S210-V	10,4	1962,5	31,1	31,9	33,6	32,2	1585,0	1542,0	1569,4	33,3	1,1
S222-V	19,5	2065,6	27,9	28,5	29,1	28,5	1923,4	1925,3	1915,6	28,7	0,2
S212_ph	19,5	2065,6	34,3	35,2	36,2	35,2	1828,5	1827,8	1808,3	36,0	0,8
S212-V	19,5	2065,6	34,3	34,9	35,8	35,0	1833,5	1834,9	1820,9	35,8	0,8
S222_g20	19,5	2065,6	30,3	31,0	32,0	31,1	1876,8	1873,2	1861,4	31,7	0,6
S222-g20-V	19,5	2065,6	31,5	32,1	32,9	32,1	1872,2	1872,9	1857,1	32,6	0,5
S222_Dr0b	19,5	2065,6	27,0	27,8	28,6	27,8	1936,3	1939,2	1906,5	28,8	1,0
S222_Dr0a-V	19,5	2065,6	27,1	27,6	28,5	27,7	1960,8	1946,7	1919,2	28,9	1,2
S232-V	19,5	2065,6	26,9	27,3	27,9	27,4	1939,1	1938,3	1932,5	27,9	0,5
S322-V	19,7	2098,3	27,6	28,0	28,6	28,1	1948,6	1943,8	1929,6	28,4	0,4
S323-V	21,5	2078,2	28,5	28,9	29,4	28,9	1952,7	1948,4	1938,2	29,1	0,2
S422-V	19,6	2102,8	27,9	28,5	29,0	28,4	1947,7	1942,2	1927,9	28,8	0,3
S222-T10c	19,5	2065,6	26,2	26,8	27,7	26,9	1948,2	1943,8	1937,0	27,1	0,2
S222-T10c-V	19,5	2065,6	26,4	26,9	27,7	27,0	1946,3	1948,3	1935,9	27,1	0,1
S222-T10d	19,5	2065,6	26,3	26,9	27,7	27,0	1946,7	1947,3	1936,0	26,9	0,0
S222-T10d-V	19,5	2065,6	26,4	26,9	27,8	27,0	1942,0	1948,1	1934,1	27,0	0,0

Two extra specimens, with suffix _ph, were prepared for photographing purpose. No further interpretation than presented in this table was made.

Appendix A2: Figures, increase in mass

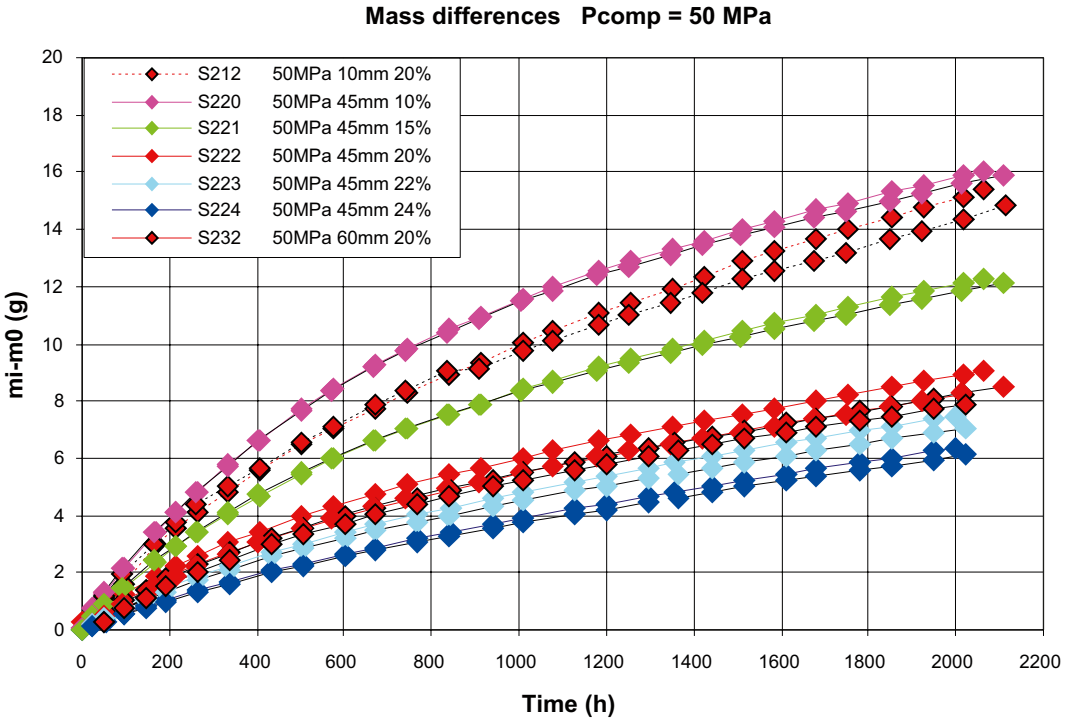

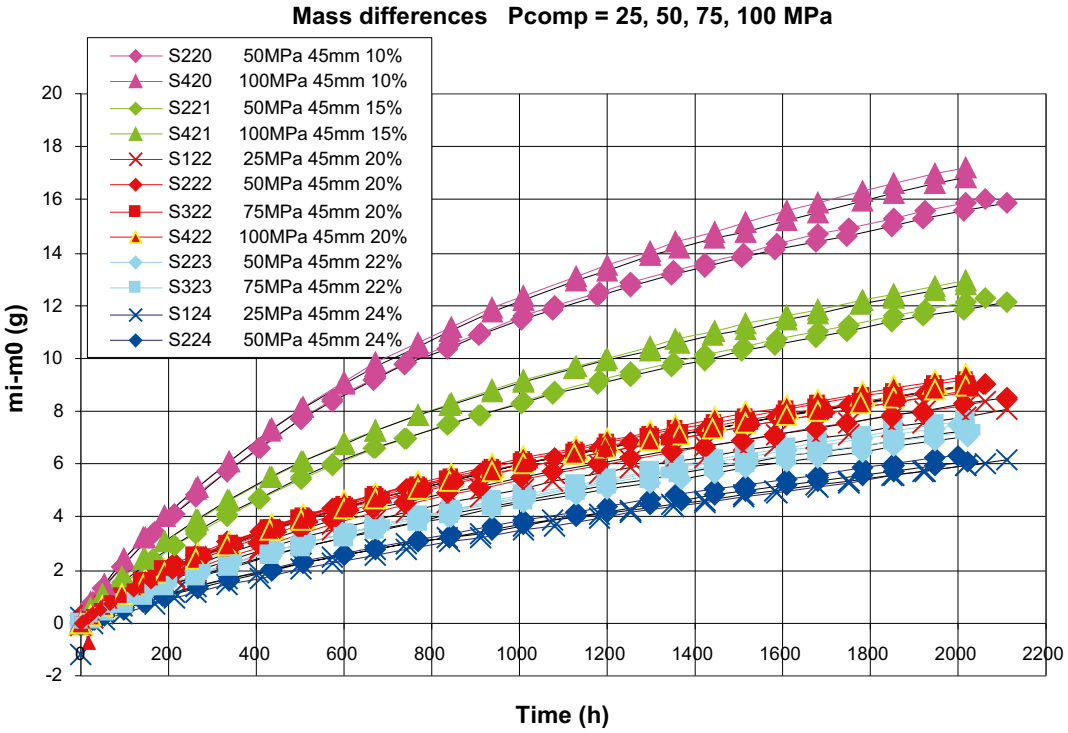

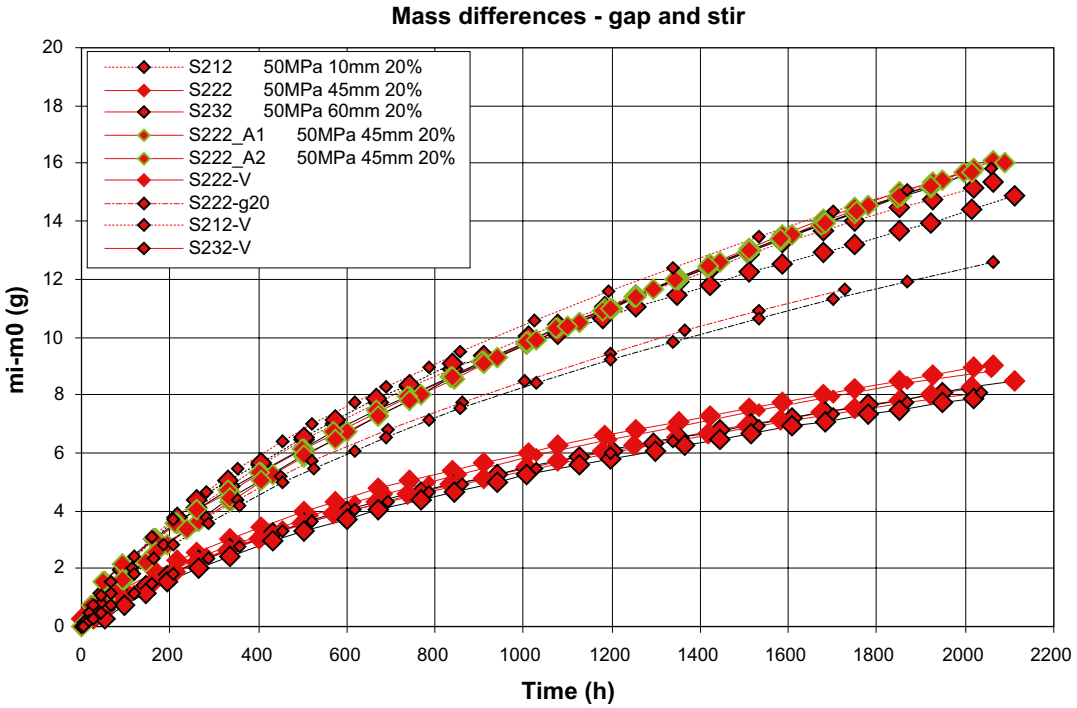
Mass differences - gap and stir
S212 50MPa 10mm 20%
S222 50MPa 45mm 20%
S232 50MPa 60mm 20%
S222_A1 50MPa 45mm 20%
S222_A2 50MPa 45mm 20%
S222-V
S222-g20
S212-V
S232-V
mi-m0 (g)
Time (h)
0
2
4
6
8
10
12
14
16
18
20
0
200
400
600
800
1000
1200
1400
1600
1800
2000
2200

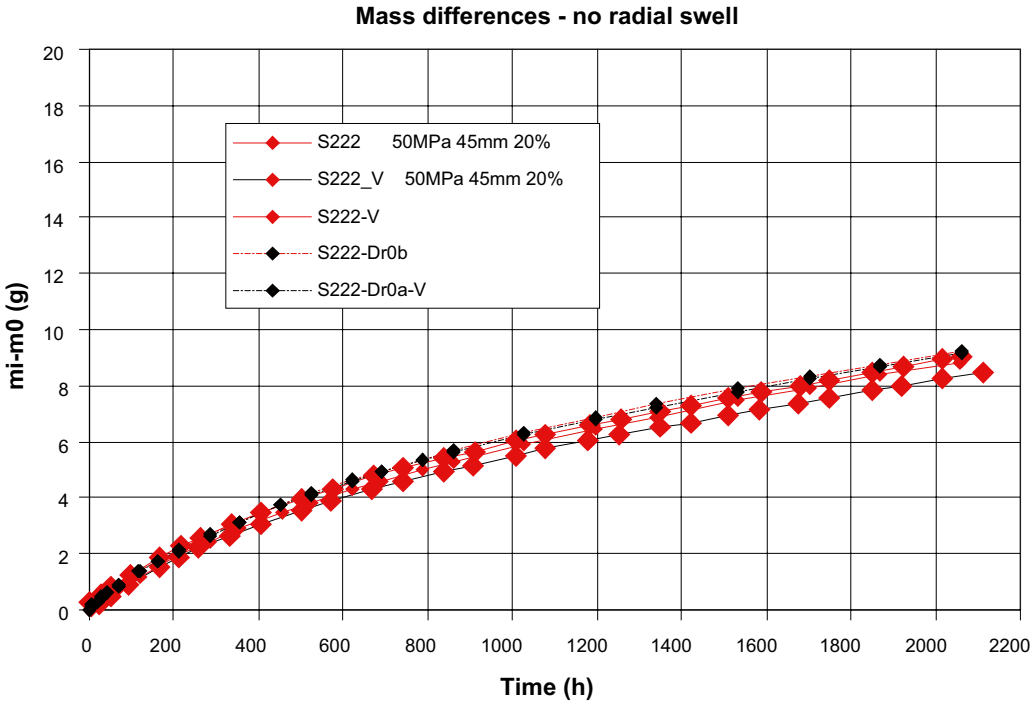
Mass differences - no radial swell
S222 50MPa 45mm 20%
S222_V 50MPa 45mm 20%
S222-V
S222-Dr0b
S222-Dr0a-V
mi-m0 (g)
Time (h)
0
2
4
6
8
10
12
14
16
18
20
0
200
400
600
800
1000
1200
1400
1600
1800
2000
2200

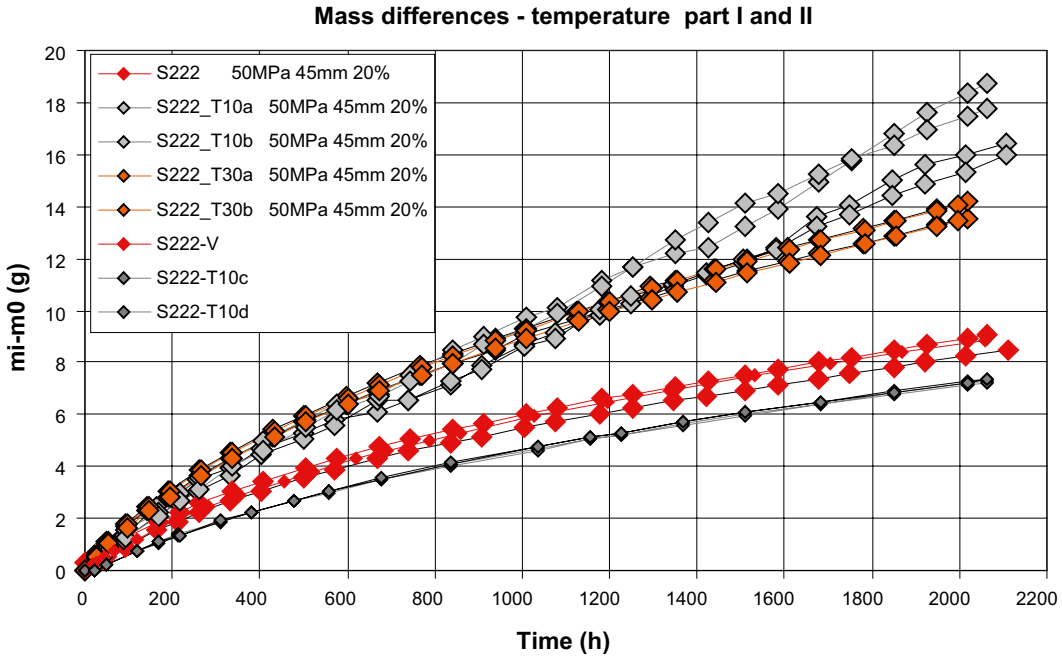
Mass differences - temperature part I and II
S222 50MPa 45mm 20%
S222_T10a 50MPa 45mm 20%
S222_T10b 50MPa 45mm 20%
S222_T30a 50MPa 45mm 20%
S222_T30b 50MPa 45mm 20%
S222-V
S222-T10c
S222-T10d
mi-m0 (g)
Time (h)
0
2
4
6
8
10
12
14
16
18
20
0
200
400
600
800
1000
1200
1400
1600
1800
2000
2200

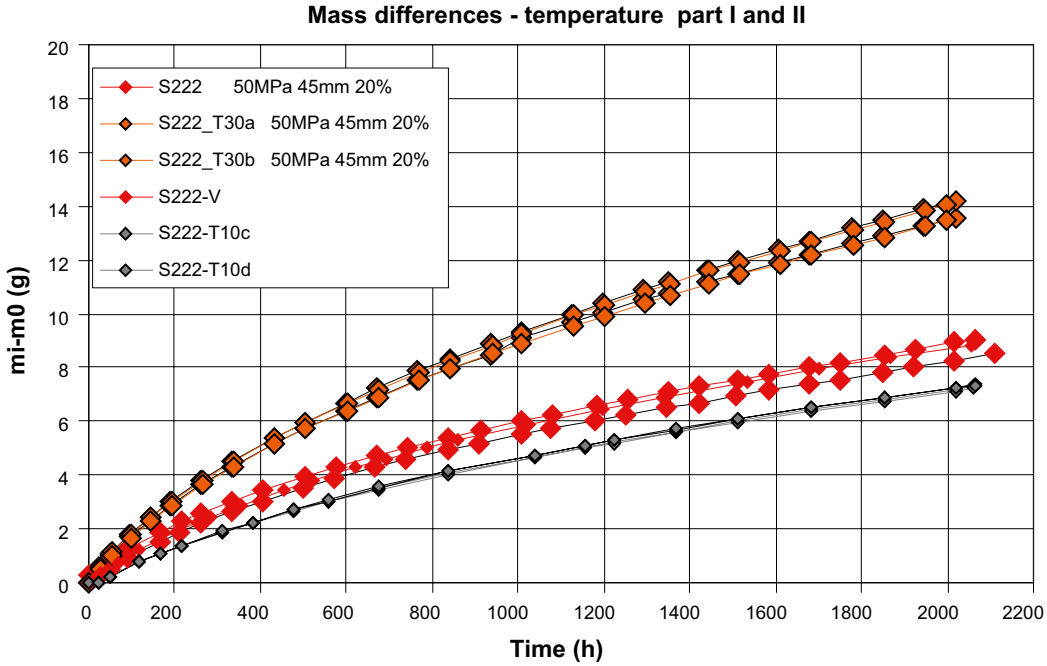
Mass differences - temperature part I and II
S222 50MPa 45mm 20%
S222_T30a 50MPa 45mm 20%
S222_T30b 50MPa 45mm 20%
S222-V
S222-T10c
S222-T10d
mi-m0 (g)
Time (h)
0
2
4
6
8
10
12
14
16
18
20
0
200
400
600
800
1000
1200
1400
1600
1800
2000
2200

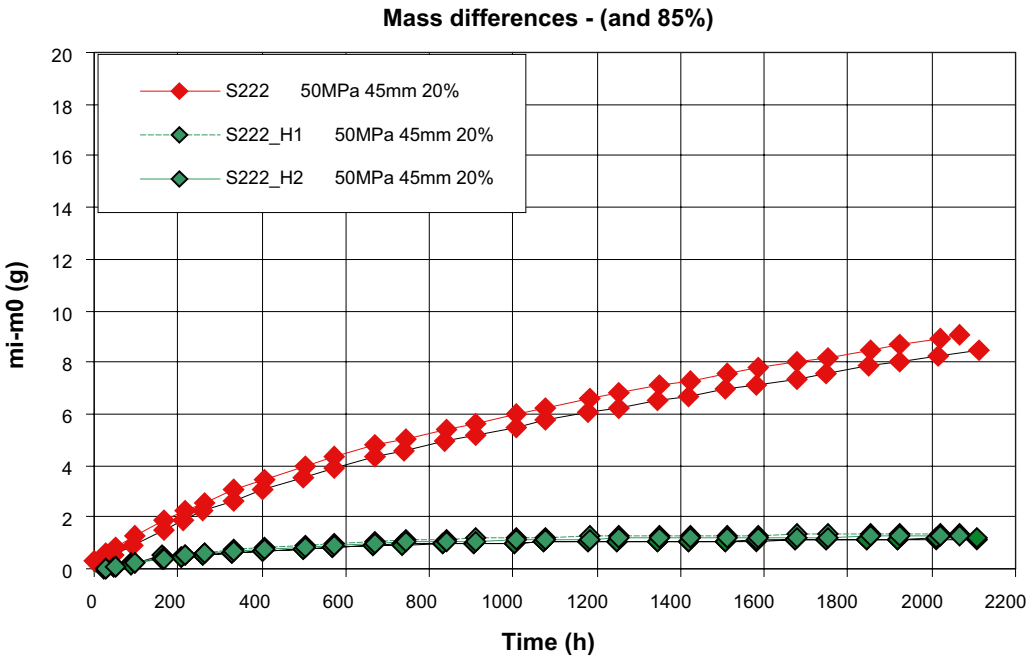
Mass differences - (and 85%)
S222 50MPa 45mm 20%
S222_H1 50MPa 45mm 20%
S222_H2 50MPa 45mm 20%
mi-m0 (g)
Time (h)
0
2
4
6
8
10
12
14
16
18
20
0
200
400
600
800
1000
1200
1400
1600
1800
2000
2200

Appendix A3: Figures, increase in height

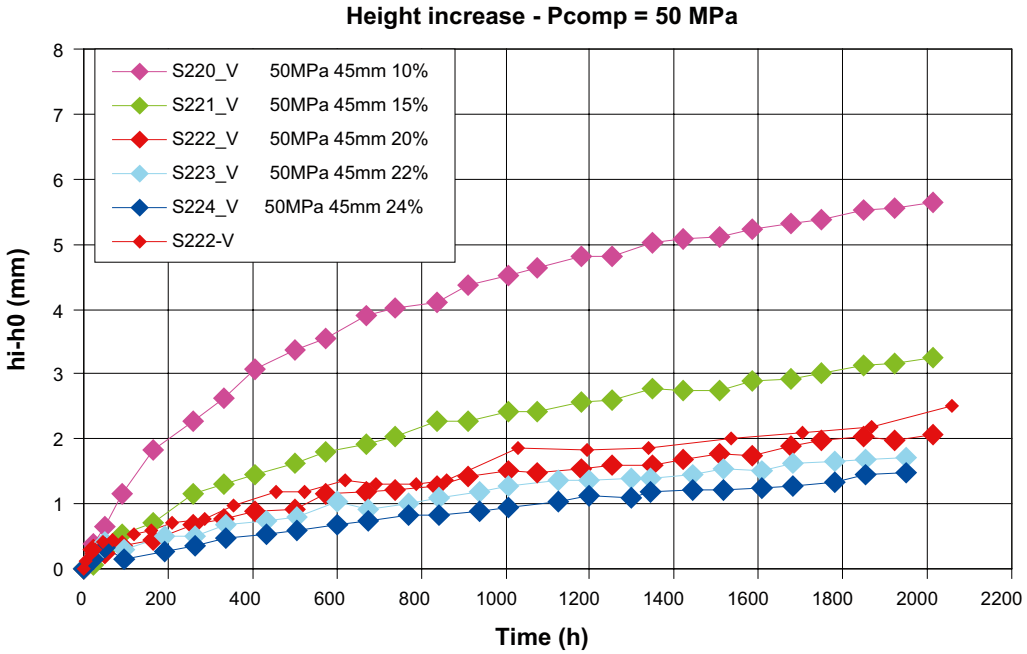

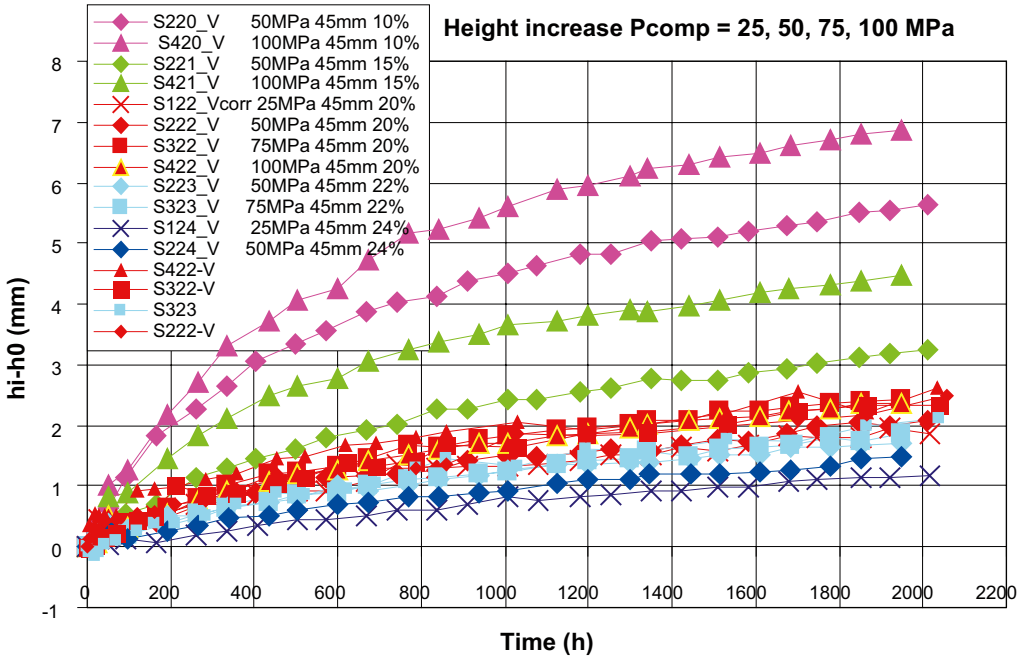

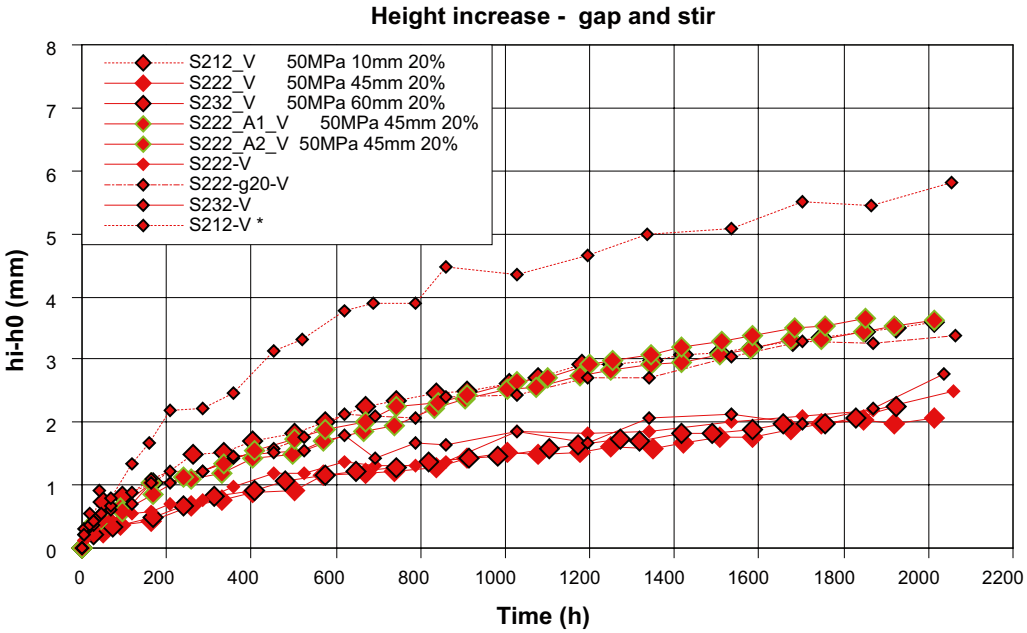
Height increase - gap and stir
S212_V 50MPa 10mm 20%
S222_V 50MPa 45mm 20%
S232_V 50MPa 60mm 20%
S222_A1_V 50MPa 45mm 20%
S222_A2_V 50MPa 45mm 20%
S222-V
S222-g20-V
S232-V
S212-V *
hi-h0 (mm)
Time (h)
0
1
2
3
4
5
6
7
8
0
200
400
600
800
1000
1200
1400
1600
1800
2000
2200

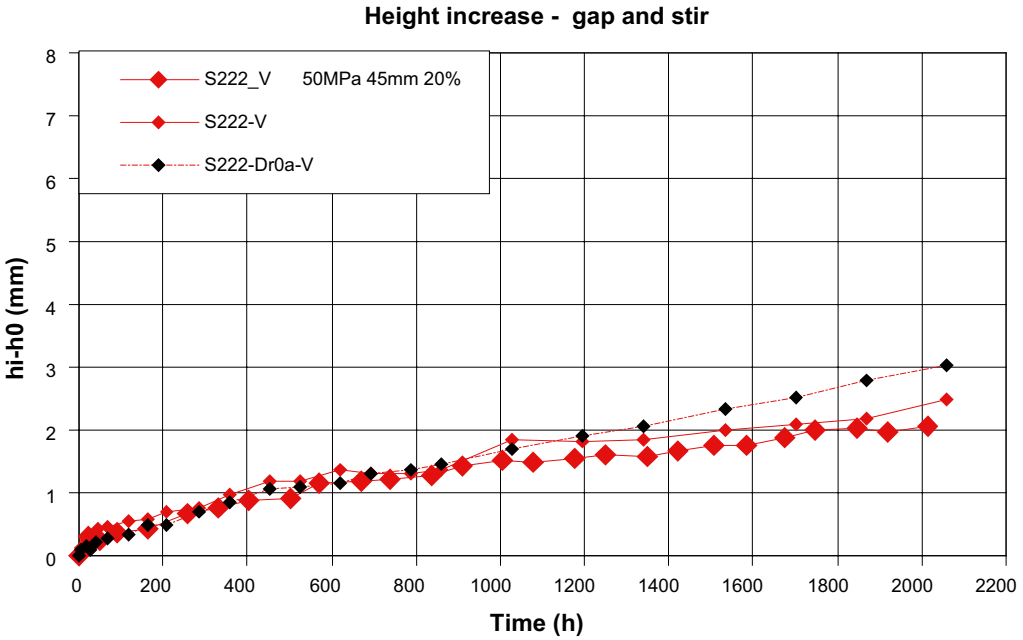
Height increase - gap and stir
S222_V 50MPa 45mm 20%
S222-V
S222-Dr0a-V
hi-h0 (mm)
Time (h)
0
1
2
3
4
5
6
7
8
0
200
400
600
800
1000
1200
1400
1600
1800
2000
2200

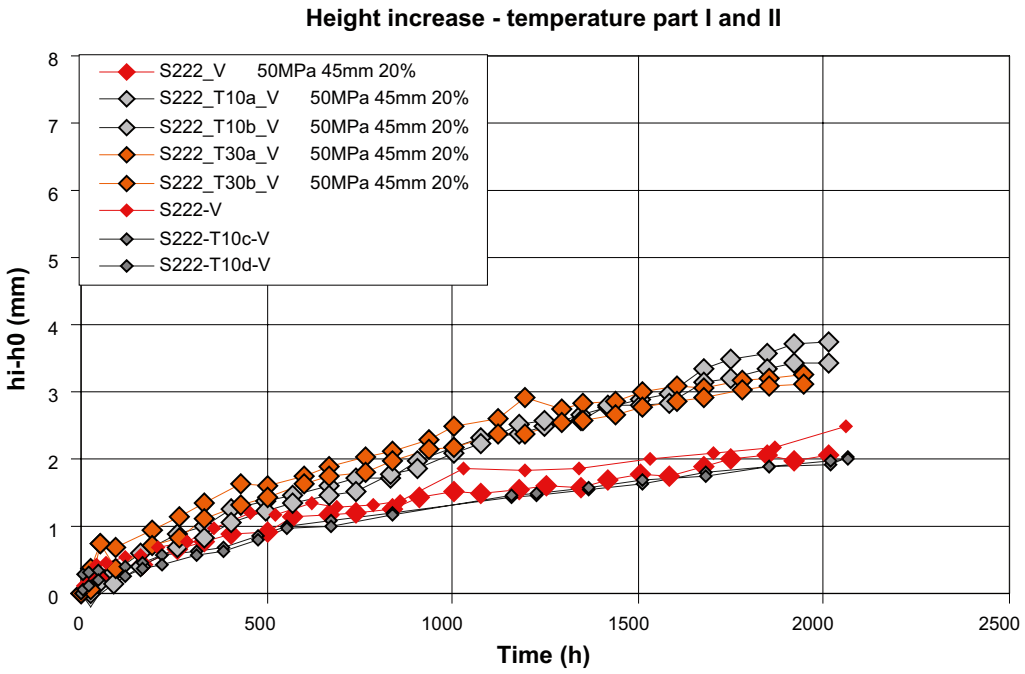
Height increase - temperature part I and II
S222_V 50MPa 45mm 20%
S222_T10a_V 50MPa 45mm 20%
S222_T10b_V 50MPa 45mm 20%
S222_T30a_V 50MPa 45mm 20%
S222_T30b_V 50MPa 45mm 20%
S222-V
S222-T10c-V
S222-T10d-V
hi-h0 (mm)
Time (h)
0
1
2
3
4
5
6
7
8
0
500
1000
1500
2000
2500

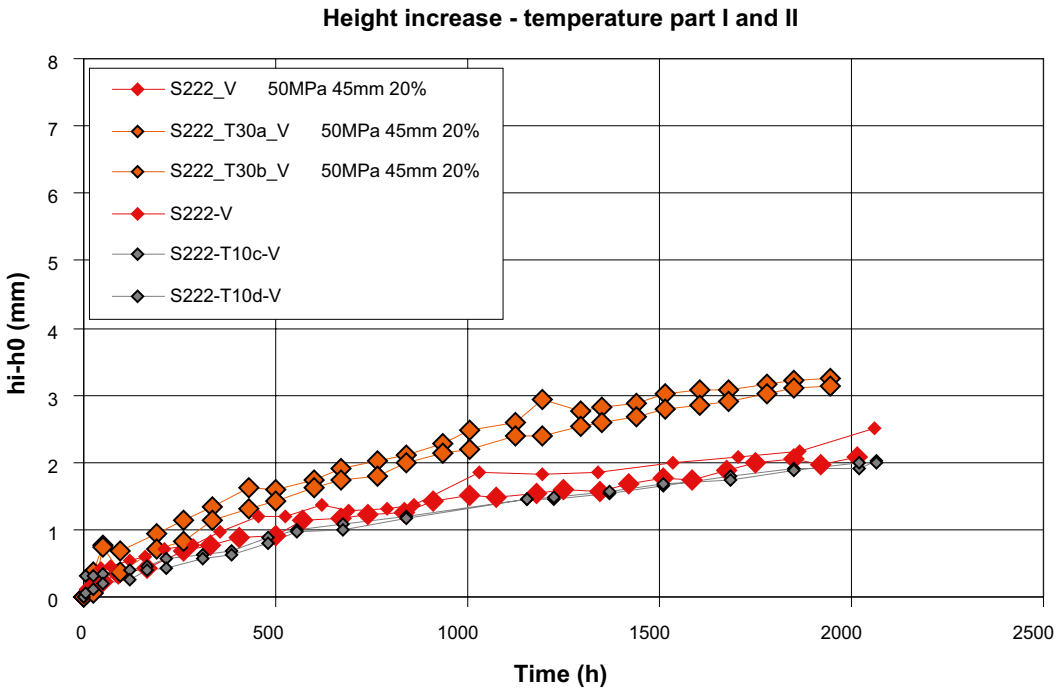
Height increase - temperature part I and II
S222_V 50MPa 45mm 20%
S222_T30a_V 50MPa 45mm 20%
S222_T30b_V 50MPa 45mm 20%
S222-V
S222-T10c-V
S222-T10d-V
hi-h0 (mm)
Time (h)
0
1
2
3
4
5
6
7
8
0
500
1000
1500
2000
2500

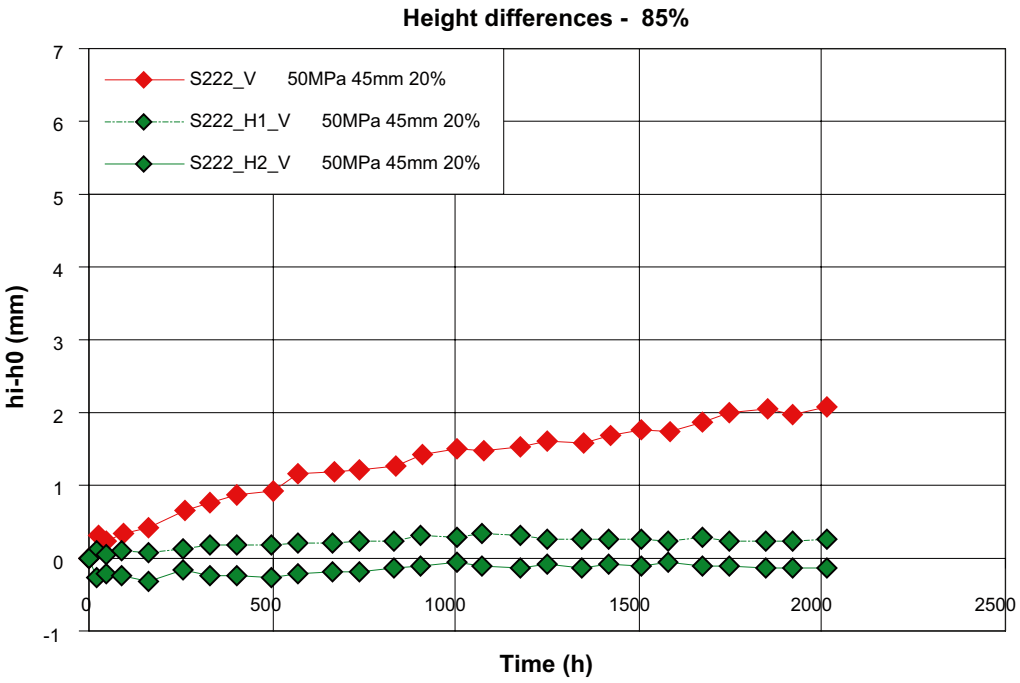
Height differences - 85%
S222_V 50MPa 45mm 20%
S222_H1_V 50MPa 45mm 20%
S222_H2_V 50MPa 45mm 20%
hi-h0 (mm)
Time (h)
7
6
5
4
3
2
1
0
-1
0
500
1000
1500
2000
2500

Appendix A4: Figures, increase in diameter

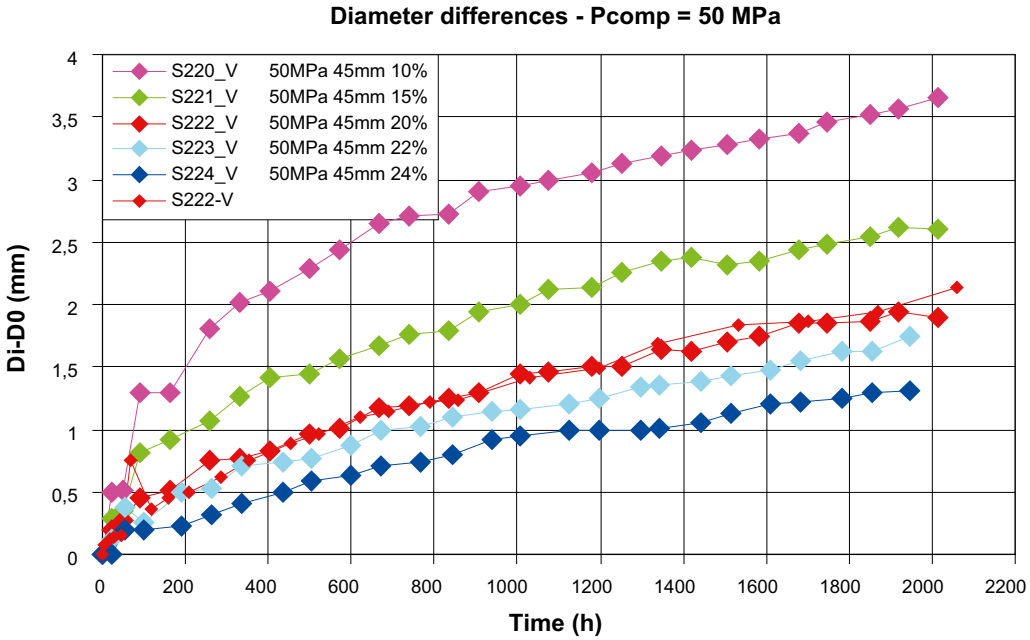

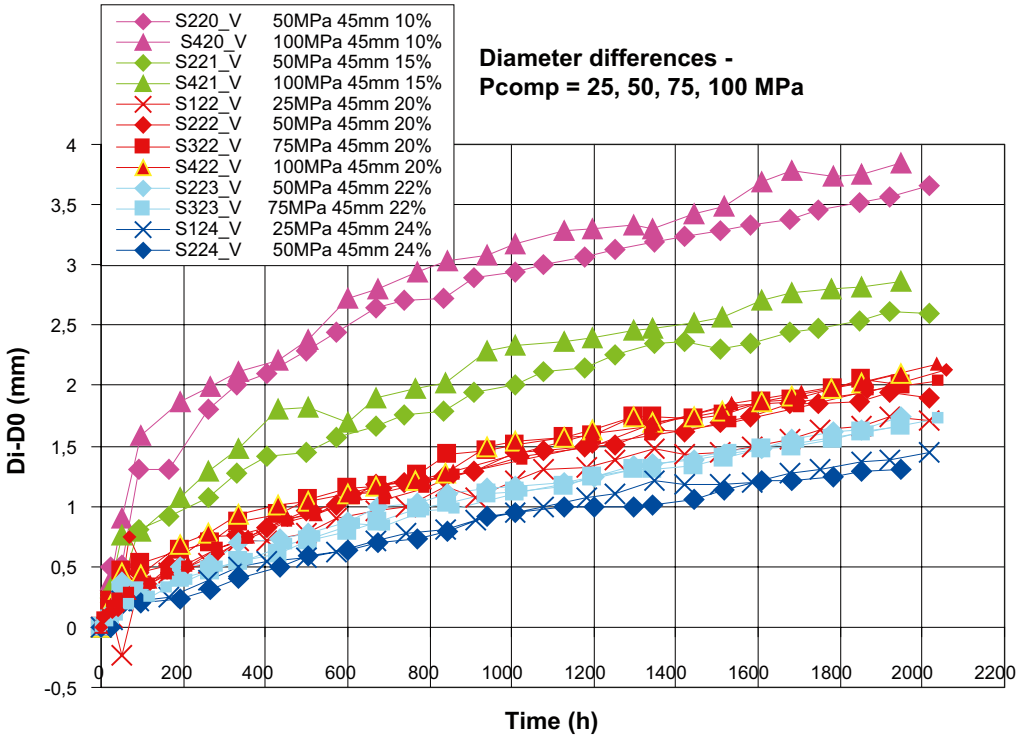

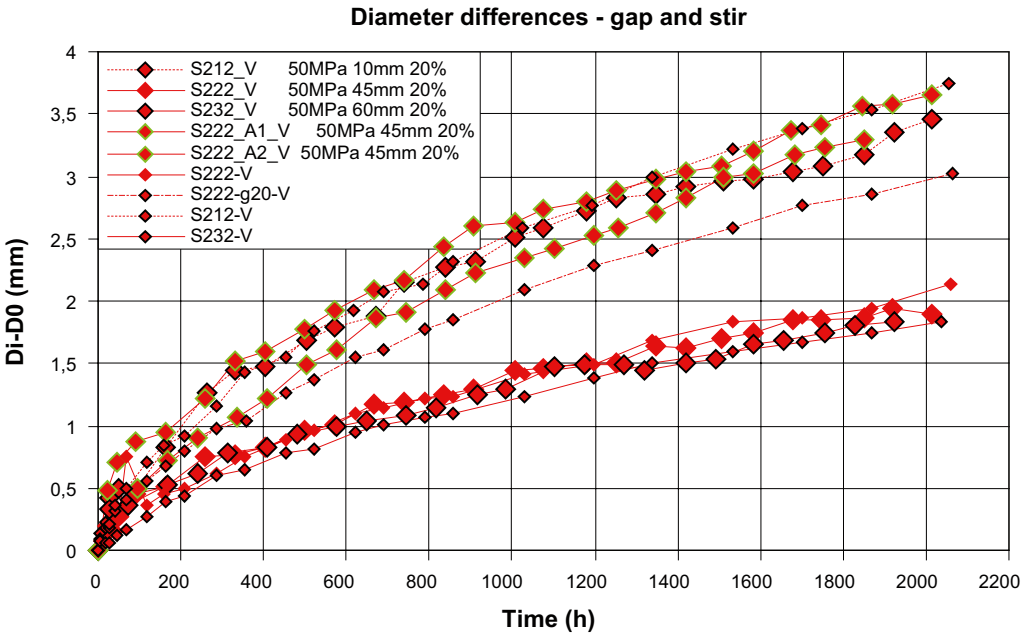
Diameter differences - gap and stir
S212_V 50MPa 10mm 20%
S222_V 50MPa 45mm 20%
S232_V 50MPa 60mm 20%
S222_A1_V 50MPa 45mm 20%
S222_A2_V 50MPa 45mm 20%
S222-V
S222-g20-V
S212-V
S232-V
Di-D0 (mm)
Time (h)
0
0,5
1
1,5
2
2,5
3
3,5
4
0
200
400
600
800
1000
1200
1400
1600
1800
2000
2200

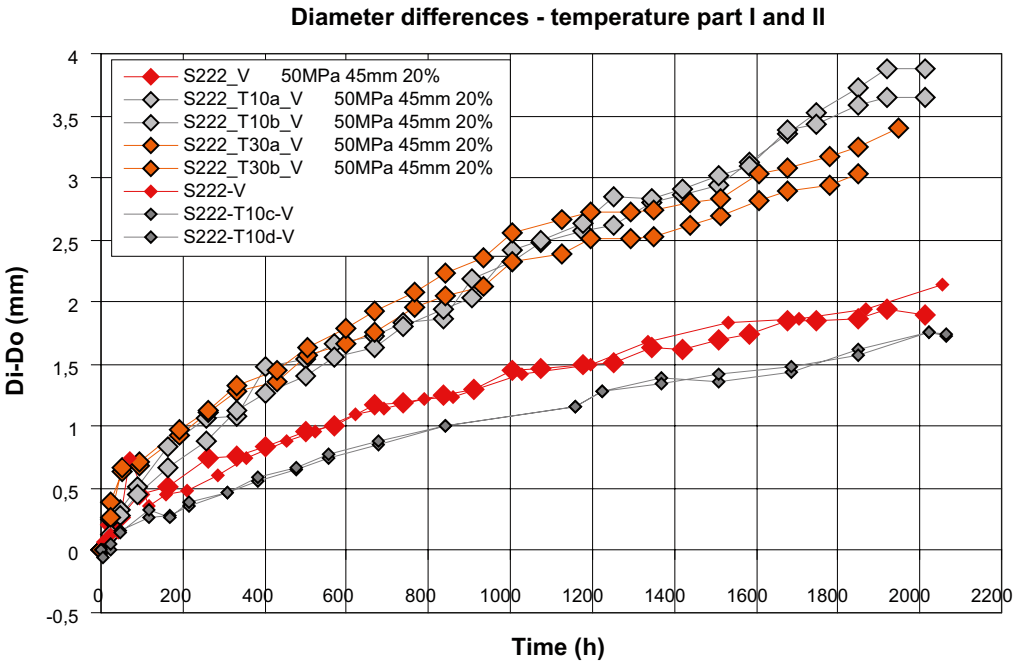
Diameter differences - temperature part I and II
S222_V 50MPa 45mm 20%
S222_T10a_V 50MPa 45mm 20%
S222_T10b_V 50MPa 45mm 20%
S222_T30a_V 50MPa 45mm 20%
S222_T30b_V 50MPa 45mm 20%
S222-V
S222-T10c-V
S222-T10d-V
Di-Do (mm)
Time (h)
-0,5
0
0,5
1
1,5
2
2,5
3
3,5
4
0
200
400
600
800
1000
1200
1400
1600
1800
2000
2200

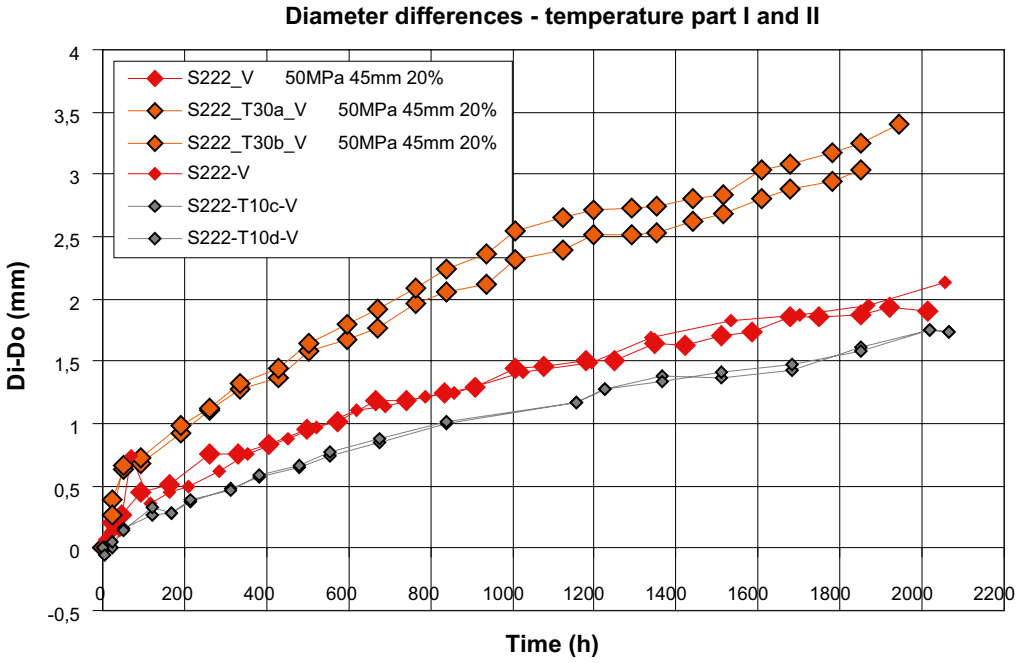
Diameter differences - temperature part I and II
S222_V 50MPa 45mm 20%
S222_T30a_V 50MPa 45mm 20%
S222_T30b_V 50MPa 45mm 20%
S222-V
S222-T10c-V
S222-T10d-V
Di-Do (mm)
Time (h)
4
3,5
3
2,5
2
1,5
1
0,5
0
-0,5
0
200
400
600
800
1000
1200
1400
1600
1800
2000
2200

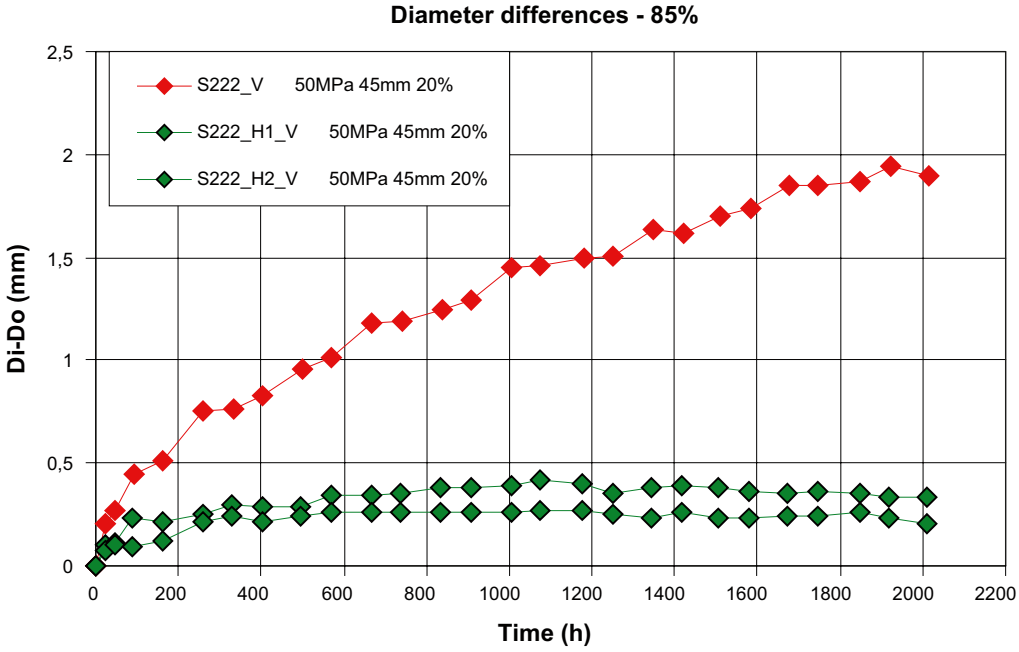
Diameter differences - 85%
S222_V 50MPa 45mm 20%
S222_H1_V 50MPa 45mm 20%
S222_H2_V 50MPa 45mm 20%
Di-Do (mm)
Time (h)
2,5
2
1,5
1
0,5
0
0
200
400
600
800
1000
1200
1400
1600
1800
2000
2200

Appendix A5: Photos of cracking, selected specimens

Both circumferential cracking and cracking on the surface towards the water

Specimen S210

Specimen S420

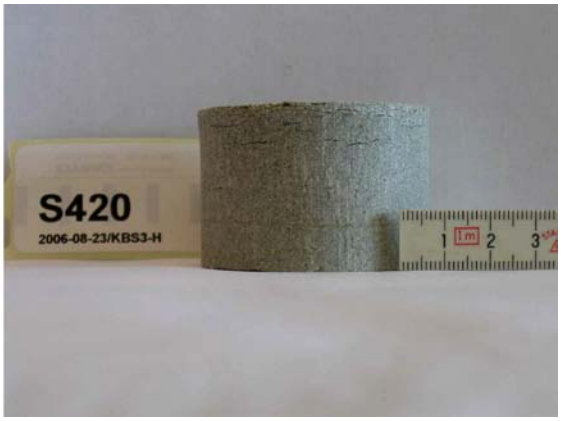

No cracking on the surface towards the water but circumferential cracking

Specimen S220

Specimen S221

Specimen S421

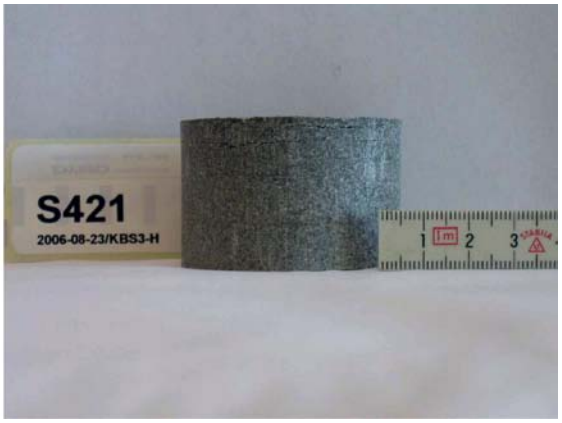

No cracking on the surface towards the water and ambiguous about circumferential cracking

Specimen S212

Specimen S222

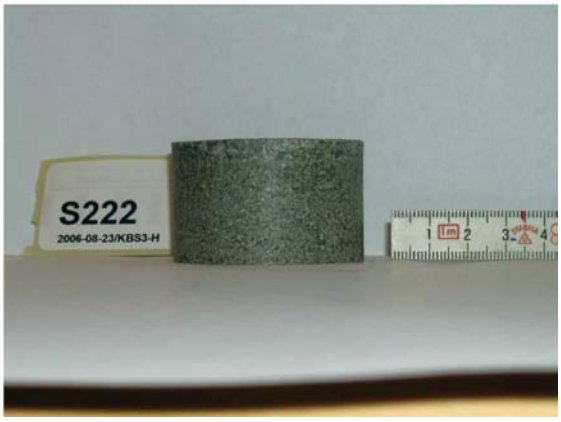

Specimen S232

Specimen S322

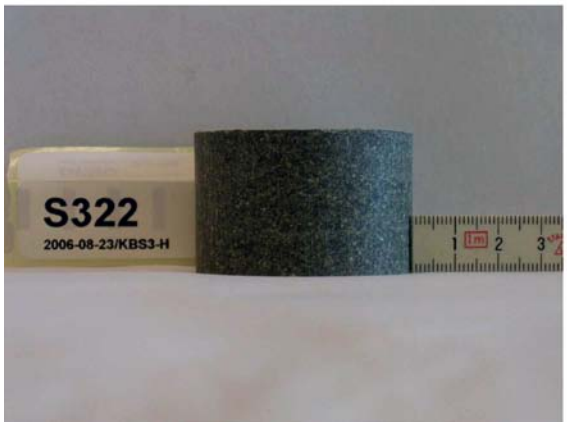

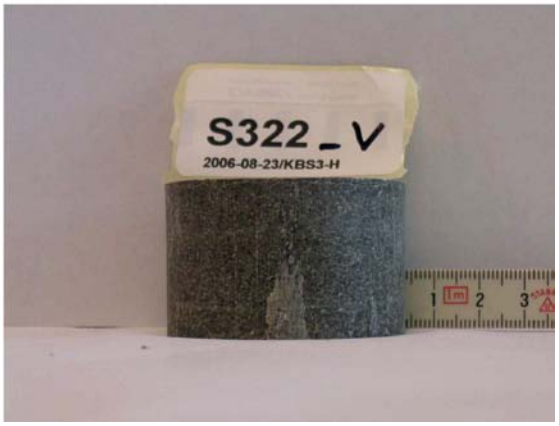

Specimen S323

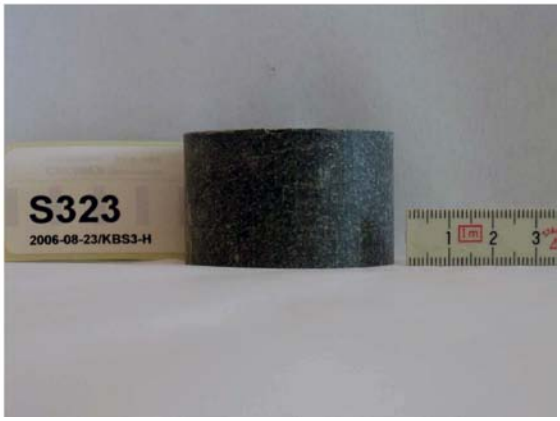

Specimen S422

Appendix A6: Selected observation during the tests

Specimen 210

After 25 days: Material fell from the sample.”

Specimen 212

After 16 days: Water droplets observed on the surface towards the water on 2 of 3 specimens. Cracking developed on the darker areas. The photos show the first observation and dismantling.

Specimen 232

After 13 days: A small crack observed on one of 3 specimens.

Specimen S420

After 24 days: Cracking observed and shown below.

Specimen S222_T10

Condensation on the membrane, on the specimen and on the inside walls of the jar at 10°C in the first part of the series. The climate boxes were exchanged for a climate room in the second part. The photos show condensation and one of the specimens at termination.

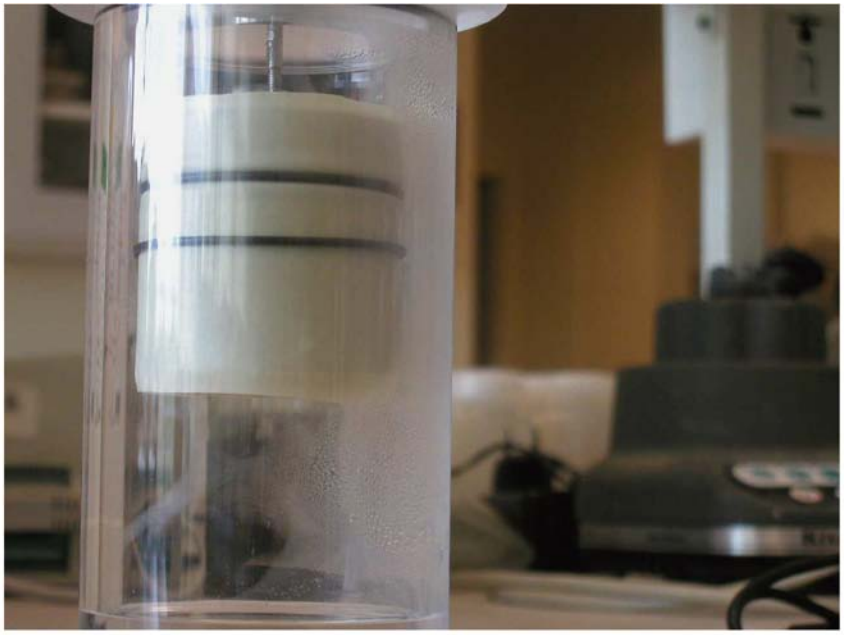

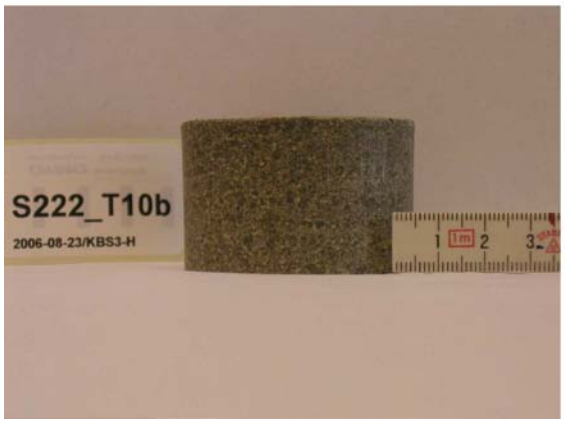

Appendix B

Appendix B1 Scale test 1:10, Test 3-1

Appendix B2 Scale test 1:10, Test 3-2

Appendix B3 Scale test 1:10, Test 3-3

Appendix B4 Scale test 1:10, Test 3-4

Appendix B5 Scale test 1:10, Test 3-5

Appendix B6 Scale test 1:10, Test 3-6

Appendix B7 Scale test 1:10, Test 3-7

Appendix B8 Scale test 1:10, Test 3-8

Appendix B9 Scale test 1:10, Test 3-9

Appendix B10 Scale test 1:10, Test 3-10

Appendix B11 Scale test 1:10, Test 3-11

Appendix B12 Scale test 1:10, Test 3-12

Appendix B13 Scale test 1:10, Test 3-13

Appendix B14 Scale test 1:10, Test 3-14

Appendix B15 Scale test 1:10, Test 3-31

Appendix B16 Scale test 1:10, Test 3-32

Appendix B17 Scale test 1:10, Test 3-33

Appendix B18 Scale test 1:10, Test 3-34

Appendix B19 Scale test 1:10, Test 3-35

Appendix B20 Hydraulic Pressure HP103

Appendix B21 Hydraulic Pressure HP203

Appendix B22 Hydraulic Pressure HP303

Appendix B23 Hydraulic Pressure HP104

Appendix B24 Hydraulic Pressure HP204

Appendix B25: Hydraulic Pressure HP404

Appendix B1: Scale test 1:10, Test 3-1

Test	Material	Water type	Slot up/down (mm)	Test length (m)
3-1	MX-80 blocks and pellets in slot	Tap water	35/35	0.94 m

Installed distance blocks

Raw material	MX-80, cores from full scale blocks
Water ratio, %	17.1
Bulk density, kg/m^3	2007
Dry density, kg/m^3	1714
Degree of saturation, %	76
Void ratio	0.622
Diameter of the blocks, mm	103.7
Test length, mm	939
Total mass of blocks installed, kg	15.87

Installed pellets

Raw material	MX-80 pellets
Water ratio, %	12.9
Total mass of pellets installed, kg	15.26

Calculated data

Final dry density, kg/m^3	1173
Void ratio	1.378
Saturated density, kg/m^3	1753

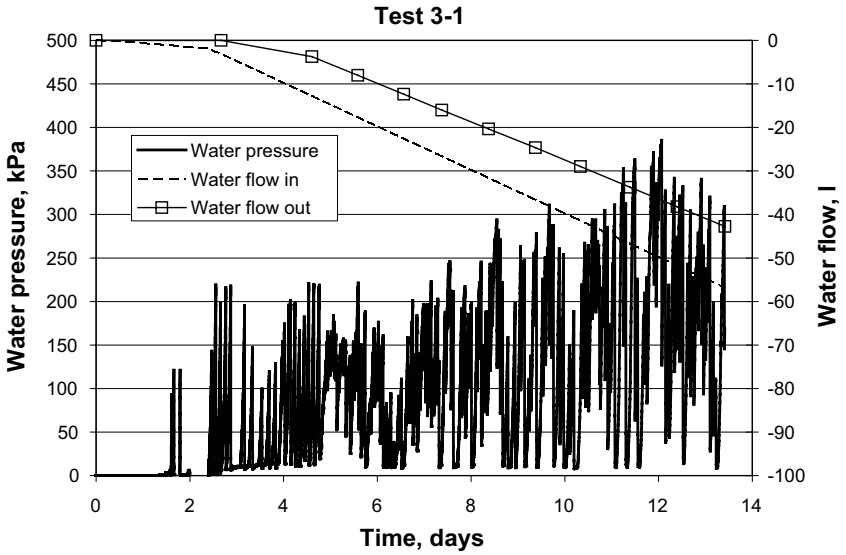

Figure B1-1. *The applied water inflow, the measured water pressure and the water outflow plotted vs. time.*

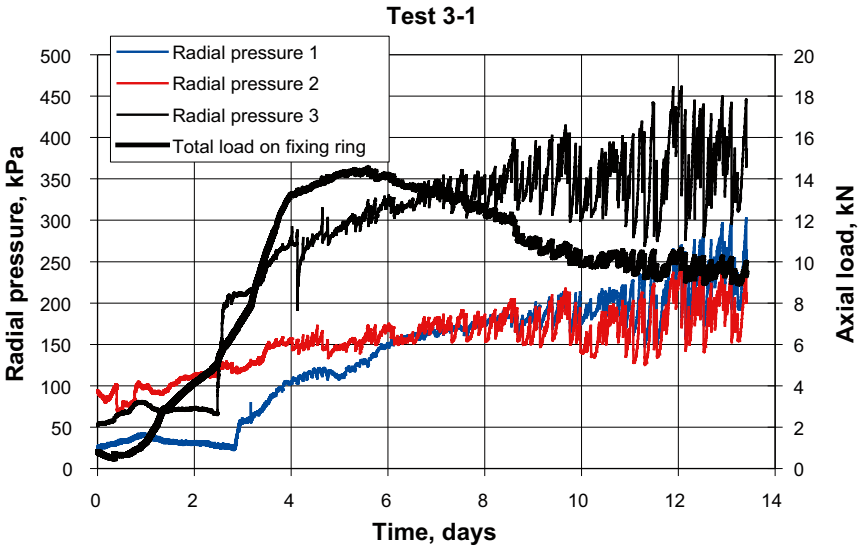

Figure B1-2. *Total load measured on the fixing ring and the radial swelling pressure plotted vs. time.*

Figure B1-3. *Picture from Test 3-1 taken during the preparation of the test showing the central block and the pellets filled slot.*

Appendix B2: Scale test 1:10, Test 3-2

Test	Material	Water type	Slot up/down (mm)	Test length (m)
3-2	MX-80 blocks	Tap water	2/0	0.94 m

Installed distance blocks

Raw material	MX-80, cores from full scale blocks
Water ratio, %	12.5
Bulk density, kg/m^3	1.93
Dry density, kg/m^3	1.72
Degree of saturation, %	56
Void ratio	0.620
Diameter of the blocks, mm	173.1
Test length, mm	944
Total mass of blocks installed, kg	42.56

Calculated data

Final dry density, kg/m^3	1611
Void ratio	0.732
Saturated density, kg/m^3	2.034

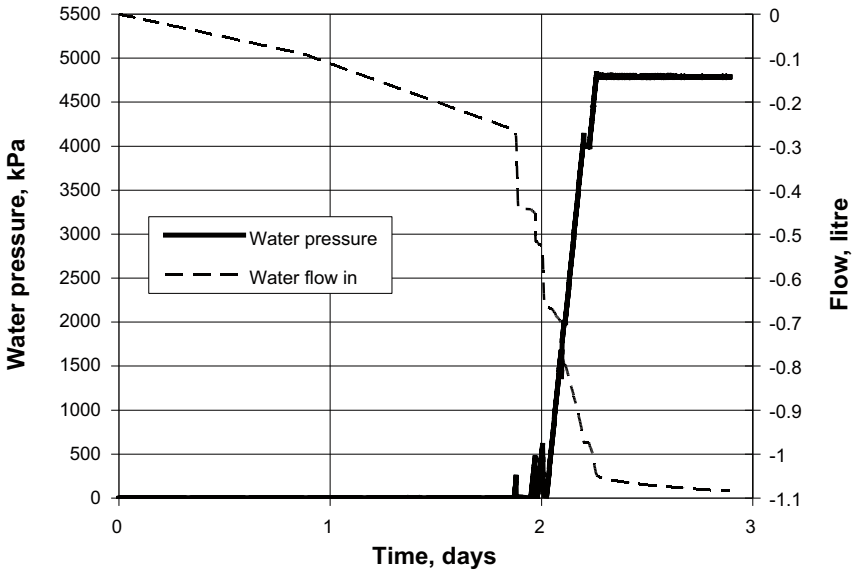

Figure B2-1. *The applied water inflow and the measured water pressure plotted vs. time.*

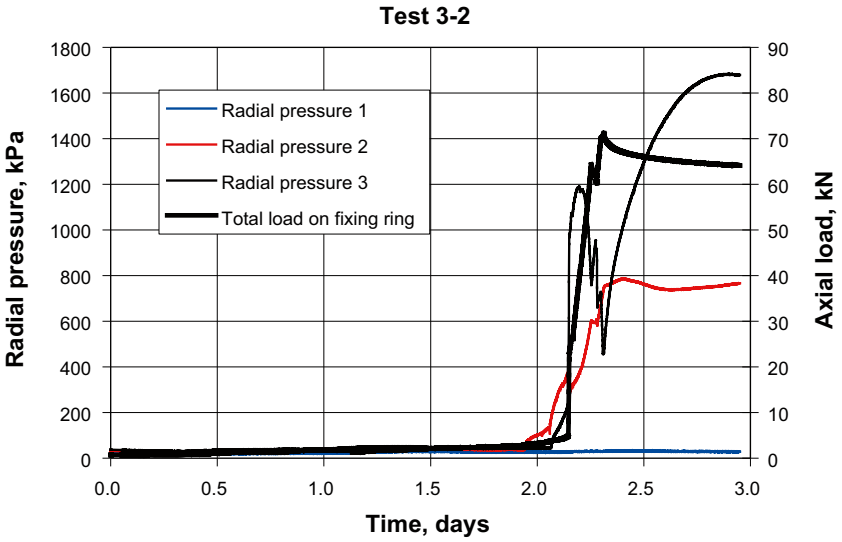

Figure B2-2. *Total load measured on the fixing ring and the radial swelling pressure plotted vs. time.*

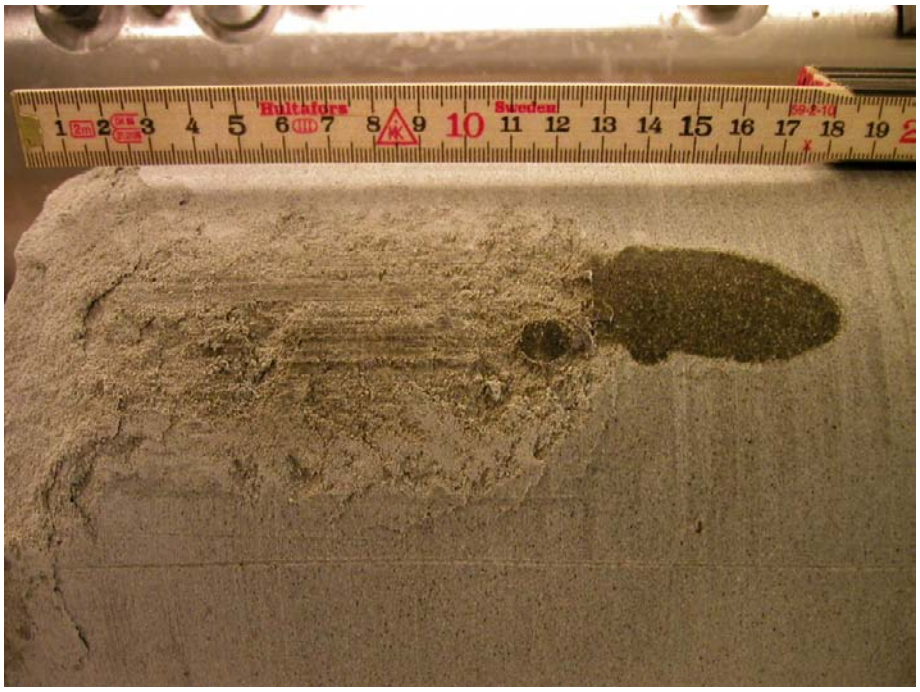

Figure B2-3. *Picture showing the outermost half of the test sample after termination of the test. The picture is taken on the bottom side and shows that the depth of the water penetration was about 71 cm (53+18). The cylindrical shaped point that could be seen on the photo is where radial pressure measurement number three has been done.*

Appendix B3: Scale test 1:10, Test 3-3

Test	Material	Water type	Slot up/down (mm)	Test length (m)
3-3	MX-80 blocks	Tap water	5/0	0.94 m

Installed distance blocks

Raw material	MX-80, cores from full scale blocks
Water ratio, %	12.5
Bulk density, kg/m^3	1.93
Dry density, kg/m^3	1.72
Degree of saturation, %	56
Void ratio	0.620
Diameter of the blocks, mm	170
Test length, mm	938
Total mass of blocks installed, kg	40.9

Calculated data

Final dry density, kg/m^3	1575
Void ratio	0.772
Saturated density, kg/m^3	2010

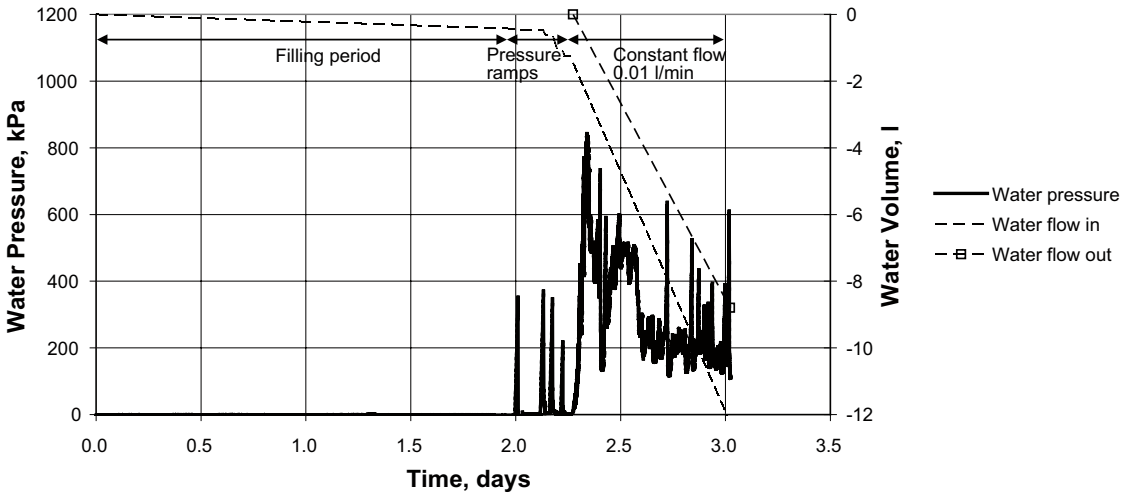

Figure B3-1. The applied water inflow and the measured water pressure plotted vs. time.

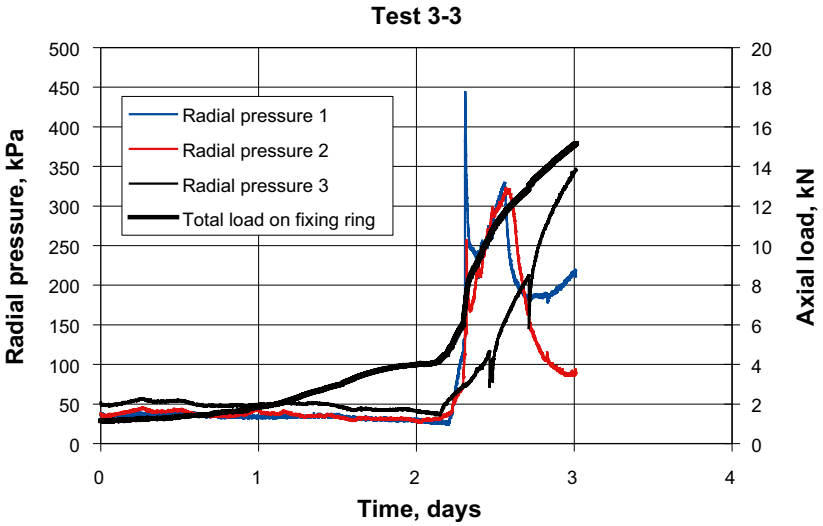

Figure B3-2. *Total load measured on the fixing ring and the radial swelling pressure plotted vs. time.*

Figure B3-3. *Picture showing the outermost part i.e. against the fixing ring. The bentonite has swollen and filled the outer slot but can obviously still not withstand high water pressures.*

Appendix B4: Scale test 1:10, Test 3-4

Test	Material	Water type	Slot up/down (mm)	Test length (m)
3-4	MX-80 blocks	Tap water	5/0	0.94 m

Layout: Pre wetting of slot

Installed distance blocks

Raw material	MX-80, cores from full scale blocks
Water ratio, %	12.5
Bulk density, kg/m^3	1.93
Dry density, kg/m^3	1.72
Degree of saturation, %	56
Void ratio	0.620
Diameter of the blocks, mm	170
Test length, mm	940
Total mass of blocks installed, kg	40.9

Calculated data

Final dry density, kg/m^3	1573
Void ratio	0.774
Saturated density, kg/m^3	2009

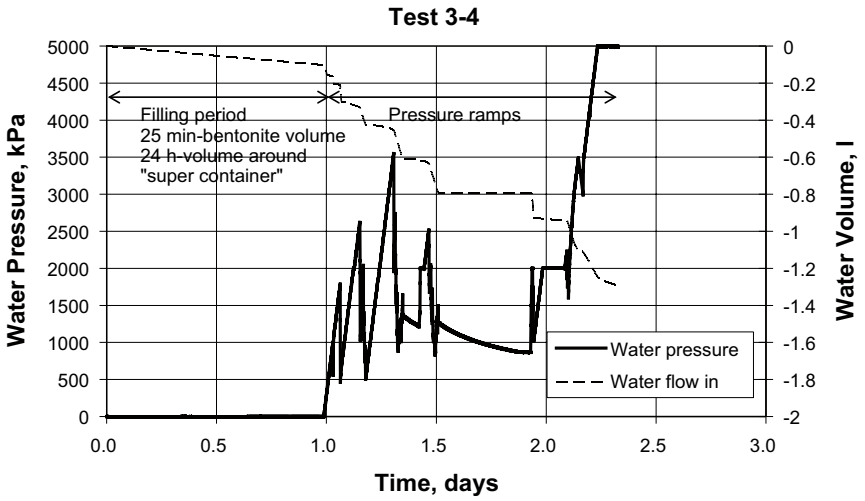

Figure B4-1. *The applied water inflow and the measured water pressure plotted vs. time.*

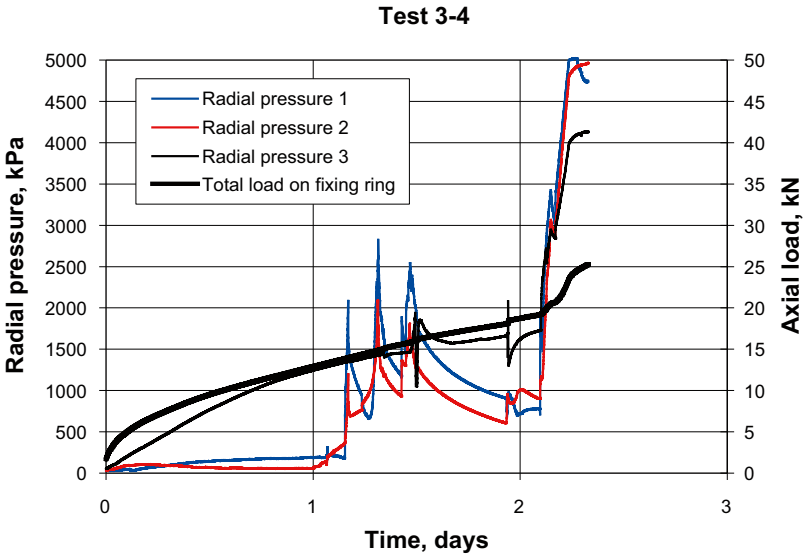

Figure B4-2. *Total load measured on the fixing ring and the radial swelling pressure plotted vs. time.*

Figure B4-3. *Picture showing the outermost part with the fixing ring. The picture shows the tubes used for the pre-filling and de-airing of the volume around the bentonite with water. Silicone was used to seal the slots.*

Appendix B5: Scale test 1:10, Test 3-5

Test	Material	Water type	Slot up/down (mm)	Test length (m)
3-5	MX-80 blocks	Tap water	10/0	0.94 m

Layout: Pre wetting of slot

Installed distance blocks

Raw material	MX-80, cores from full scale blocks
Water ratio, %	12.5
Bulk density, kg/m^3	1.93
Dry density, kg/m^3	1.72
Degree of saturation, %	56
Void ratio	0.620
Diameter of the blocks, mm	165
Test length, mm	940
Total mass of blocks installed, kg	38.48

Calculated data

Final dry density, kg/m^3	1479
Void ratio	0.886
Saturated density, kg/m^3	1949

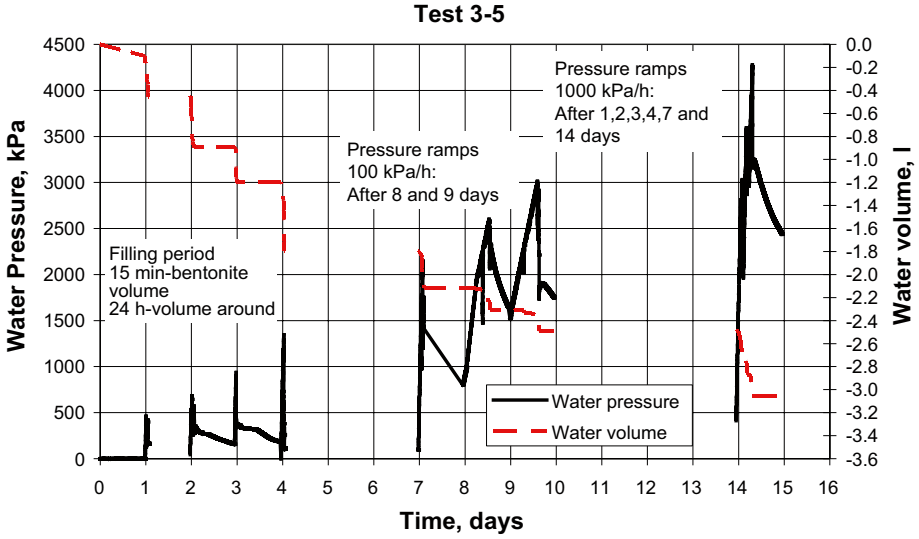

Figure B5-1. The applied water inflow and the measured water pressure plotted vs. time.

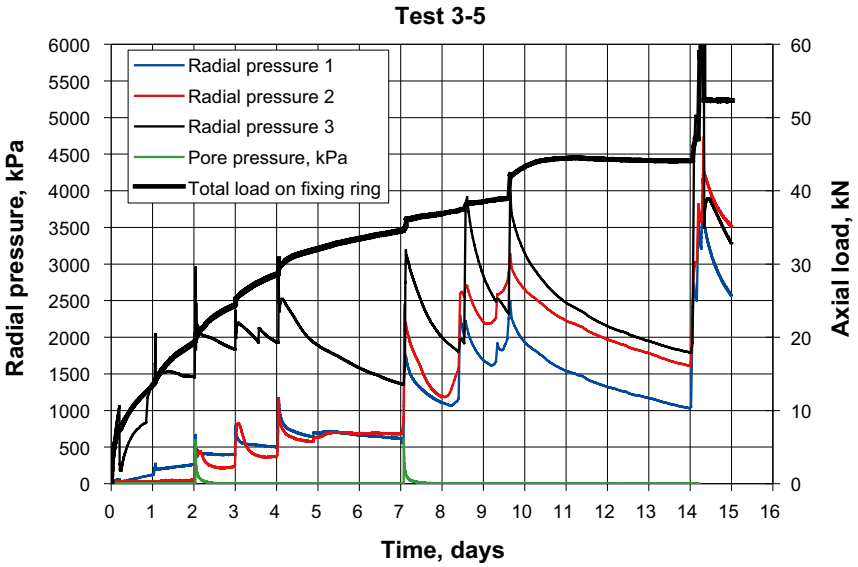

Figure B5-2. *Total load measured on the fixing ring and the radial swelling pressure plotted vs. time.*

Figure B5-3. *Picture from the middle of the sample about 0.5m from the pressure side. The water ratio of the outermost cm clay at the top was 64 %.*

Appendix B6: Scale test 1:10, Test 3-6

Test	Material	Water type	Slot up/down (mm)	Test length (m)
3-6	MX-80 blocks and pellets	Tap water	15/15	0.94 m

Layout: Pre wetting of pellet filled slot

Installed distance blocks

Raw material	MX-80, cores from full scale blocks
Water ratio, %	12.5
Bulk density, kg/m^3	1930
Dry density, kg/m^3	1716
Degree of saturation, %	56
Void ratio	0.620
Diameter of the blocks, mm	145
Test length, mm	939
Total mass of blocks installed, kg	29.81

Installed pellets

Raw material	MX-80 pellets
Water ratio, %	12.9
Total mass of pellets installed, kg	6.7

Calculated data

Final dry density, kg/m^3	1402
Void ratio	0.99
Saturated density, kg/m^3	1900

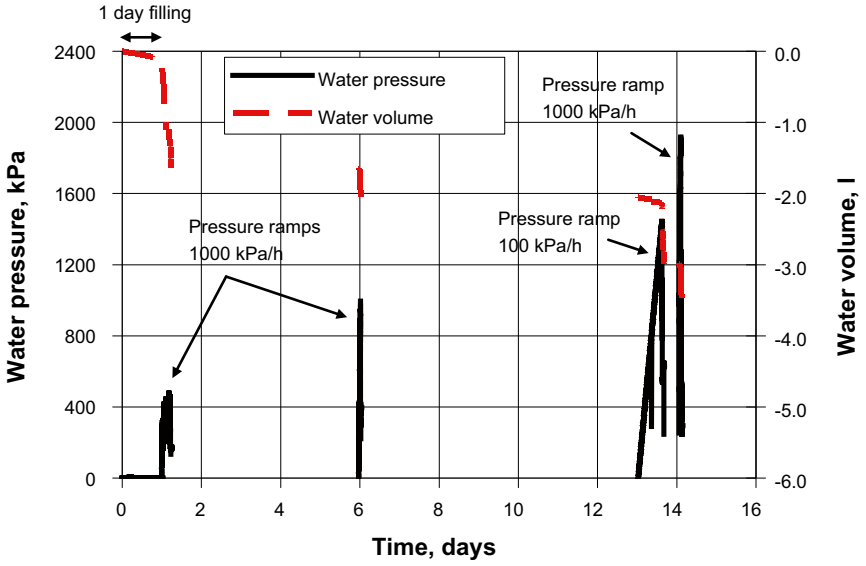

Figure B6-1. The applied water inflow and the measured water pressure plotted vs. time.

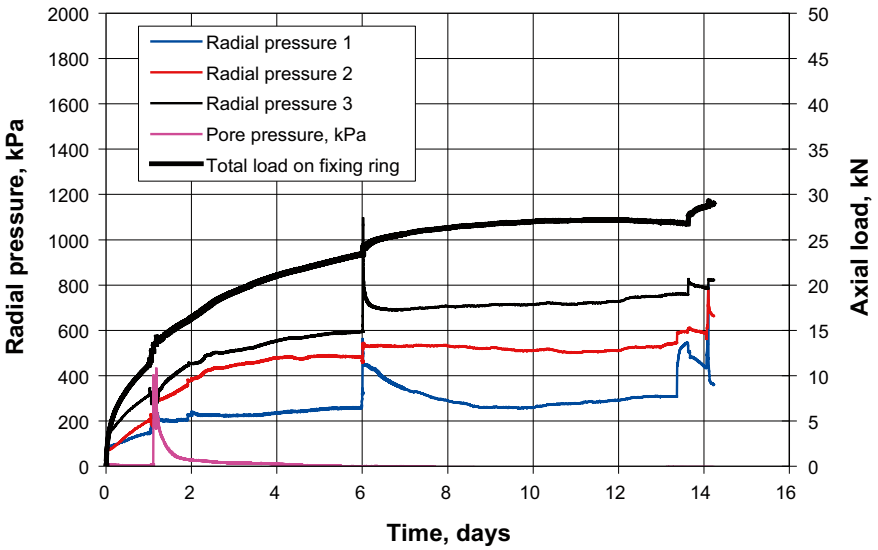

Figure B6-2. *The total load measured on the fixing ring and the radial swelling pressure plotted vs. time.*

Figure B6-3. *Picture from the middle of the sample about 0.5m from the super container side. The water ratio in the outermost 10 mm varied between 40-49% (four samples in different directions.*

Appendix B7: Scale test 1:10, Test 3-7

Test	Material	Water type	Slot up/down (mm)	Test length (m)
3-7	MX-80 blocks	3.5 % salt	5/0	0.94 m

Layout: Pre wetting of slot. Planned movement of fixing ring after 8 days.

Installed distance blocks

Raw material	MX-80, cores from full scale blocks
Water ratio, %	12.5
Bulk density, kg/m^3	1.93
Dry density, kg/m^3	1.72
Degree of saturation, %	56
Void ratio	0.620
Diameter of the blocks, mm	170
Test length, mm	920
Total mass of blocks installed, kg	39.9

Calculated data

Final dry density, kg/m^3	1533
Void ratio	0.820
Saturated density, kg/m^3	1984

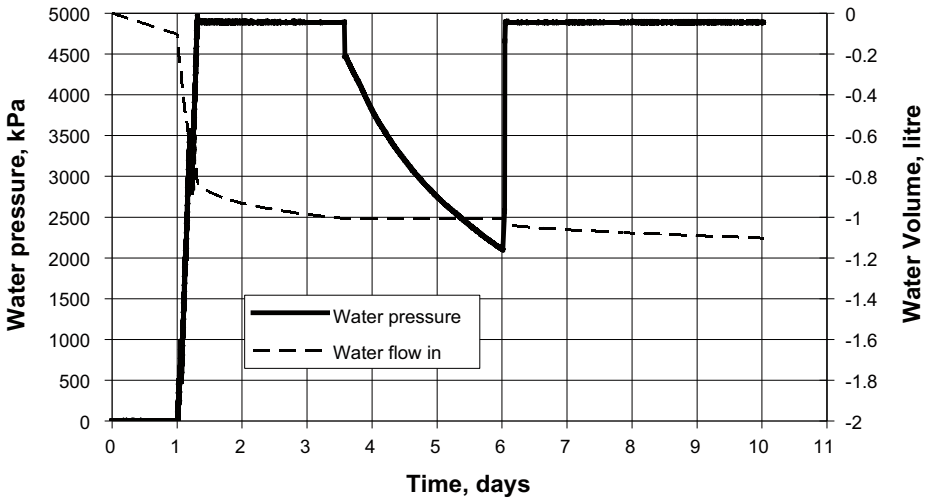

Figure B7-1. *The applied water inflow and the measured water pressure plotted vs. time.*

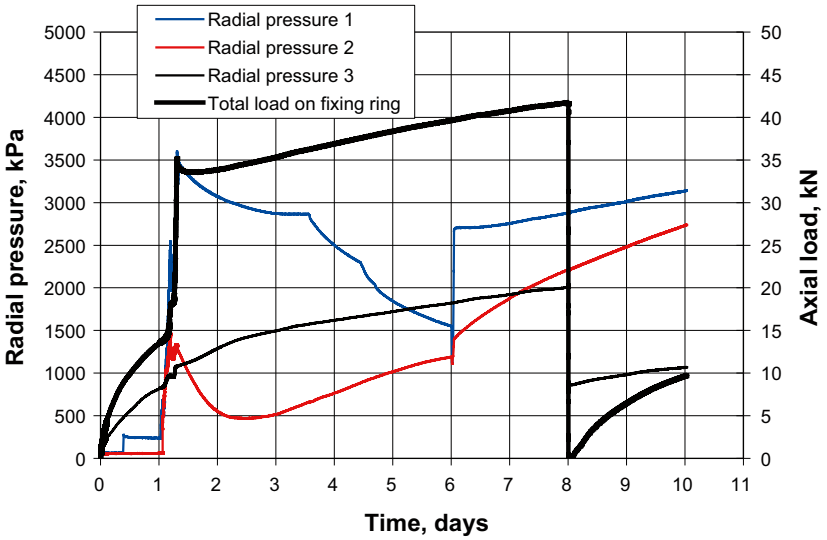

Figure B7-2. *The total load measured on the fixing ring and the radial swelling pressure plotted vs. time.*

Figure B7-3. *Picture showing the surface just inside the dummy simulating the super container. Due to the planned movement of the fixing ring and the followed movement of the distance blocks was the complete area wetted. The depth of the saturated clay was measured to about 6 cm. The water ratio was between 80 % in the centre and up to 90 % in the outermost parts.*

Appendix B8: Scale test 1:10, Test 3-8

Test	Material	Water type	Slot up/down (mm)	Test length (m)
3-8	MX-80 blocks	3.5 % salt	10/0	0.94 m

Layout: Pre wetting of slot

Installed distance blocks

Raw material	MX-80, cores from full scale blocks
Water ratio, %	12.5
Bulk density, kg/m^3	1.93
Dry density, kg/m^3	1.72
Degree of saturation, %	56
Void ratio	0.620
Diameter of the blocks, mm	165
Test length, mm	944
Total mass of blocks installed, kg	38.48

Calculated data

Final dry density, kg/m^3	1479
Void ratio	0.886
Saturated density, kg/m^3	1949

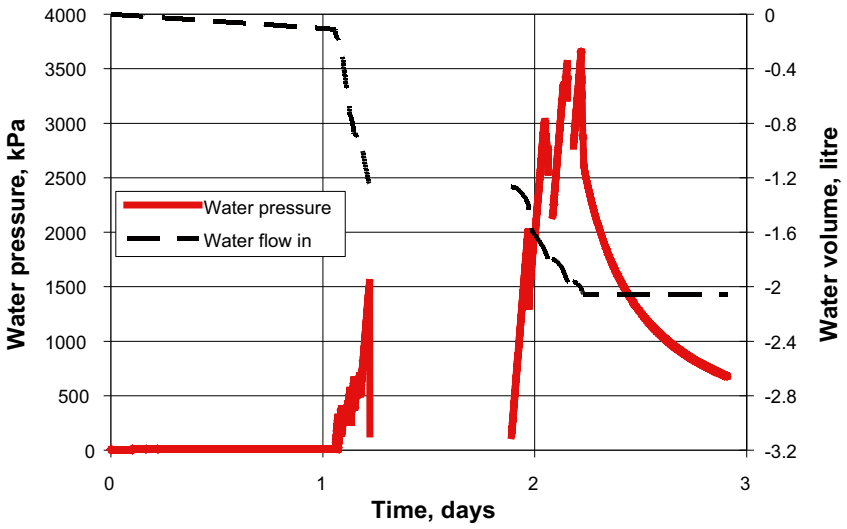

Figure B8-1. *The applied water inflow and the measured water pressure plotted vs. time.*

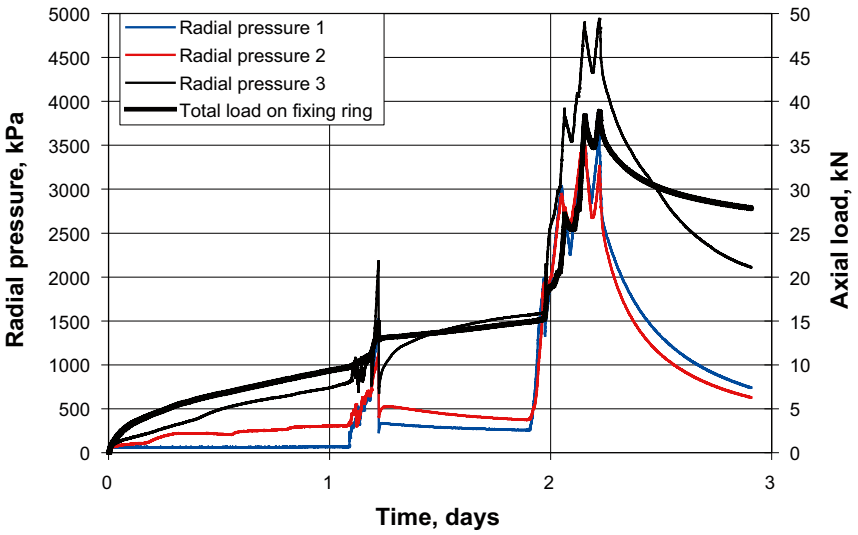

Figure B8-2. *The total load measured on the fixing ring and the radial swelling pressure plotted vs. time.*

Figure B8-3. *Picture showing the fixing ring. Bentonite was squeezed out between the ring and the steel tube.*

Appendix B9: Scale test 1:10, Test 3-9

Test	Material	Water type	Slot up/down (mm)	Test length (m)
3-9	MX-80 blocks	3.5 % salt	5/5	0.94 m

Layout: Pre wetting of slot

Installed distance blocks

Raw material	MX-80, cores from full scale blocks
Water ratio, %	12.5
Bulk density, kg/m^3	1.93
Dry density, kg/m^3	1.72
Degree of saturation, %	56
Void ratio	0.620
Diameter of the blocks, mm	165
Test length, mm	941
Total mass of blocks installed, kg	38.3

Calculated data

Final dry density, kg/m^3	1472
Void ratio	0.896
Saturated density, kg/m^3	1944

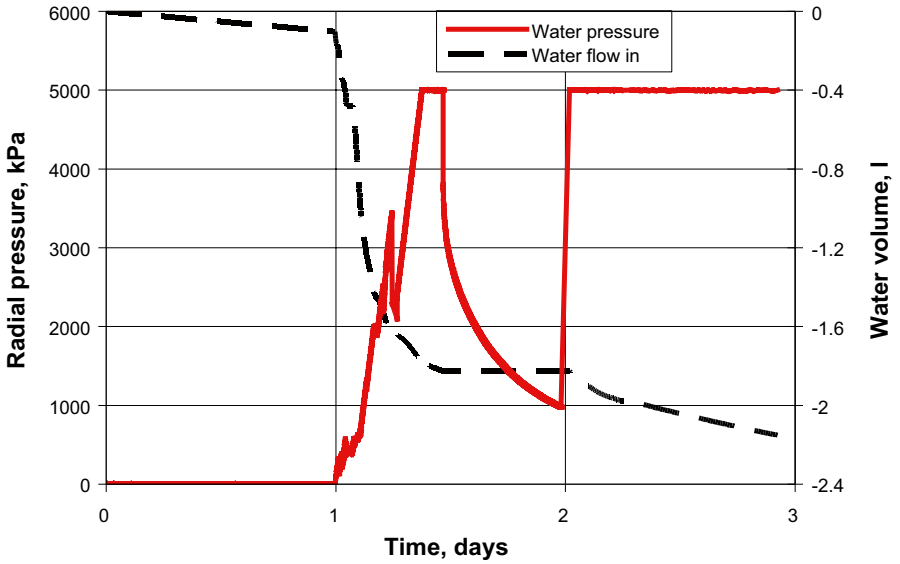

Figure B9-1. *The applied water inflow and the measured water pressure plotted vs. time.*

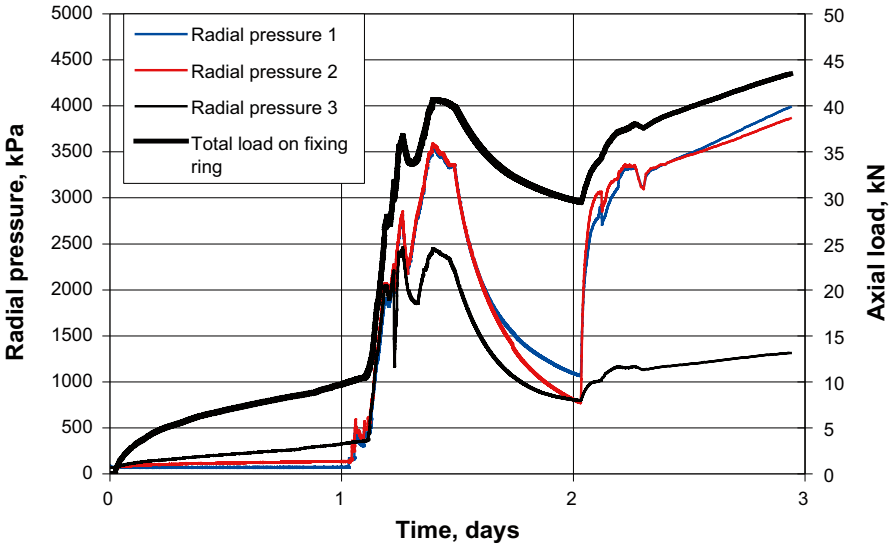

Figure B9-2. *The total load measured on the fixing ring and the radial swelling pressure plotted vs. time.*

Figure B9-3. *Picture from the middle of the sample about 0.5m from the super container. The water ratio was determined in some positions here: Uppermost 5mm=30%, next 5 mm=29%, next 5 mm=28%, next 5 mm=25%, and in the centre=17%*

Appendix B10: Scale test 1:10, Test 3-10

Test	Material	Water type	Slot up/down (mm)	Test length (m)
3-10	MX-80 blocks	3.5 % salt	5/5	0.94 m

Layout: Pre wetting of slot

Installed distance blocks

Raw material	MX-80, cores from full scale blocks
Water ratio, %	12.5
Bulk density, kg/m^3	1.93
Dry density, kg/m^3	1.72
Degree of saturation, %	56
Void ratio	0.620
Diameter of the blocks, mm	165
Test length, mm	941
Total mass of blocks installed, kg	38.5

Calculated data

Final dry density, kg/m^3	1481
Void ratio	0.883
Saturated density, kg/m^3	1950

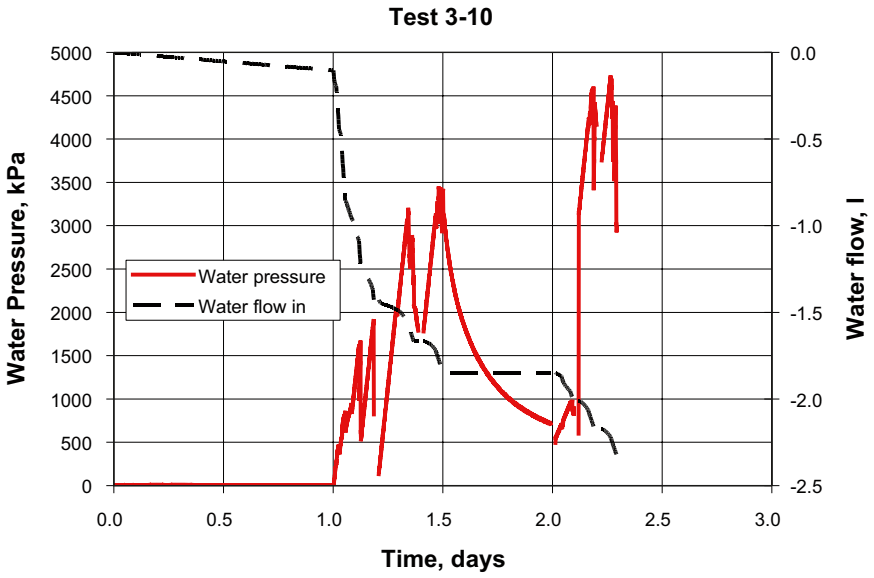

Figure B10-1. *The decided inflow and the applied water pressure. After 1 day was a pressure ramp of 1 MPa/h applied. After some internal piping the sample could take about 3.5 MPa. The pressure equipment run out of water but was filled up again the next morning. The pressure was raised rather fast to 3 MPa and then the ramp was applied again. At 4.5 MPa piping was achieved with material leaking out at the axial load cells, see pictures.*

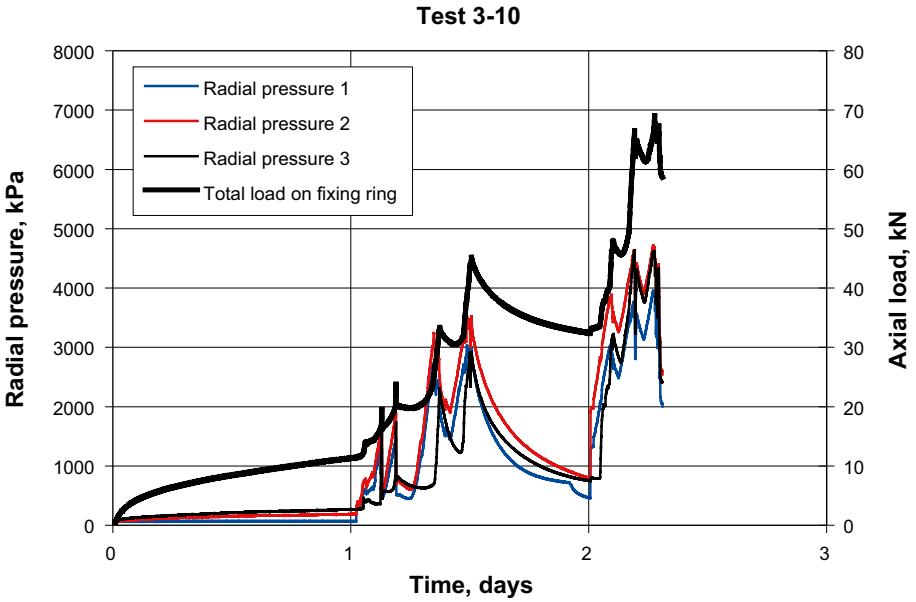

Figure B10-2. *The swelling pressure in three different points and the axial load plotted vs. time. The dip in load and swelling pressure depends on that the pressuring device run out of water, Figure 19:1.*

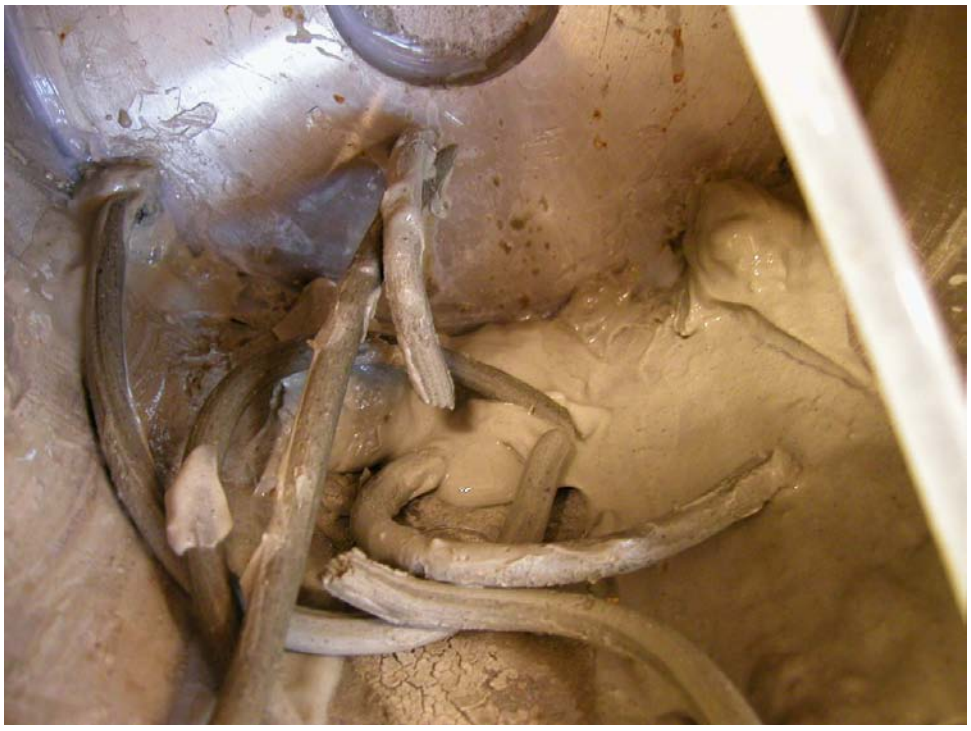

Figure B10-3. *Picture showing the fixing ring . Clay /gel has been pressed out through the tube inlets used for the pre wetting of the slot*

Appendix B11: Scale test 1:10, Test 3-11

Test	Material	Water type	Slot up/down (mm)	Test length (m)
3-11	MX-80 blocks	3.5 % salt	5/5	0.94 m

Layout: Pre wetting of slot

Installed distance blocks

Raw material	MX-80, cores from full scale blocks
Water ratio, %	12.5
Bulk density, kg/m^3	1.93
Dry density, kg/m^3	1.72
Degree of saturation, %	56
Void ratio	0.620
Diameter of the blocks, mm	165
Test length, mm	940
Total mass of blocks installed, kg	38.56

Calculated data

Final dry density, kg/m^3	1470
Void ratio	0.898
Saturated density, kg/m^3	1943

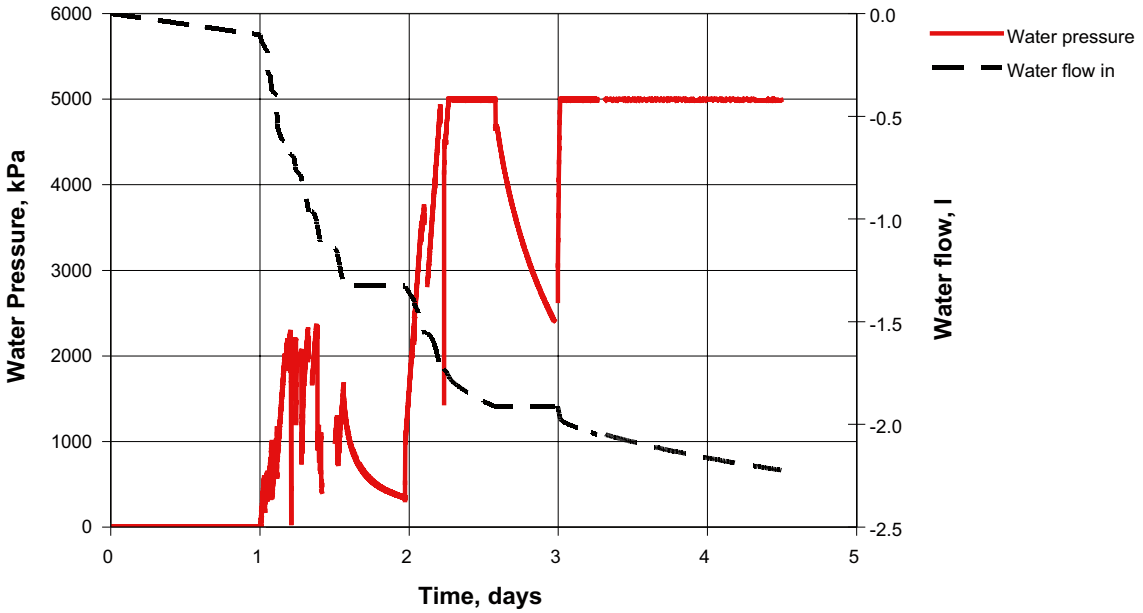

Figure B11-1. *The decided inflow and the water pressure plotted vs. time.. After 1 day was a pressure ramp of 1 MPa/h applied. After some internal piping (and the pressurizing device run out of water after 1.5 days) the sample could take 5 MPa.*

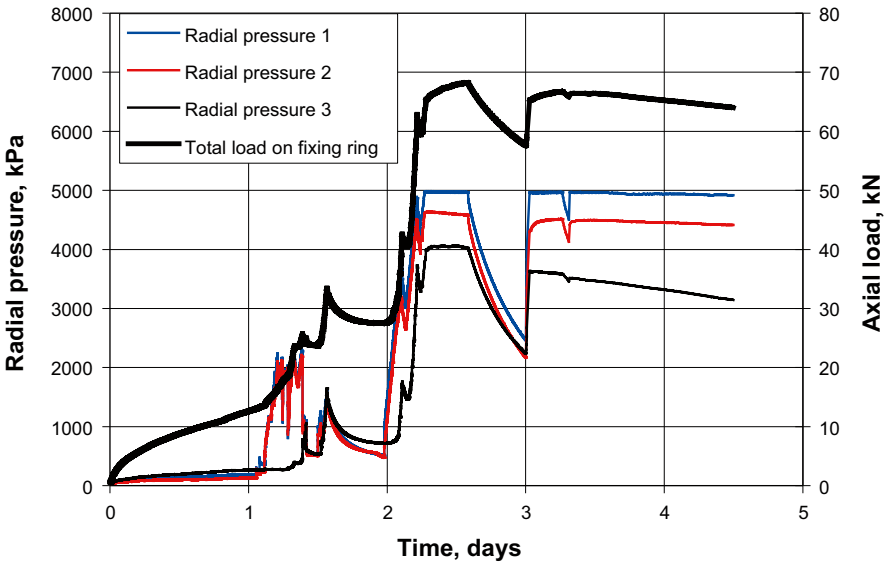

Figure B11-2. *Swelling pressure in three different points and the axial load plotted vs. time. The dip in load and swelling pressure depends on that the pressuring device run out of water, Figure 21:1.*

Figure B11-3. *Picture showing the surface just inside the dummy simulating the super container. There is a large dry surface in the middle.*

Appendix B12: Scale test 1:10, Test 3-12

Test	Material	Water type	Slot up/down (mm)	Test length (m)
3-12	MX-80 blocks	3.5 % salt	10/10	0.94 m

Layout: Pre wetting of slot, drainage tube in order to control test conditions

Installed distance blocks

Raw material	MX-80, cores from full scale blocks
Water ratio, %	12.5
Bulk density, kg/m^3	1.93
Dry density, kg/m^3	1.72
Degree of saturation, %	56
Void ratio	0.620
Diameter of the blocks, mm	155
Test length, mm	941
Total mass of blocks installed, kg	34.2

Calculated data

Final dry density, kg/m^3	1302
Void ratio	1.143
Saturated density, kg/m^3	1835

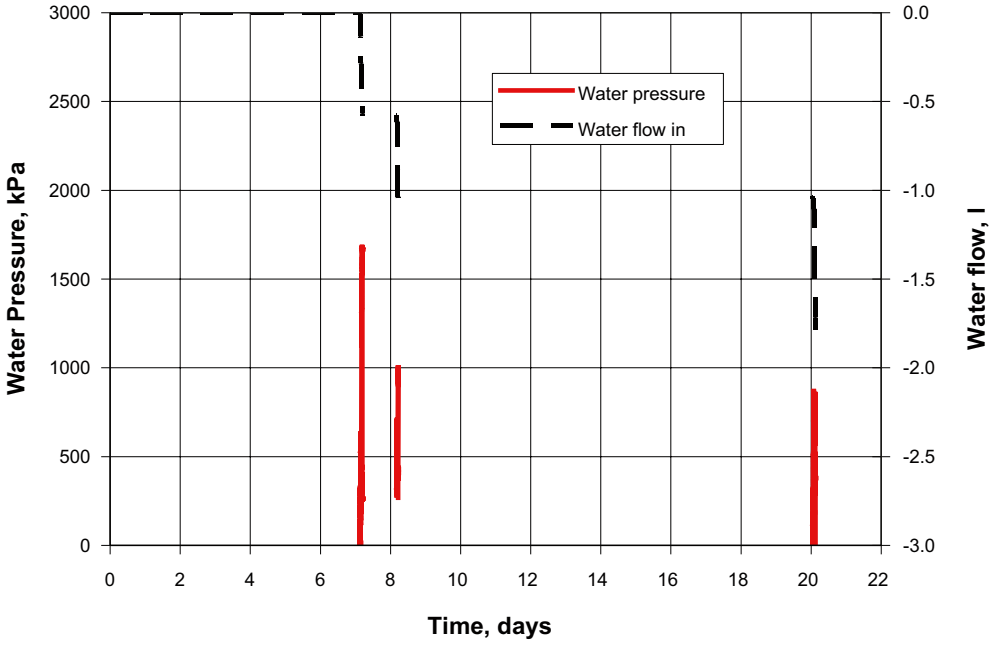

Figure B12-1. *The water inflow and the water pressure plotted vs. time. After 7 days was a pressure ramp of 1 MPa/h applied. Piping occurs and a new pressure ramp was applied after 24 hours. A last attempt was done 12 days later but the clay could not withstand the water pressure.*

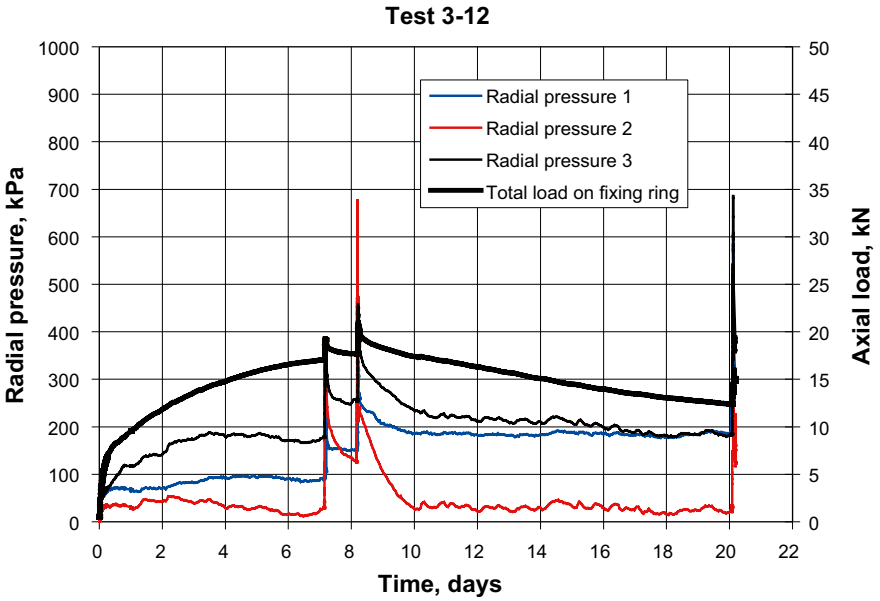

Figure B12-2. *The swelling pressure in three different points and the axial load plotted vs. time. All measurements were very sensitive to the applied water pressure ramps.*

Figure B12-3. *Picture from the middle of the sample about 0.5m from the super container. The dark ring has a width of 35-40 mm.*

Appendix B13: Scale test 1:10, Test 3-13

Test	Material	Water type	Slot up/down (mm)	Test length (m)
3-13	MX-80 blocks	3.5 % salt	10/10	0.94 m

Layout: Pre wetting of slot, no access to additional water. Long term test.

Installed distance blocks

Raw material	MX-80, cores from full scale blocks
Water ratio, %	17.0
Bulk density, kg/m^3	2090
Dry density, kg/m^3	1790
Degree of saturation, %	85.2
Void ratio	0.553
Diameter of the blocks, mm	155
Test length, mm	944
Total mass of blocks installed, kg	32

Calculated data

Final dry density, kg/m^3	1380
Void ratio	1.022
Saturated density, kg/m^3	1885

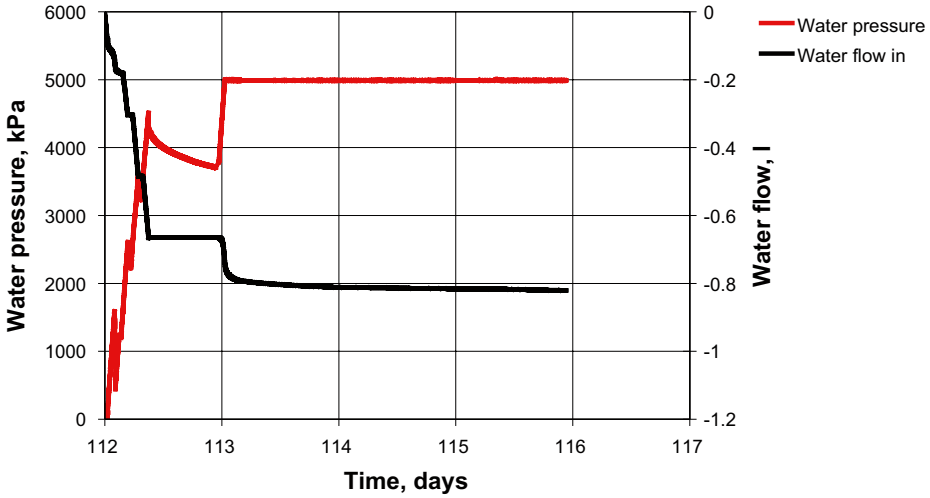

Figure B13-1. *After 112 days without access to additional water a pressure ramp was applied. The diagram shows the water pressure and the water inflow plotted vs. time. During the pressure ramp, internal piping occurred a number of times. The amount of water injected was quite large which meant that the pressurizing equipment had to be filled up a number of times. 24 hours after starting the pressure ramp the maximum pressure, 5 MPa, was reached. The dip in pressure after about 8 hours depends on that the pressurising device run out of water in the middle of the night.*

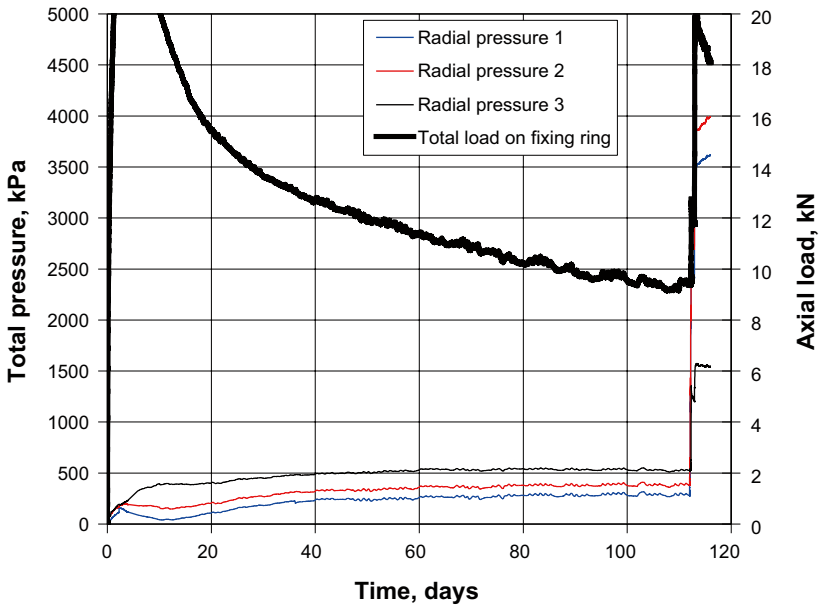

Figure B13-2. *The radial swelling pressure in three different points and the axial load on the fixing ring plotted vs. time.*

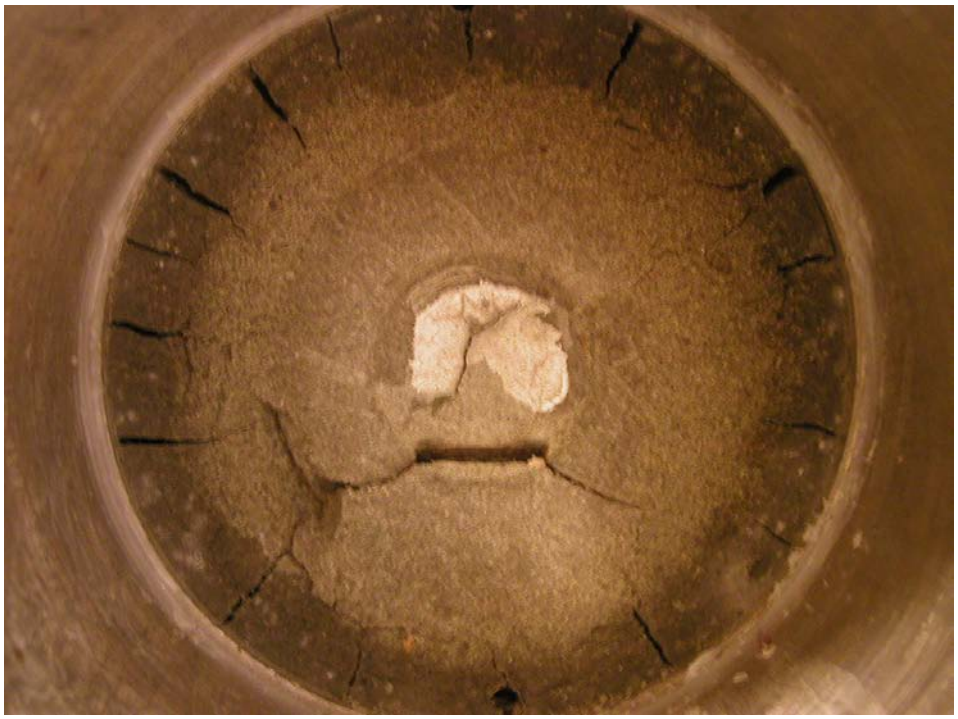

Figure B13-3. *Picture showing the distance block after removal of the fixing ring.*

Appendix B14: Scale test 1:10, Test 3-14

Test	Material	Water type	Slot up/down (mm)	Test length (m)
3-14	MX-80 blocks	3.5 % salt	10/10	0.94 m

Layout: Pre wetting of slot. Blocks with Sr=94%.

Installed distance blocks

Raw material	MX-80, cores from full scale blocks
Water ratio, %	21.7
Bulk density, kg/m^3	2060
Dry density, kg/m^3	1693
Degree of saturation, %	95.0
Void ratio	0.642
Diameter of the blocks, mm	171
Test length, mm	925
Total mass of blocks installed, kg	43.6

Calculated data

Final dry density, kg/m^3	1380
Void ratio	1.022
Saturated density, kg/m^3	1885

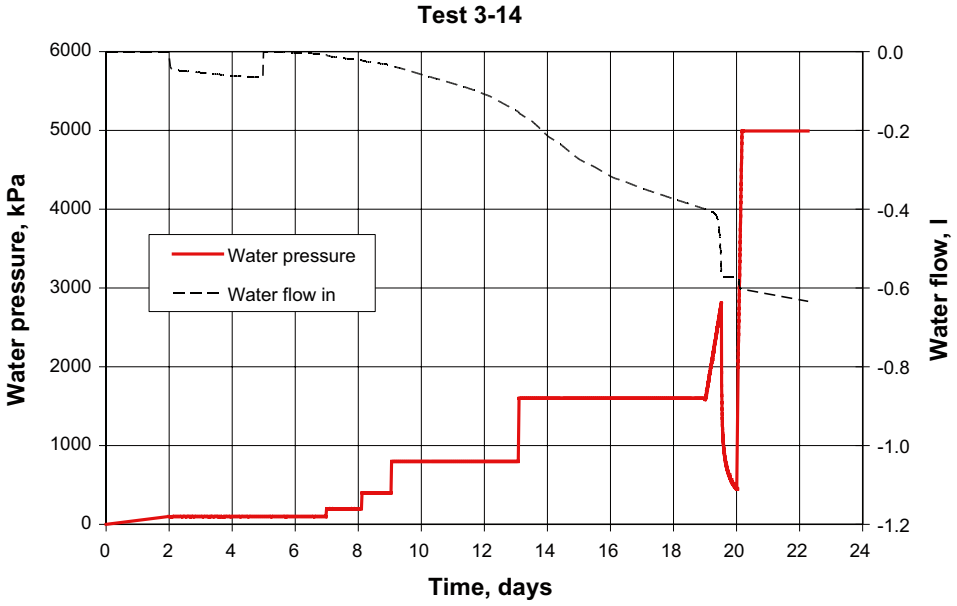

Figure B14-1. *The applied water pressure and the measured water inflow plotted vs. time. The dip in pressure after about 19 days depended on that the pressurising device run out of water in the middle of the night.*

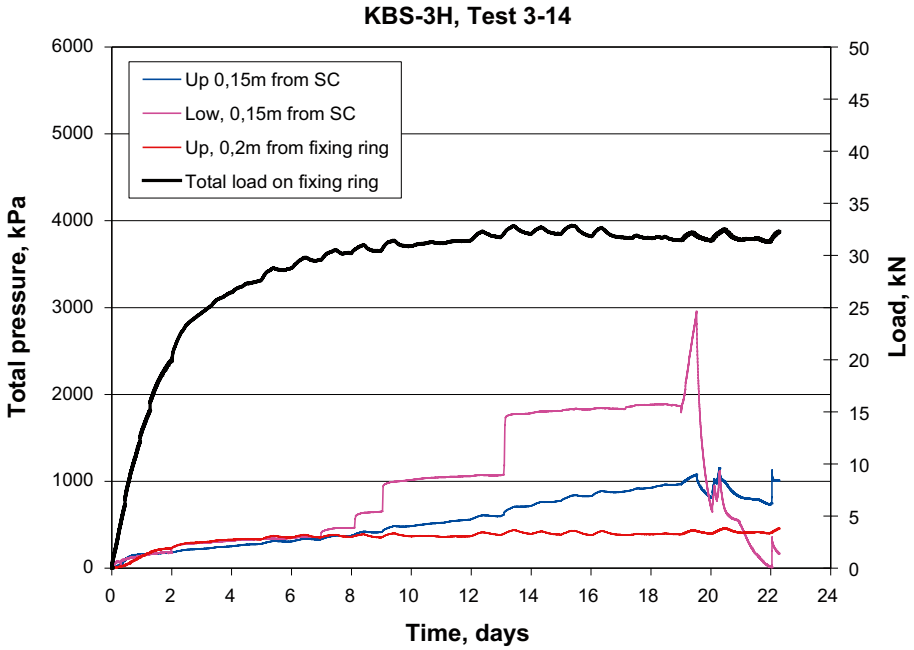

Figure B14-2. *The radial swelling pressure in three different points and the axial load on the fixing ring plotted vs. time.*

Appendix B15: Scale test 1:10, Test 3-31

Test	Material	Water type	Slot up/down (mm)	Test length (m)
3-31	MX-80 blocks	3.5 % salt	10/10	3.08 m

Layout: Pre wetting of slot

Installed distance blocks

Raw material	MX-80, cores from full scale blocks
Water ratio, %	13.5
Bulk density, kg/m^3	1950
Dry density, kg/m^3	1720
Degree of saturation, %	60.6
Void ratio	0.617
Diameter of the blocks, mm	155
Test length, mm	3080
Total mass of blocks installed, kg	112.05

Calculated data

Final dry density, kg/m^3	1343
Void ratio	1.078
Saturated density, kg/m^3	1861

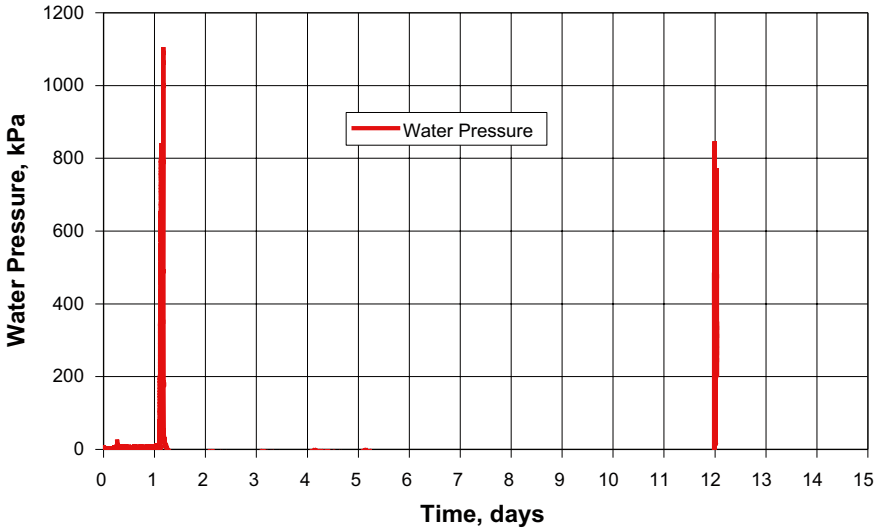

Figure B15-1 . *The applied water pressure plotted vs. time.. After 1 day was a pressure ramp of 1 MPa/h applied. Piping occurs at 1100 kPa. A new pressure ramp was applied after additional 11 days with almost the same result.*

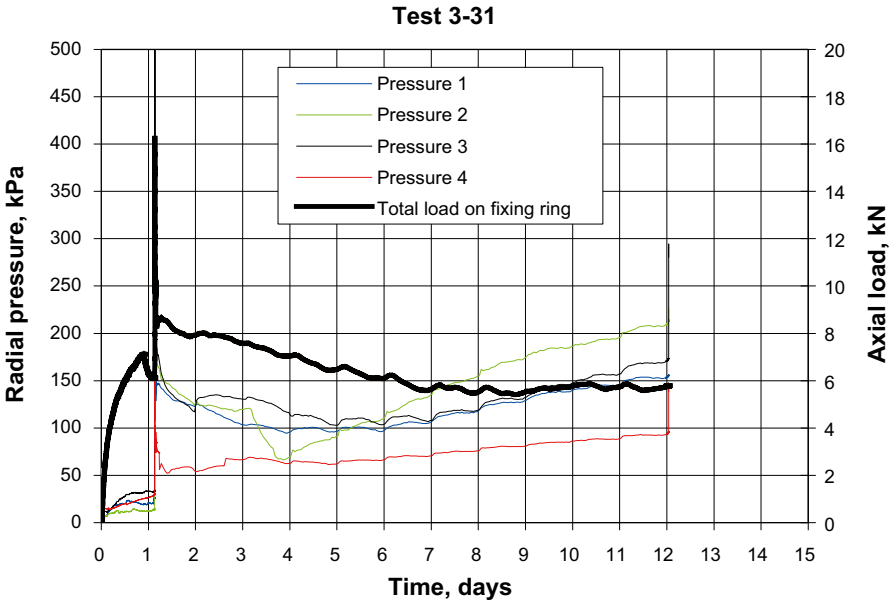

Figure B15-2 . *The radial swelling pressure in three different points and the axial load on the fixing ring plotted vs. time.*

Figure B15-3 . *Picture showing the surface just inside the dummy simulating the super container.*

Appendix B16: Scale test 1:10, Test 3-32

Test	Material	Water type	Slot up/down (mm)	Test length (m)
3-32	MX-80 blocks	3.5 % salt	10/10	3.08 m

Layout: Pre wetting of slot. Drainage tube in order to control test conditions.

Installed distance blocks

Raw material	MX-80, cores from full scale blocks
Water ratio, %	17.0
Bulk density, kg/m^3	2090
Dry density, kg/m^3	1790
Degree of saturation, %	85.2
Void ratio	0.553
Diameter of the blocks, mm	155
Test length, mm	3099
Total mass of blocks installed, kg	123.6

Calculated data

Final dry density, kg/m^3	1414
Void ratio	0.973
Saturated density, kg/m^3	1907

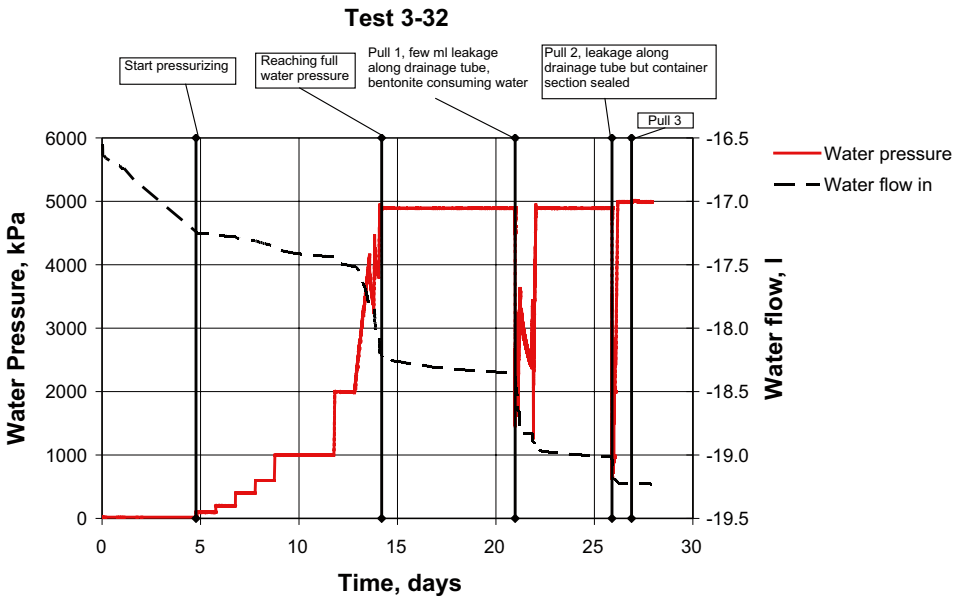

Figure B16-1. The water inflow and the applied water pressure plotted vs. time. After 5 days the increasing of the water pressure was started in steps. Fourteen days after test start could the sample seal for 5 MPa. 27 days after test start was the drainage tube retrieved. This could probably have been done earlier.

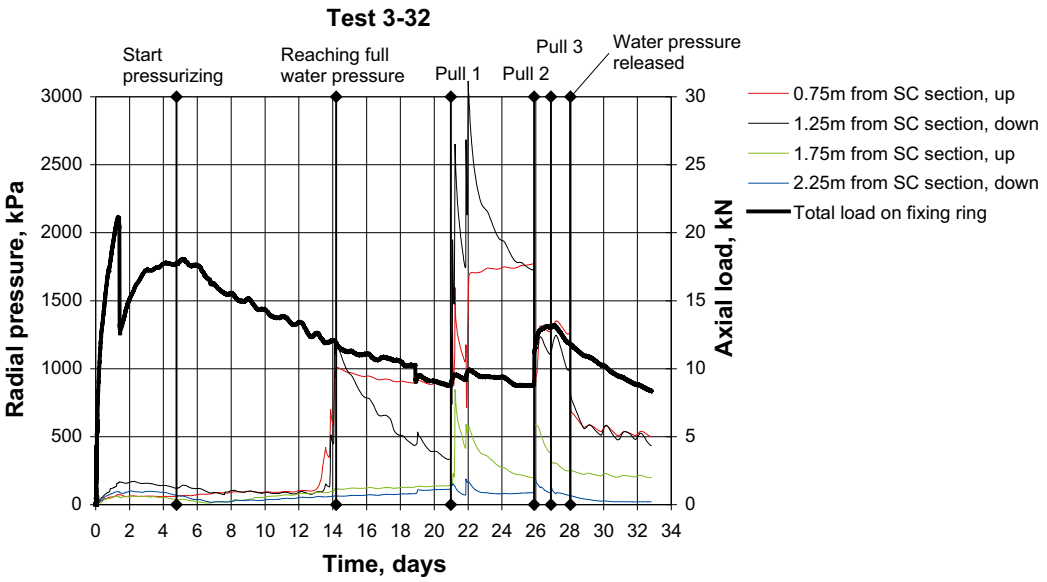

Figure B16-2. *The radial swelling pressure built up in three different points and the axial load on the fixing ring plotted vs. time.*

Figure B16-3. *Picture showing the fixing ring after dismantling. The bentonite had swelled through the central hole in the fixing ring (totally about 12 mm).*

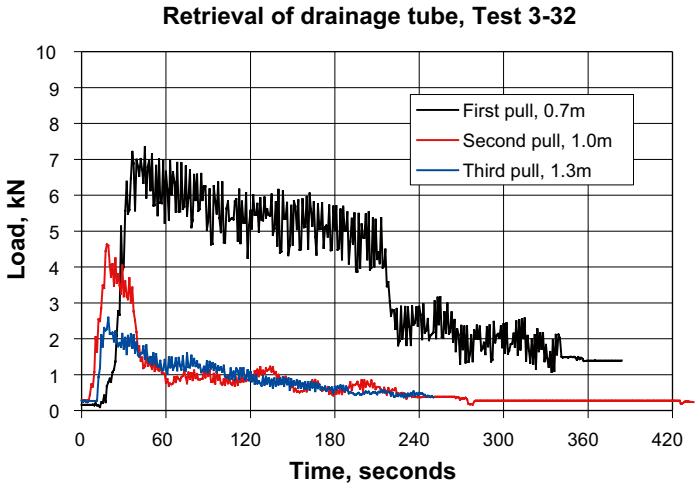

Figure B16-4. *The force needed in order to retrieve the drainage tube plotted vs. time. The tube was pulled out in steps. After the first pull, the bentonite had a healing time of about 5 days (to swell and seal the remaining hole) and additional 1 day after the second pull.*

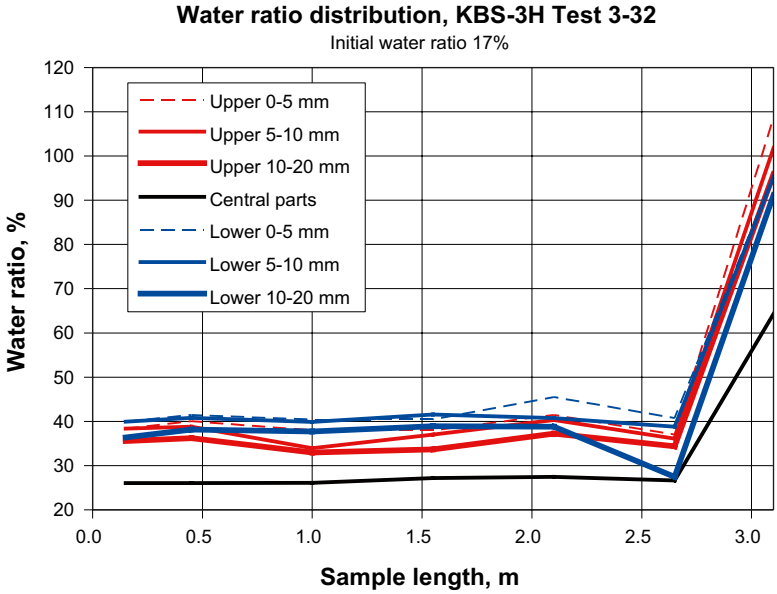

Figure B16-5. *The water ratio distribution in the clay plotted vs. the sample length. After finishing the test was sample taken at different radius at the outermost parts and also some sample in the middle parts.*

Appendix B17: Scale test 1:10, Test 3-33

Test	Material	Water type	Slot up/down (mm)	Test length (m)
3-33	MX-80 blocks	3.5 % salt	10/10	3.08 m

Layout: Pre wetting of slot. Drainage tube in order to control test conditions.

Distance blocks

Installed distance blocks

Raw material	MX-80, cores from full scale blocks
Water ratio, %	17.3
Bulk density, kg/m^3	2110
Dry density, kg/m^3	1799
Degree of saturation, %	88.2
Void ratio	0.545
Diameter of the blocks, mm	155
Test length, mm	3080
Total mass of blocks installed, kg	122.75

Calculated data

Final dry density, kg/m^3	1413
Void ratio	0.974
Saturated density, kg/m^3	1907

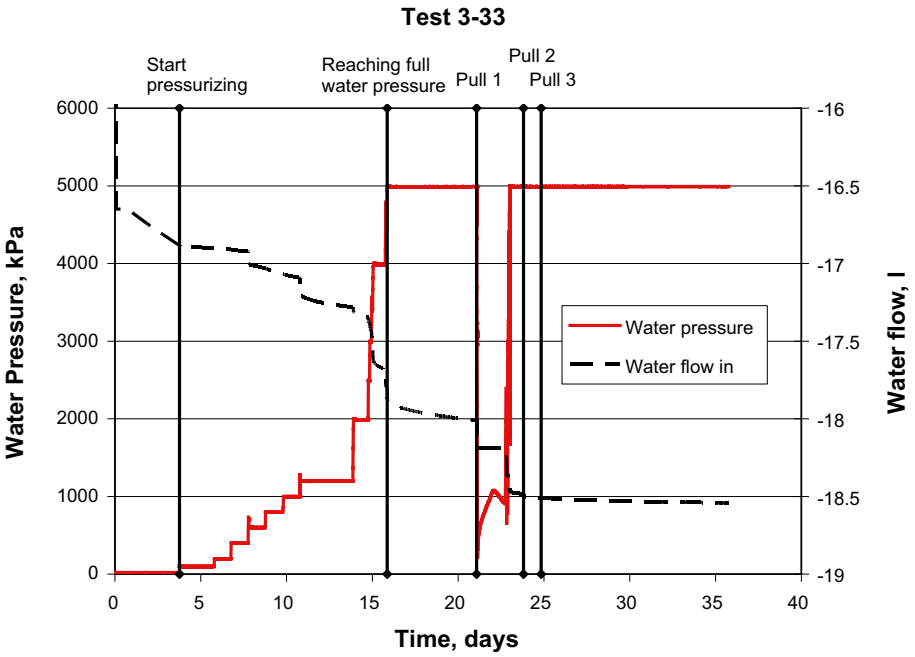

Figure B17-1 . The water inflow and the water pressure plotted vs. time. After 4 days the increasing of water pressure started in steps. Fourteen days after test start can the sample seal for 5 MPa. 25 days after test start is the tube retrieved. This can probably be done faster.

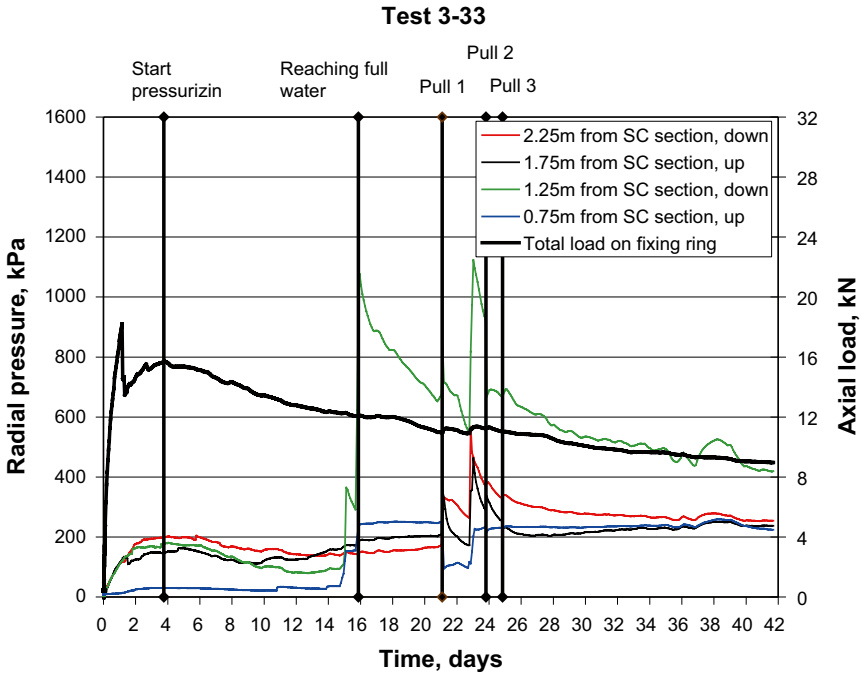

Figure B17-2. *The radial swelling pressure in three different points and the axial load on the fixing ring plotted vs. time.*

Figure B17-3. *Cut about 1.5 m from the super container. The remaining hole from the drainage tube can still be seen.*

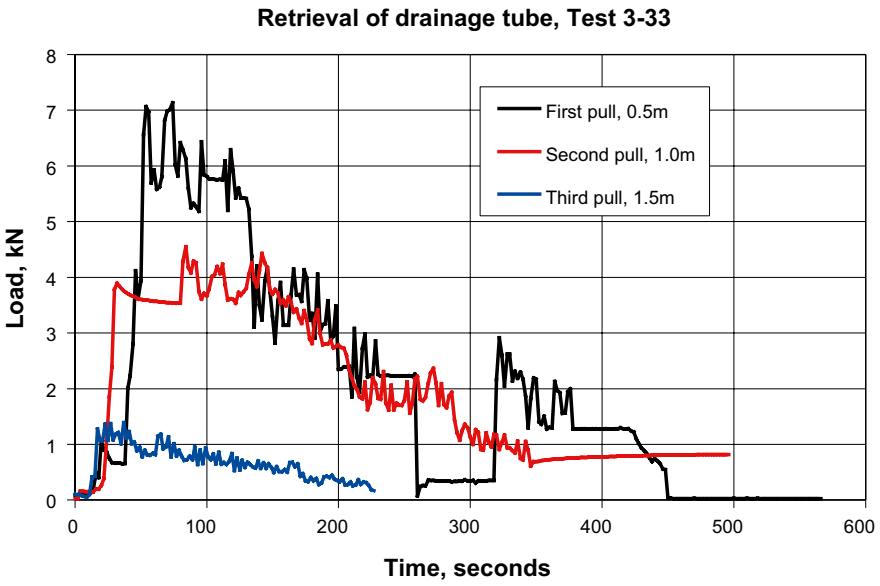

Figure B17-4. *The force needed in order to retrieve the drainage tube plotted vs. time. The tube was pulled out in steps. After the first pull, the bentonite had a healing time of about 3 days (to swell and seal the remaining hole) and additional 1 day after the second pull.*

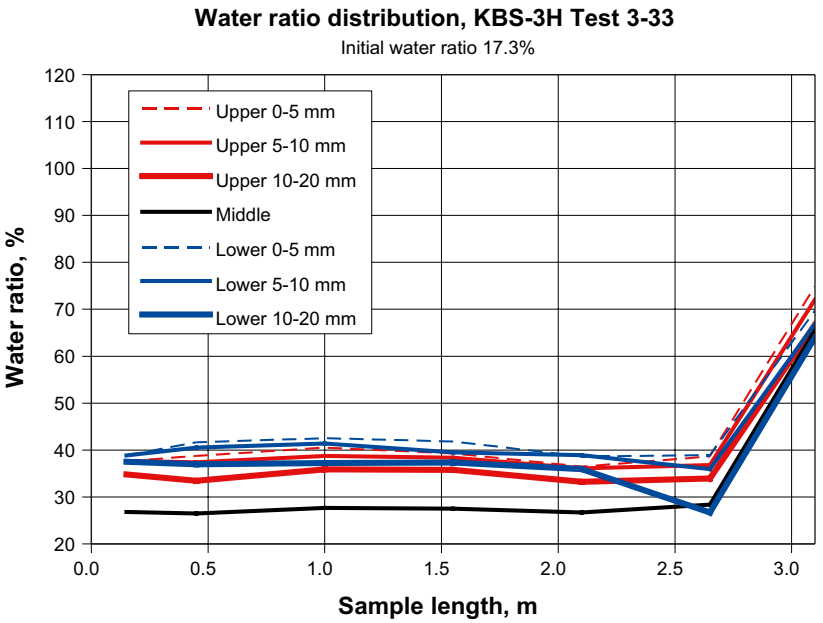

Figure B17-5. *The water ratio distribution in the clay plotted vs. the sample length. After finishing the test samples were taken at different radius at the outermost parts and also some sample in the middle parts.*

Appendix B18: Scale test 1:10, Test 3-34

Test	Material	Water type	Slot up/down (mm)	Test length (m)
3-34	MX-80 blocks	3.5 % salt	10/10	3.08 m

Layout: Pre wetting of slot. Blocks with Sr=94%.

Installed distance blocks

Raw material	MX-80, cores from full scale blocks
Water ratio, %	21.7
Bulk density, kg/m^3	2060
Dry density, kg/m^3	1693
Degree of saturation, %	94
Void ratio	0.642
Diameter of the blocks, mm	171
Test length, mm	1464
Total mass of blocks installed, kg	69.4

Calculated data

Final dry density, kg/m^3	1619
Void ratio	0.723
Saturated density, kg/m^3	2039

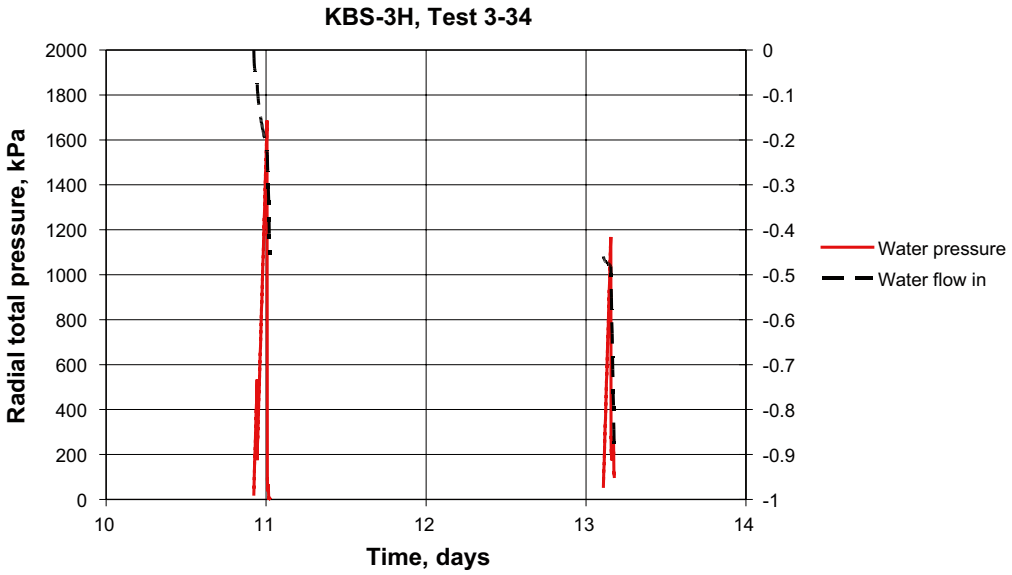

Figure B18-1. The water inflow and the water pressure plotted vs. time for the two pressure ramps.

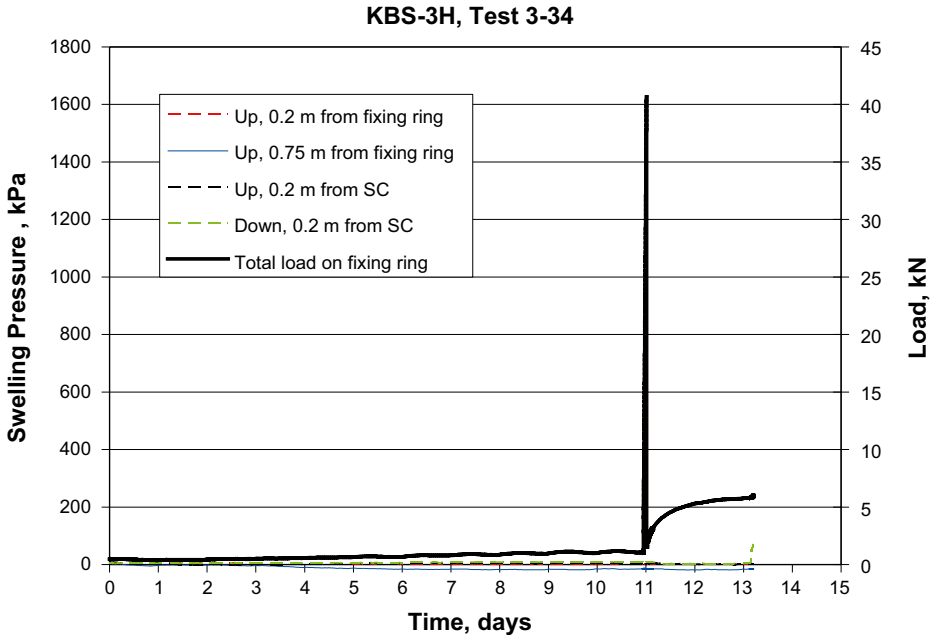

Figure B18-2. *The radial swelling pressure in three different points and the axial load on the fixing ring plotted vs. time.*

Figure B18-3. *Picture showing a distance block about 0.5m from the super container. Only a part of the slot was filled with water due to the fact that the bentonite closest to the super container swelled and sealed very fast and the water had no access to the slot volume inside. When the water pressure ramp was applied the bentonite could not withstand the pressure.*

Appendix B19: Scale test 1:10, Test 3-35

Test	Material	Water type	Slot up/down (mm)	Test length (m)
3-35	MX-80 blocks	3.5 % salt	10/10	3.08 m

Layout: Pre wetting of slot. Drainage tube in order to control test conditions. Sr=94%.

Installed distance blocks

Raw material	MX-80, cores from full scale blocks
Water ratio, %	21.7
Bulk density, kg/m^3	2060
Dry density, kg/m^3	1693
Degree of saturation, %	94
Void ratio	0.642
Diameter of the blocks, mm	173.2
Test length, mm	1443.8
Total mass of blocks installed, kg	58.2

Calculated data

Final dry density, kg/m^3	1676
Void ratio	0.664
Saturated density, kg/m^3	2075

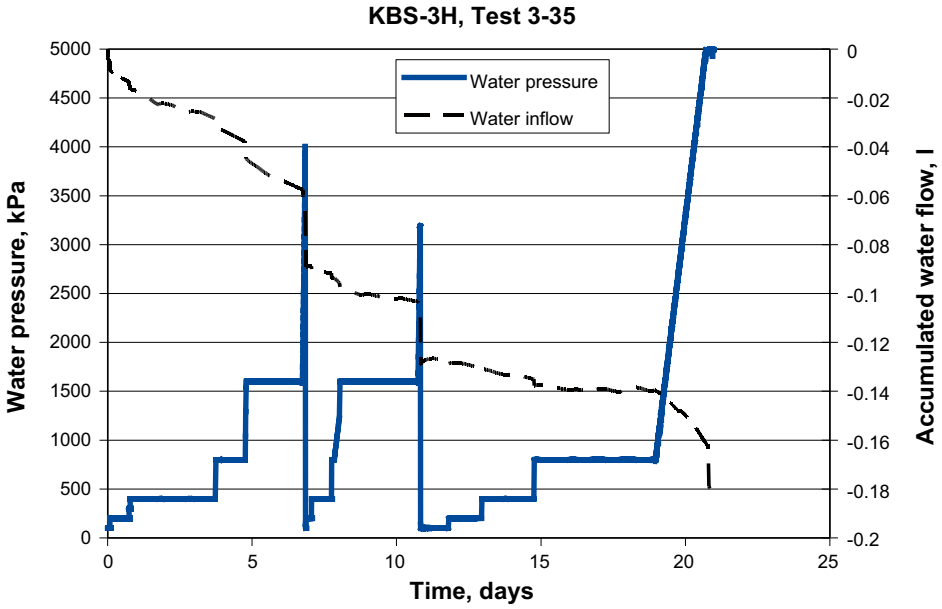

Figure B19-1. *The water inflow and the water pressure ramps plotted vs time.*

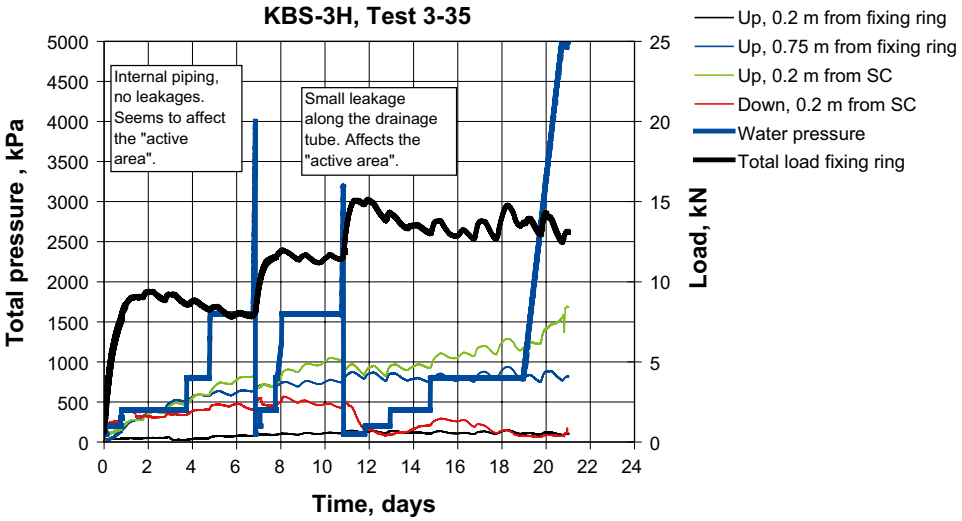

Figure B19-2. *The radial swelling pressure in three different points and the axial load on the fixing ring plotted vs. time. The applied water pressure is also shown in the diagram.*

Appendix B20: Hydraulic Pressure HP103

Test	Material and water	Water inflow rate	Water pressure increase rate	Initial axial slot (mm)
HP103	MX-80 blocks, 3.5% salt in water	0.1 l/min	0.1 MPa/h	2

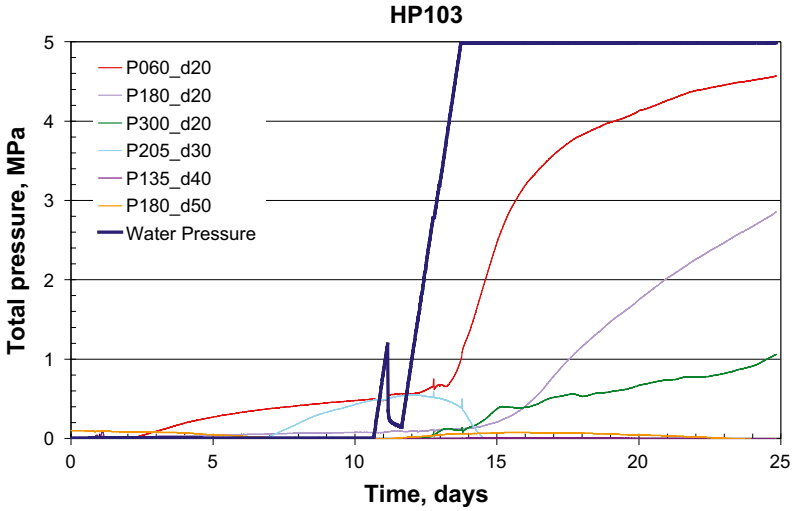

Figure B20-1. The applied water pressure and the measured axial pressure at different radial distance from the rock on the super container plotted vs. time. The label of each pressure sensor shows the position of the sensor on the super container end plate (angel and distance from rock surface). The three outermost sensors, placed on a distance of 20 mm from the rock surface, starts to react slowly and with an evident delay after reaching full water pressure in the super container section.

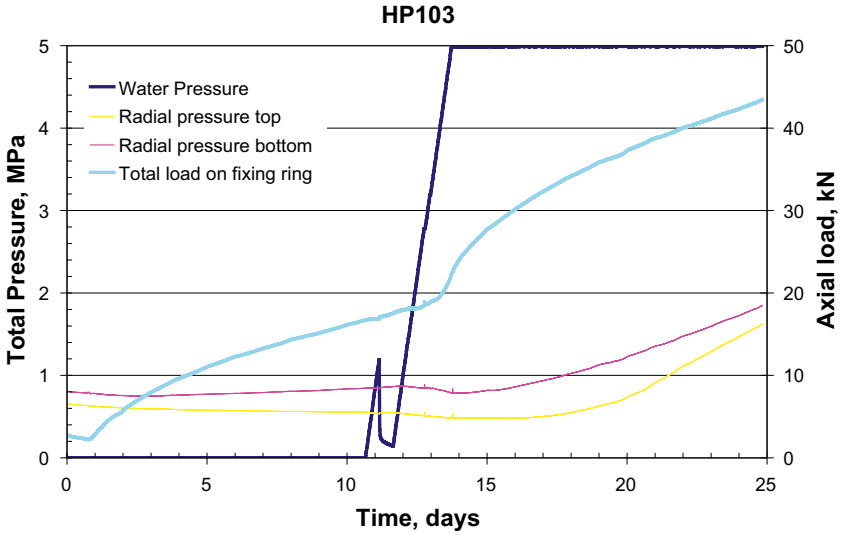

Figure B20-2. The applied water pressure, the measured radial swelling pressure and the total axial load on the fixing ring as function of time.

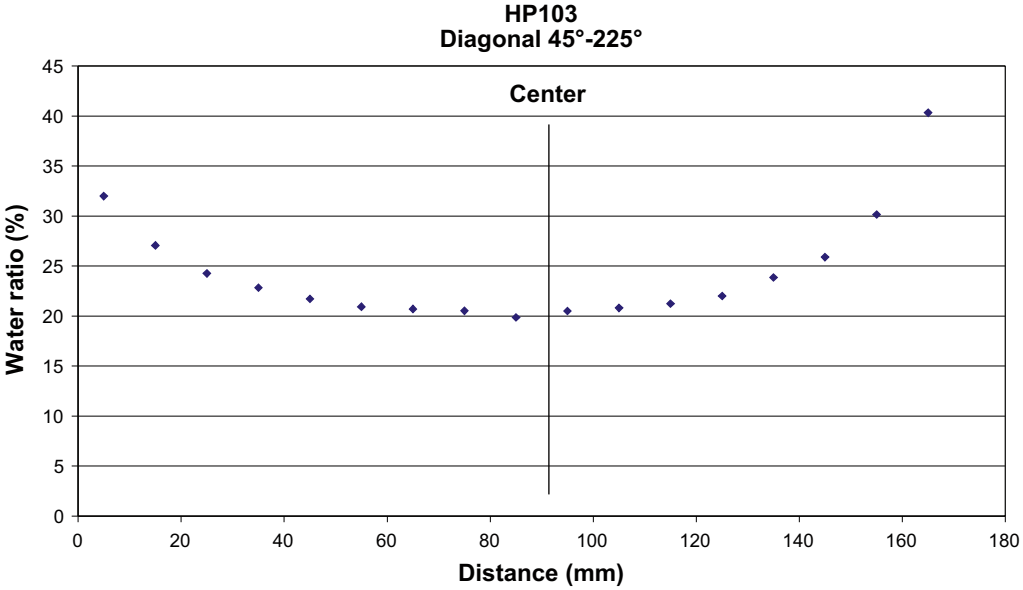

Figure B20-3. *The water ratio distribution on the distance block surface closest to the super container end plate. The distribution indicates the size of the "active area" and supports the pressure measurements.*

Appendix B21: Hydraulic Pressure HP203

Test	Material and water	Water inflow rate	Water pressure increase rate	Initial axial slot (mm)
HP203	MX-80 blocks, 3.5% salt in water	0.1 l/min	1 MPa/h	2

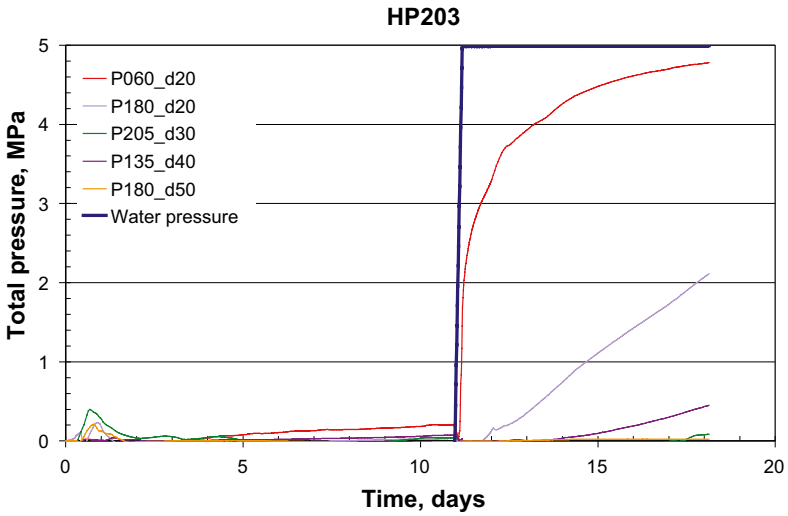

Figure B21-1. The applied water pressure and the measured axial pressure at different radial distance from the rock on the super container plotted vs. time. The label of each pressure sensor shows the position of the sensor on the super container end plate (angel and distance from rock surface). Three sensors, two placed on a distance of 20 mm from the rock surface and on placed on a distance of 40 mm from the rock surface, starts to react slowly and with an evident delay after reaching full water pressure in the super container section.

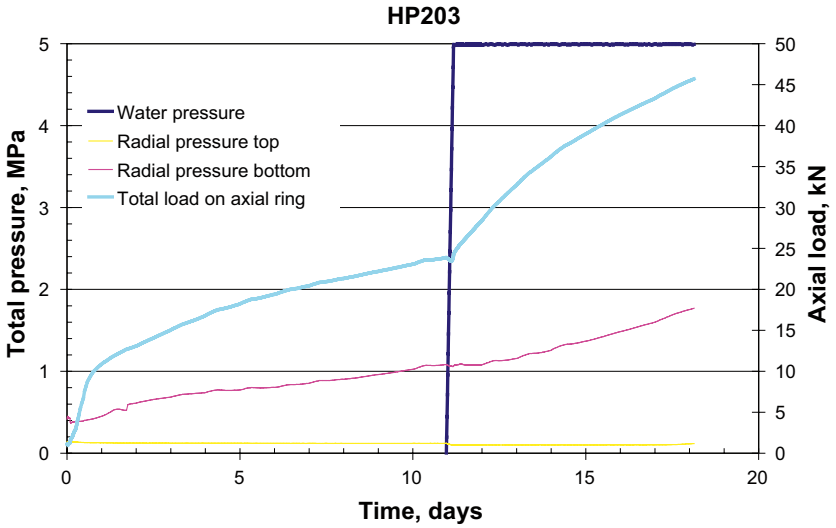

Figure B21-2. The applied water pressure, the measured radial swelling pressure and the total axial load on the fixing ring as function of time.

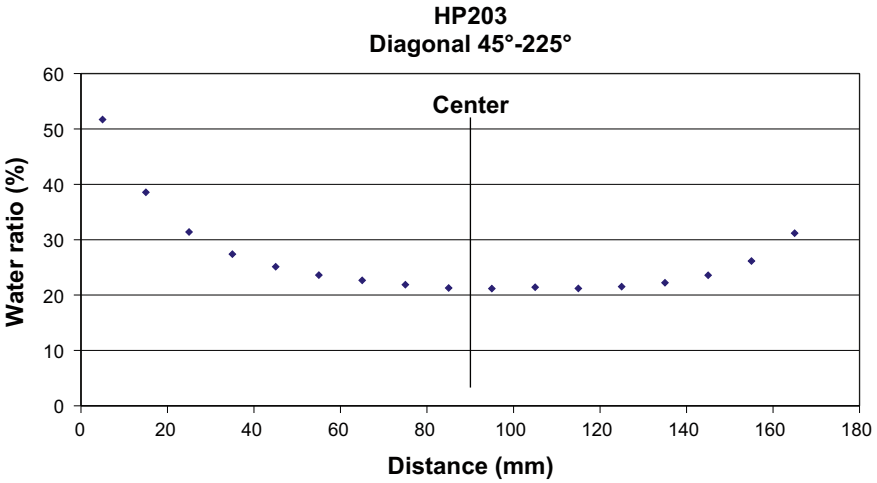

Figure B21-3. *The water ratio distribution on the distance block surface closest to the super container end plate. The distribution indicates the size of the "active area" and supports the pressure measurements.*

Appendix B22: Hydraulic Pressure HP303

Test	Material and water	Water inflow rate	Water pressure increase rate	Initial axial slot (mm)
HP303	MX-80 blocks, 3.5% salt in water	1 l/min	1 MPa/h	2

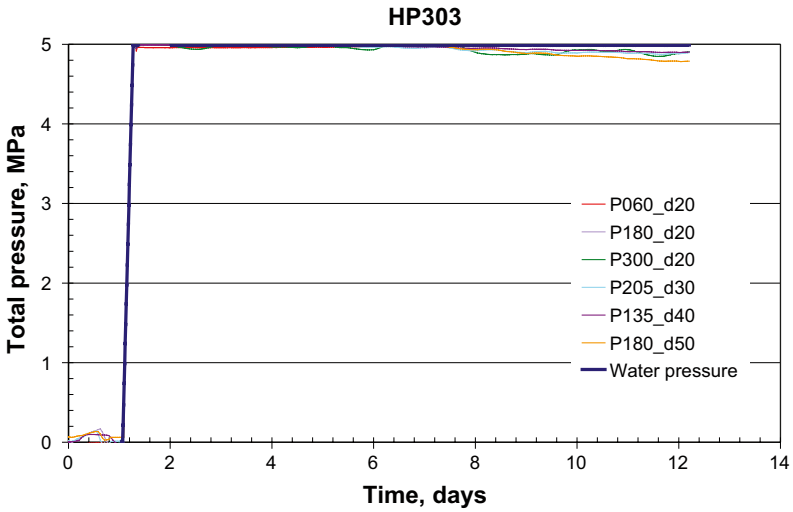

Figure B22-1. The applied water pressure and the measured axial pressure at different radial distance from the rock on the super container plotted vs. time. The label of each pressure sensor shows the position of the sensor on the super container end plate (angel and distance from rock surface). All pressure sensors react immediately when the water pressure was increased.

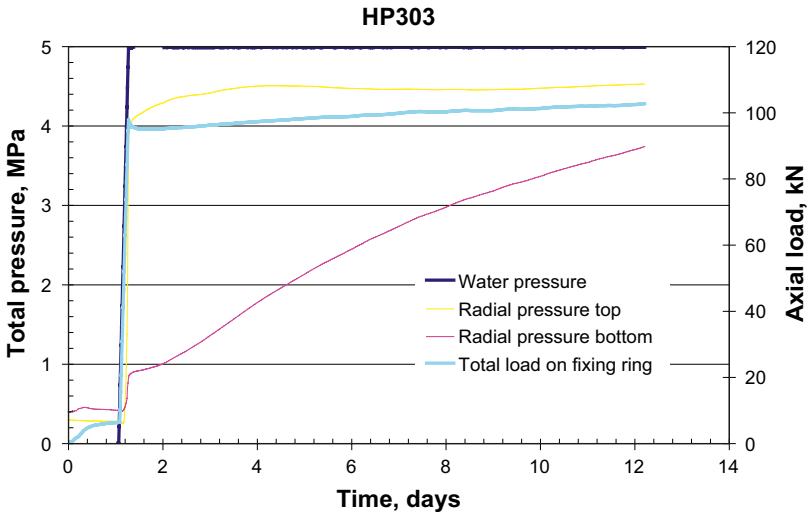

Figure B22-2. Diagram showing the applied water pressure, the measured radial swelling pressure and the total axial load on the fixing ring as function of time.

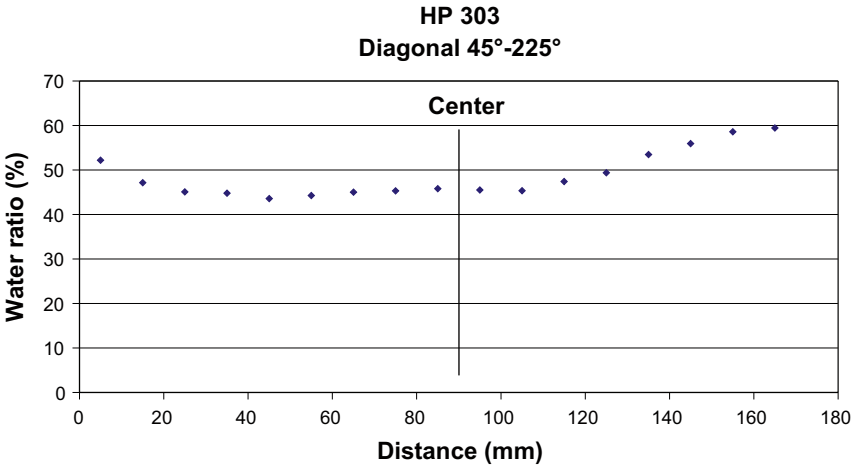

Figure B22-3. *Water ratio distribution on the distance block surface closest to the super container end plate. The distribution indicates the size of the "active area" and supports the pressure measurements.*

Appendix B23: Hydraulic Pressure HP104

Test	Material and water	Water inflow rate	Water pressure increase rate	Initial axial slot (mm)
HP104	MX-80 blocks, 3.5% salt in water	0,1 l/min	0,1 MPa/h	5

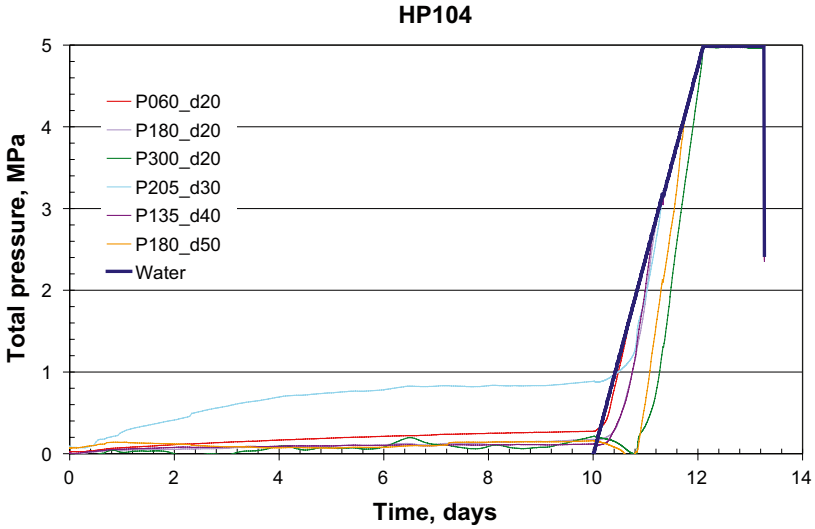

Figure B23-1. The applied water pressure and the measured axial pressure at different radial distance from the rock on the super container plotted vs. time. The label of each pressure sensor shows the position of the sensor on the super container end plate (angel and distance from rock surface). All pressure sensors react almost immediately when the water pressure was increased.

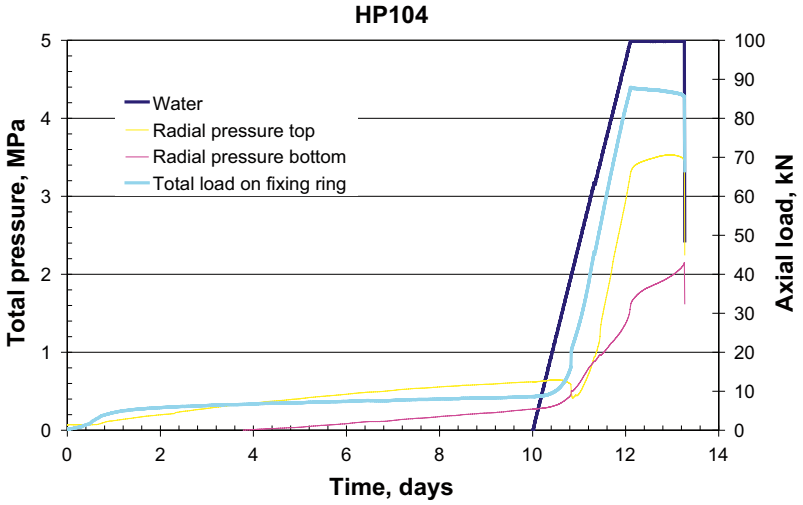

Figure B23-2. The applied water pressure, the measured radial swelling pressure and the total axial load on the fixing ring as function of time.

Appendix B24: Hydraulic Pressure HP204

Test	Material and water	Water inflow rate	Water pressure increase rate	Initial axial slot (mm)
HP204:2	MX-80 blocks, 3.5% salt in water	0,1 l/min	1 MPa/h	5

Test was repeated depending on leakage in the first test setup.

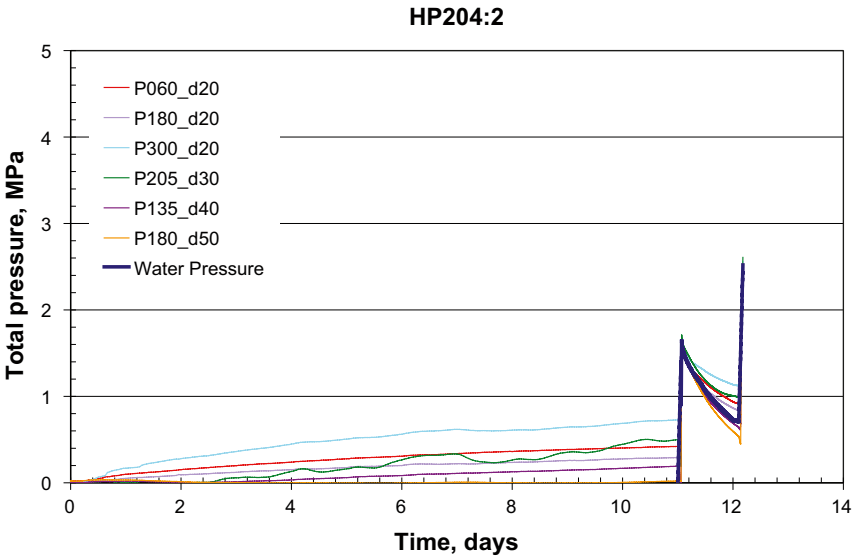

Figure B24-1. The applied water pressure and the measured axial pressure at different radial distance from the rock on the super container plotted vs. time. The label of each pressure sensor shows the position of the sensor on the super container end plate (angel and distance from rock surface). All pressure sensors react almost immediately when the water pressure was increased.

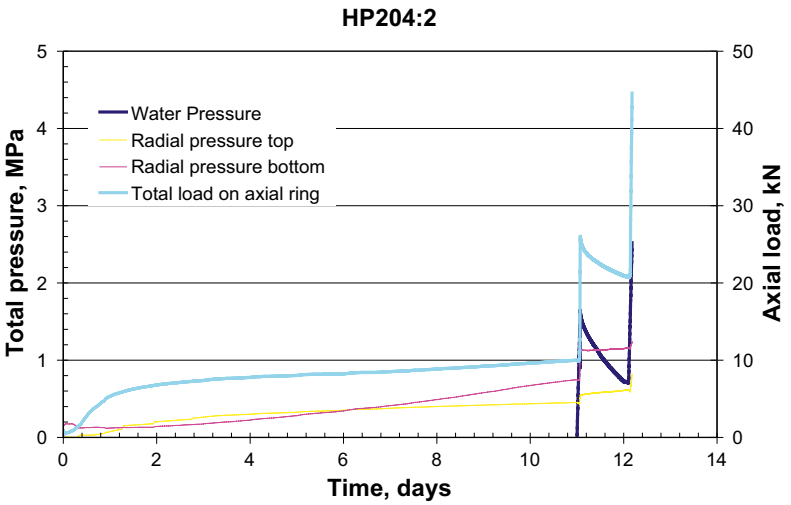

Figure B24-2. The applied water pressure, the measured radial swelling pressure and the total axial load on the fixing ring as function of time.

Appendix B25: Hydraulic Pressure HP404

Test	Material and water	Water inflow rate	Water pressure increase rate	Initial axial slot (mm)
HP404	MX-80 blocks, 3.5% salt in water	Controlled	Controlled	5

Special test with controlled conditions.

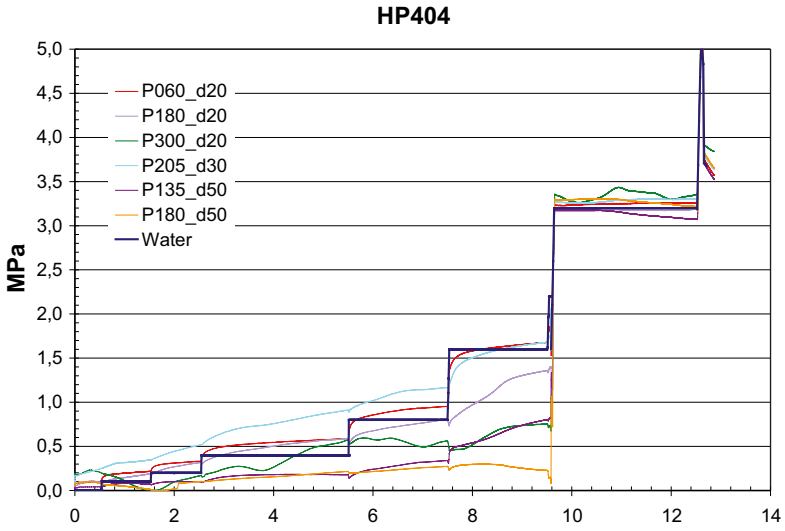

Figure B25-1. *The applied water pressure and the measured axial pressure at different radial distance from the rock on the super container plotted vs. time. The label of each pressure sensor shows the position of the sensor on the super container end plate (angel and distance from rock surface). All pressure sensors react almost immediately when the water pressure was increased.*

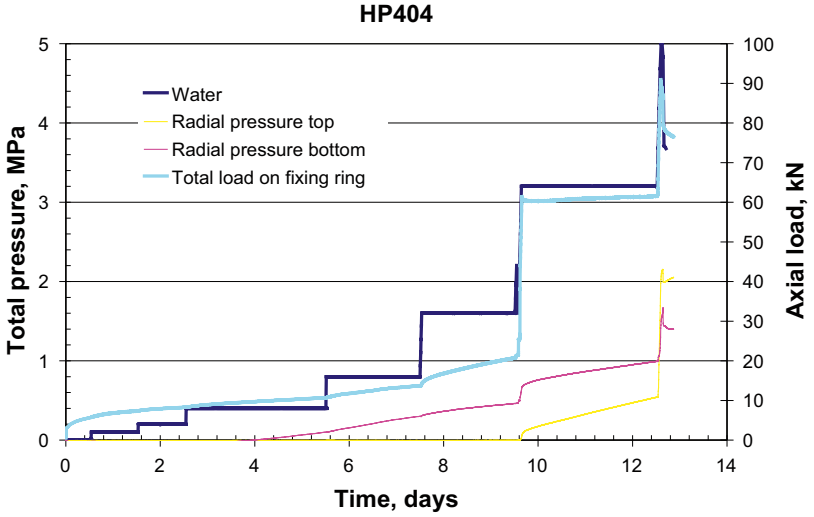

Figure B25-2. *The applied water pressure, the measured radial swelling pressure and the total axial load on the fixing ring as function of time.*

Appendix C1: Test type 1 – Measured RH, P_a and P_r vs. time from each test.

(Labels to the right show: initial water content_slot width_salt content of the added water)

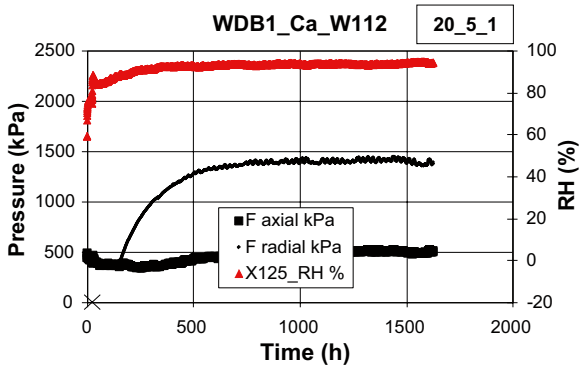

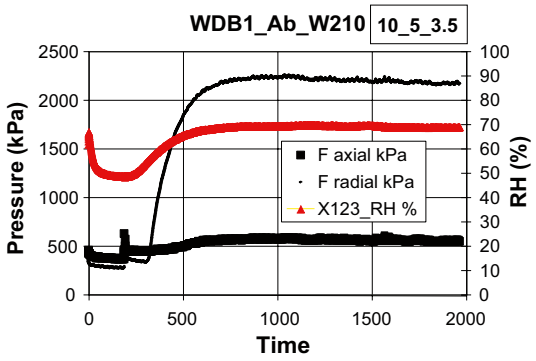

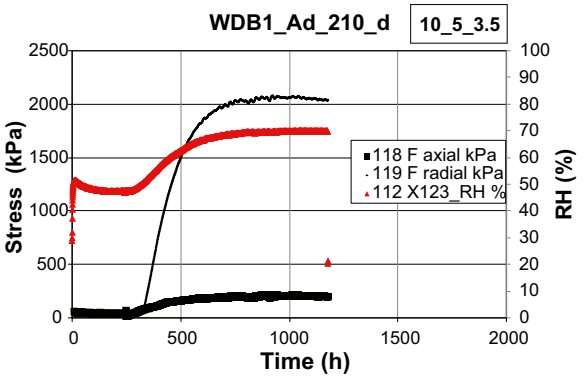

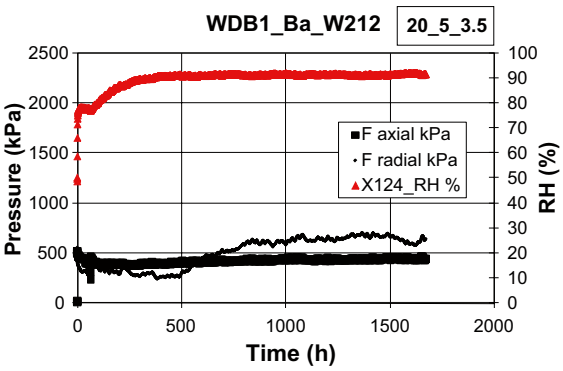

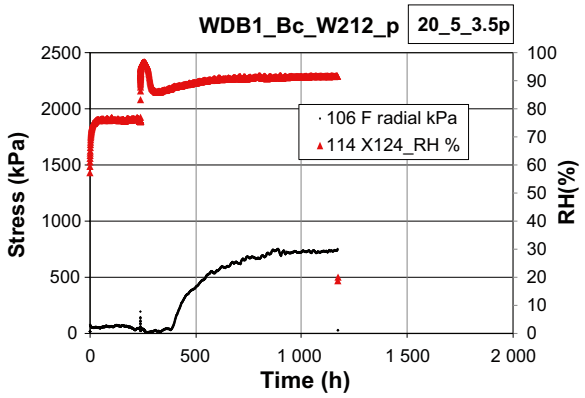

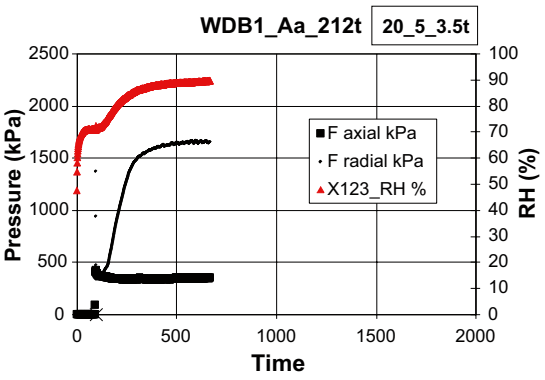

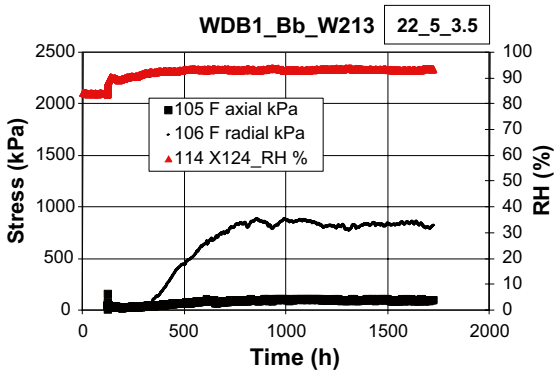
WDB1_Bb_W213
22_5_3.5
105 F axial kPa
106 F radial kPa
114 X124_RH %
Stress (kPa)
RH (%)
Time (h)

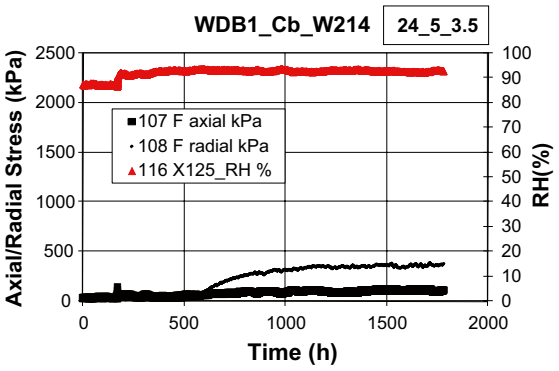
WDB1_Cb_W214
24_5_3.5
107 F axial kPa
108 F radial kPa
116 X125_RH %
Axial/Radial Stress (kPa)
RH(%)
Time (h)

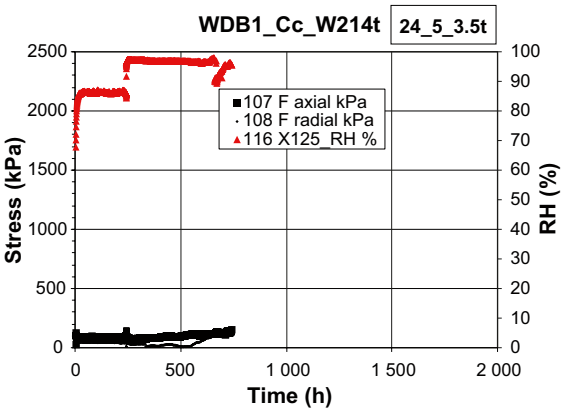
WDB1_Cc_W214t
24_5_3.5t
107 F axial kPa
108 F radial kPa
116 X125_RH %
Stress (kPa)
RH (%)
Time (h)

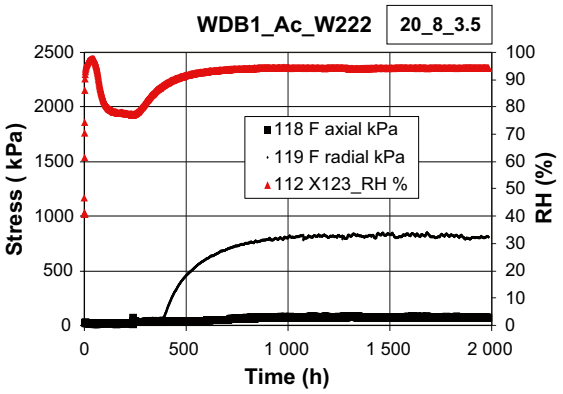
WDB1_Ac_W222
20_8_3.5
118 F axial kPa
119 F radial kPa
112 X123_RH %
Stress (kPa)
RH (%)
Time (h)

Appendix C2: Test type 1 – Profiles of water ratio and dry density for all specimens.

(Labels show: *initial water content_slot width_salt content of the added water*)

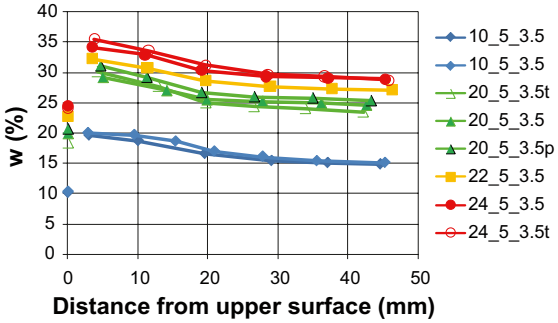

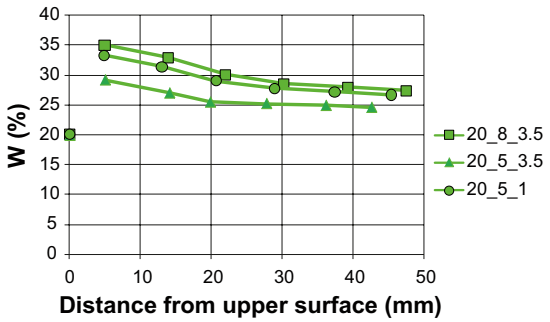

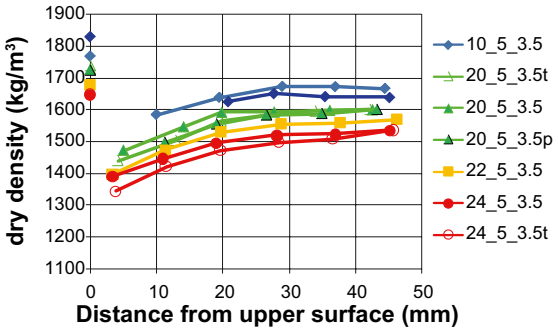

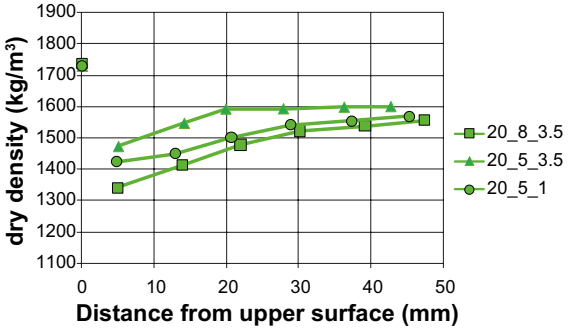

Appendix C3: Test type 1 – Photos after each test.

(Labels to the right show: *initial water content_slot width_salt content of the added water*)

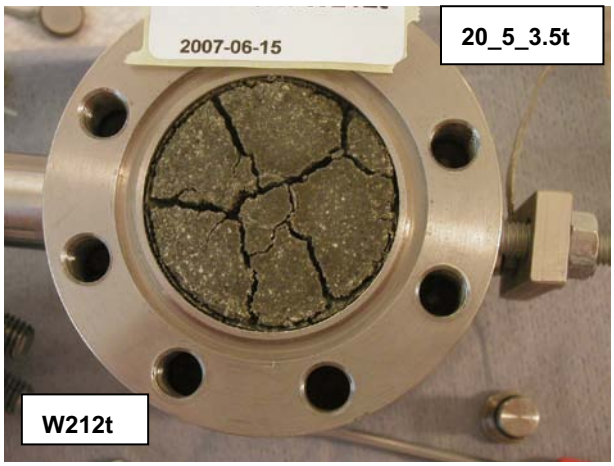

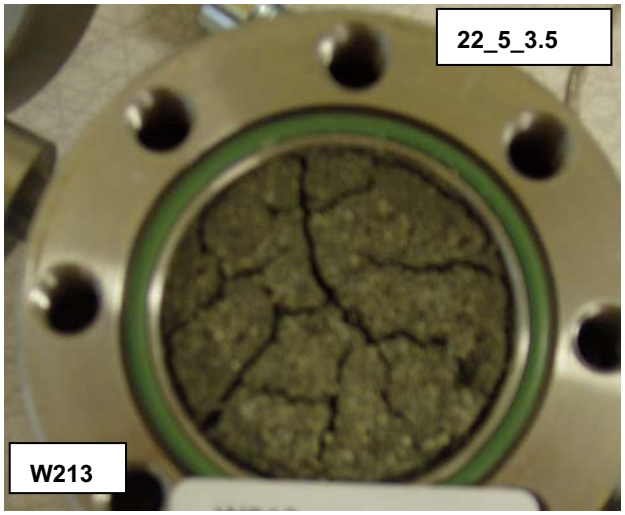
22_5_3.5
W213

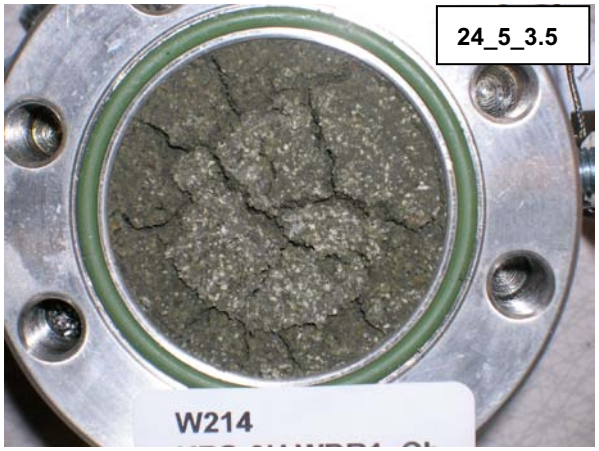
24_5_3.5
W214


2008-03-14 /ad
24_5_3.5t
W214t


20_8_3.5
W222
KBS-3H WDB1_Ac
2007-12-27/ad

Appendix C4: Test type 1 – Photos during one test made for illustration purpose with the upper lid made of acrylic plastic.

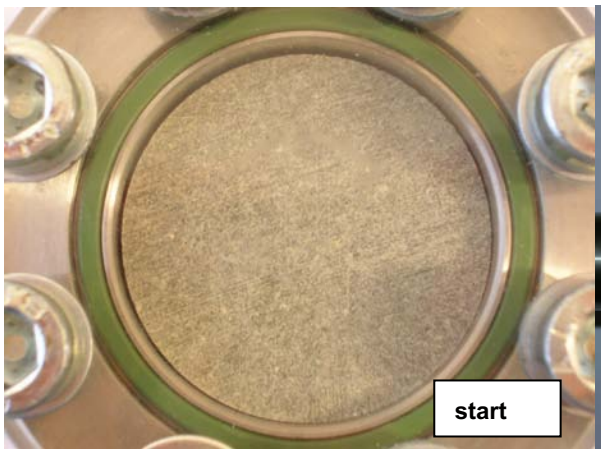

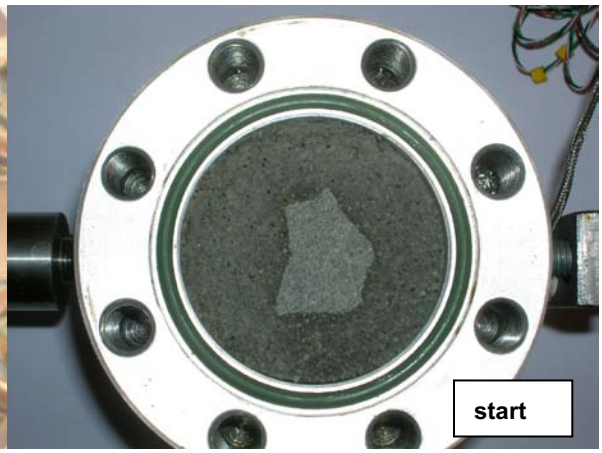

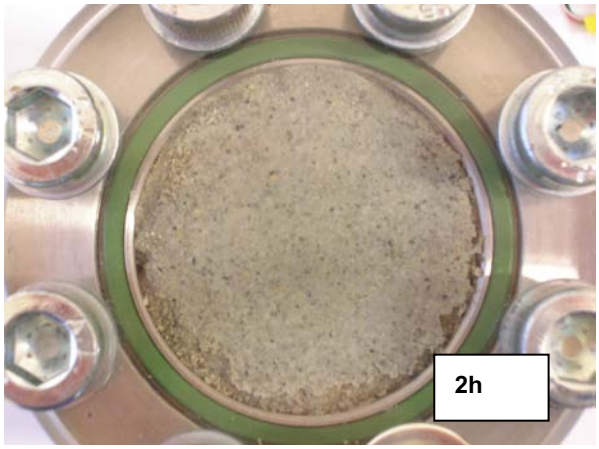

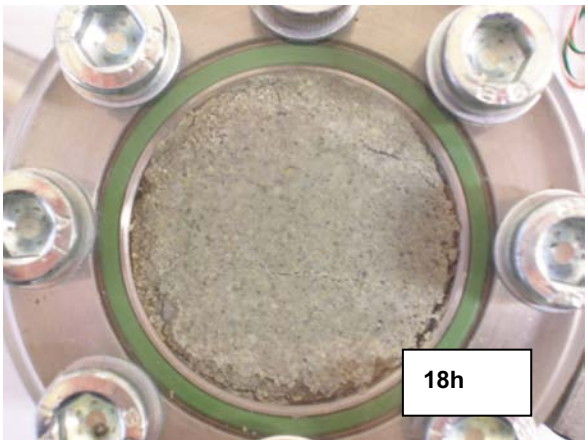

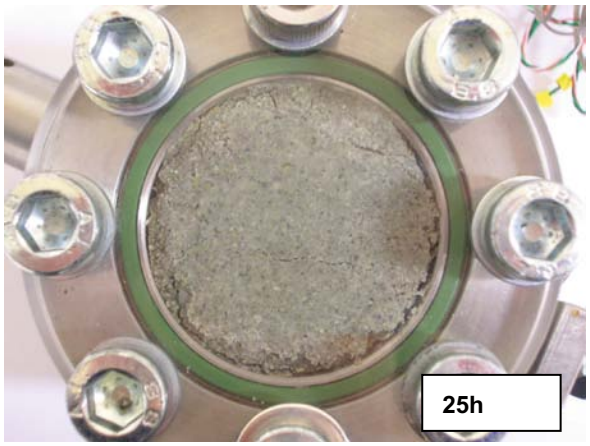

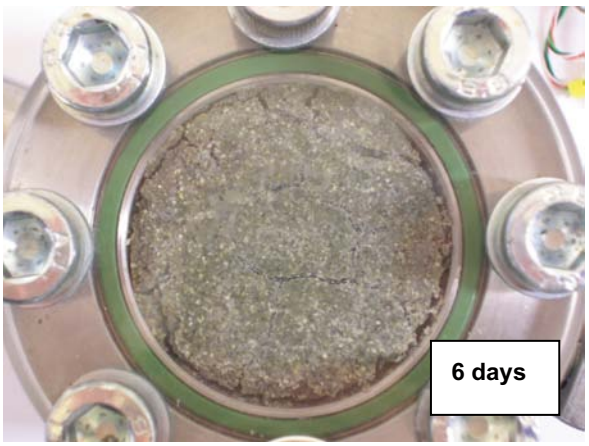

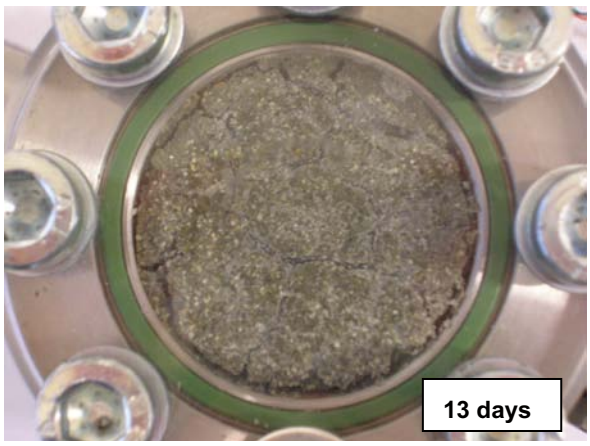
13 days

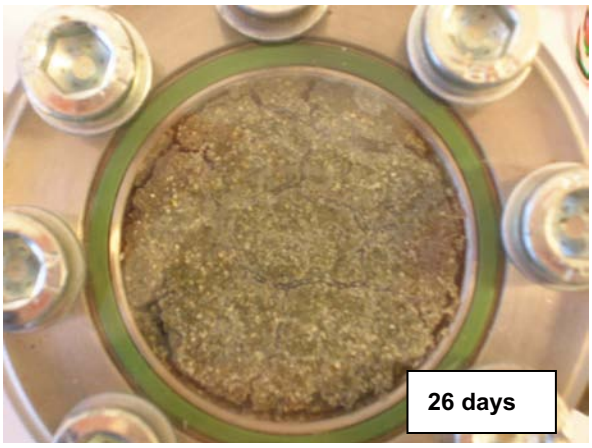
26 days

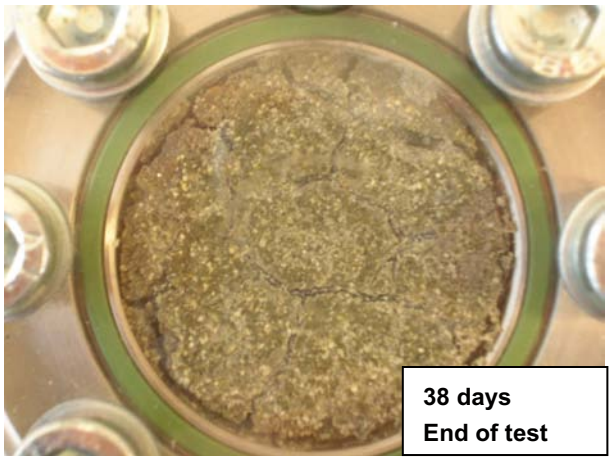
38 days
End of test


W212_p
KBS-3H WDB1_Bc
2008-03-17 /ad